

SUMMARY.

The electron transfer properties of titanium dioxide pigments have been investigated by the adsorption of electron donors and acceptors and the detection of radical species by electron spin resonance spectroscopy. Electron transfer was found to be a thermal process, no photo-assistance being observed. A powerful electron acceptor, dichlorodicyano p benzoquinone was used for a quantitative determination of the electron donor abilities of a number of pigments. The adsorption of electron acceptors from solution has been followed by ultra-violet absorption spectroscopy and ultra-violet and visible reflectance spectroscopy.

Room temperature fluorescence of pigments and of compounds on pigments has been examined and compared with solution fluorescence.

The photo-reduction of pigments in the presence of alcohols was studied and the formation of small quantities of photo-produced superoxide anion adsorbed on pigments has been confirmed.

The photo-electric properties of pigments have been studied by use of a simple wet electrochemical cell containing a layer of pigment deposited on an inert substrate. Photo-voltages of a number of pigments have been measured and found to correlate well with their known durabilities in paint media; providing a rapid test for the estimation of pigment durabilities. The photo-voltages and equilibrium dark potentials are discussed in terms of the band model for titanium dioxide.

Small photo-currents have been observed for pigments; anodic photo-currents flowing at positive biasing and small cathodic photo-currents at negative biasing. The initial photo-currents show

a transient part which decays to leave a level photo-current. The spectral distribution of the photo-current has been determined and the temperature dependence of photo-voltage and photo-current examined.

Anodic photo-currents have been sensitized by addition of a variety of alcohols to the electrolyte and are discussed in terms of the reaction of alcohols with photo-holes.

Addition of small quantities of potassium iodide and bromide to the electrolytes have been found to decrease the photo-voltage, and for potassium iodide even resulting in a change in the direction of the photo-voltage. Anodic photo-currents are likewise decreased and can become cathodic.



**A Study of the Photo-chemical Properties
of Titanium Dioxide**

by

Richard Michael Slater

**A Thesis
presented for the degree of
Doctor of Philosophy
in the Faculty of Science
of the
University of Leicester
1975**

UMI Number: U419145

All rights reserved

INFORMATION TO ALL USERS

The quality of this reproduction is dependent upon the quality of the copy submitted.

In the unlikely event that the author did not send a complete manuscript and there are missing pages, these will be noted. Also, if material had to be removed, a note will indicate the deletion.



UMI U419145

Published by ProQuest LLC 2015. Copyright in the Dissertation held by the Author.
Microform Edition © ProQuest LLC.

All rights reserved. This work is protected against
unauthorized copying under Title 17, United States Code.



ProQuest LLC
789 East Eisenhower Parkway
P.O. Box 1346
Ann Arbor, MI 48106-1346



THESIS
499737
22 3 76

x753028244

To Liz and Pussy

STATEMENT

The experimental work described in this thesis has been carried out by the author in the laboratories of the Department of Chemistry of the University of Leicester and partly in the Research Laboratories of Laporte Industries, Organics and Pigments Division, between October, 1972 and July, 1975.

No part of this work has been presented, or is concurrently being presented, for any other degree.

Signed

R. Slater

September, 1975.

R.M. Slater.

ACKNOWLEDGEMENTS.

I would like to thank my supervisor, Dr. R.S. Davidson, for his support and encouragement.

My thanks go to the Staff of the Research Laboratories of Laporte Industries, Organics and Pigments Division, especially Mr. R. Lait, Dr. R. Pearse, Dr. H. Chambers, Dr. R. Fell, Mr. B. Watson, and Mr. J.H. Collings, for many valuable discussions, technical assistance, and for the supply and analysis of titanium dioxide pigments.

I am also indebted to Mrs. N. Johnson for typing this thesis and to the Science Research Council for the award of a maintenance grant.

	<u>Page</u>
4.2b Results	74
4.3 Sensitized Photo-Oxidation of 9-Methylanthracene by Methylene Blue on Titanium Dioxide	84
4.4 Discussion	86
<u>Chapter 5.</u>	<u>Photo-Electric Properties of Titanium Dioxide Cell Systems.</u>
5.1 Introduction	90
5.2 Photo-Voltage Measurement	92
5.3 Photo-Current Measurement	119
5.4 Photo-Current Sensitization	131
5.5 Spectral Distribution and Light Intensity Variation of Photo-Current	138
5.6 Temperature Dependence of the Photo-Electric Effects of Titanium Dioxide	145
5.7 Effect of Anions on the Photo-Electric Effect of Titanium Dioxide	152
5.8 Effect of Amines on Pigment Photo-Currents	165
5.9 Chalking Mechanisms	171

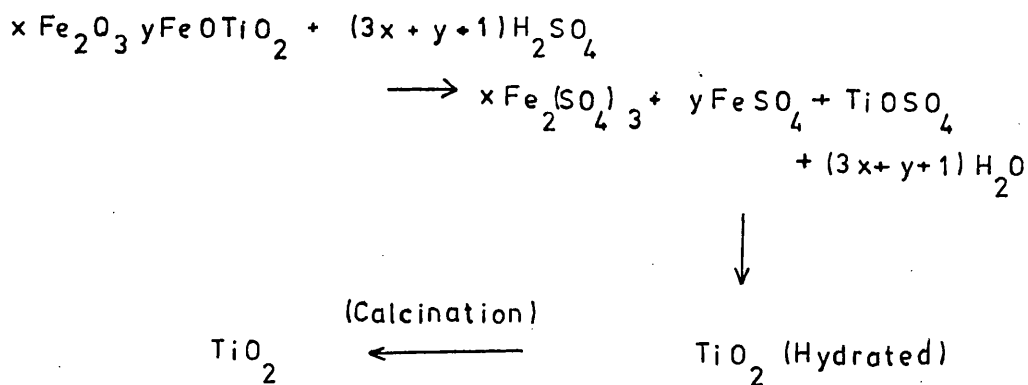
CHAPTER 1

GENERAL INTRODUCTION

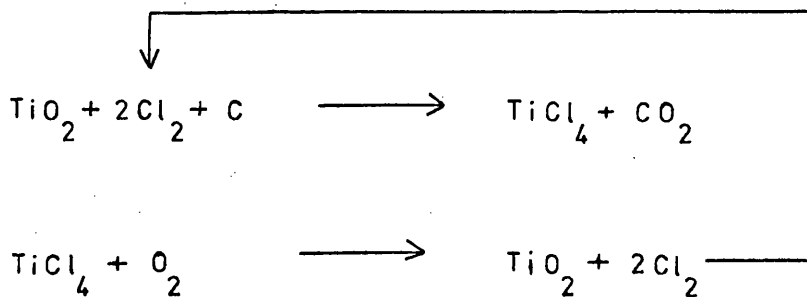
1.1 Introduction.

Titanium dioxide has been of commercial importance for many years as a white pigment in paints and plastics. It is manufactured from the mineral ilmenite, (which can be represented by $x\text{Fe}_2\text{O}_3 \cdot y\text{FeOTiO}_2$ where $x \approx 0.3$ and $y \approx 0.5$ for a typical weathered ilmenite), by the sulphate process in which titanium dioxide is precipitated from sulphate solution and calcined at about 900°C . It is also manufactured by the chloride process in which titanium tetrachloride is made by reaction of gaseous chlorine with mineral rutile and coke at high temperature. The titanium tetrachloride is reacted with oxygen at high temperature to form titanium dioxide¹ and chlorine gas which is recycled.

(a) Sulphate Process.



(b) Chloride Process.



Titanium dioxide exists in three crystalline forms, rutile, anatase, and brookite. All three structures are based on octahedral co-ordination of O^{2-} ions around Ti^{4+} ions with varying degrees of distortion. It is only the rutile and anatase forms of titanium dioxide which find commercial use.

A white paint film consists of titanium dioxide particles embedded in an organic binder and it is from this use that the photochemistry of titanium dioxide gains its importance. Paint films pigmented with titanium dioxide are known to slowly degrade under the action of sunlight. The organic medium is destroyed leading to loss of gloss and eventually to pigment particles being freed at the paint surface resulting in "chalking", so called because a paint film in this condition is covered in a loose white chalk of titanium dioxide. The organic binders composing the paint film can be broadly divided into two types².

(1) Those binders such as linseed oil, nitrocellulose and alkyds which are photochemically unstable, i.e. they are directly degraded by ultra-violet light.

(2) Modern photochemically stable binders such as fluorinated hydrocarbons, silicone alkyds, polyesters and polyurethane which are of high durability due to their resistance to direct decomposition by ultra-violet light.

For the photochemically unstable binders the presence of titanium dioxide pigment has a protective effect so that the unpigmented binder degrades at a faster rate than the pigmented binder. This protective effect is due to the pigment strongly absorbing the ultra-violet light striking the film. It is calculated³ that for a film having a pigment volume concentration of 10% the pigment will absorb 99% of the ultra-

-violet light reaching the film, and this protection increases with increasing pigment volume concentration⁴. The photochemical contribution to the breakdown of the organic media is therefore greatly reduced, but there is another mechanism of breakdown of the paint film which is the photocatalytic pathway. This is due to the energy that the titanium dioxide receives through its ultra-violet absorption resulting in the production of a reactive species at the pigment surface which attacks the organic media and contributes to its breakdown. The nature of the species responsible for the photocatalytic action is still not firmly established. A discussion of the mechanism of the photocatalytic process is included at the end of Chapter 5.

The extent of the photocatalytic reaction will depend upon the type of titanium dioxide pigment used and much has been done in recent years to minimize the photocatalytic activity of pigments. It can be seen that for photostable binders pigmented with titanium dioxide the major contribution to the degradation will be due to the photocatalytic reaction since the photochemical degradation of the binders is minimal and for these binders the degradation increases with increasing pigment volume concentration since the photocatalytic reaction is increased⁴.

To decrease the photocatalytic activity of the pigments the pigment particles are surrounded with a thin layer of titania, silica or alumina mixtures which are in hydrated form. The pigment particles are only of the order of 0.2 microns in diameter and the thin coating of the order of 3nm in thickness is deposited by co-precipitation of mixtures of the hydrous oxides from solution in which the pigment particles are suspended. The surface coating physically covers the titanium dioxide surface but it is by no means perfect; exposed

titanium dioxide surface still occurring. The surface treatment of pigments is illustrated in Figs. 1 and 2. Fig 1 shows an electron micrograph of base (uncoated) pigment particles and Fig. 2 shows an electron micrograph of coated pigment particles, the surface coating being the "blurring" effect around each particle which shows that the coating is of uneven thickness.

The characterization of the titanium dioxide surface is important since the photocatalytic breakdown of the paint media occurs either at the pigment surface or a reactive species produced at the surface is freed enabling it to react with resin molecules. Commercial pigments made by the sulphate process contain strongly adsorbed sulphate ions⁵ due to the precipitation of the pigment from sulphate solution and these adsorbed ions are carried through the process to the final pigment. Likewise pigments manufactured by the chloride process contain adsorbed chloride ions.

The presence of hydroxyl groups on the surface of titanium dioxide was demonstrated by Yates⁶ who detected hydroxyl groups and adsorbed water on rutile by their infra-red absorptions at 3680cm^{-1} and 1605cm^{-1} respectively. Numerous⁷⁻¹¹ other investigations of the infra-red spectroscopy of titanium dioxide surfaces led to the proposal of the existence of different types of surface hydroxyl groups having basic and acidic properties¹². Hydroxyl groups giving rise to a 3670cm^{-1} absorption band have been assigned as terminal hydroxyl groups attached to the metal cation and having acidic properties, and hydroxyl groups giving rise to a 3700cm^{-1} absorption band being assigned to bridged hydroxyl groups on oxide sites having basic properties. Other absorptions observed at 3690cm^{-1} and 3420cm^{-1} have

Fig. 1. Electron Micrograph of Base Pigment Particles on a Graphite Grid.
Magnification 150,000X.

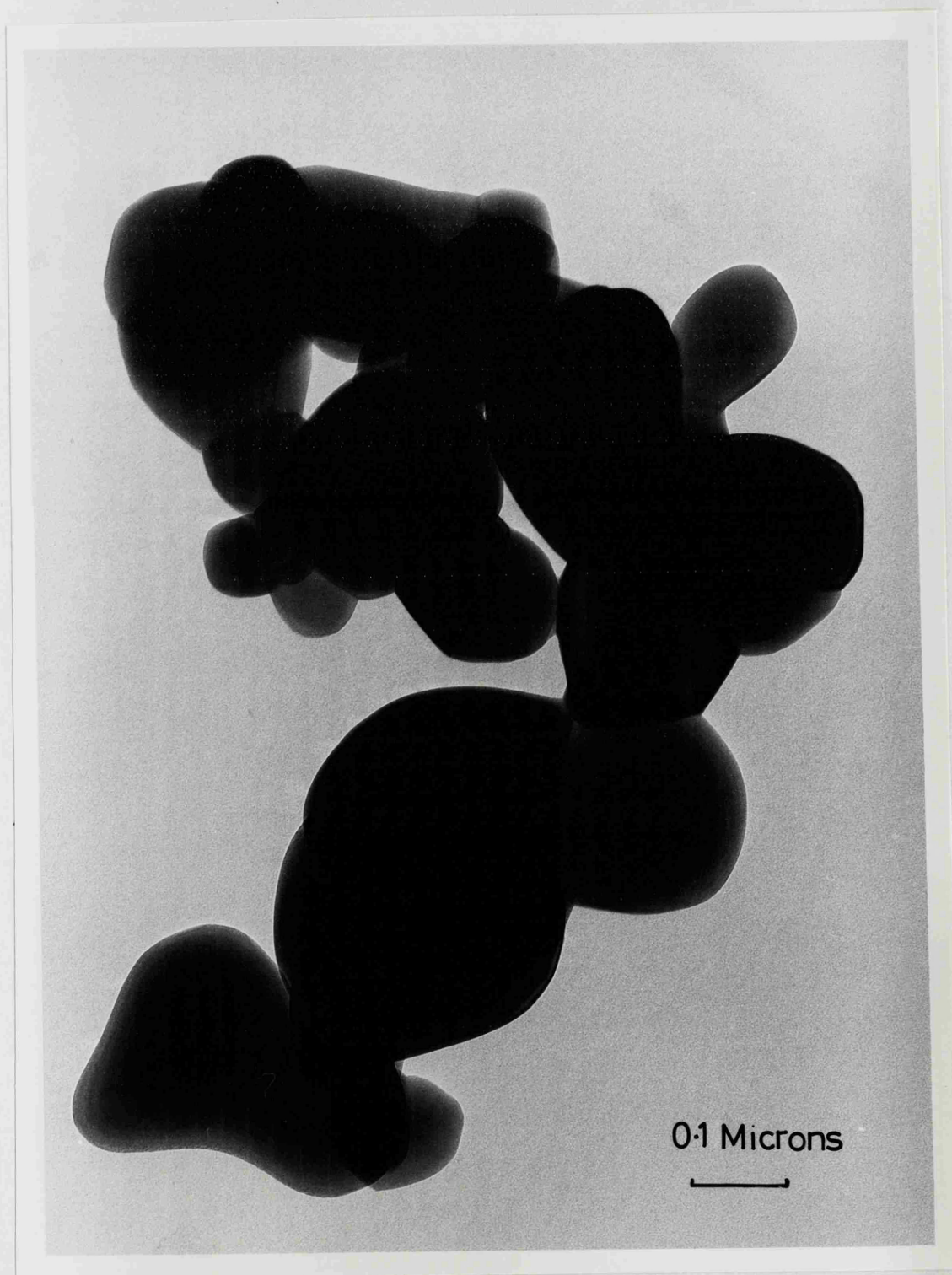
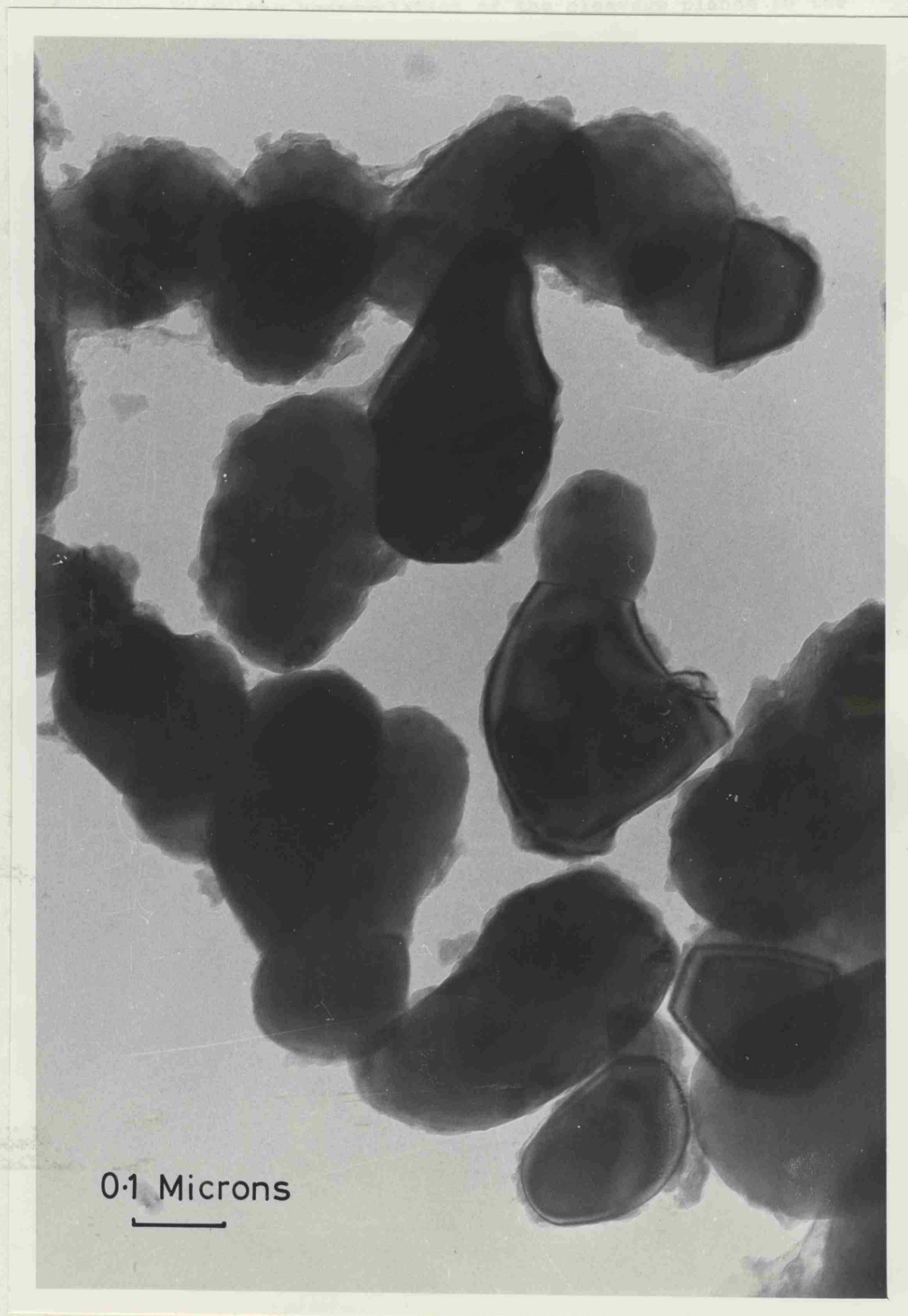
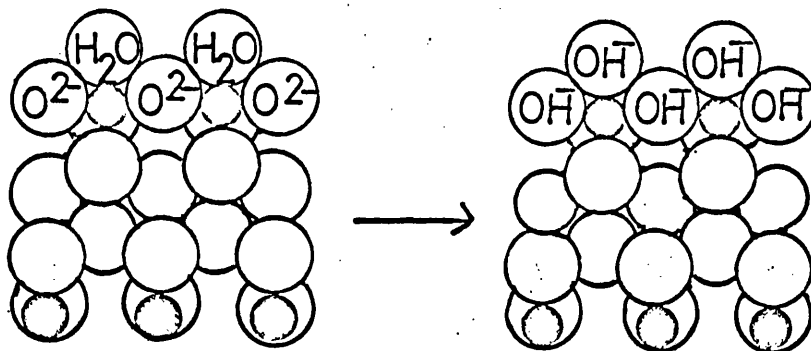


Fig. 2. Electron Micrograph of Coated Pigment Particles on a Graphite Grid.

Magnification 150,000X.



been assigned to hydrogen bonding interacting hydroxyl groups of terminal and bridged types respectively. Attempts^{7,13,14} at correlating the observed infra-red absorption frequencies of the hydroxyl groups to the hydroxylation of the cleavage planes in the crystal structures have been made. The unsatisfied co-ordination spheres of the surface ions would be completed by adsorption of water molecules. The water molecules would be able to react with surface O^{2-} ions to form adsorbed hydroxyl groups.



The amphoteric nature of the titanium dioxide surface has been demonstrated by Boehm¹⁵⁻¹⁹ by the chemical reaction of surface hydroxyl groups with compounds such as ammonia, fluoride ion, thionyl chloride, and phosphate ion. Parfitt has also studied the interaction of hydroxyl groups with pyridine²⁰, ammonia²¹, and hydrogen chloride²².

An investigation by Smith²³ of the infra-red spectroscopy of hydroxyl groups on pigments indicated that coatings of alumina and silica applied as surface treatments on pigments lose their identities with respect to surface hydroxylation compared with bulk silica and alumina as judged by the loss of the characteristic silica and alumina surface hydroxyl group bands.

Adsorbed carbon dioxide from the atmosphere will also be expected on the pigment since carbon dioxide has been shown to be readily adsorbed^{6,12,24} but is easily removed by evacuation at room temperature.

The purpose of the project was to study the photochemical properties of pigmentary titanium dioxide with reference to its photocatalytic action in paint media using a number of different directions of investigation. These included the investigation of the electron transfer properties of pigments, the fluorescence of pigment-dye systems and the properties of simple cell systems containing titanium dioxide.

1.2 Titanium Dioxide Samples.

The titanium dioxide samples used in the experiments were pigmentary samples prepared by Laporte Industries Ltd. The pigments and some of their characteristics are listed in Table 1.

Pigments D and E are surface treated pigments prepared from pigment A. Pigments G and H are surface treated pigments prepared from pigment F. Pigment A differs from pigment C in containing zinc oxide incorporated into the lattice as a rutilizing agent and as an antichalking treatment. An organic surface treatment (approximately 0.1 to 0.3%) is added to pigment D and G as an aid to dispersibility²⁵. Surface treated pigments generally have a higher surface area than base pigments.

Analysis of the pigments, mainly by mass spectroscopy was performed by the Analytical Laboratories of Laporte Industries, Organics and Pigments Division. The percentage weight loss at 105°C represents

Table 1.

Pigment	Crystal Structure	Approximate Surface Area m^2/g	Surface Treatment	% wt. loss 105°C	% wt. loss on ignition	Additional Information.
A	Rutile	6.8	None	0.13	0.35	Contains 0.74% ZnO in the lattice
B	Rutile	7.6	None	0.09	0.23	Contains 0.01% ZnO in the lattice
C	Rutile	7.9	None	0.08	0.27	Contains 0.08% ZnO in the lattice
D	Rutile	15.8	medium coating of alumina/titania	0.56	1.64	Organic Treatment. Contains 0.59% ZnO in the lattice.
E	Rutile	13.2	medium coating of silica/alumina/titania	0.50	1.39	Contains 0.64% ZnO in the lattice.
F	Rutile	6.4	None	-	-	Zinc Oxide free (0.0007%)
G	Rutile	13.6	heavy coating of alumina/titania	0.72	2.03	Organic Treatment. Zinc oxide free (0.0003%)
H	Rutile	14.3	heavy coating of alumina/titania	-	-	Zinc oxide free (0.0002%)
I	Anatase	10.7	None	0.1	0.23	Zinc oxide free. (0.0003%)

the amount of loosely bound molecular water that the pigment contains. The percentage weight loss upon ignition is due to loss of both molecular water and surface hydroxyl groups²⁶. The pigments A-E and I contain the following impurities apart from the additives mentioned; approximately 50p.p.m. Fe_2O_3 , SnO_2 , W_3O_3 , and PbO ; 100p.p.m. ZrO_3 and only a few p.p.m. of V_2O_5 , CrO_3 , MnO , CoO , and NiO . The pigments F, G, and H were of higher purity containing approximately 30p.p.m. Fe_2O_3 and only a few p.p.m. of ZrO_3 , PbO , SnO_3 , W_3O_3 , V_2O_5 , CrO_3 , MnO , CoO and NiO .

CHAPTER 2

ELECTRON SPIN RESONANCE AND ELECTRON TRANSFER

PROPERTIES OF TITANIUM DIOXIDE PIGMENTS.

2.1 Introduction.

Electron spin resonance is a very sensitive technique for the detection of free radicals and metal ions having unpaired electron spin. Pure titanium dioxide does not give any electron spin resonance absorption^{27,28}, since both Ti^{4+} and O^{2-} ions are diamagnetic. Investigations of the electron spin resonance of single crystals of rutile titanium dioxide specifically doped with small quantities of transition metal ions have been carried out. From these studies information has been gained on the environment of these ions in the titanium dioxide lattice. The electron spin resonance of single crystals gives information along the three principal crystal axes since each axis can be aligned with the magnetic field direction. For powdered samples some but not all of the directional information is lost, due to the random orientations of the spins to the magnetic field direction. The observation of the electron spin resonance absorptions of transition metal ions in the titanium dioxide lattice is generally only observable at the low temperature of 77K or below due to spin lattice relaxation of the ions²⁹. Electron spin resonance spectra of several ions in titanium dioxide have been reported and the hyperfine coupling from the natural abundances of magnetic isotopes have been observed. It has been inferred from these studies that Fe^{3+} ³⁰ and Co^{2+} ³¹ ions in titanium dioxide replace Ti^{4+} ions in the lattice. The presence of impurity ions does play an important part in its colour and photropy, i.e. the properties of some preparations of titanium dioxide to change colour or darken on exposure to light³² which has been attributed to the presence of Fe^{3+} ions in the lattice. Ni^{2+} ions were inferred from electron spin resonance studies to occupy interstitial positions

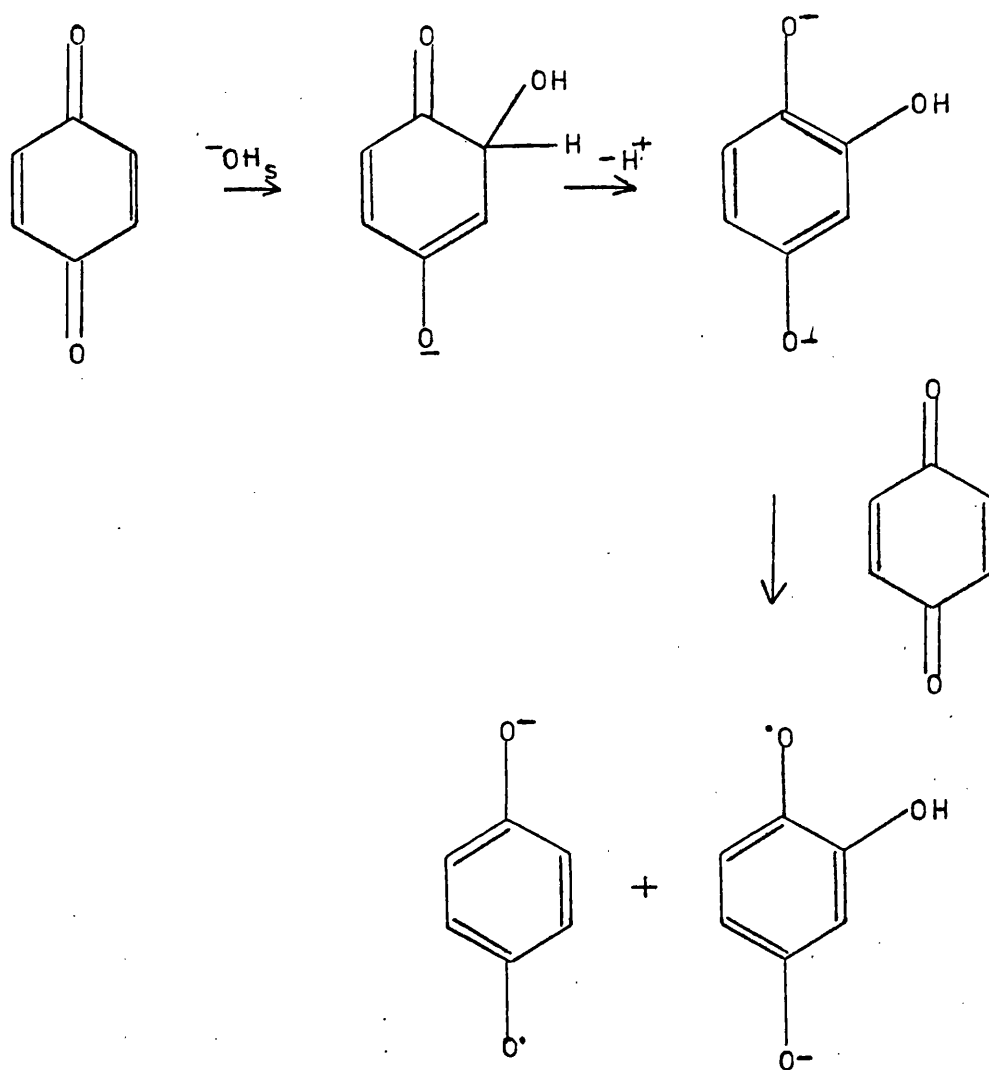
in titanium dioxide. Titanium dioxide doped with Mn^{3+} ³³, Mo^{5+} ²⁷, and Cr^{3+} ³⁴ has also been studied by electron spin resonance.

The electron transfer from metal oxides to adsorbed electron acceptors and from adsorbed electron donors to metal oxides has been the subject of a number of studies. It was hoped to determine the electron transfer properties of pigmentary titanium dioxide by its reaction with selected donor and acceptor molecules. The donating or accepting of an electron by an adsorbed molecule to a metal oxide would lead to the formation of radical cations or anions which could be detected by electron spin resonance and ultra-violet reflectance spectroscopy.

The electron donor properties of activated alumina have been studied using powerful electron acceptors to trap electrons from the alumina surface. The formation of the p benzoquinone free radical anion and tetrachloro p benzoquinone anion radical adsorbed on alumina ³⁵ was detected by an unresolved electron spin resonance absorption at $g = 2$ and assignments were made on the basis of ultra-violet spectral data. No hyperfine interactions are expected for the chloranil anion radical whereas the p benzoquinone anion radical in solution gives a five line spectrum due to hyperfine splittings from four equivalent hydrogen nuclei. Tetracyanoethylene, another powerful electron acceptor, was used to investigate the electron donor properties of catalytic alumina by Flockhart et al ³⁶. The tetracyanoethylene anion radical identified by its nine line spectrum was formed when tetracyanoethylene was adsorbed onto alumina from the vapour phase and from benzene or hexane solution, the characteristic colour of the anion being formed on the oxide.

The anion radicals of trinitrobenzene and other nitrobenzenes³⁷ were also formed on catalytic alumina, the electron spin resonance spectra showing hyperfine coupling from only one nitrogen nucleus which suggested that the adsorbed anion-alumina surface behaved as an ion pair, the unpaired electron being centred on one of the nitro groups. The nitrobenzene anion radical was also observed on zinc oxide³⁸. Electron transfer to tetracyanoethylene was used to determine the variation of the electron donor properties of alumina and silica-alumina with activation temperature by quantitative measurements of the adsorbed tetracyanoethylene anion radical^{39,40}. Trinitrobenzene was also used to determine the radical forming activity of alumina with activation temperature.⁴¹ The electron transfer to nitrobenzene adsorbed from benzene solution onto alumina was reported to be photo-assisted^{40,42}, irradiation of the alumina-nitrobenzene systems with ultra-violet light giving an increased electron spin resonance absorption from the nitrobenzene anion.

Two mechanisms were considered for the formation of the semiquinone radical on alumina³⁵ which were, either a charge transfer mechanism where a lewis base site transfers one electron to the orbital of the electron acceptor, or the reaction of a surface hydroxide ion at the quinone 2 position followed by loss of a proton producing the hydroxyhydroquinone dianion which could react with a quinone molecule to form hydroxy-p-benzosemiquinone and p-benzosemiquinone along the lines of a scheme suggested by Eigen⁴³.



The Al-OH^- surface group on alumina was suggested³⁹ as an electron donor site on alumina dehydrated below 500°C - 600°C and surface Al^+ ions and Al-O^- groups as the electron donor sites present on aluminas activated above 500°C - 600°C . Flockhart⁴⁰ also proposed a surface hydroxyl ion as the electron donor site for alumina activated below 350°C . For alumina activated above 500°C the oxide ion defect was proposed as the electron donor site. This site consists of two surface O^{2-} ions occupying adjoining surface sites which can act as an electron donor site.

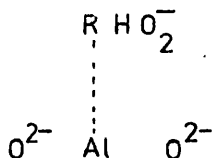
The interdependence of radical anion and radical cation formation on the surface of alumina and silica-alumina was demonstrated by Flockhart^{41,42}. Reduction of trinitrobenzene still occurred with surfaces saturated with electron donors such as anthracene and perylene, in fact an enhancement of the anion radical concentration was observed on perylene treatment alumina surfaces and likewise an enhancement of the perylene radical cation concentration was observed on adsorption of trinitrobenzene on alumina although oxygen was found to be necessary for radical cation formation. The mutual dependence of radical cation and anion formation suggested the possibility of the existence of a range of sites on alumina of varying donor and acceptor strengths which can mutually interact.

The electron acceptor properties of silica-alumina and alumina have been studied by electron donation from suitable donor molecules and the radical cations formed detected by the same methods as radical anions. The formation of the perylene radical cation identified by its hyperfine interactions was reported over activated silica-alumina⁴⁴. The participation of oxygen in the electron transfer process was not clear at first. The presence of a small quantity of oxygen was needed for the electron transfer from perylene to occur, proposed mechanisms being electron transfer to oxygen from a perylene-surface proton complex and electron transfer from a perylene-lewis acid (electron acceptor) site complex⁴⁴. Radical cations of perylene, diphenylamine, aniline and naphthalene were also detected on silica-aluminas^{46,47}.

Rooney⁴⁸ detected the radical cations of perylene, naphthalene and anthracene although benzene, toluene, oxylene, and hexamethylbenzene were found not to give radical species on silica-alumina. The electron acceptor sites were found to be destroyed by adsorption of water or

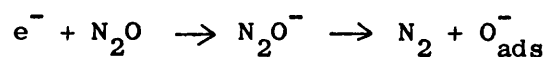
ethanol on the catalyst. The gas phase adsorption of diphenylamine, benzidine and dimethyl p phenyldiamine on alumina-silica gels⁴⁹ also produced radical cations detected by electron spin resonance. Gas phase adsorption of naphthalene, anthracene, perylene, and tetracene on the catalyst gave electron spin resonance absorptions from the radical cations and two bands in the electronic spectra were attributed to the radical cations and the presence of carbonium ions formed by addition of H^+ to the hydrocarbons.

Electron transfer from perylene and anthracene to alumina was observed⁵⁰ but electron transfer from naphthalene did not occur. The variation of electron accepting ability of alumina and silica-alumina with activation temperature was determined using perylene as the electron donor. Oxygen^{50,51} was found to be necessary for the electron transfer to alumina since if oxygen was carefully excluded no perylene cations were observed. Addition of a small quantity of oxygen resulted in the formation of radical cations but increasing the oxygen pressure above 1.5mm of mercury resulted in collision broadening of the electron spin resonance spectrum. Oxygen was also found to be involved in the electron transfer to silica-alumina⁵². An exposed aluminium ion produced on dehydration of the alumina, in the presence of oxygen was proposed as the electron acceptor site. RH is the electron donor molecule, oxygen being converted to an $O_2^{\cdot-}$ radical.



There has been much less research on the electron transfer properties of titanium dioxide than on alumina and silica alumina where interest was stimulated by their use as catalysts. A study⁵³ was reported of anion radicals formed by vapour adsorption of the electron acceptors tetrachloro, tetrabromo, tetraiodo, and tetrafluoro-p-benzoquinones, trinitrobenzene and tetracyanoethylene on zinc oxide, magnesium oxide, and titanium dioxide (crystal type and preparation not specified) all activated by evacuation at 500°C for 2-3 hours. An electron spin resonance absorption at $g = 2.004$ was observed for the p-benzoquinone anion radical on zinc oxide, magnesium oxide and titanium dioxide with a corresponding electronic spectrum absorption band at 440 nm on titanium dioxide attributed to the radical anion. The electron transfer to p-benzoquinone from rutile powder is also reported by Zafif' yants.⁵⁴ Sulphur dioxide adsorbed on partly reduced titanium dioxide and zinc oxide produces an electron spin resonance spectrum attributed to SO_2^- radicals⁵⁵.

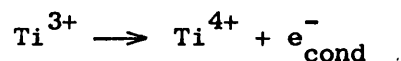
Cunningham⁵⁶ observed the decomposition of nitrous oxide to nitrogen over activated titanium dioxide. He proposed the following electron transfer mechanism for the decomposition.



The decomposition is photo-assisted over zinc oxide but not over titanium dioxide. Cunningham makes a distinction between the direction donation of an electron from a Ti^{3+} ion,



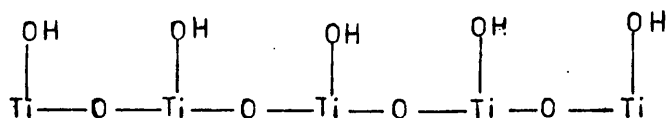
and the indirect donation possibility of



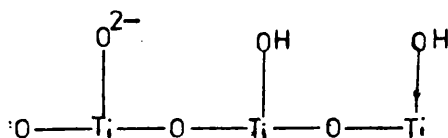
where the Ti^{3+} ion first donates an electron to the conduction band which then acts as the electron donor.

Che et al⁵⁷ studied the electron donor abilities of magnesium oxide and titanium dioxide (anatase, high surface area, laboratory produced) with varying activation treatments by the use of tetracyanoethylene and trinitrobenzene as electron acceptors. A nine line spectrum from the tetracyanoethylene anion radical was observed on titanium dioxide activated by evacuation or heating in oxygen below 300°C . Above 300°C the spectrum produced was unresolved. The adsorption of trinitrobenzene on titanium dioxide and magnesium oxide treated below 300°C resulted in a spectrum composed of three main lines each with hyperfine components of five lines which was attributed to a major anisotropic interaction with one nitrogen nucleus and a lesser anisotropic interaction with two nitrogen nuclei. Activation of titanium dioxide above 300°C resulted in only the three main hyperfine lines being observed for the trinitrobenzene anion radical. The electron donor ability of titanium dioxide measured by the tetracyanoethylene anion radical concentration formed was found to be small after activation of titanium dioxide at 200°C , reaching one maximum at an activation temperature of 250°C and a second maximum at 500°C - 600°C . The electron donor sites were proposed to be surface hydroxyl ions, and O^{2-} ions in weak co-ordination for samples activated at high temperatures since all surface hydroxyl groups would have been removed.

The hydrated titanium dioxide surface can be simply represented as ⁵⁷



Upon activation at elevated temperatures dehydration between two adjacent hydroxyl groups leads to a water molecule being released and an O^{2-} ion being formed.



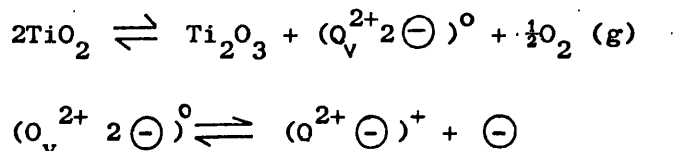
Ti^{3+} ions formed by activation of titanium dioxide by high temperature evacuation ⁵⁸ were proposed as addition donor sites.



where A is an acceptor molecule.

The adsorption of the electron acceptor 7,7,8,8-tetracyanoquinodimethane (TCNQ) from acetonitrile solution was used to study the electron donor abilities of a number of oxides ⁵⁹ including titanium dioxide (anatase, laboratory prepared). The concentration of the TCNQ anion radicals being measured from its unresolved electron spin resonance spectrum and the metal oxides were activated at 100°C under vacuum. Titanium dioxide was found to be a much less powerful electron donor than magnesium oxide, alumina or zinc oxide. The electronic spectra of TCNQ adsorbed on the oxides showed two bands, 400 nm and below assigned to physically

adsorbed TCNQ and around 600 nm assigned to the dimer of the TCNQ anion radical. The electron donor properties of titanium dioxide were partly attributed to its n type semiconductor properties written formally as



where O_v is an oxide ion vacancy and \ominus is a free electron.

This scheme is equivalent to the proposal of Ti^{3+} ions as electron donors since loss of oxygen from titanium dioxide results in the formation of Ti^{3+} ions. The surface hydroxyl ion was also considered as a potential electron donor site. The electron donor abilities of mixed oxides including silica-titania and alumina-titania were determined by the same method⁶⁰. This showed that mixed oxides can have less electron donor ability than either of the two pure oxides. The influence of the solvent used for TCNQ upon the adsorption was also studied⁶¹.

Radical ions from naphthalene derivatives were formed on oxides including titanium dioxide⁶²; the radicals formed were not positively identified as cations or anions. The anthracene radical cation was observed on rutile²⁸ by an unresolved electron spin resonance absorption. An electronic spectral study of the electron donation to titanium dioxide from tetramethyl-p-phenylenediamine, diphenylamine, N-methylphenylamine, N-ethylphenylamine, and ferrocene adsorbed from the vapour⁶³ phase was made. Absorption bands from radical cations were only seen on admission of air to the samples. The radical species formed from diphenylamine on titanium dioxide in the presence of oxygen which showed three sets of hyperfine interactions in its electron spin

resonance spectrum was attributed to the $\text{Ph}_2\text{N}^\bullet$ radical.⁶⁴ The proposed mechanism of formation was H^\bullet abstraction from diphenylamine by an O_2^\bullet radical ion known to be formed on partly reduced titanium dioxide by reaction with oxygen.



All studies of electron transfer properties of oxides have involved activation of the oxides either by evacuation at high temperatures or heating in oxygen at high temperatures. In studying the electron transfer properties of titanium dioxide pigments the intention was to determine the electron transfer properties with as little disturbance from their condition as used commercially in paint manufacture as possible. To facilitate this a search was made for possible electron acceptors and donors suitable for reaction with the pigments.

2.2 Electron Spin Resonance of Titanium Dioxide Pigments.

2.2(a) Experimental.

All electron spin resonance measurements were made on a Varian Associates X band E3 Spectrometer. Samples of the pigments were packed and sealed in bora-silica glass tubes of 4 mm OD to a height sufficient to fill the spectrometer cavity. Measurements were made at room temperature and at liquid nitrogen temperature 77K. g values were determined using diphenyldipicrylhydrazyl as an external standard having a g value of 2.0036 and by using the approximation⁶⁵,

$$g_x = 2.0036 \pm \frac{2.0036 \times \Delta H}{H}$$

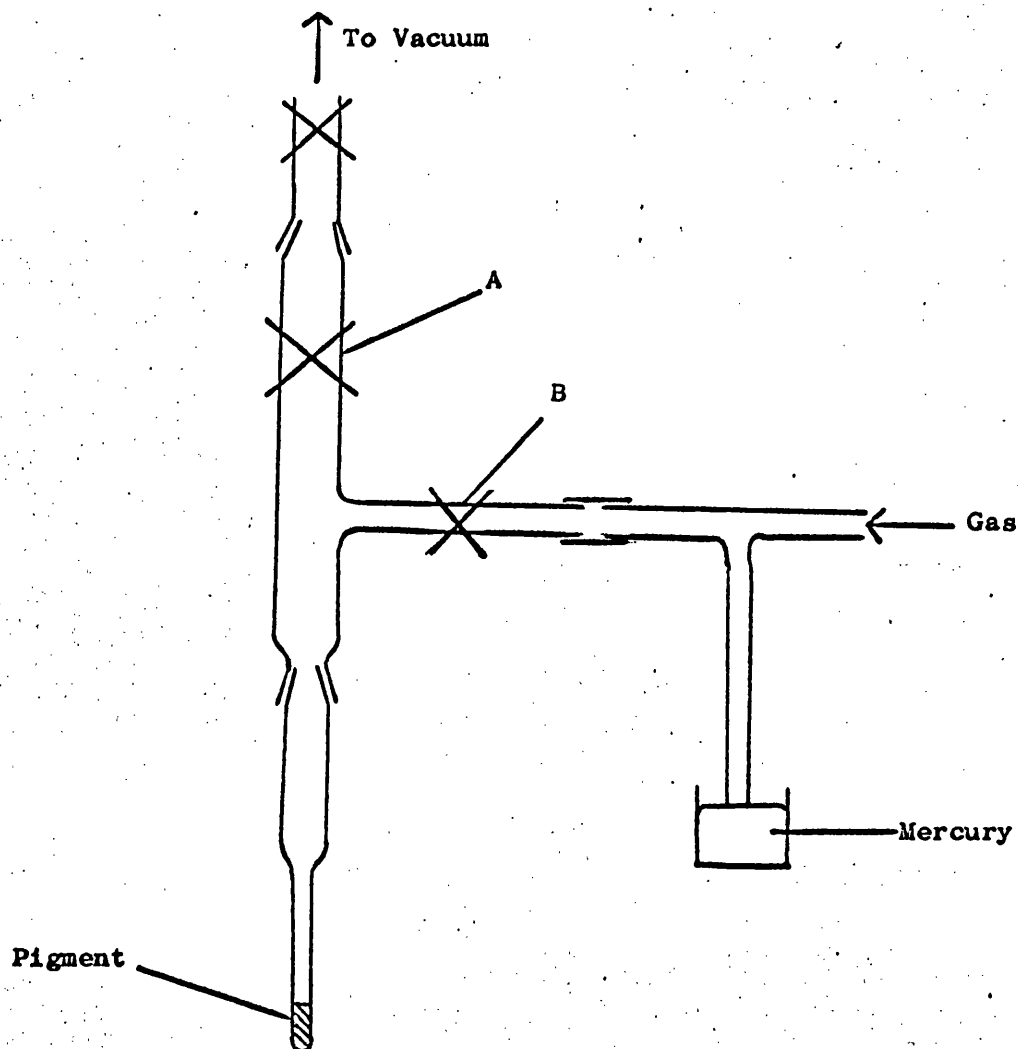
Where ΔH is the difference in magnetic field strength between g_x and $g = 2.0036$ and H is the value of the field strength at $g = 2.0036$.

The approximation is only valid for g values near $g = 2$.

Evacuation of the tubes containing the pigments when required was performed on a high vacuum line fitted with a mercury diffusion pump and McLeod gauge. The tubes were attached to wider pyrex tubing and fitted to the vacuum line by a ground glass joint. After evacuation the tubes were sealed off by collapsing the bora-silica tubing at a point above the sample.

When an atmosphere of a gas was required above a pigment sample the apparatus in Fig 3 was used.

Fig. 3.



The system was evacuated, i.e. tap A open and tap B closed and this part of the system could be removed for electron spin resonance measurements. Gases could be released into the system by opening tap B.

The grades of gases used were, nitrogen - oxygen free grade 99.9% minimum, oxygen - commercial grade 99.5% minimum, helium - Grade A 99.8% minimum.

2.2(b) Results.

At room temperature none of the pigments showed any electron spin resonance absorption except for pigment I which showed the weak absorption shown in fig. 4. At 77K this spectrum became more intense and more features were observed (fig. 5). Pigments F, G and H showed no absorption at 77K but G and H did show some base line drift.

The electron spin resonance spectra at 77K for pigments A, D and E were identical and is shown in fig. 6. The spectra for pigments B and C at 77K were similar to pigments A, D and E but were of weaker intensity.

Fig. 4. E.S.R. Spectrum of Pigment I at Room Temperature.

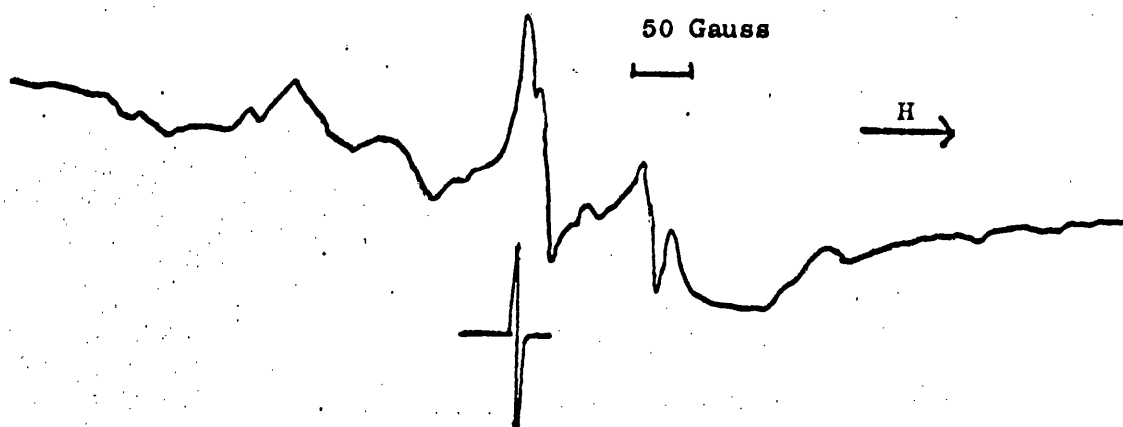


Fig. 5. E.S.R. Spectrum of Pigment I at 77K.

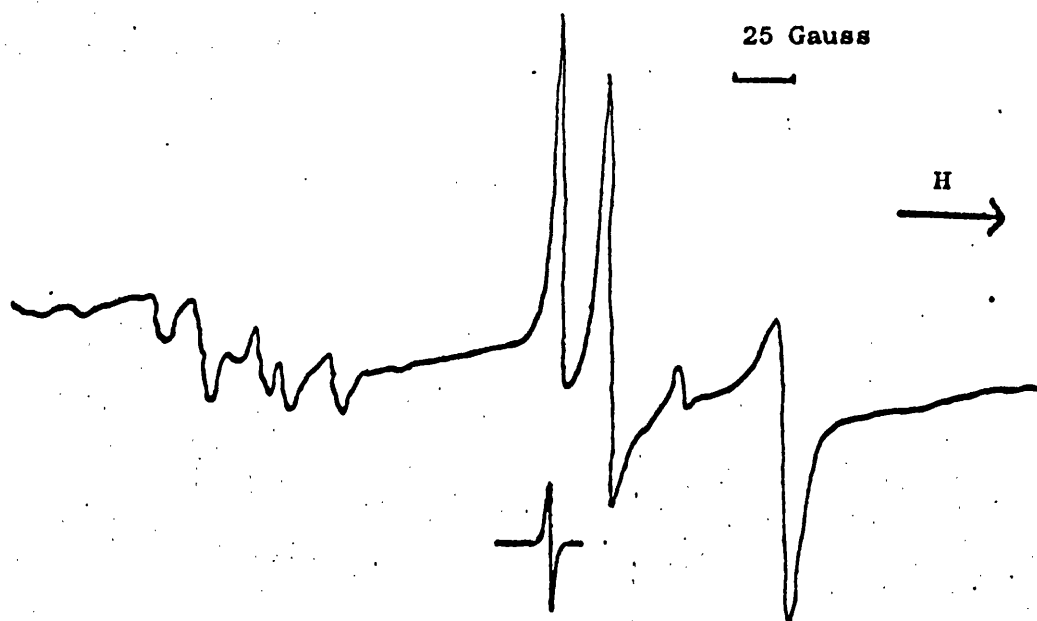
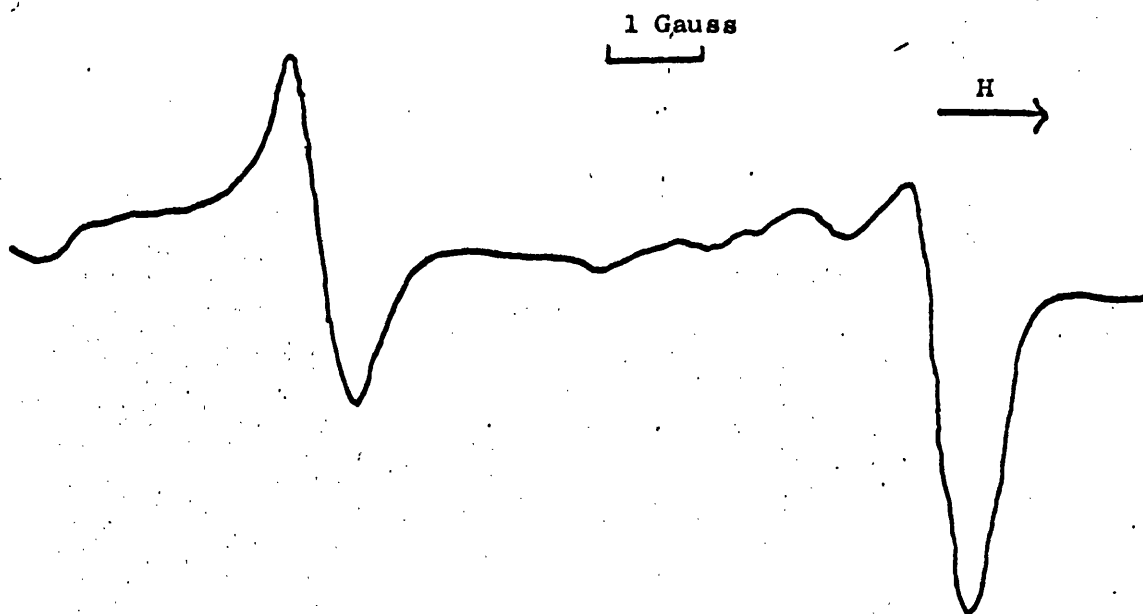


Fig. 6. E.S.R. Spectrum of Pigments A, D and E at 77K.



The electron spin resonance spectrum from sample I was found to be unaffected by evacuation of the sample for one hour at 200°C.

It was observed that evacuation of a sample of pigment E at approximately 10^{-5} torr pressure for one hour at room temperature completely removed the electron spin resonance absorptions at $g = 1.9428$ and $g = 1.906$ observed at 77K. Upon releasing air into the evacuated tube, by cutting the top of the tube, the two absorptions returned immediately. Samples of pigments A, B and D were also evacuated for 1 hour at room temperature. For these pigments the absorptions did not disappear completely but upon releasing air into the tubes the intensity of the signals increased. Samples of A, B and D were evacuated at 100°C and approximately 10^{-5} torr pressure for one hour. Under these conditions the absorptions were completely removed from B and D and returned on exposing the sample to air. Sample A still showed the absorptions but they were of low intensity and upon exposing the sample to air the spectrum intensity greatly increased.

Attempts were made using sample E and the apparatus described in section (a) to observe which gas was responsible for the reformation of the electron spin resonance absorptions. Sample E was evacuated for one hour at room temperature and its electron spin resonance spectrum measured at 77K to ensure that the absorptions had been removed. Gases were then released into the system via tap B. However it was found that the absorptions returned on exposure of the pigment to nitrogen, oxygen, and helium.

The intensities of the absorptions from 0.15g of pigment E compared to a Mn^{2+} standard in zinc sulphide before and after irradiation of the sample with ultra-violet light from a 2kw Xenon lamp showed no change.

2.2(c) Discussion.

The base line drift observed in the e.s.r. spectra of pigments at 77K is probably due to the presence of transition metal impurities in low concentrations having more than one unpaired electron which would give broad absorptions²⁹. This is supported by there being no base line drift in the room temperature spectra when the transition metal ions would not show any absorption due to spin lattice relaxation. The e.s.r. absorptions shown by pigment I at 77K are unsymmetrical showing the anisotropic character of a powder spectrum. These absorptions are likely to be due to bulk impurities since they are not removed by evacuation of the pigment at 200°C. The absorptions at 77K shown by pigments A, B, C, D and E also show asymmetry due to powder spectra. The absorptions arise on pigments containing zinc oxide in the lattice. The pigments F, G and H, which contain very little zinc oxide (less than 0.0007%) do not show these absorptions. Pigments B and C which give low intensity spectra contain an intermediate quantity of zinc oxide (0.01 and 0.08%). The removal of the absorptions by evacuation suggests that the radical is loosely held on the surface and the dependence upon zinc oxide presence may indicate that the radical is associated with zinc ions in the surface of the pigment. The reappearance of the radical or radicals upon letting air into the system suggests that the radical is reformed on the adsorption of a component of air but attempts to identify the gas were unsuccessful due to being unable to deliver gases of sufficient purity above the pigment sample. The e.s.r. absorptions are of quite low intensity, and are recorded towards the limit of sensitivity of the spectrometer and therefore only a very low

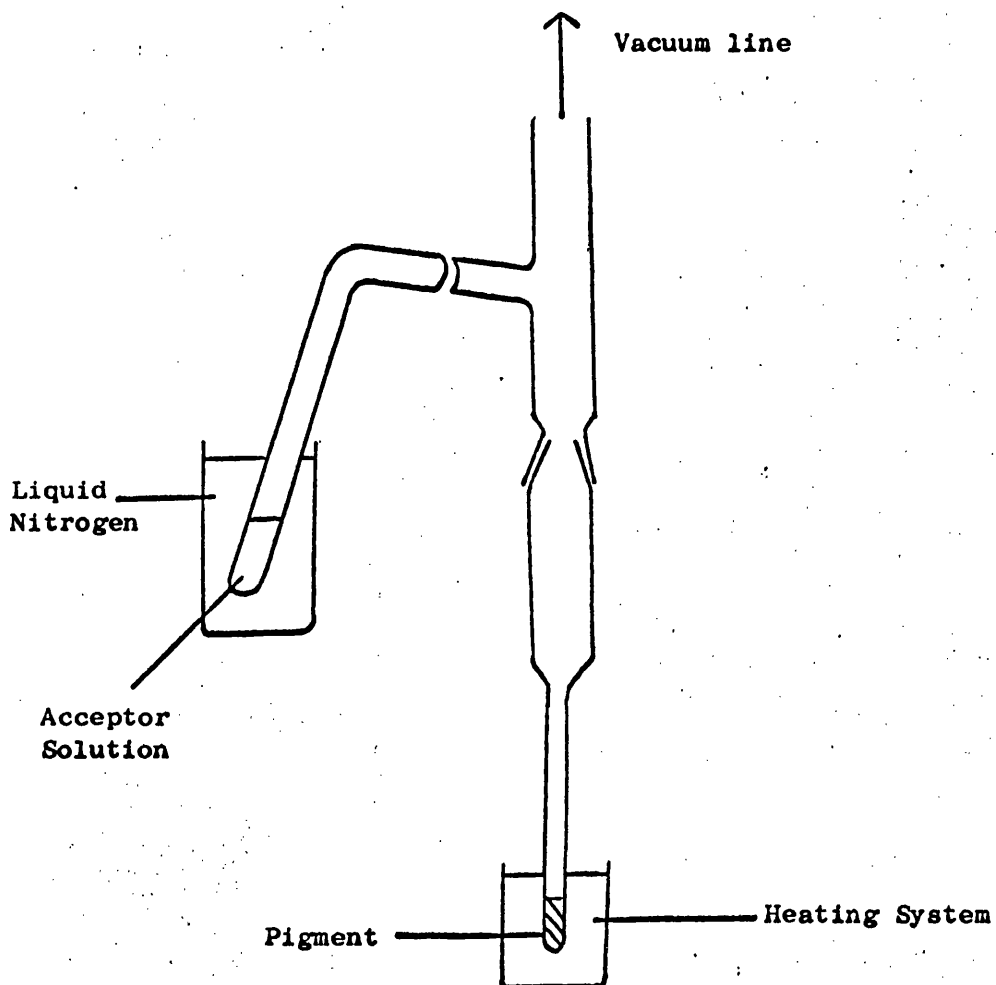
concentration of the gas would be required to reform the radicals.

2.3 Electron Transfer Properties of Titanium Dioxide.

2.3(a) Experimental.

The apparatus in fig. 7 was used for the adsorption of electron acceptors from solution onto titanium dioxide under vacuum.

Fig. 7.



The solution of the electron acceptor could be degassed by freeze thaw cycles and then maintained at 77K while the pigment sample was heated under vacuum for the required length of time. The titanium dioxide was allowed to cool to room temperature and the electron acceptor solution (usually in sodium dried benzene) was poured over onto the pigment by rotating the side arm. The sample tube was then sealed off by collapsing the tubing above the level of the solution in the tube. The sample tube was shaken to ensure complete mixing of the pigment and solution and the e.s.r. spectrum was recorded at room temperature.

Adsorption of electron acceptors in the presence of air was performed by injecting the electron acceptor solution into an e.s.r. tube containing the pigment sample, the spectrum being recorded at room temperature after the sample was shaken.

Adsorption of electron donors under vacuum was performed by the same method as for the electron acceptors, or the electron donors were adsorbed onto the pigment by evaporation of the solvent using a rotary evaporator and the pigment samples were then heated under vacuum and the sample tube sealed off.

Water treated pigments were prepared by storing pigment samples in a saturated water vapour atmosphere in a desiccator for 48 hours prior to their use.

The salt $K^+ DDQ^-$ was prepared by a method analogous to the preparation of $Li^+ TCNQ^-$ ⁶⁶. 0.2g of DDQ was dissolved in dry acetonitrile and added to a boiling acetonitrile solution of 0.44g of potassium iodide. Dark red crystals appeared on cooling and were filtered off and dried under vacuum.

2.3(b) Results.

A strong asymmetric, partially resolved spectrum at $g = 2.0024$ was obtained when TCNE (0.02M in benzene) was adsorbed on sample I activated at 200°C for one hour under vacuum. The pigment developed a blue colouration. The adsorption was repeated using activation temperatures of 100°C, 50°C, and room temperature and gave very similar spectra to that obtained on the sample activated at 200°C, (fig. 8). The samples were irradiated with ultra-violet light in the spectrometer cavity but no increases in the absorption intensities were observed. The adsorption of benzene alone on pigment I evacuated at 200°C did not produce any changes in the background e.s.r. spectrum of I.

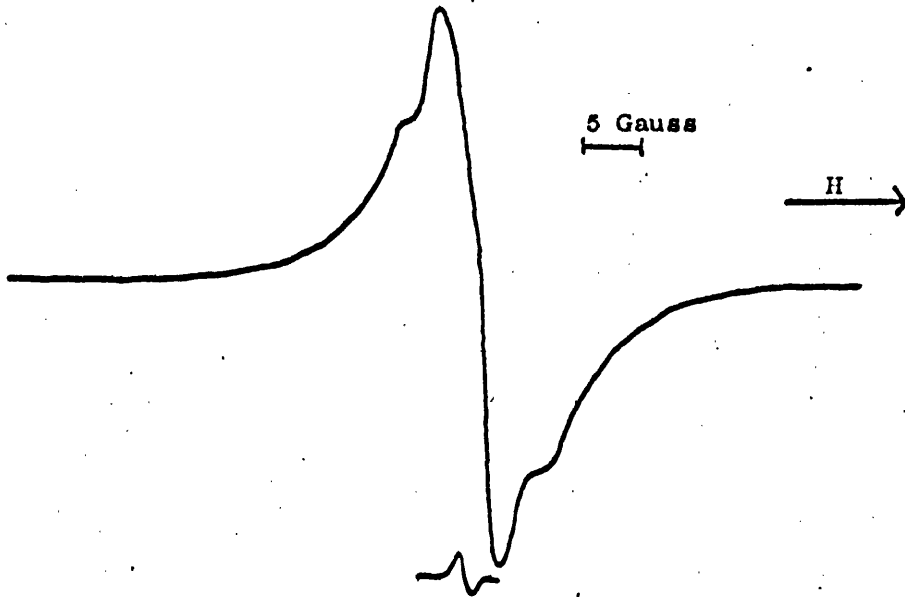
Trinitrobenzene (0.02M in benzene) was adsorbed on pigments A and I activated at 200°C. The spectrum (fig. 9) was of low intensity.

Tetrachloro p benzoquinone (2×10^{-2} molar in benzene) adsorbed on pigment I activated at 200°C for one hour gave a species having an unresolved spectrum centred on $g = 2.0037$ with a width of approximately 30 gauss. Evacuation for one hour at room temperature of pigment I with subsequent adsorption of tetrachloro p benzoquinone gave no e.s.r. absorption. Irradiation of both systems did not change the e.s.r. spectra. Adsorption of 9,10-anthraquinone from benzene solution on pigment I activated at 200°C for one hour under vacuum did not lead to any detectable radicals being formed.

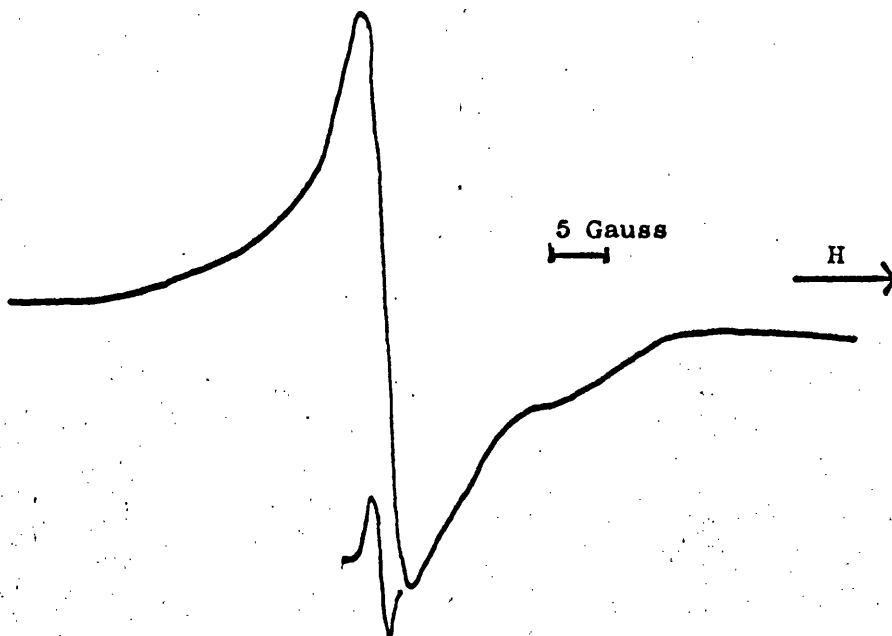
In order to find an electron acceptor that would accept electrons from titanium dioxide pigments without any prior treatment the following acceptors were adsorbed from benzene solutions onto pigment samples without any evacuation treatment; - tetrachloro p benzoquinone, tetrachloro o benzoquinone, tetracyanoethylene (TCNE),

Fig. 8. E.S.R. of TCNE on Pigment I.

(a) 200°C Activation.



(b) 50°C Activation.



(c) Room Temperature Activation.

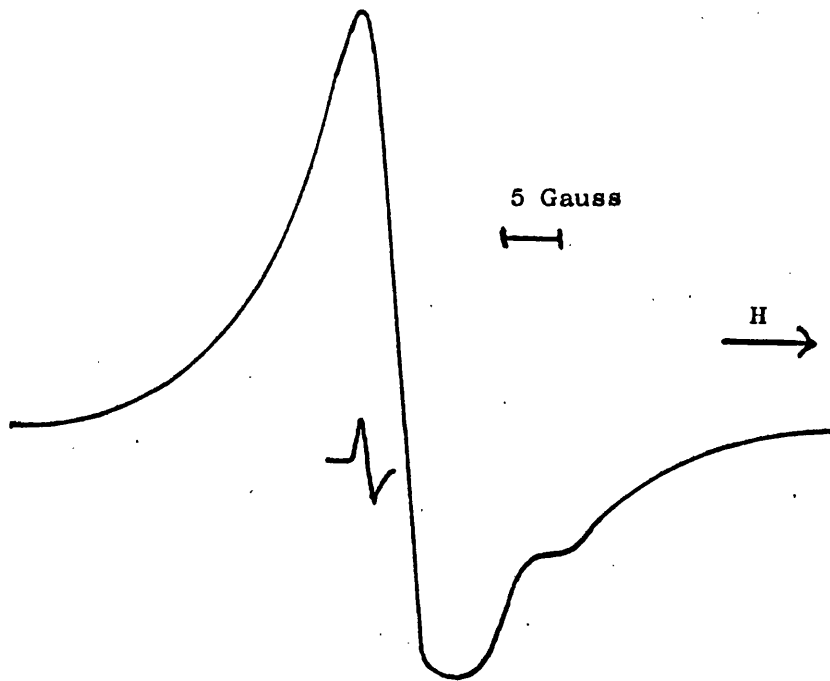
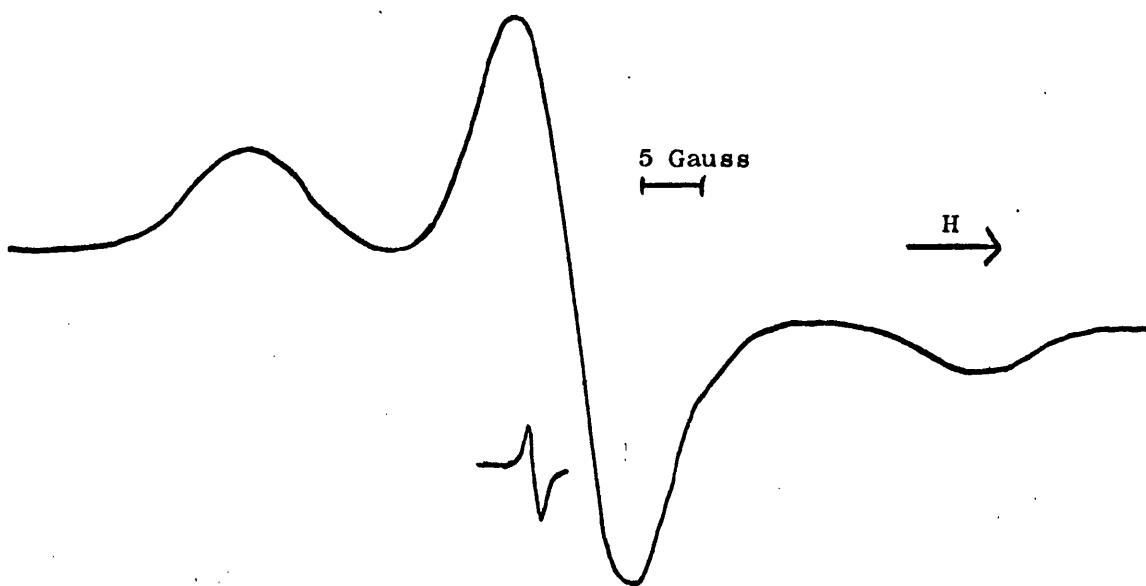


Fig. 9. E.S.R. Spectrum of Trinitrobenzene Adsorbed on Pigment I.

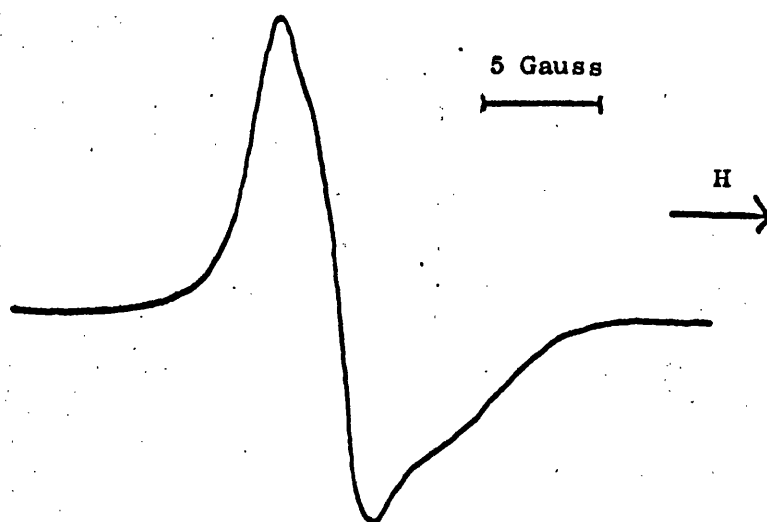


trinitrobenzene, tetracyanoquinodimethane (TCNQ), and dichlorodicyano p benzoquinone (DDQ).

Tetrachloro p benzoquinone, tetrachloro o benzoquinone, TCNQ, and TCNE gave low intensity unresolved e.s.r. spectra with all pigments except pigment I. Adsorption of trinitrobenzene did not give a detectable spectrum. Evacuation of pigment I for one hour on a vacuum line or drying in an evacuated desiccator for two hours followed by adsorption of TCNQ resulted in an observable e.s.r. spectrum.

The adsorption of DDQ resulted in the formation of an intense asymmetric unresolved e.s.r. spectrum centred at $g = 2.0046$ (fig. 10) and the pigments becoming dark green coloured. The spectrum is approximately 25 gauss in width. Untreated sample I gave an absorption upon adsorption of DDQ. The e.s.r. absorption intensities were not increased by ultra-violet irradiation and adsorption of DDQ in total darkness still resulted in an e.s.r. absorption.

Fig. 10. E.S.R. Spectrum of DDQ on Pigment A.



Adsorption on Water-treated Pigments.

Water-treated pigments were found by weight measurements to contain 5 - 10% of water. Adsorption of p and o tetrachlorobenzoquinone from benzene solution onto water-treated pigments in air still gave low intensity unresolved e.s.r. spectra. TCNE was adsorbed onto water-treated pigments A, E, G and I. On pigment E a strong well resolved nine line spectrum was observed (fig. 11) overall width of approximately 17 gauss and hyperfine coupling of 1.5 gauss.

Pigments A and G gave partially resolved spectra (figs. 12 and 13) which decayed to unresolved absorptions. Water-treated pigment I gave no e.s.r. spectrum upon adsorption of TCNE.

Adsorption on pigments A, E, G, and I or 0.044M benzene solution of DDQ resulted in the immediate formation of strong narrow unresolved e.s.r. absorptions which gradually resolved into a hyperfine structure of five lines after approximately 30 minutes. The hyperfine coupling was 0.5 gauss (figs. 14 a,b,c).

The e.s.r. spectrum of an acetonitrile solution of K^+DDQ^- at room temperature gave a strong symmetrical unresolved spectrum of 11 gauss width. The spectrum of a degassed acetonitrile solution of K^+DDQ^- is shown in fig. 15 a and b. Five lines with a hyperfine coupling of 0.6 gauss were observed. Side bands with a hyperfine coupling of 0.5 gauss were observed at higher instrument gain.

Electron Donors.

Adsorption of anthracene and perylene in benzene solutions on pigment I heated for 1 hour at 200°C under vacuum did not result in the formation of any radical species. Adsorption of 2% w/w anthracene on

Fig. 11. E.S.R. Spectrum of TCNE on Water-Treated Pigment E.

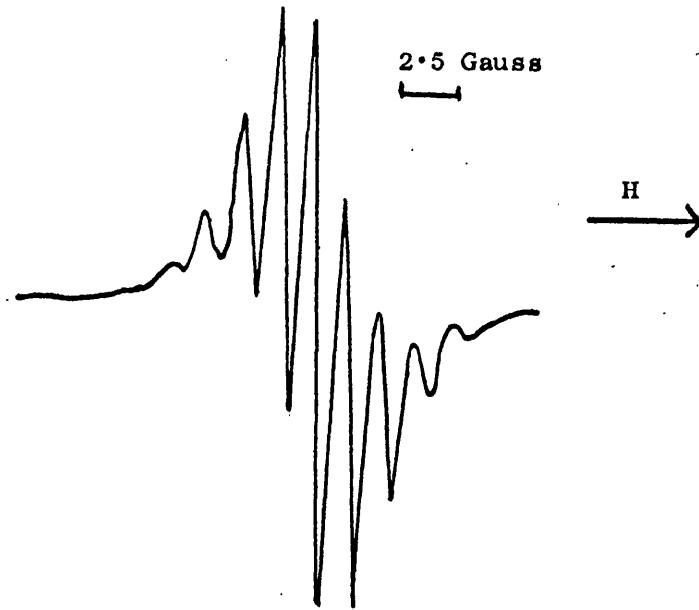


Fig. 12. E.S.R. Spectrum of TCNE on Water-Treated Pigment A.

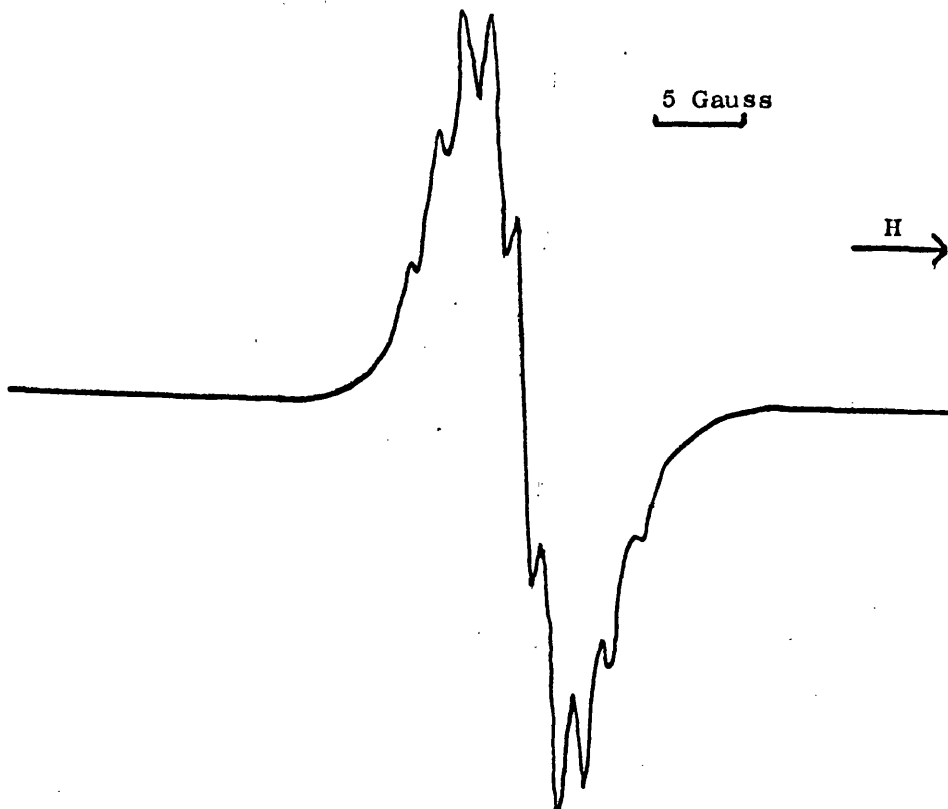


Fig. 13. E.S.R. Spectrum of TCNE on Water-Treated Pigment G.

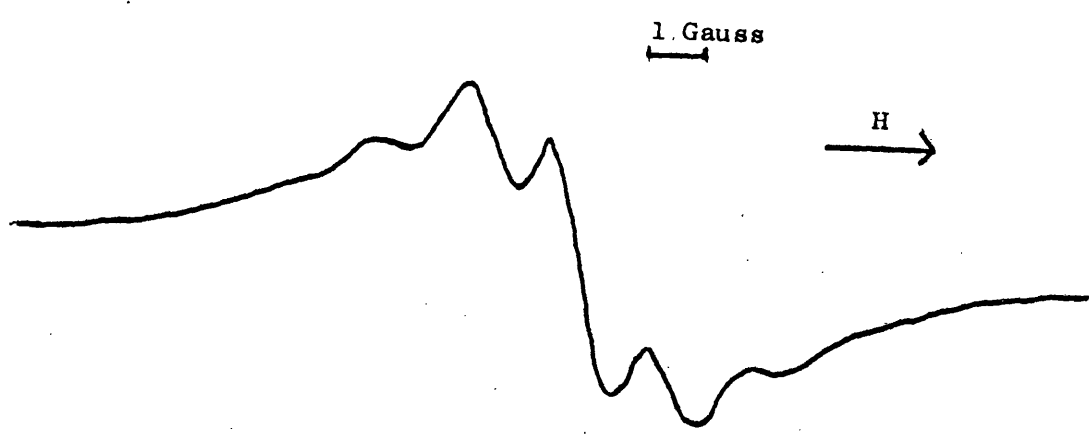


Fig. 14(a). E.S.R. Spectrum of DDQ on Water-Treated Pigment A.

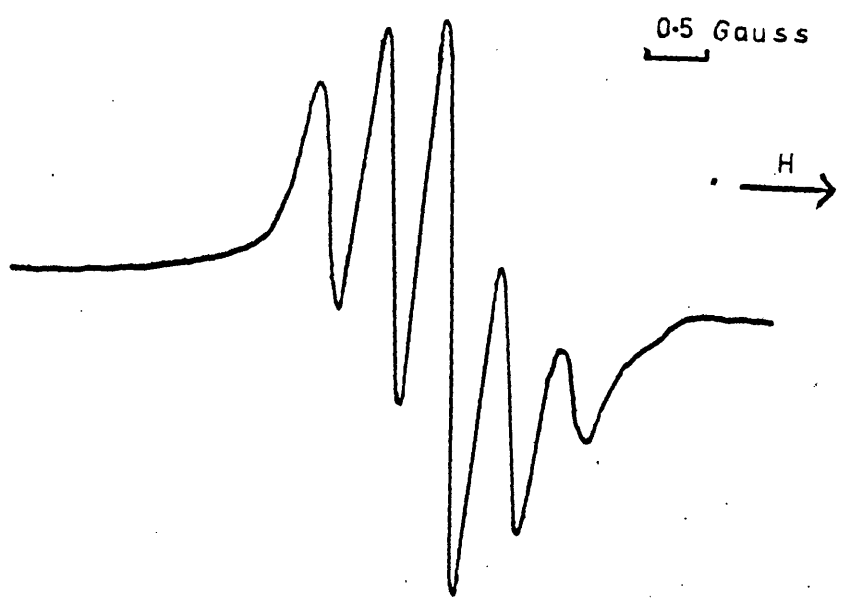


Fig. 14(b). E.S.R. Spectrum of DDQ on Water-Treated Pigment G.

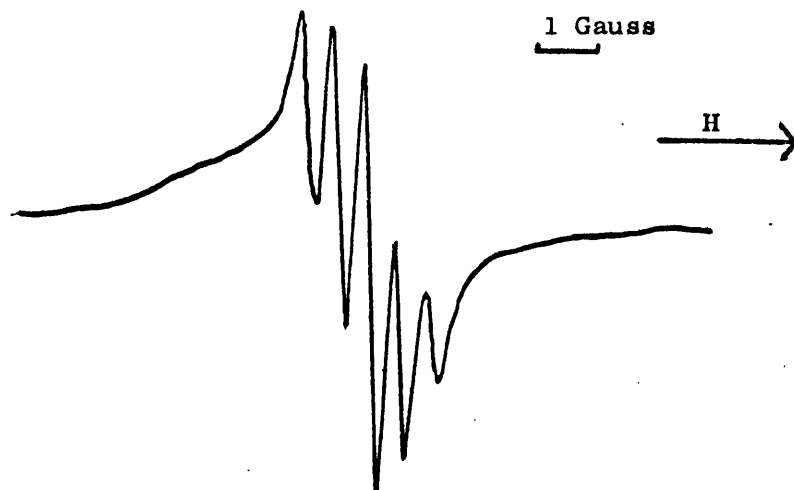


Fig. 14(c). E.S.R. Spectrum of DDQ on Water-Treated Pigment I.

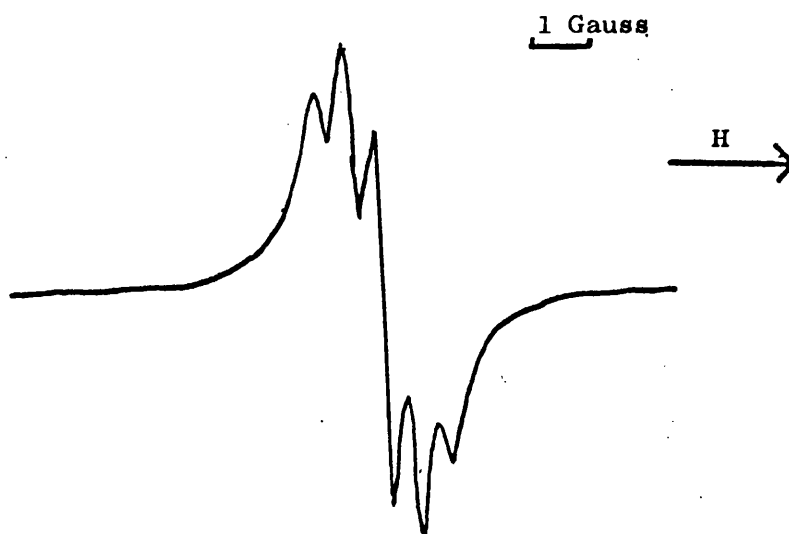
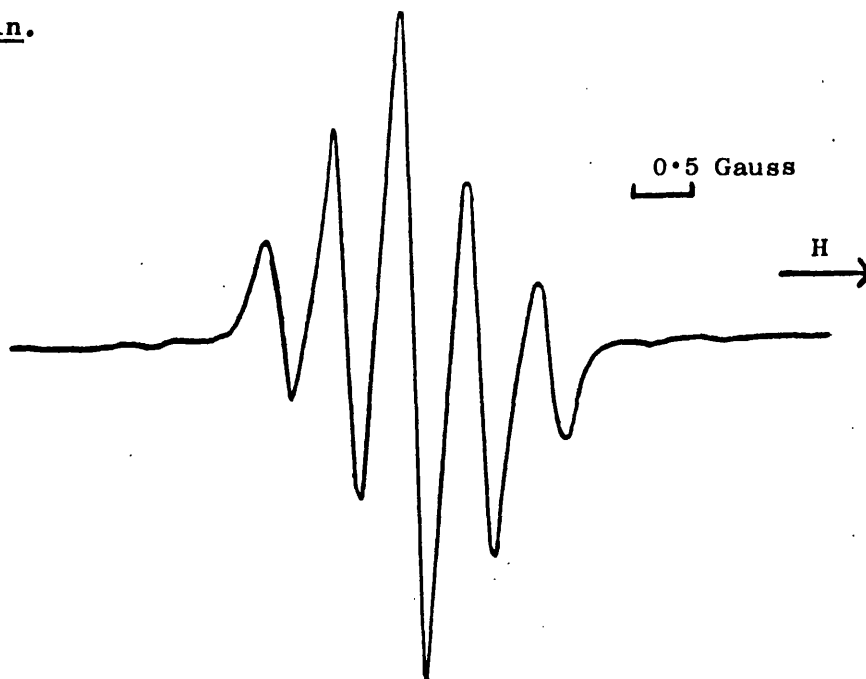
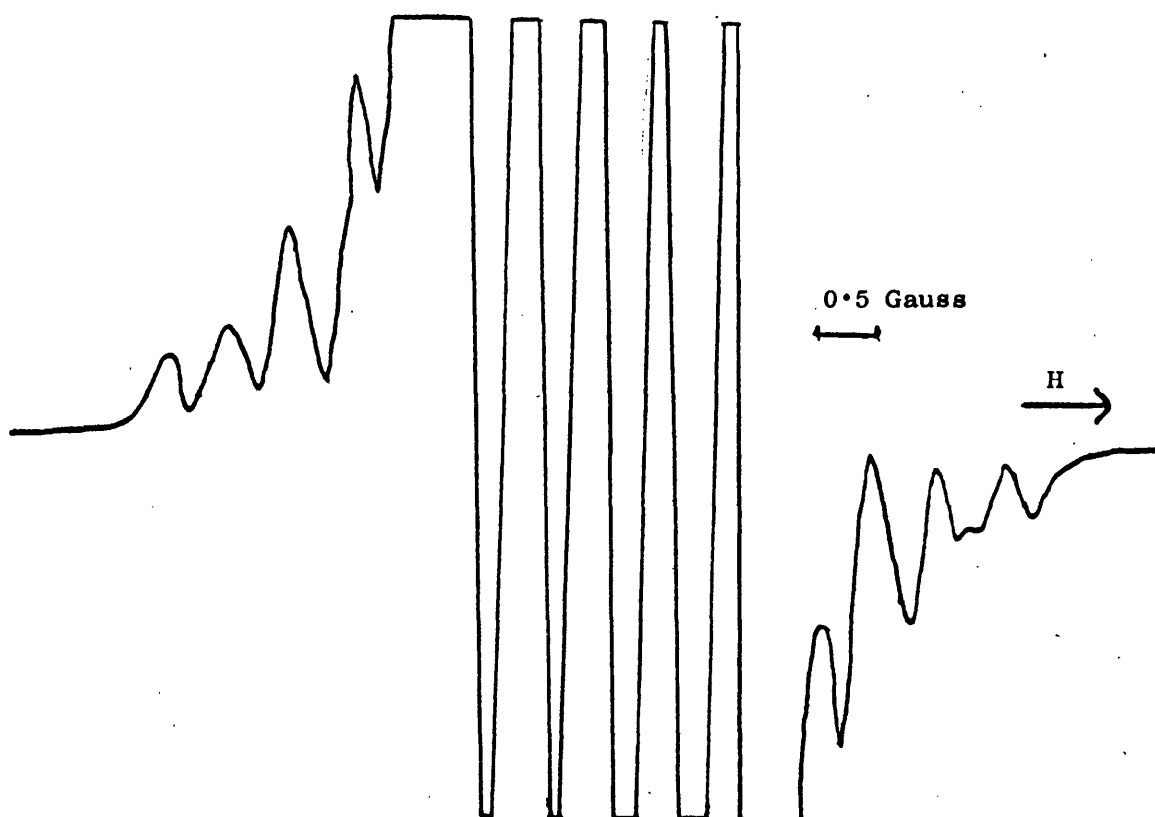


Fig. 15. E.S.R. Spectrum of K^+DDQ^- in Acetonitrile Solution.

(a) Low Gain.



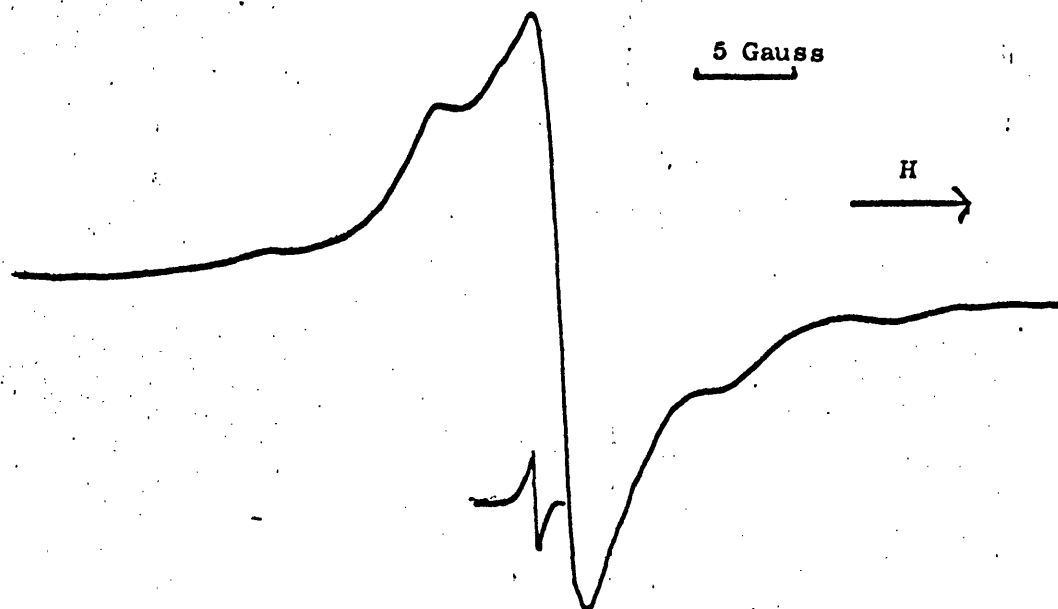
(b) High Gain.



I by evaporation of an n butanol anthracene solution onto the pigment and evacuation of the sample at 200°C for one hour resulted in the formation of an asymmetric unresolved e.s.r. absorption at $g = 2.0014$ with a width of approximately 43 gauss. No absorption was obtained when the sample was evacuated at 100°C .

Adsorption of 8% w/w perylene onto pigment I by evaporation of a benzene solution and evacuation of the sample at 200°C for one hour produced an asymmetrical e.s.r. absorption at $g = 1.9996$ with a width of approximately 40 gauss. Adsorption of diphenylamine on I, also by benzene solution evaporation, followed by activation at 200°C resulted in a broad partially resolved spectrum at $g = 2.0028$ being about 65 gauss in width, shown in fig. 16.

Fig. 16. E.S.R. Spectrum of Diphenylamine on Pigment I.



Absorption of 8% carbazole, aniline, tri p tolylamine and 1,4-diaza-bicyclo 2,2,2 octane D.A.B.C.O. onto pigment I by solution evaporation and activation at 200°C failed to produce any radical species.

2.3(c) Discussion.

Pigmentary titanium dioxide samples would be expected to be less active as electron acceptors and donors than laboratory prepared samples due to their generally having a lower surface area of around $10\text{m}^2/\text{g}$ instead of as much as $200\text{m}^2/\text{g}$. The e.s.r. spectra of radicals adsorbed on the dry untreated pigments are much broader than the solution spectra of the radicals and there is a lack of hyperfine coupling which arises from the restriction in the acceptor or donor molecules motion by adsorption to the titanium dioxide surface. Direct identification of the radicals formed on dry pigments is not possible due to the absence of hyperfine coupling, although it is most likely that the electron acceptors form the corresponding anion radicals, this being supported by the observation of hyperfine splittings for radicals observed on alumina⁴⁰ and for TCNE on anatase⁵⁷.

The g values of the radicals are all close to the free spin value of 2.0023 as expected for organic radicals. The formation of the radicals is a thermal process since the radical concentrations are not increased by the action of ultra-violet light and electron transfer occurs in the total absence of light.

The electron donation from titanium dioxide to electron acceptors will be dependent upon the "electron affinity" of the acceptor and upon the "ionization potential" of the donor site. It may be more useful to consider reduction potential values of the acceptors since

this is a solution reaction whereas the electron affinity refers to the gas phase addition of an electron. Table 2 lists the electron affinities and reduction potentials of the acceptors. The reduction potentials refer to the reaction



The sign convention adopted is the reduction potentials take the sign of the energy of the above reaction so that strong electron acceptors have negative values of $E^{\frac{1}{2}}(\text{red})$.

The g value of the trinitrobenzene radical on titanium dioxide corresponds closely to that reported by Che⁵⁷. Trinitrobenzene has a lower electron affinity (Table 2) and electron transfer to trinitrobenzene only occurred on activated titanium dioxide. The three part spectrum was similar to that reported by Che⁵⁷ which was attributed to hyperfine interaction from only one nitrogen nucleus. DDQ is the most powerful electron acceptor used and is the only acceptor found suitable for a comparative study of the electron donor properties of untreated pigments.

The radicals formed on water-treated pigments are directly identifiable by their hyperfine splitting pattern. The radical formed from adsorption of TCNE on water treated pigments is the TCNE anion radical showing hyperfine coupling of 1.5 gauss with nine lines due to the coupling from four equivalent nitrogen nuclei. The radical anion in solution shows a hyperfine splitting of 1.56 gauss^{71a}. The spectra are remarkably isotropic, but, the radical is only present on the titanium dioxide and is not observable in the solution above the

Table 2.

	E_A	(ev)	$E_{red}^{\frac{1}{2}}$ (ev) SCE
DDQ	1.91 ⁶⁷		-0.51 ⁶⁹ acetonitrile
TCNE	1.53 ⁶⁷	2.38 ⁶⁸	-0.24 ⁷⁰ acetonitrile
TCNQ	1.7 ⁶⁷	2.46 ⁶⁸	-0.19 ⁷⁰ acetonitrile
o chloranil	1.5(5) ⁶⁷	1.95 ⁶⁸	
p chloranil	1.37 ⁶⁷	2.05 ⁶⁸	-0.01 ⁶⁹ acetonitrile
TNB	0.7 ⁶⁷		+0.31 ⁷⁰ aq ph 7.4
9,10-Anthraquinone		1.07 ⁶⁸	+0.94 ⁶⁹ acetonitrile
		1.03 ⁶⁹	

pigment. The isotropy of the spectra indicates that the radical must be quite loosely bound to the surface. Adsorption of TCNE on water-treated alumina⁴⁰ did not result in electron transfer to the TCNE. TCNE anion radicals formed by electron transfer from hydroxide ions in solution have been reported^{71b}.

The radical formed from adsorption of DDQ on water-treated pigments can be identified as the DDQ anion radical from its hyperfine splitting pattern and by comparison with the spectrum of K^+DDQ^- . The side bands observed in the spectrum of K^+DDQ^- are most likely due to C^{13} $I = \frac{1}{2}$ CN hyperfine interactions⁷². Hyperfine interactions from chlorine nuclei in semiquinone molecules have not been observed⁷³ which may be due to the chlorine quadrupole moment causing relaxation of the chlorine nuclear spin states which averages the hyperfine splittings to zero. The five intense lines are due to hyperfine coupling from the two equivalent nitrogen nuclei, $I = 1$. The lines are overlapping slightly and cover the central C^{13} lines.

It is possible that on the water-treated pigments electron transfer may occur between physically adsorbed water and the electron acceptors. The observation of narrow resolved spectra on water-treated samples occurs only with DDQ and TCNE which are the two most powerful acceptors used. On dry samples OH groups may act as donors.

The electron transfer from a donor molecule would depend upon the "ionization potential" of the donor and the electron affinity of the acceptor site. Again it may be more useful to consider the oxidation potential of the donor molecule, Table 3. The need for the presence of oxygen for the electron donation to titanium dioxide to occur is implicated since no radicals are formed when the donors are

Table 3.

	EA (ev)	$E_{red}^{1/2}$ SCE	IP	$E_{ox}^{1/2}$ SCE
Benzene	-1.5 ⁶⁷		9.24 ⁶⁷	2.30 ⁷⁵ acetonitrile
Naphthalene	-0.3 ⁶⁷	2.48 ⁷⁴ ethanol	8.26, 8.12 ⁶⁷	1.54 ⁷⁵ acetonitrile
Anthracene	0.42 ⁶⁷	1.96 ⁷⁴ ethanol	7.3-7.66 ⁶⁷	1.34 ⁷⁶ methylene chloride
Perylene	0.85 ⁶⁷	1.75 ⁷⁴ ethanol	7.15, 7.07 ⁶⁷	0.85 ⁷⁵ acetonitrile
Aniline			8.23 ⁷⁷	0.864 ⁷⁸ water pH 1
Diphenylamine			7.4 ⁷⁹	1.008 versus NHE ⁸⁰
Tri p tolylamine			7.4 ⁸³	= 0.728 versus SCE
D.A.B.C.O.			7.52 ⁸⁴	0.75 ⁸² acetonitrile
Carbazole		2.77 75% Dioxan		

adsorbed onto activated pigment from degassed benzene solution.

The radicals observed when anthracene and perylene were adsorbed on activated pigments are most likely due to the radical cations but they cannot be directly identified due to the lack of hyperfine coupling. No electron donor reacted with untreated pigments. It appears that donor molecules with ionization potentials of less than approximately 7.4 eV are capable of donating electrons to titanium dioxide. The radical formed from diphenylamine may well be due to $\text{Ph}_2\text{N}^\bullet$ as proposed by Che⁶⁴. The spectrum showed only a partly resolved triplet splitting which would be due to the nitrogen hyperfine interaction.

2.4 Quantitative Study of the Electron Donor Properties of Pigments.

2.4(a) Experimental.

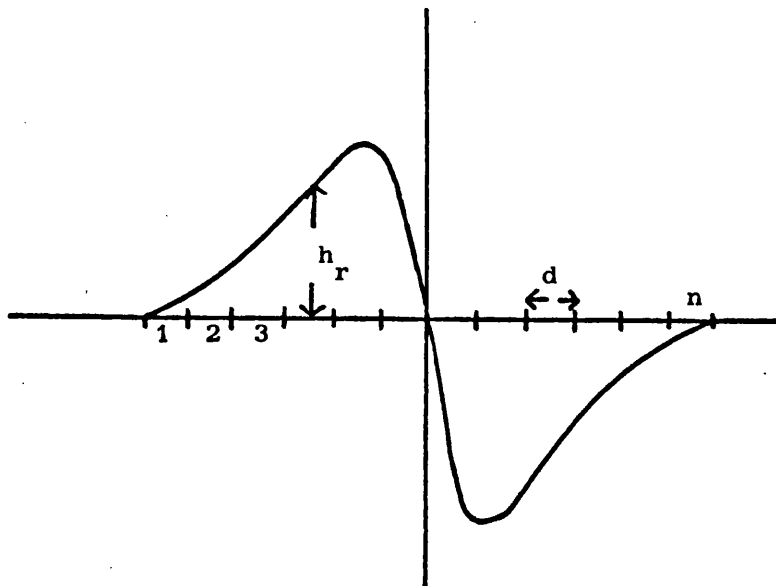
A quantitative study of the electron donor properties of untreated and water-treated pigments was made using DDQ as the electron acceptor. 0.1 g of pigment sample was packed into 4 mm O.D. tubes and 0.5 ml of a freshly prepared 0.044 M benzene solution of DDQ* was injected into the tubes and thoroughly mixed with the pigment by shaking. The e.s.r. spectrum at room temperature was recorded after 20 minutes and immediately afterwards the e.s.r. spectrum of 0.2 ml of a standard solution of DPPH in benzene sealed in an identical bora-silica tube was recorded at the same spectrometer settings. The number of radicals formed on the pigments was calculated by a comparison of the areas under the absorption curves of the DDQ spectra and of the DPPH spectra knowing the number of spins present in the DPPH solutions.

* A freshly prepared solution was used since DDQ is known to decay at the rate of 30% every 24 hours in benzene solution⁸⁶.

The area under the absorption curves was determined from the first derivative curves by mathematical double integration using the approximation

$$A = \frac{1}{2} d^2 \sum_{r=1}^n (n-2r+1)h_r$$

where d is the width of a division, h_r is the height of the r th division and n is the total number of divisions⁸⁵.



2.4(b) Results.

The DPPH standards used contained the following number of DPPH radicals,

Standard	Weight DPPH(g)	Mols.	Number of Spins
1	6.8×10^{-4}	1.73×10^{-6}	1.04×10^{18}
2	2.32×10^{-4}	5.88×10^{-7}	3.55×10^{17}
3	1.55×10^{-4}	3.93×10^{-7}	2.37×10^{17}
4	1.16×10^{-4}	2.94×10^{-7}	1.77×10^{17}
5	5.8×10^{-5}	1.47×10^{-7}	8.87×10^{16}
6	2.9×10^{-5}	7.36×10^{-8}	4.43×10^{16}
7	1.45×10^{-5}	3.68×10^{-8}	2.22×10^{16}
8	7.25×10^{-6}	1.84×10^{-8}	1.11×10^{16}
9	4.83×10^{-6}	1.23×10^{-8}	7.38×10^{15}
10	3.62×10^{-6}	9.19×10^{-9}	5.53×10^{15}
11	1.81×10^{-6}	4.59×10^{-9}	2.76×10^{15}
12	1.2×10^{-6}	3.05×10^{-9}	1.89×10^{14}
13	4.5×10^{-7}	1.14×10^{-9}	6.87×10^{13}

The number of radicals formed was determined three times for most pigments. The results are illustrated in fig. 17. Fig. 18 shows the number of radicals per square metre of pigment surface.

The electron donor properties of two specially prepared alumina/titania surface coatings used in the surface treatment of pigment H were determined twice by comparison with pigment A. The determinations gave the following results for the relative number of radicals formed on these coatings.

Fig. 17. Electron Donor Properties of Pigments/g.

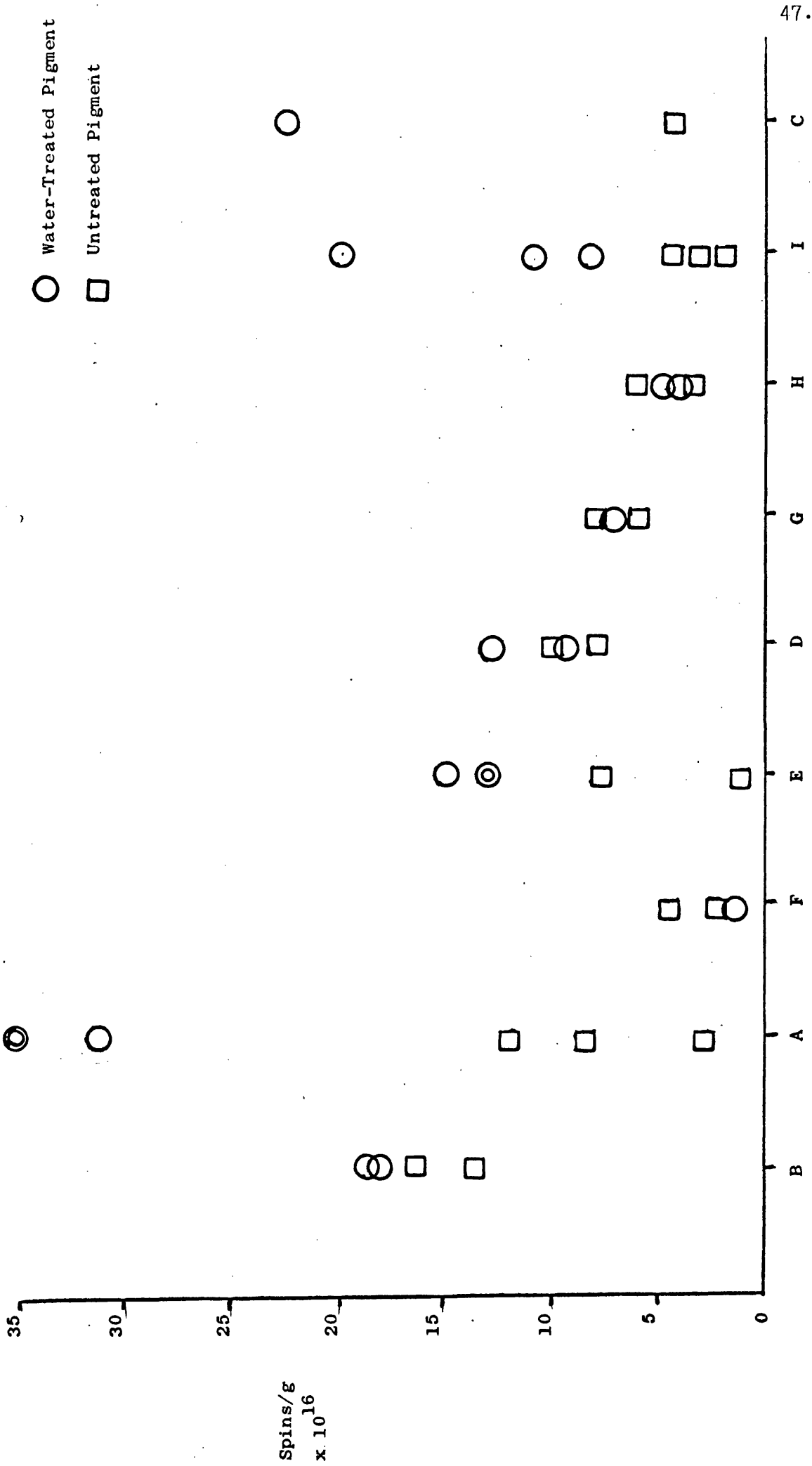
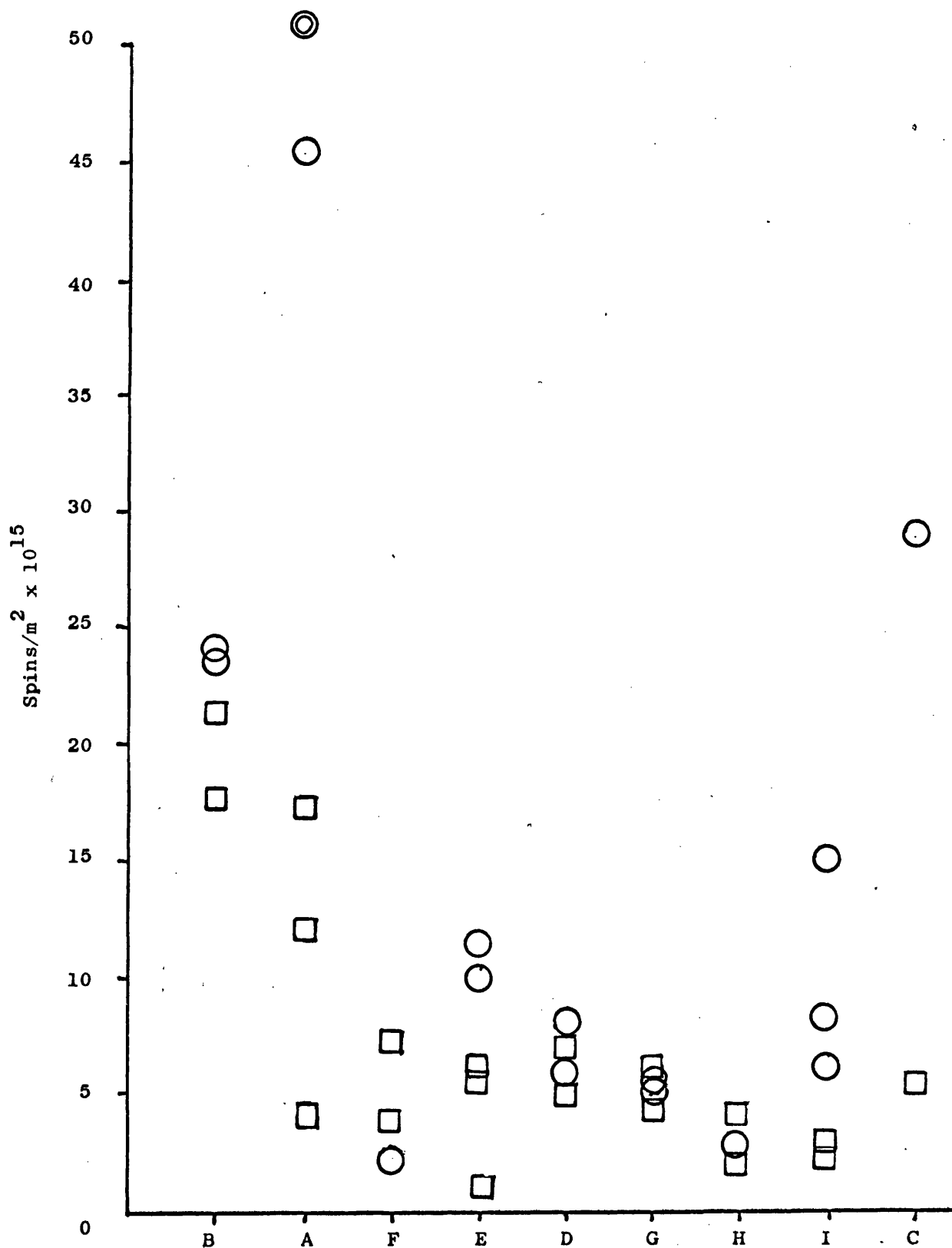


Fig. 18. Electron Donor Properties of Pigments/m².



	1st Determination	2nd Determination	Average
Pigment A	1	1	1
Coating A	17.4	22.9	20
Coating B	11.5	15.87	13.5

Upon adsorption of DDQ the pigments obtained various intensities of a green colouration.

A Bayer zinc oxide pigment studied as a comparison gave a similar DDQ radical spectrum with a dry sample to that observed on titanium dioxide pigments. The spin concentration was determined as 1.3×10^{18} spins/g. Water-treated zinc oxide became intensely red coloured upon adsorption of DDQ but gave no detectable spectrum.

2.4(c) Discussion.

The values of the spin densities of DDQ anion radicals formed on dry pigments range from about 15×10^{16} spin/g for pigment B to about 5×10^{16} spins/g for dry pigment H, a factor of approximately three. The zinc oxide pigment had a far greater electron donor ability. The errors in quantitative e.s.r. are large and this is reflected in the spread of results. A plot of DDQ radicals per square metre of surface reveals that the uncoated pigments A and B have a greater electron donor ability per unit area than the coated pigments. The uncoated pigments C and F gave a spin concentration comparable to the coated pigments. The water-treated samples of pigments A and C gave much increased radical concentrations than the dry pigments and this is especially noticeable since the spectrum intensity is much increased due to the narrowness of the spectrum. A and C are both uncoated

pigments containing zinc oxide in the lattice and the presence of zinc oxide may be effecting this behaviour since pigment B containing a lower concentration of zinc oxide does not show this large increase in radical concentration for a water-treated sample. It must be noted, however, that water-treated zinc oxide is itself inactive towards DDQ.

The alumina/titania treatments showed a larger donor ability per gram than any of the pigments and it is likely that when the treatment is applied to the surface of titanium dioxide as a thin layer its donor properties are considerably different.

The e.s.r. studies of electron acceptors on pigments only indicate radical species on the surface, they do not reveal diamagnetic species adsorbed on the surface. The adsorption of electron acceptors on pigments can be followed by ultra-violet absorption spectroscopy.

2.5 Adsorption and Ultra-Violet Reflectance Studies of Electron Acceptors on Titanium Dioxide.

2.5(a) Experimental.

6 mls of a 1.84×10^{-3} M benzene solution of DDQ were shaken with 0.4 g of pigment in a 3" x 1" glass sample tube and 6 mls of a 1.84×10^{-3} M benzene solution of TCNE was shaken with 0.2g of pigment. The suspension was centrifuged at intervals to firmly settle the pigment down and a small portion of the acceptor solution was removed, and returned after measurement of the optical density at 407 nm for DDQ and at 384 nm for TCNE. 10mls of a 0.313×10^{-3} M benzene solution of TCNQ (saturated solution) shaken with 0.2g of pigment was used for the adsorption of TCNQ the optical density being measured at 404nm. Optical density measurements were made on a Pye Unicam SP800 spectro-

photometer using quartz cells of path length 0.2cm for DDQ and TCNE solutions and 0.1cm for TCNQ solutions.

The concentrations of solutions and cell path lengths were chosen so as to enable direct measurement of the optical density of the solutions without any dilution being necessary since preliminary experiments using a 4.4×10^{-2} M DDQ solution showed only small random variations in the optical density after shaking with pigment due to inaccuracy of dilution compared with the small uptake of DDQ on the pigment.

Samples for ultra-violet reflectance spectral measurements of DDQ adsorption on the dry pigments were prepared by shaking 0.8g of pigment with 8 mls of a 4.4×10^{-2} M benzene solution of DDQ for three hours followed by separation by filtration and drying at room temperature in evacuated drying pistols. The samples were pressed into a circular recess in an aluminium plate and the ultra-violet reflectance spectra were recorded using magnesium oxide as a reference on a Beckman DK2A reflectance spectrophotometer.

2.5(b) Results.

Shaking the benzene solution of DDQ alone for the period that the adsorption was followed did not result in any appreciable change in the concentration of DDQ. From the optical density measurements the number of moles of electron acceptor adsorbed onto one gram of pigment could be calculated. The uptake of the electron acceptors on several pigments are plotted in figs. 19 and 20. The adsorption of electron acceptors on a Bayer zinc oxide pigment was determined as a comparison, and the zinc oxide was found to be a much stronger

Fig. 19. Adsorption of DDQ on Pigments.

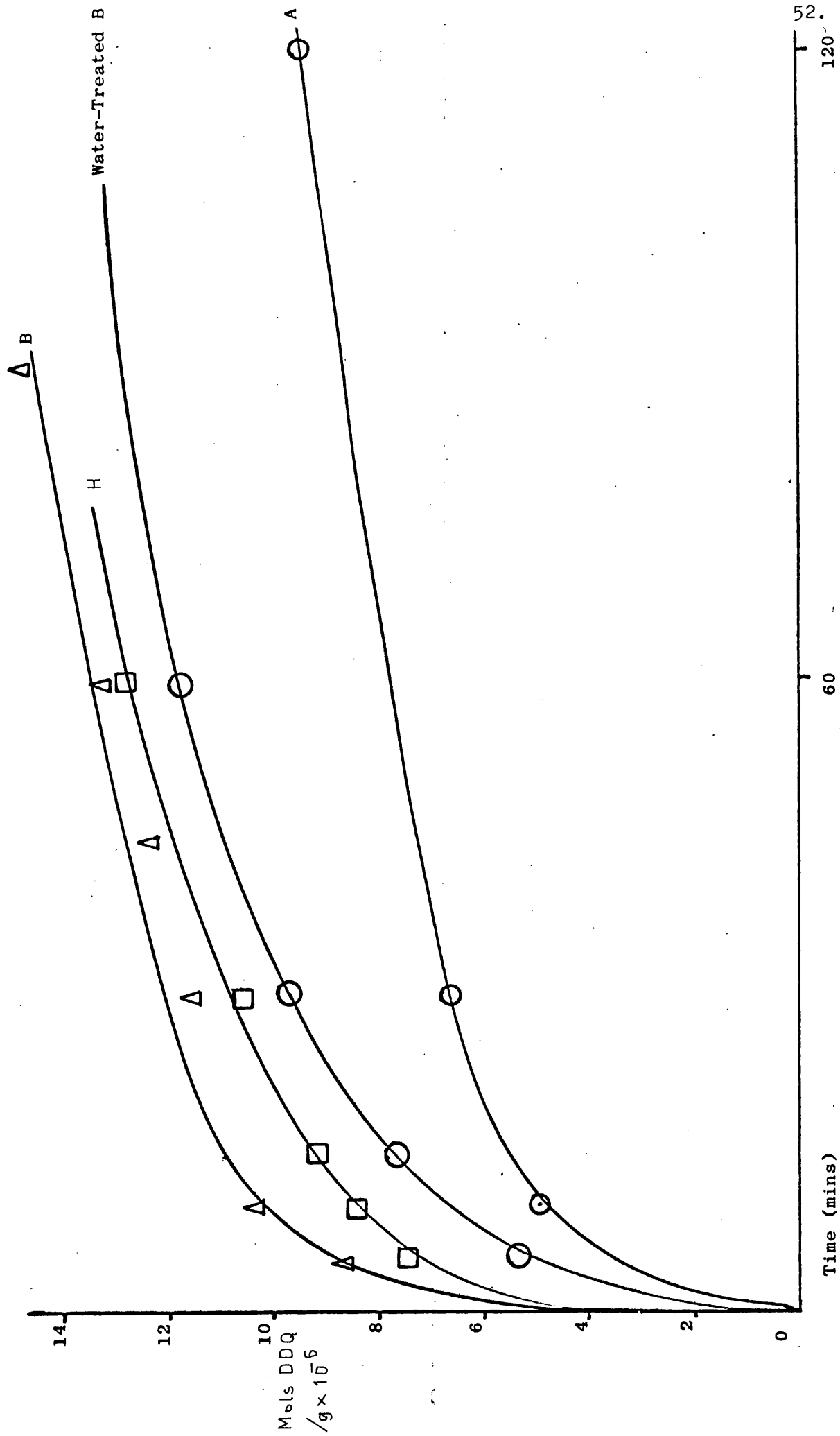
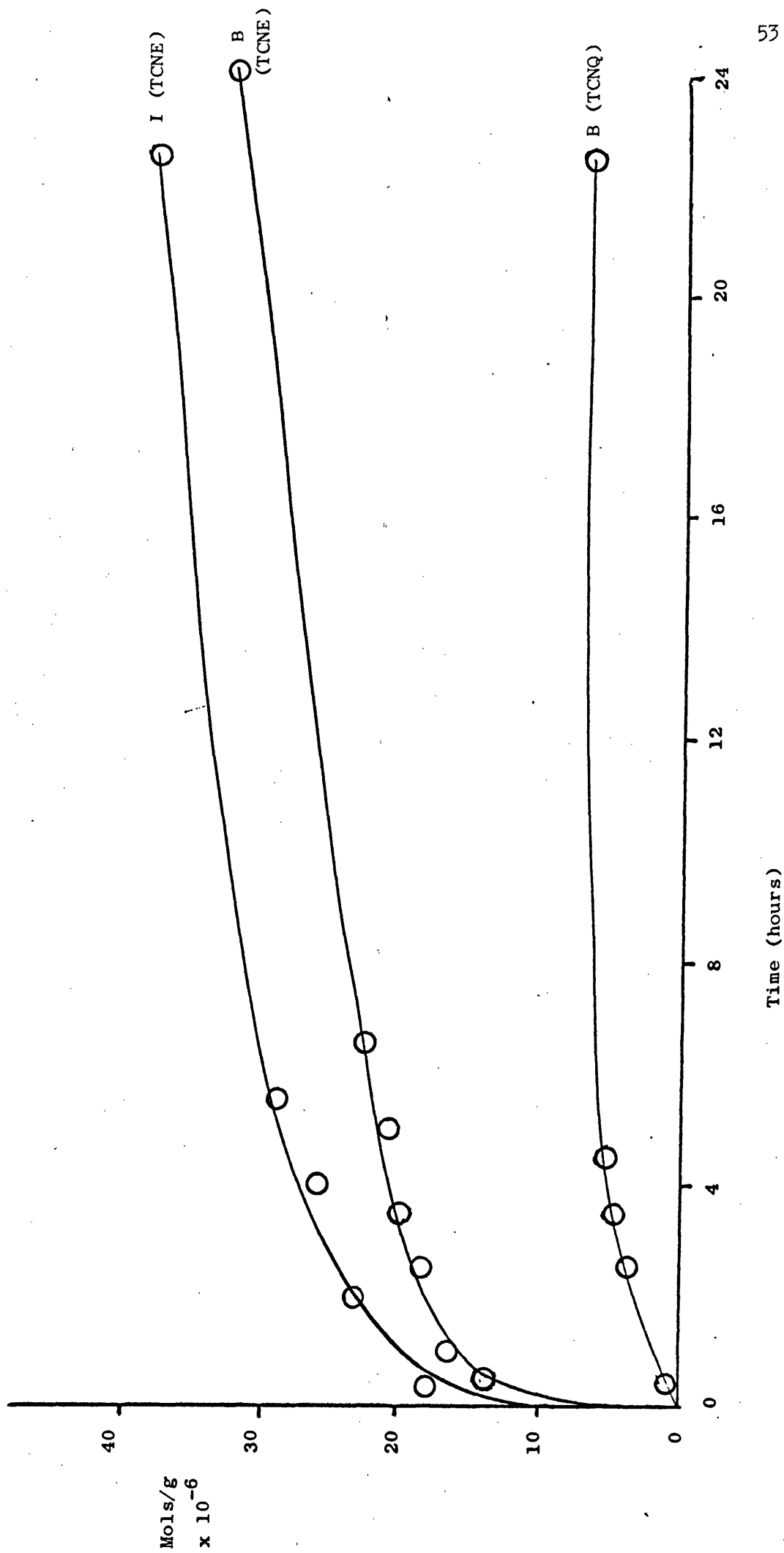


Fig. 20. Adsorption of TCNE and TCNQ on Pigments.



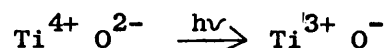
adsorber of electron acceptors than titanium dioxide.

The ultra-violet and visible reflectance spectra of adsorbed DDQ are shown in fig. 21. The visible absorption spectrum of K^+DDQ^- in acetonitrile solution is shown in fig. 22.

2.5(c) Discussion.

Zinc oxide adsorbed more DDQ than the titanium dioxide pigments. The adsorption will be influenced by the concentrations of the acceptor solutions although when using more concentrated solutions the amount of acceptor adsorbed was undetectable. It is obvious from the adsorption measurements that far more DDQ is adsorbed in a diamagnetic state than is adsorbed with electron transfer to form the radical anion.

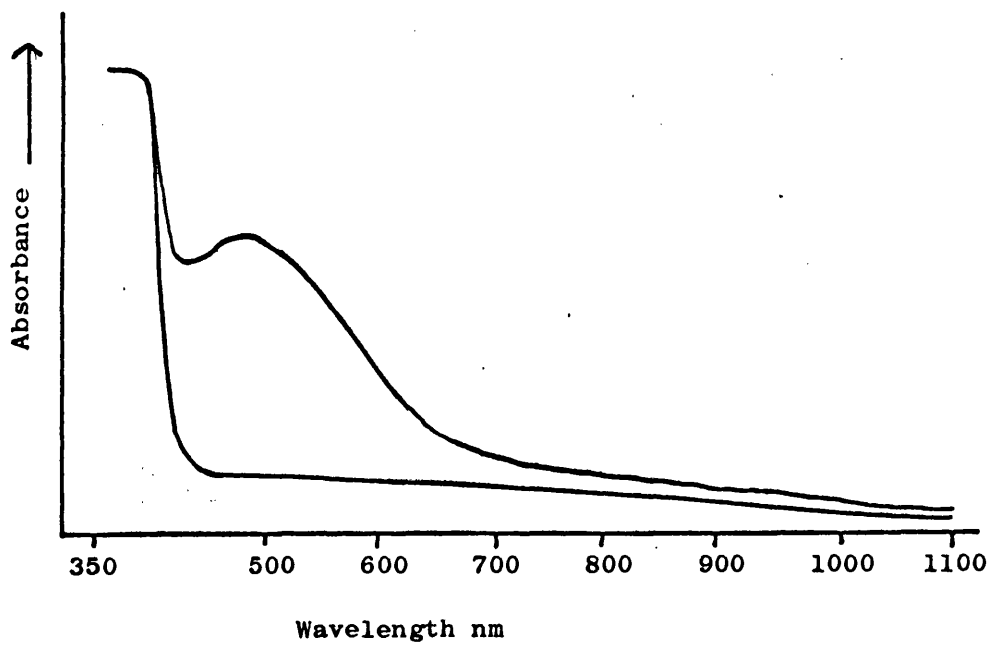
The reflectance spectra show the onset of the absorption of rutile and anatase at about 410nm and 390nm respectively. The absorption wavelengths co-incide with the band gap energy of n type titanium dioxide, approximately 3.0ev and the absorption is due to transition of electrons from the valence band to the conduction band. Since the valence band consists of the filled 2p orbitals of O^{2-} ions and the empty conduction band consists of the 3d orbitals of Ti^{4+} ions the transition can be represented by



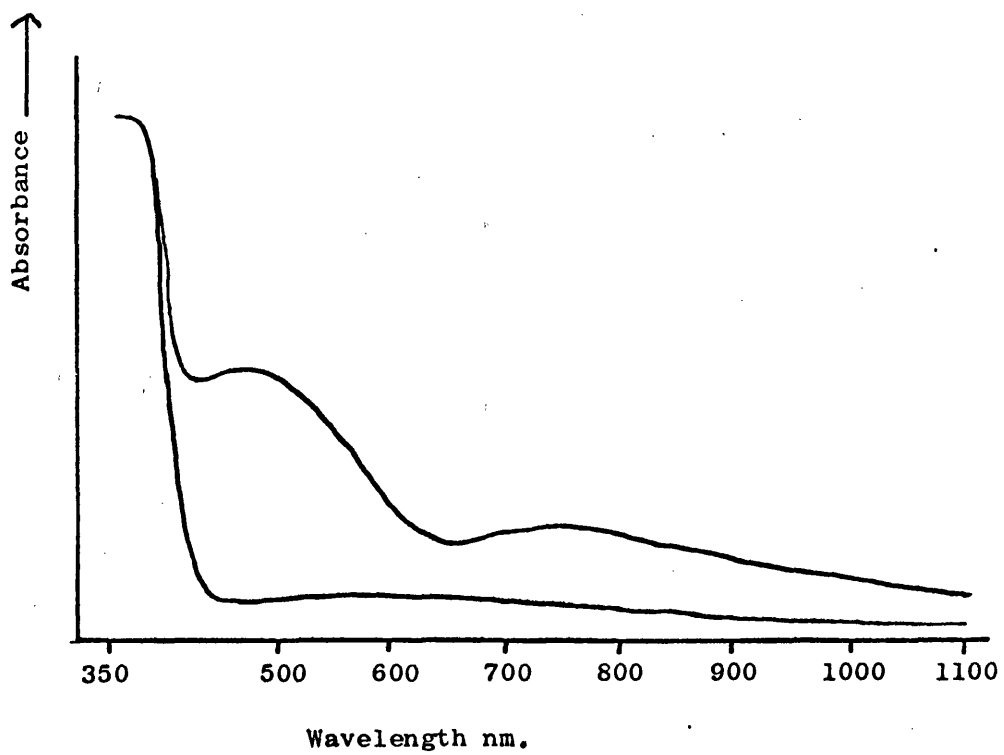
Two broad bands are observed in the reflectance spectra, one, centred around 500nm and the other around 750nm. DDQ molecules in benzene solution have an absorption band centred on 407nm. The ultra-violet absorption spectrum of K^+DDQ^- in acetonitrile (fig. 22) agrees well with that reported for Na^+DDQ^- by Iida⁸⁷, which was attributed to the radical anion monomer. The reflectance spectrum for solid K^+DDQ^- ⁸⁷ shows bands at 752nm, 488nm, and 400nm, the low energy transition was attributed to a

Fig. 21. Ultra-Violet and Visible Reflectance Spectra of DDQ on Pigments.

Pigment E.



Pigment G.



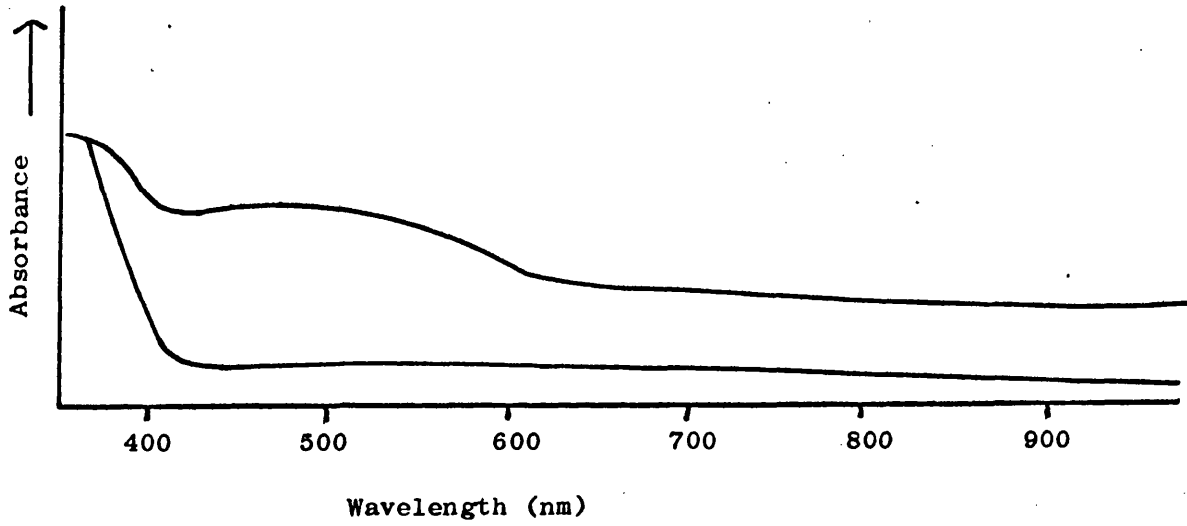
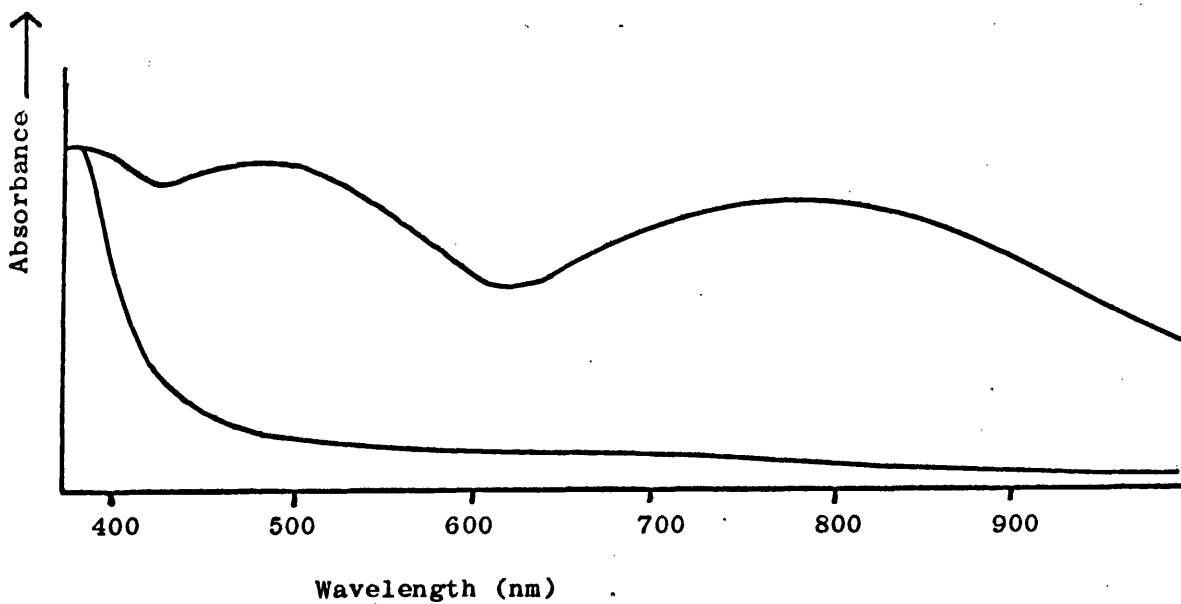
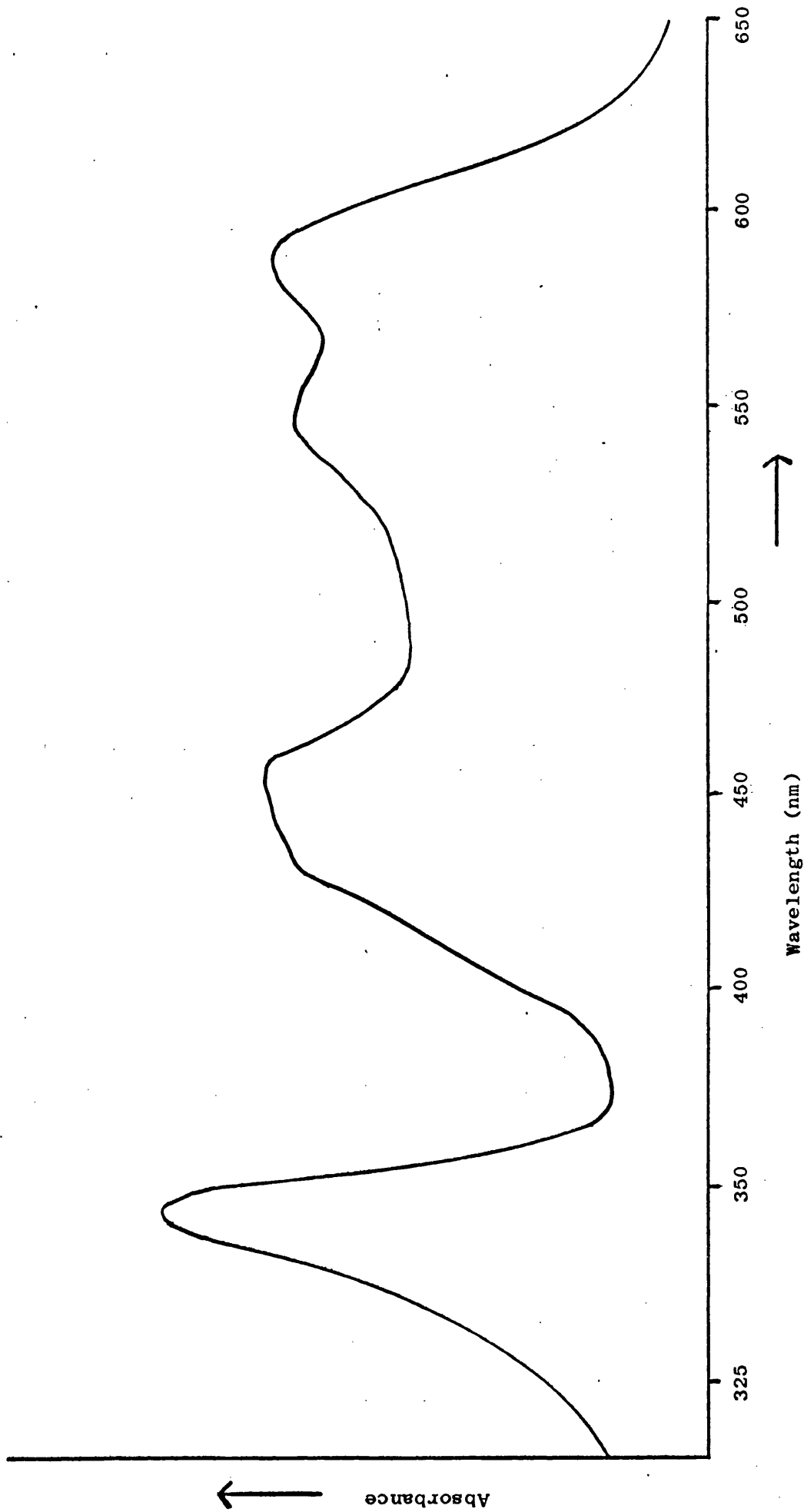
Pigment I.Zinc Oxide.

Fig. 22. Visible Spectrum of $K^+ DDQ$.

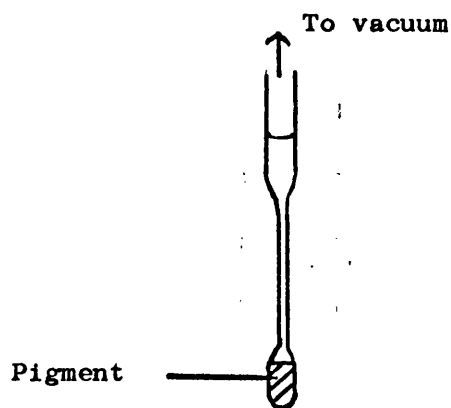


$\pi \rightarrow \pi$ transition of the monomer radical anion perturbed by the field of the other radicals close by in the solid, for the reflectance spectra of DDQ on pigments bands below 400nm are not observed due to the absorption by the pigment. The bands at 500nm and 750nm are more intense on zinc oxide than on titanium dioxide. Molecules adsorbed on the pigment surface can be expected to be perturbed from the solution environment. The long wavelength band observed may be due to the adsorbed anion radical and the band around 500nm due partly to adsorbed molecular DDQ and the anion radicals.

2.6 Electron Donation to Paraquat and Diquat.

2.6(a) Experimental.

Adsorption of paraquat dichloride and diquat dibromide from methanol solutions for e.s.r. measurements was effected using the apparatus in fig. 7, except that the 4mm O.D. tube was drawn down to produce the following shaped tube.



The methanol solutions were degassed by freeze thaw cycles and poured over onto the pigment which was not activated by heating. The tube was sealed off and immediately stored in the dark.

2.6(b) Results.

Adsorption of concentrated methanolic paraquat solutions (0.39M) on pigment A resulted in a blue colouration being observed forming at the pigment-solution interface. The tubes were stored in the dark since irradiation of degassed paraquat solutions leads to the formation of the radical cation⁸⁸. On storing the tube overnight an intense blue colouration was observed in the solution part of the system. Measurement of the e.s.r. spectrum at room temperature was done by positioning the narrow part of the tube in the spectrometer cavity, this being necessary due to the high dielectric loss from methanol. Degassing of the paraquat solution in the absence of pigment and storage overnight in the dark did not lead to any blue colouration being formed.

Adsorption of diquat dibromide on pigment A in the same manner resulted in a dark green colouration developing in the solution overnight. The e.s.r. spectra observed for paraquat and diquat solutions over pigment A are illustrated in figs. 23 and 24.

The measurement of the ultra-violet absorption spectrum of the radicals in solution was attempted by using an apparatus consisting of a 1cm cell containing a pigment sample with an attached side arm and facilities for attachment to a vacuum line for degassing. The blue colouration from paraquat was only produced when using high concentrations of paraquat, i.e. 0.39M, when using 1.56×10^{-2} and 7.8×10^{-2} M solutions no colouration was produced and the intensity of colouration produced when using the 0.39M solution was too intense for ultra-violet spectrum measurement.

Fig. 23. E.S.R. Spectrum of Paraquat on Pigment A.

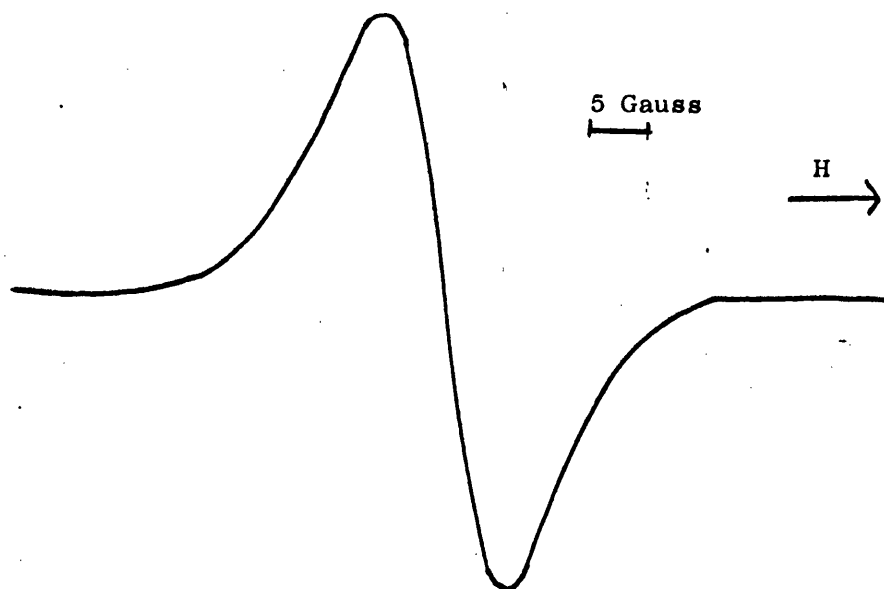
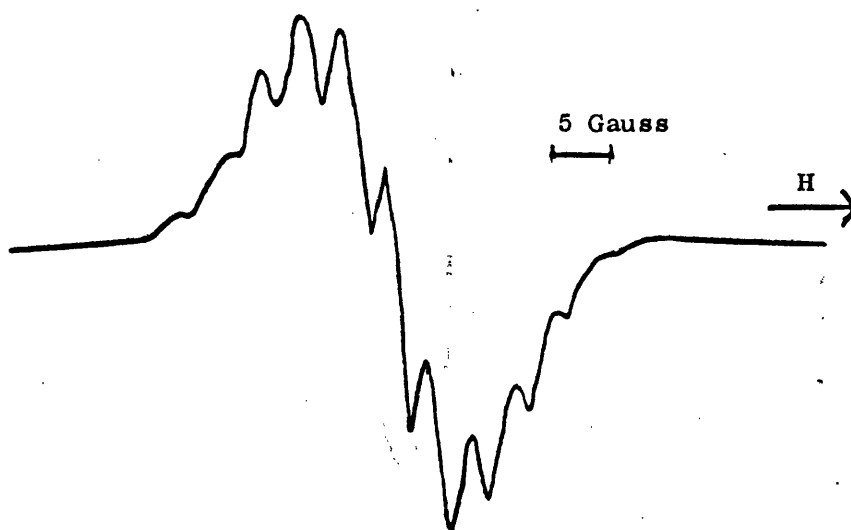


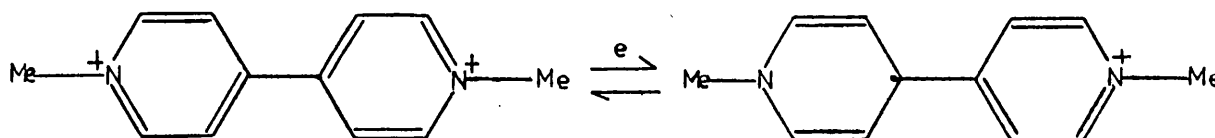
Fig. 24. E.S.R. Spectrum of Diquat on Pigment A.



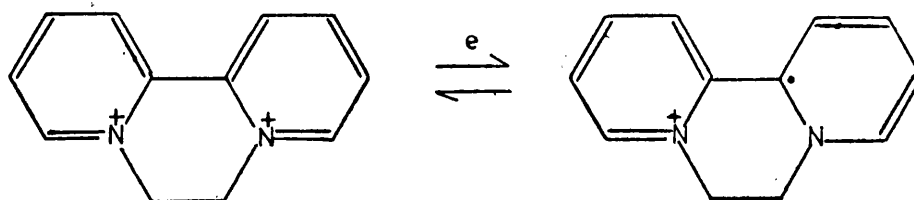
2.6(c) Discussion.

The reduction potentials of paraquat and diquat are -0.446V and -0.349V ^{89,90} versus the normal hydrogen electrode with a convention of more positive values of reduction potentials indicating molecules which are easier to reduce. These figures convert to $+0.68\text{V}$ and $+0.589$ versus the saturated calomel electrode using the convention of more negative values of reduction potentials indicating molecules which are easier to reduce. These figures suggest that paraquat and diquat are less powerful acceptors than those previously used.

The blue colouration of the radical monocation of paraquat is formed by the one electron reduction of paraquat dichloride.



and likewise the green colouration of the diquat monocation is formed by the one electron reduction of diquat dibromide



The reductions are effected by reducing agents such as zinc dust and sodium dithionite^{91,92}.

From the colouration of the methanol solutions of paraquat and diquat above pigment A it is apparent that the monocations have been formed by reduction and unlike the adsorption of the other electron acceptors the radicals produced are in solution and not trapped on the pigment surface. The participation of titanium dioxide in the electron transfer is established by the lack of reaction in the absence of pigment. Since the monocations are desorbed into solution, to maintain electroneutrality of the solution negative ions must be adsorbed onto the pigment or other cationic species desorbed from the pigment.

The radical monocations are readily oxidized back to the dications by oxygen and the presence of small quantities of oxygen in the systems may be responsible for lack of formation of the radicals when using dilute solutions of paraquat.

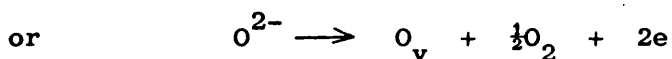
The e.s.r. spectra observed are symmetrical as expected for radicals in solution but no hyperfine coupling was observed for the paraquat free radical cation and the diquat radical cation e.s.r. spectrum was only partially resolved. Resolved spectra have been observed for the photo-produced radicals in solution⁸⁸ but the concentration of radicals is important for the observation of hyperfine lines.

CHAPTER 3

PHOTO-REDUCTION OF TITANIUM DIOXIDE AND
PHOTO-PRODUCTION OF OXYGEN RADICALS ON TITANIUM DIOXIDE.

3.1 Introduction.

Titanium dioxide can be thermally reduced by heating under vacuum or heating with reducing agents such as carbon monoxide, hydrogen, and ethylene. The reduction results in a broad asymmetric e.s.r. absorption being observed at 77K^{58,93,94} and the titanium dioxide takes on a blue or grey appearance. Loss of an oxygen atom from titanium dioxide frees two electrons to remain in the crystal. There are two possibilities for these electrons; they can either reduce Ti^{4+} ions to Ti^{3+} ions or the electrons can remain in the vacancies left by the departing oxygen atom.



where O_v = anion vacancy.

Both cases would give rise to e.s.r. absorption but most workers conclude that the asymmetric absorption at $g = 1.96$ is due to Ti^{3+} ions.

A study⁹⁴ of the thermal reduction of anatase and rutile by various methods led to the proposal for the existence of two kinds of paramagnetic centres in reduced titanium dioxide. These were Ti^{3+} ions in lattice or interstitial sites giving e.s.r. absorptions at $g_L = 1.99$, $g_{||} = 1.96$ in anatase and $g_L = 1.966$, $g_{||} = 1.96$ in rutile, and the other being a Ti^{3+} ion associated with one or two oxygen vacancies giving an e.s.r. absorption at $g_L = 1.966$, $g_{||} = 1.946$ in both rutile and anatase.

Rutile and anatase were found to be reduced by ultra-violet light in the presence of isobutane and it was noted that evacuated anatase but not rutile was reduced by the action of ultra-violet

light alone. Earlier work⁹⁵⁻⁷ indicated that titanium dioxide could be reduced, as detected by its blue colouration, by irradiation in the presence of mandelic acid, glycerol, formaldehyde, tartaric acid and alcohol. A study⁹⁸ of the photo-oxidation of binders by titanium dioxide revealed that irradiation of titanium dioxide with adsorbed alkyd resins resulted in reduction to Ti^{3+} . It was also observed that titanium dioxide modified with silicon dioxide formed a lower concentration of Ti^{3+} ions after a standard reduction treatment of evacuation at $450^{\circ}C$ for six hours.

Oxidation of reduced titanium dioxide with oxygen results in the formation of the superoxide anion $O_2^{\cdot-}$ adsorbed on the surface and the Ti^{3+} e.s.r. absorption disappears^{99,100}.



The formation of $O_2^{\cdot-}$ is confirmed by its e.s.r. spectrum.

E.s.r. studies of the adsorption of O^{16} and O^{17} enriched oxygen on thermally reduced titanium dioxide¹⁰⁰ led to the observation of hyperfine lines from the $O_2^{\cdot-}$ anion and the equivalence of the two oxygen nuclei indicates that the ion is adsorbed with the oxygen - oxygen axis parallel to the adsorption site.

A study¹⁰¹ of the number of Ti^{3+} centres in a reduced titanium dioxide sample compared to the number of paramagnetic centres formed after oxidation showed that the number of paramagnetic oxygen species was only 7% of the number of Ti^{3+} ions suggesting that the bulk of the reoxidation results in the formation of diamagnetic O^{2-} ions.

$O_2^{\cdot-}$ ions, detectable by e.s.r. spectroscopy, are produced by irradiation of titanium dioxide in the presence of oxygen and can be reacted with alkanes¹⁰²⁻³. The wavelengths found active in the

formation of $O_2^{\cdot-}$ were 200nm to 600nm. Only the 200-350nm range is of band gap energy or greater and can produce electrons and holes by excitation of electrons from the valence band to the conduction band. Trapping of a photo-electron by oxygen would lead to an $O_2^{\cdot-}$ ion being formed. The promotion of electrons from donor levels in the band gap was used to explain the formation of $O_2^{\cdot-}$ ions with light of longer wavelength.

$O_2^{\cdot-}$ ions produced on thermally reduced titanium dioxide have been reacted with ethylene, carbon monoxide, and sulphur dioxide¹⁰⁴.

The formation of the paramagnetic species O^- on titanium dioxide was inferred⁶⁴ but there seems to be no definite evidence for its formation^{93,100}.

A great deal of confusion arose from the use of titanium dioxide samples prepared by precipitation using aqueous ammonia. It was shown¹⁰⁵⁻⁷ that the trace of ammonia trapped by titanium dioxide, after heating in oxygen, yields paramagnetic species containing nitrogen and oxygen. The e.s.r. absorptions from these radicals had previously been assigned to surface O_2^+ ions¹⁰⁸ or a TiO^{3+} species with analysis of Ti^{47} and Ti^{49} hyperfine interactions¹⁰⁹.

The intention of the following study was to examine the photo-reduction of pigments by a number of agents and to detect the formation of $O_2^{\cdot-}$ anions on the pigments.

3.2(a) Experimental.

Samples of pigments were placed in e.s.r. tubes and degassed solvents were placed over them using the apparatus in fig. 7, and then sealed off as before. A 2KW Xenon lamp with a blue filter allowing

only light of wavelengths 300-400nm through was used, the light being focussed on the pigment sample tube which was supported in a beaker of water to ensure that there was no heating effect. The sample tubes were rotated at intervals to give a more even irradiation of the available surface. Irradiation was at room temperature and normally for a period of seven hours. The e.s.r. spectra of the pigments were recorded at 77K after the irradiations.

For irradiations with oxygen the apparatus in fig. 3 was used to place an oxygen atmosphere above the pigment and after the irradiation period the oxygen was evacuated at room temperature for a few minutes to a pressure of approximately 10^{-4} torr.

3.2(b) Results.

Irradiation of evacuated samples of pigments A and E did not effect any change in their e.s.r. spectra at 77K. An evacuated sample of pigment I showed blue colouration on the surfaces exposed to ultra-violet light after irradiation. Its e.s.r. spectrum at 77K is shown in fig. 25. A broad asymmetric absorption with $g_{\perp} = 1.999$, and $g_{\parallel} = 1.967$ is superimposed on the background impurity spectrum.

Irradiation of pigment A in degassed methanol, ethanol, n butanol, isopropanol and benzyl alcohol produced a blue colouration in the pigment and the e.s.r. spectrum at 77K in fig. 26 which consists of an asymmetric absorption with $g_{\perp} = 1.973$, $g_{\parallel} = 1.940$.

For comparative purposes the spectrum of the O_2^- ions was produced on a reduced laboratory sample of titanium dioxide prepared by hydrolysis of tetra-n-butyltitanate and reduced by evacuation at $200^{\circ}C$ for one hour. Upon opening the sample tube to air and plunging

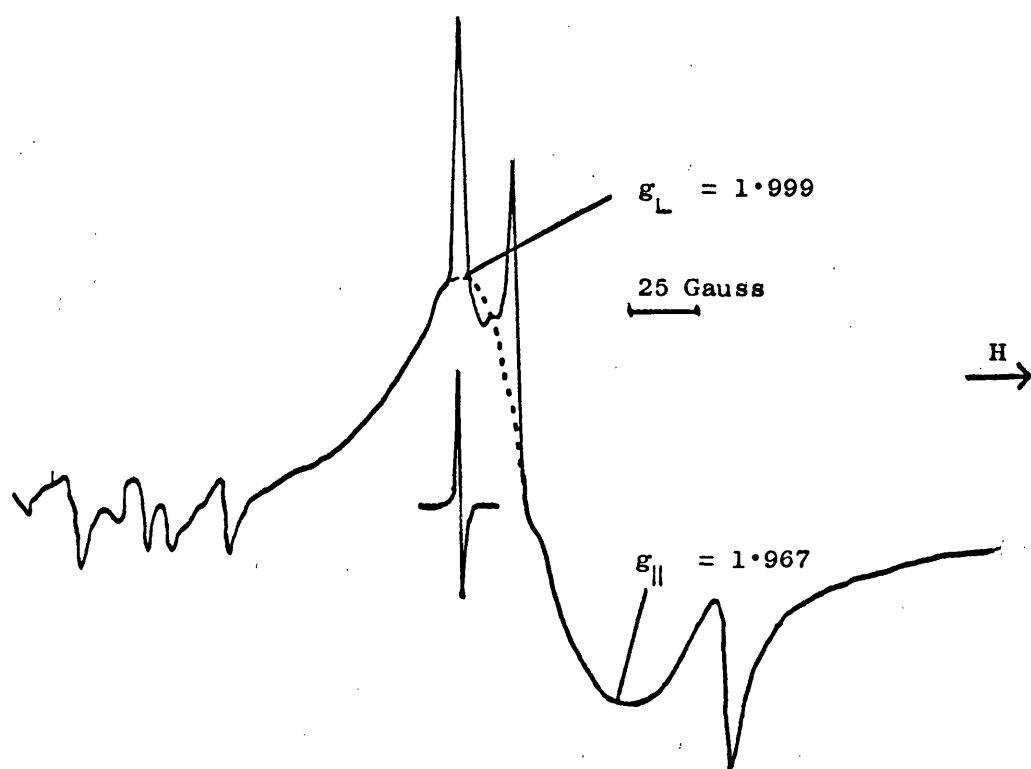
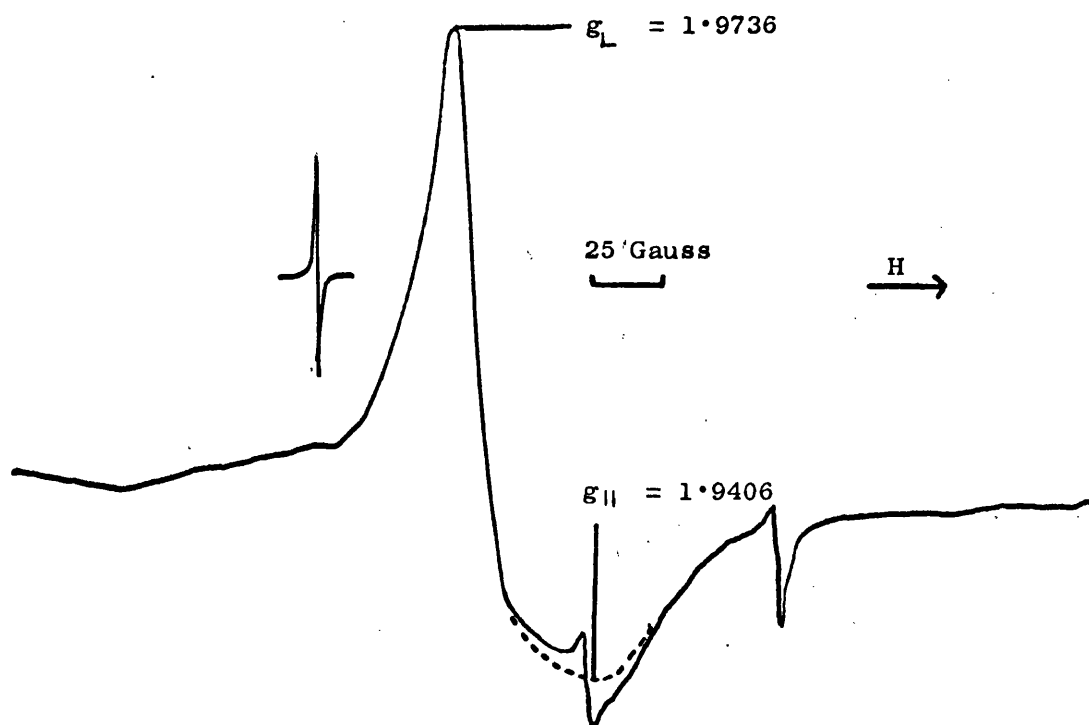
Fig. 25. E.s.r. Spectrum of Irradiated Pigment I at 77K.Fig. 26. E.s.r. Spectrum of Pigment A - Irradiated with Alcohols.

Fig. 27. E.s.r. Spectrum of O_2^- on Laboratory Titanium Dioxide at 77K.

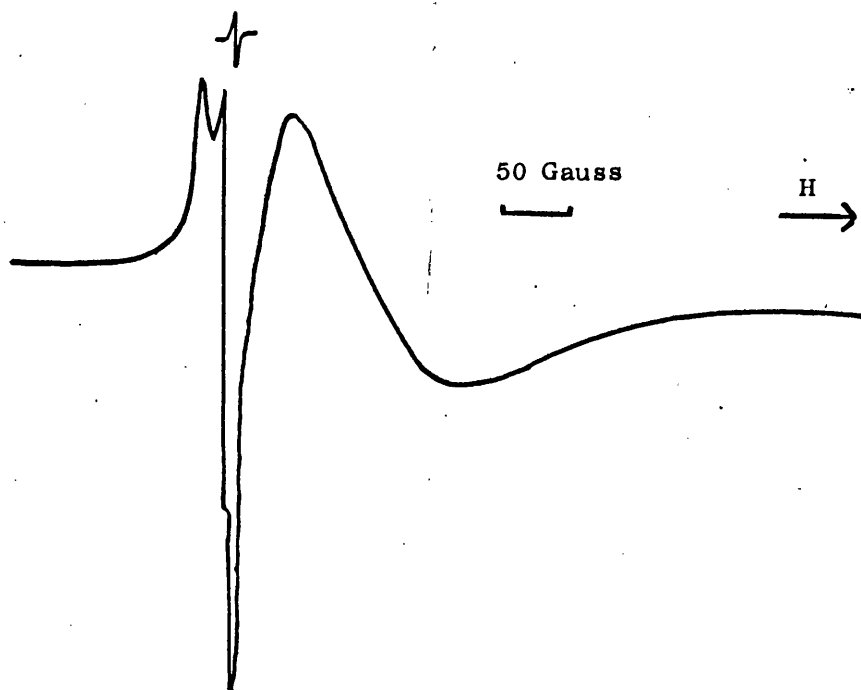


Fig. 28. E.s.r. Spectrum of O_2^- at 77K after Warming to Room Temperature.

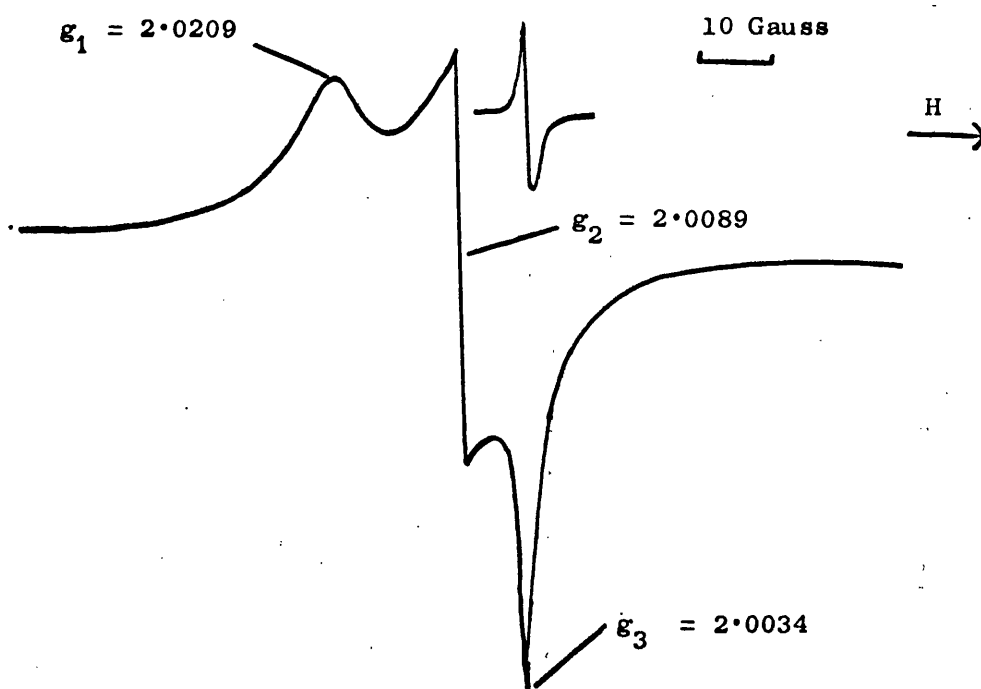


Fig. 29. E.s.r. Spectrum at 77K of Pigment I Irradiated with Oxygen.

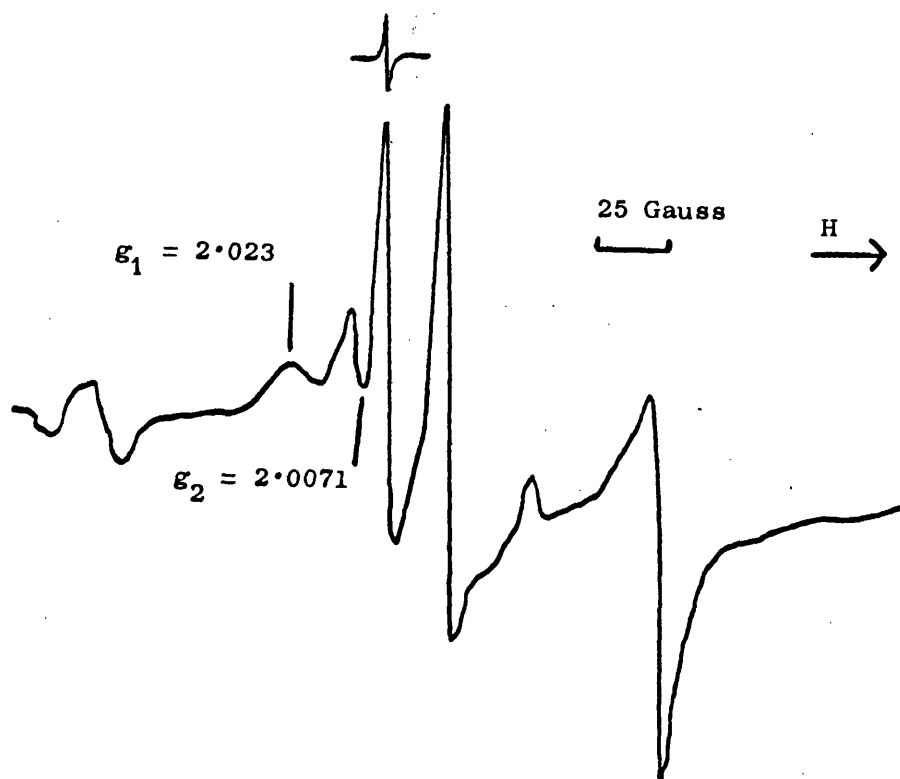
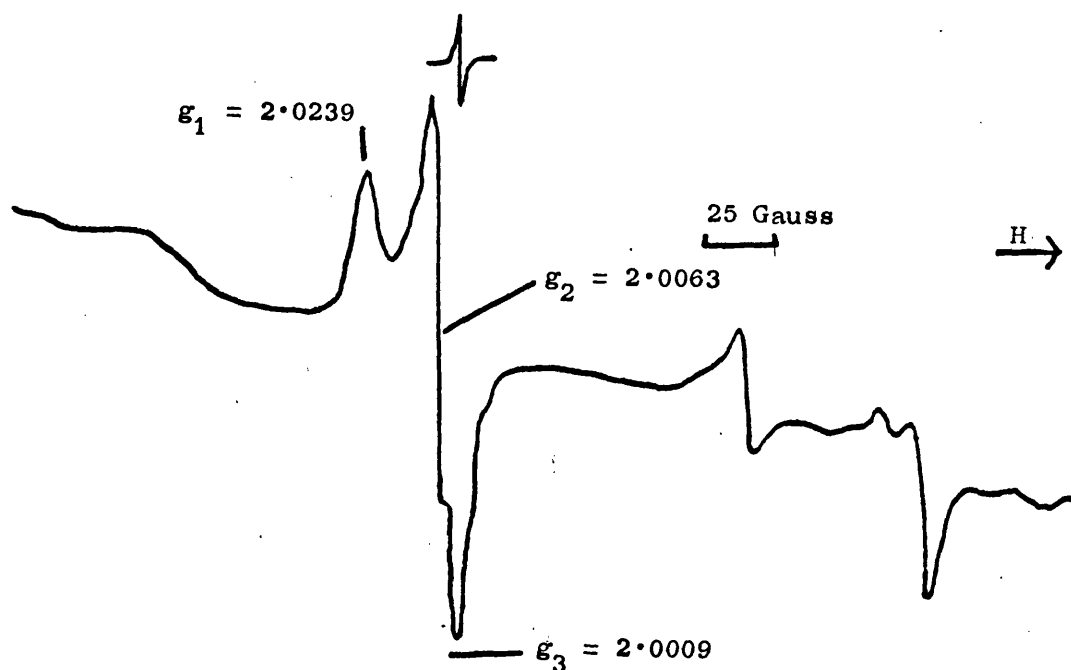


Fig. 30. E.s.r. Spectrum at 77K of Pigment E Irradiated with Oxygen.



it into liquid nitrogen the e.s.r. spectrum in fig. 27 was recorded. After warming to room temperature and recooling to 77K the spectrum in fig. 28 was recorded.

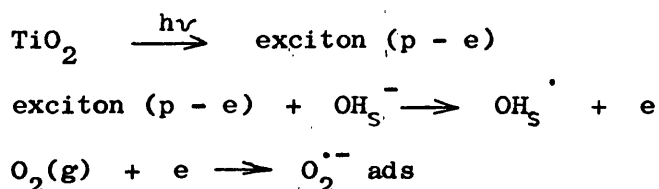
Irradiation of pigment I with oxygen and removal of the oxygen after irradiation gave an e.s.r. spectrum at 77K as shown in fig. 29. Upon letting air into the system the spectrum returned to that shown in fig. 5. Irradiation of pigment E with oxygen followed by removal of the oxygen gave an e.s.r. spectrum at 77K as shown in fig. 30. On letting air into the system the spectrum returned to that shown in fig. 6.

3.2(c) Discussion.

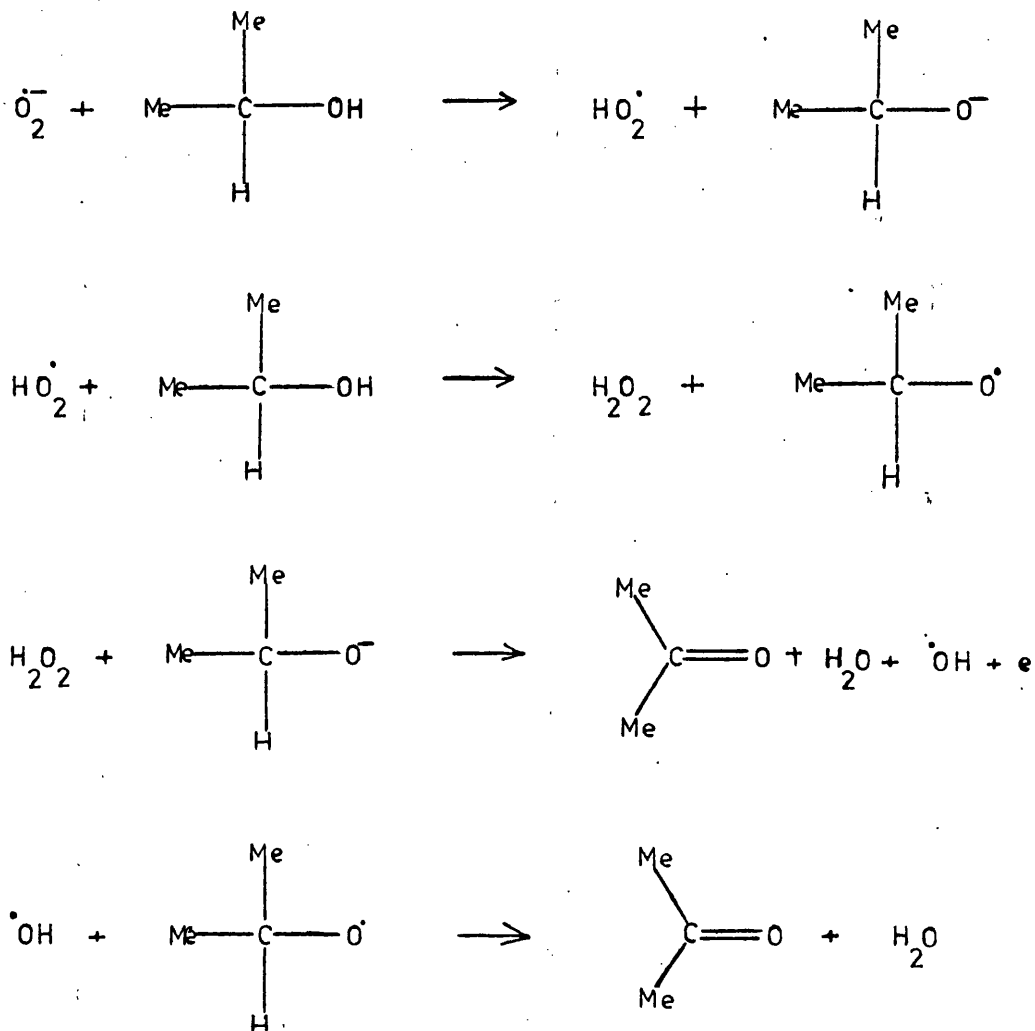
The rutile samples A and E were not reduced by ultra-violet irradiation alone, whereas the anatase pigment I showed reduction; this confirms the result of Che⁹⁴ where an absorption with $g_{\perp} = 1.99$, $g_{\parallel} = 1.96$ was observed. The centre of the absorption due to Ti^{3+} ions is most likely displaced by the background signals.

The g values for the Ti^{3+} e.s.r. absorption for the rutile pigment corresponds well with that reported for the photo-reduction of rutile with isobutane⁹⁴ where $g_{\perp} = 1.973$ and $g_{\parallel} = 1.946$ compared with values of $g_{\perp} = 1.9736$ and $g_{\parallel} = 1.9406$ observed for reduced pigment A.

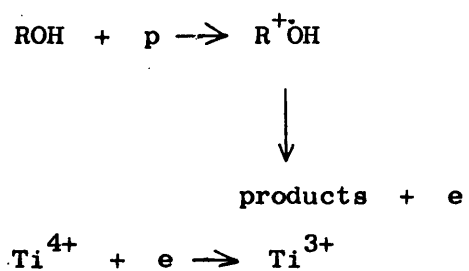
Pigment A is photo-reduced in the presence of alcohols. Isopropanol is known to be photo-oxidised in the presence of irradiated titanium dioxide and oxygen to acetone¹¹⁰. A proposed mechanism involves the reaction of photo-produced $O_2^{\cdot-}$ by the trapping of a photo-electron while the hole is trapped by a surface hydroxyl group.



A reaction scheme proposed for acetone formation is given.

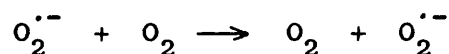


In the presence of oxygen the titanium dioxide is maintained in a fully oxidized state; in the absence of oxygen reduction of the oxide could occur. This probably occurs by a process of hole injection into the alcohol molecule.



The reaction of alcohols with irradiated pigments is discussed in Chapter 5.

The spectrum for the $O_2^{\cdot-}$ ion on laboratory titanium dioxide was observable in the presence of oxygen due probably to the high intensity of the e.s.r. spectrum. Usually samples have to be evacuated to prevent exchange broadening of the spectrum by the reaction.



The g values for the $O_2^{\cdot-}$ radical on laboratory titanium dioxide agree well with literature values.¹⁰⁰ The broad part of the spectrum is due to Ti^{3+} ions which are oxidized to Ti^{4+} ions on warming the sample to room temperature.

The e.s.r. spectra for the photo-produced oxygen radicals observed on pigments I and E are of low intensity and can be assigned to the $O_2^{\cdot-}$ radical by comparison with the e.s.r. spectrum of $O_2^{\cdot-}$ on laboratory titanium dioxide and by comparison with the literature. Part of the $O_2^{\cdot-}$ spectrum of pigment I is obscured by the background impurity spectrum but the g values $g_1 = 2.023$ and $g_2 = 2.0071$ agree closely with the values of $g_1 = 2.0234$, $g_2 = 2.0098$, and $g_3 = 2.0035$ for photo-produced $O_2^{\cdot-}$ on anatase¹⁰².

The g values for $O_2^{\cdot-}$ on pigment E $g_1 = 2.0239$, $g_2 = 2.0063$, $g_3 = 2.0009$ compare well with g values for thermally produced $O_2^{\cdot-}$ on rutile $g_1 = 2.0216$, $g_2 = 2.0106$, $g_3 = 2.002$ ¹¹¹.

CHAPTER 4

FLUORESCENCE OF TITANIUM DIOXIDE PIGMENTS

AND OF ADSORBED MOLECULES.

4.1 Introduction.

Comparatively little research has been reported on the fluorescent properties of titanium dioxide. Ghosh¹¹² reported the observation of a weak luminescence band at 850 nm for a reduced rutile crystal excited with light of wavelength 365nm. This luminescence was found to be strongest in the temperature range -50°C to -100°C and was tentatively attributed to the radiation released upon the recombination of an electron from the conduction band with a positive hole at a luminescence centre; the involvement of interstitial Ti^{3+} ions was inferred.

For tungsten doped titanium dioxide¹¹³ a red-orange luminescence was observed at 2.02ev (614nm) which did not occur in undoped samples. The luminescence transition was proposed to be from the excited state of an acceptor level, (lying just beneath the conduction band) to the ground state of the acceptor level, (lying above the valence band).

The observation of a green emission (510nm) at 77K was reported¹¹⁴ for a thin film of 75nm thickness of amorphous titanium dioxide; the luminescence was identified with direct band gap transitions from the excitation spectrum.

Many other inorganic materials fluoresce such as zinc oxide, zinc sulphide and calcium sulphide^{115,116}. Zinc oxide shows a luminescence at approximately 500nm and also in the near ultra-violet region at 372nm¹¹⁶. The luminescence is supposed to arise from recombination of electrons and holes. At room temperature oxygen suppresses the luminescence, presumably by trapping conduction band electrons at the surface.

Investigations of the fluorescence of dyes on inorganic substrates have been made^{117,118} and emission shifts have been observed for dyes

on metal hydroxides and oxides¹¹⁹ and for pyrene and naphthalene on alumina and magnesium oxide¹²⁰.

4.2(a) Experimental.

The fluorescence spectra were recorded on a Baird Atomic Spectrofluorimeter. An attachment for the instrument was constructed, consisting of a copper disc into which the pigment sample was pressed. The disc could be moved backwards and forwards on a ratchet mechanism so that the beam of exciting light could be focussed onto the pigment sample maximizing the fluorescence intensity. The spectra were recorded at room temperature.

Pigment samples doped with organic compounds were prepared by solvent evaporation and dried at room temperature overnight in evacuated drying tubes. Benzene was the solvent for anthracene and perylene, acetonitrile was used for eosin and fluorescein and methanol for methylene blue.

4.2(b) Results.

The fluorescence spectra of all pigments was recorded with λ excitation = 330nm. The pigments all showed a weak fluorescence which was the same for all rutile pigments showing bands at 420nm and 520nm (fig. 31).

Fig. 32 shows the fluorescence spectrum for pigment I (anatase) which shows bands at 406nm and 520nm. The fluorescence spectrum of zinc oxide with λ excit. = 300nm is given in fig. 33.

The fluorescence spectrum of pigment A containing 2% w/w anthracene shows bands at 423nm, 446nm, and 473nm, λ excitation 350nm

Fig. 31. Fluorescence Spectrum of Pigments A - H.

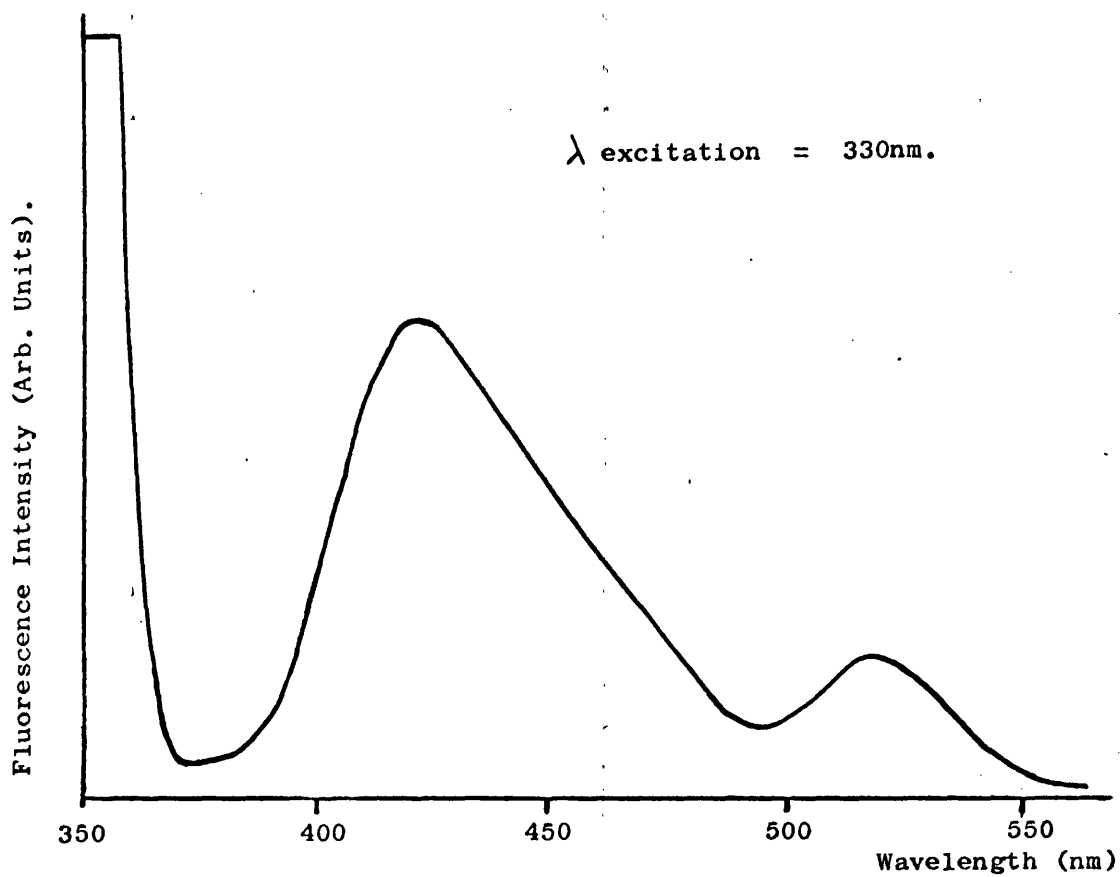


Fig. 32. Fluorescence Spectrum of Pigment I.

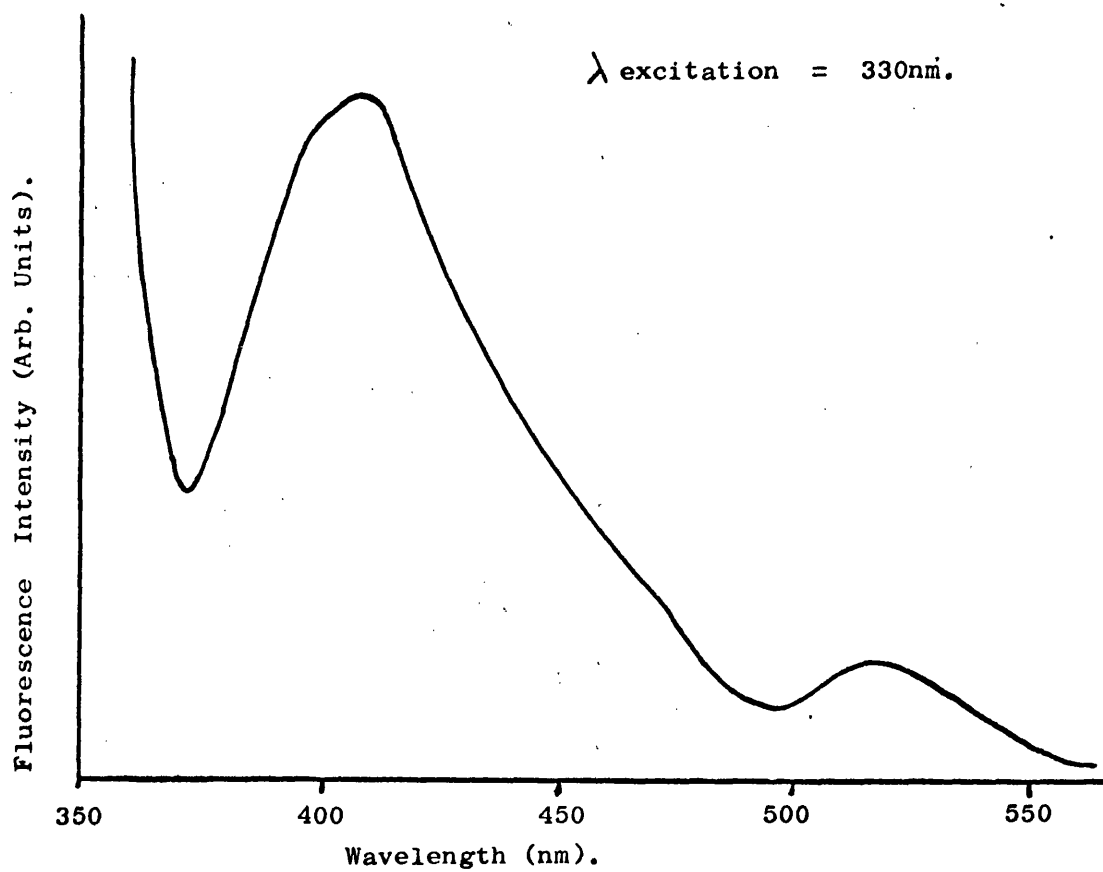


Fig. 33. Fluorescence Spectrum of Zinc Oxide.

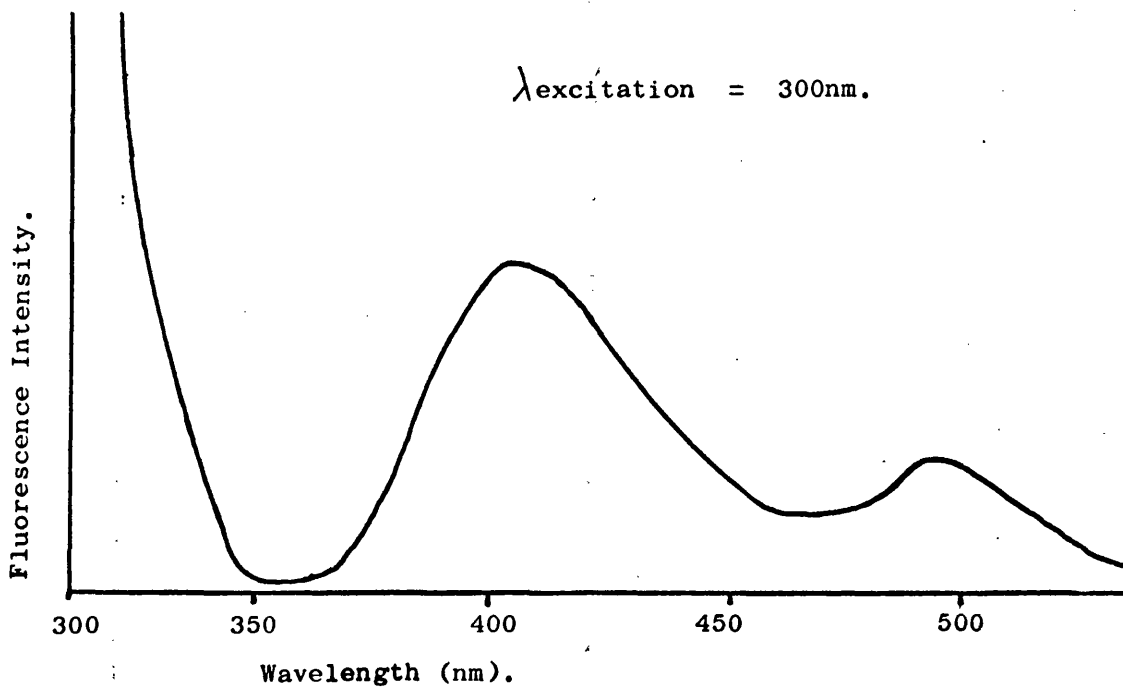


Fig. 34a. Fluorescence Spectrum of Anthracene on Pigment A.

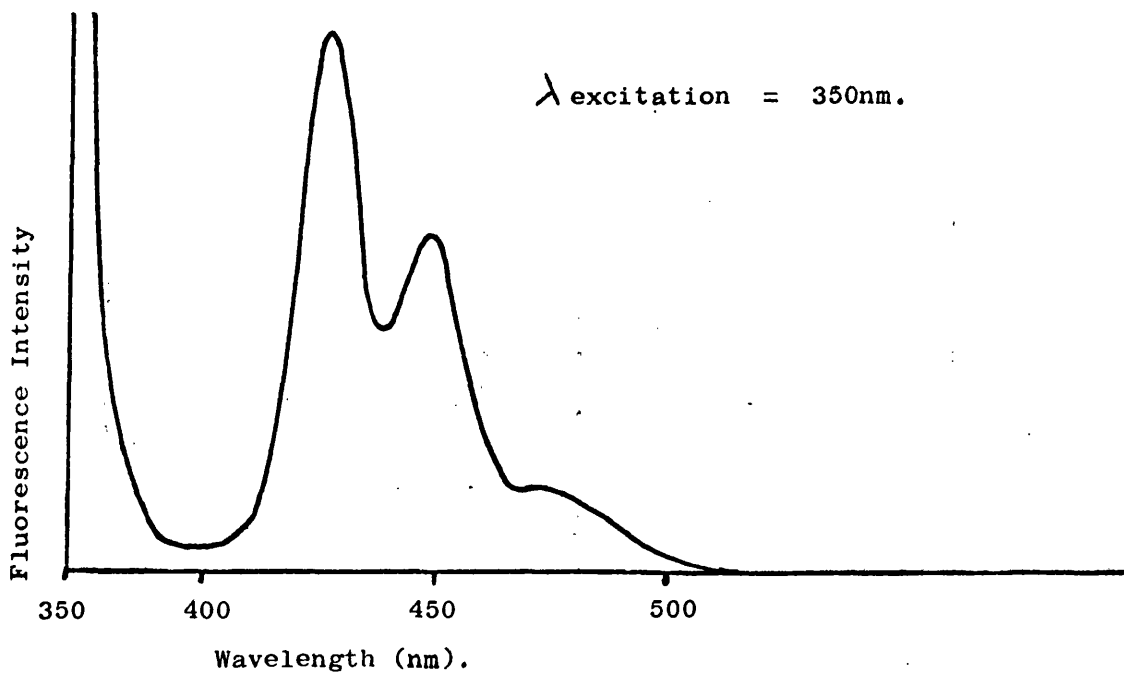


Fig. 34b. Excitation Spectrum of Anthracene on Pigment A.

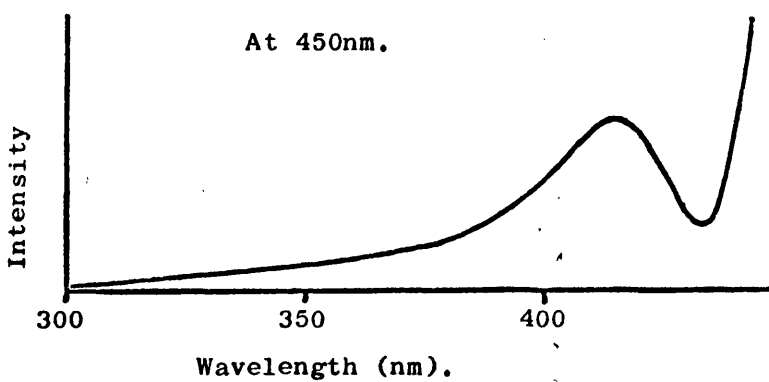


fig. 34a. The pigment fluorescence is weak compared to the fluorescence of compounds on titanium dioxide and so does not distort the observed spectra. The excitation spectrum at 470nm for anthracene on pigment A, i.e. the variation of the intensity of fluorescence at 470nm with variation in the wavelength of exciting light is shown in fig. 34b, having a maximum at 418nm. Pigment I containing 2% w/w anthracene shows the same fluorescence bands but the maximum in the excitation spectrum occurs at 408nm.

The fluorescence spectrum of 5×10^{-6} m/g of perylene on pigment A using λ excitation = 430nm is shown in fig. 35a, having a major band at 555nm and other bands at 512nm and 485nm. The excitation spectrum (at 610nm), (fig. 35b) has a maximum at 475nm.

Fig. 36a shows the fluorescence of 10^{-6} m/g eosin on pigment A (λ excitation 450nm) centred on 556nm and the excitation spectrum at 610nm (fig. 36b) is centred at 547nm.

10^{-6} m/g fluorescein on pigment A fluoresces at 523nm and the excitation spectrum at 630nm has a maximum at 482nm (fig. 37a and b).

10^{-6} m/g methylene blue fluoresces at 683nm (λ excitation 600nm) and the excitation spectrum maximum is at 654nm (fig. 38 a and b). The results are summarized and compared with solution fluorescence in Table 4.

The ultra-violet reflectance spectra of anthracene and perylene on pigment A only shows slight distortion from the rutile reflectance spectrum due to most of the anthracene absorption occurring in the same range as the rutile absorption.

The ultra-violet reflectance spectra of 10^{-6} m/g methylene blue on pigment A and zinc oxide are shown in figs. 39 a and b with the absorption spectrum of a methanolic solution of methylene blue drawn in for comparison.

Fig. 35a. Fluorescence Spectrum of Perylene on Pigment A.

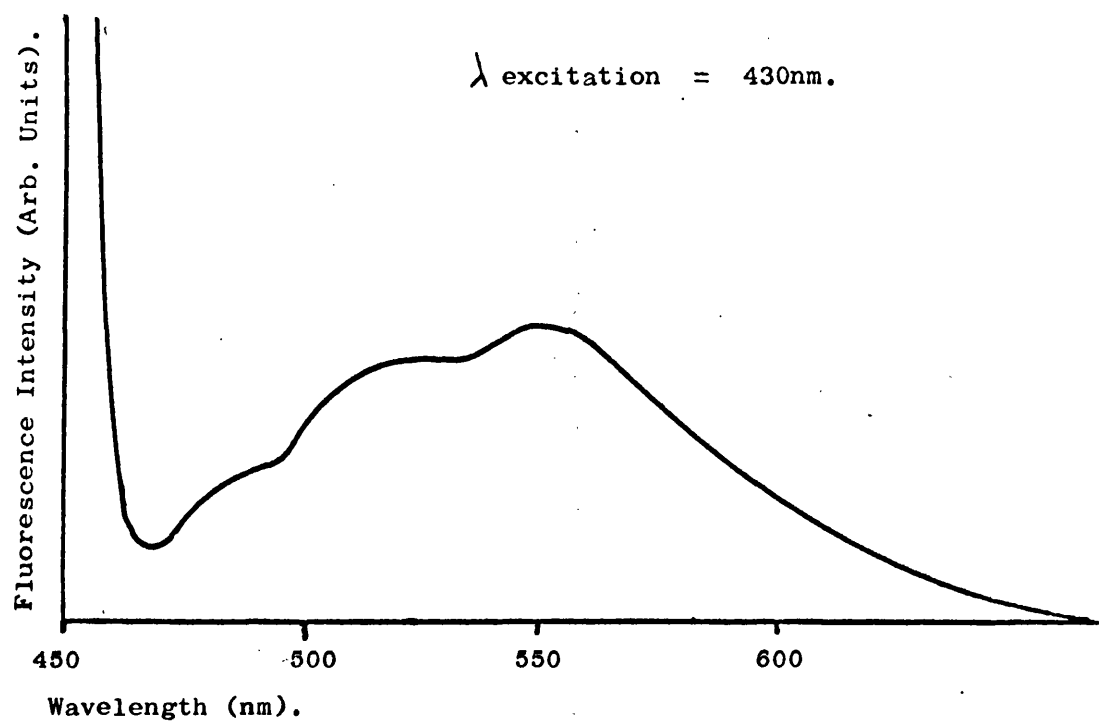


Fig. 35b. Excitation Spectrum of Perylene on Pigment A. (610nm).

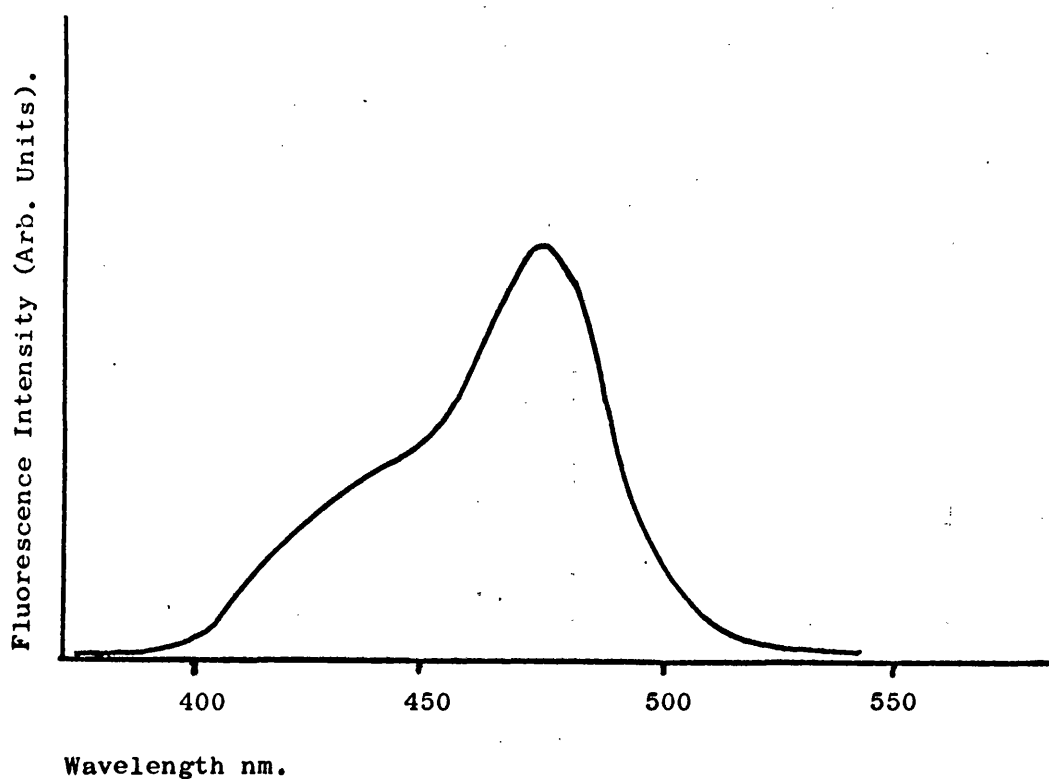


Fig. 36a. Fluorescence Spectrum of Eosin on Pigment A.

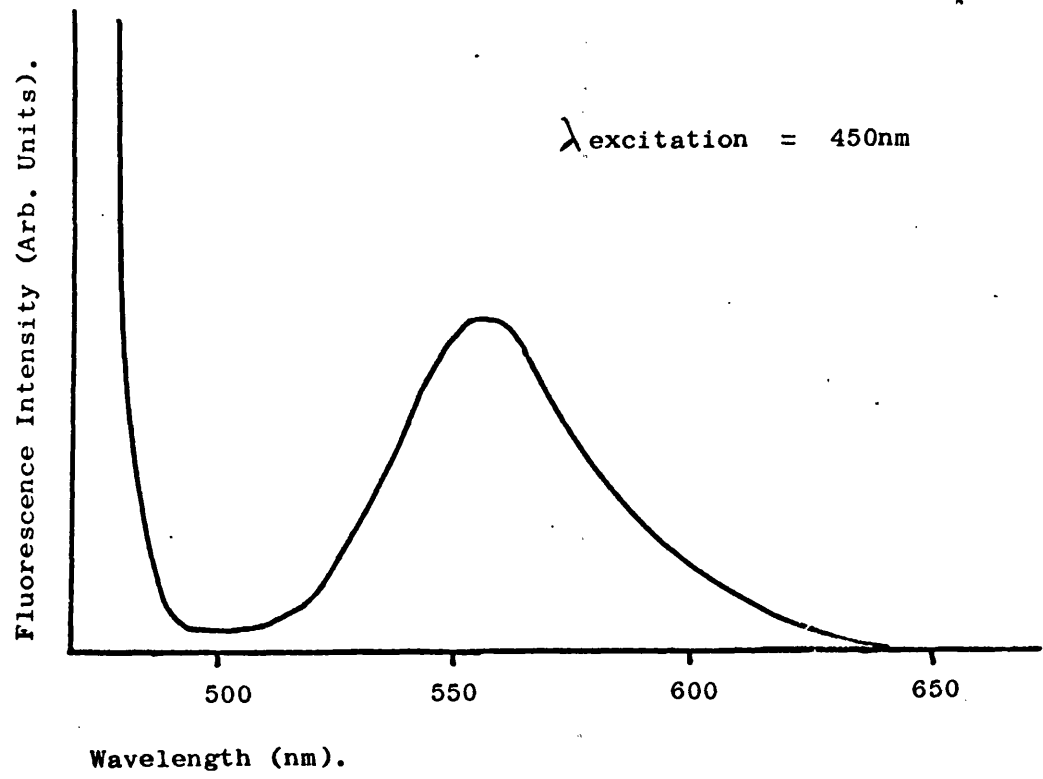


Fig. 36b. Excitation Spectrum of Eosin on Pigment A (610 nm).

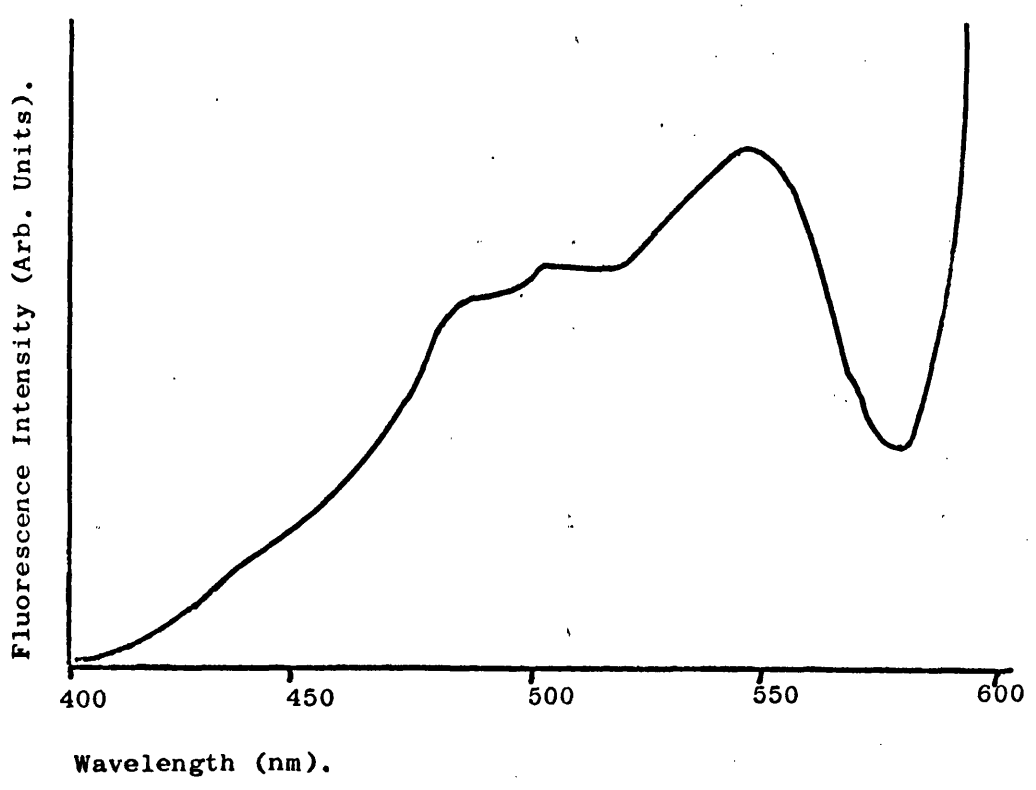


Fig. 37a. Fluorescence Spectrum of Fluorescein on Pigment A.

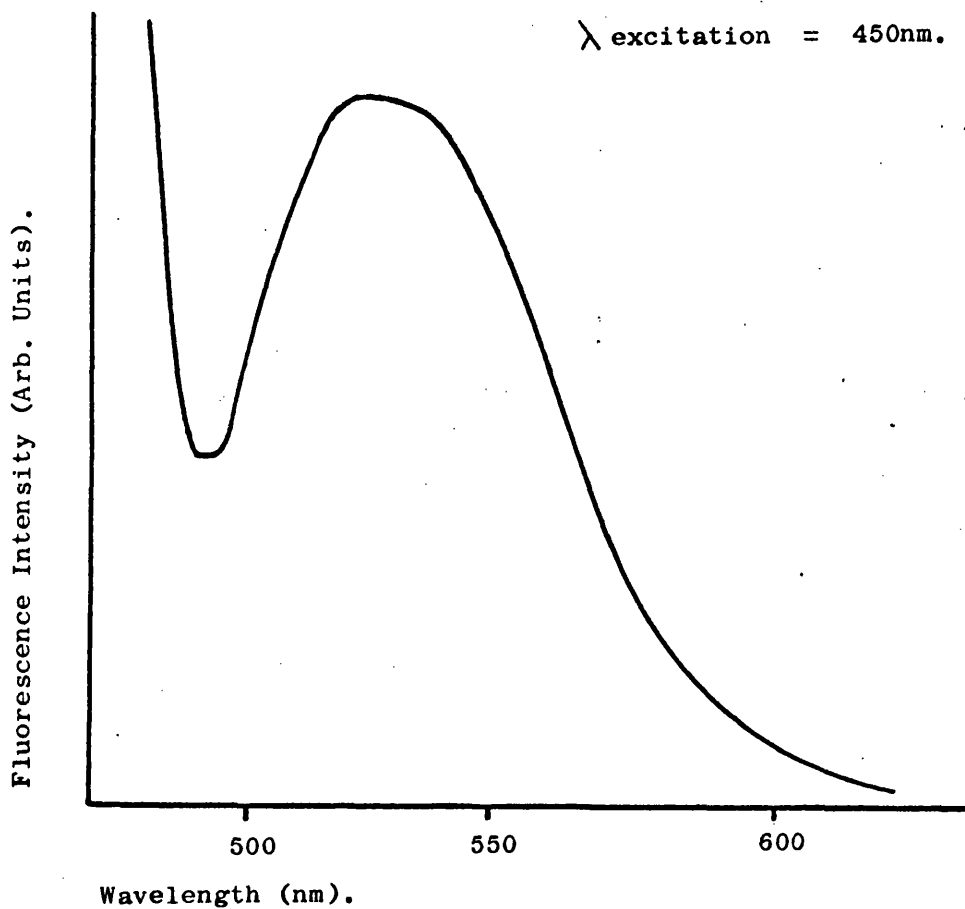


Fig. 37b. Excitation Spectrum of Fluorescein on Pigment A. (630nm).

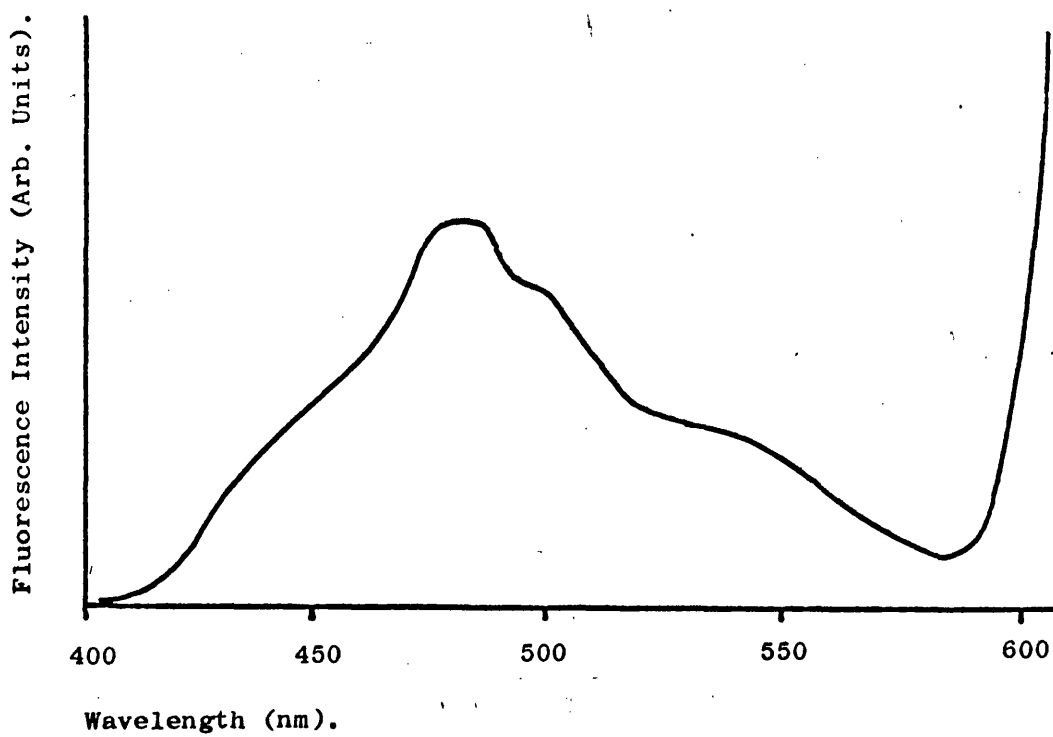


Fig. 38a. Fluorescence Spectrum of Methylene Blue on Pigment A.

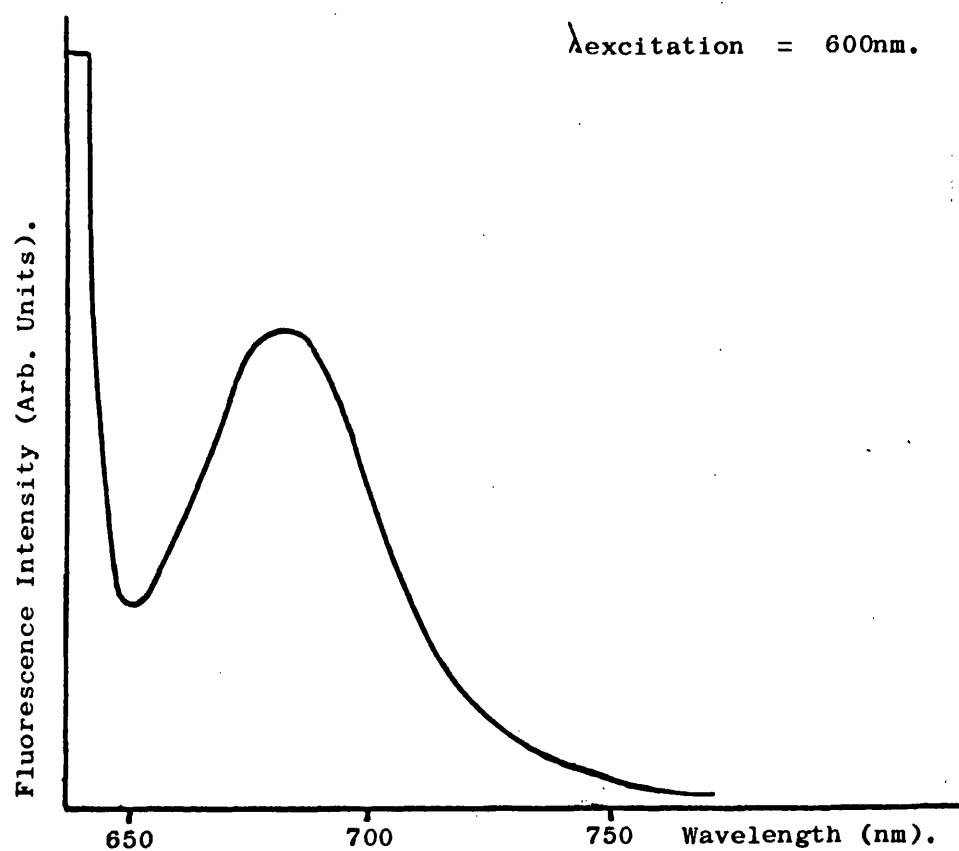


Fig. 38b. Excitation Spectrum of Methylene Blue on Pigment A. (700 nm).

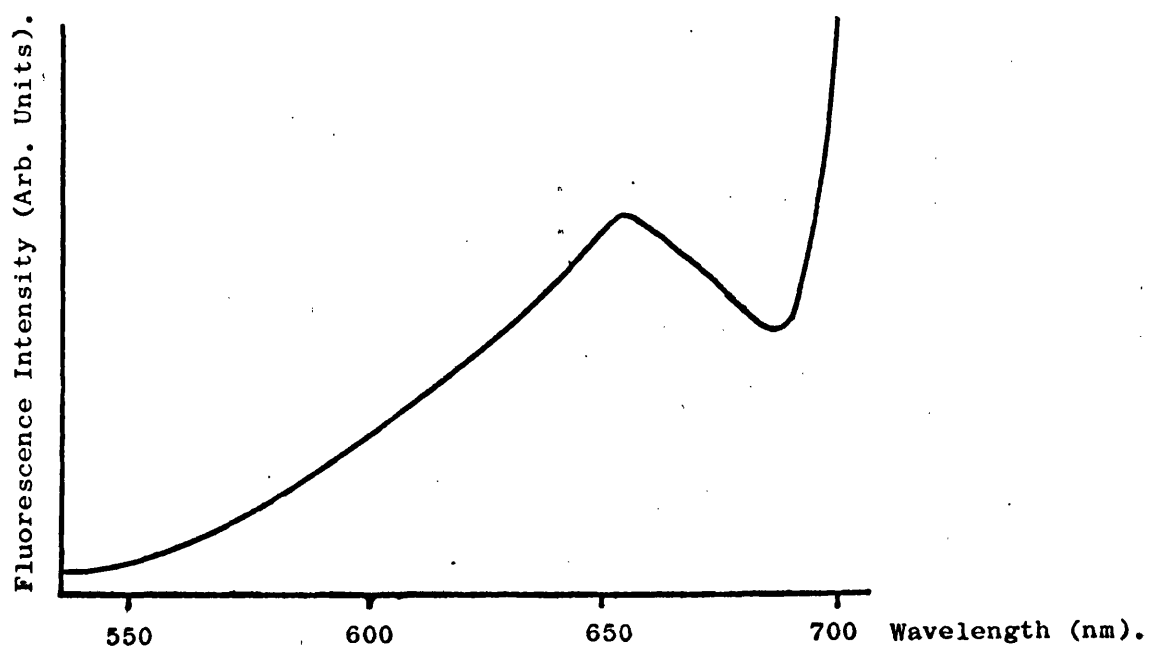


TABLE 4.

Compound	λ_{max} sol. fluor.	λ_{max} fluor. on TiO_2	λ_{shift} on TiO_2	λ_{max} fluor. on ZnO	λ_{shift} on ZnO	λ_{max} excit. sol.	λ_{max} excit. on TiO_2	λ_{max} excit. shift on TiO_2	λ_{max} excit. on ZnO	λ_{max} excit. shift on ZnO
Anthracene	400nm. in EtOH	423nm	+23nm	423nm	23nm	368nm	418nm (rutile) 408nm (anatase)	50nm 40nm	413nm	45nm
Methylene Blue	683nm in H_2O	683nm	0nm	674nm	-9nm	665nm	654nm	-11nm	652nm	-13nm
Eosin	545nm in H_2O	556nm	+11nm	568nm	23nm	526nm	547nm	21nm	530nm	+4nm
Fluorescein	520nm in H_2O	523nm	3nm	546nm	26nm	496nm	482nm	-14nm	475nm	-21nm
Perylene	449nm in benzene	555nm		555nm		440nm	475nm	35nm	488nm	48nm

Fig. 39a. Ultra-Violet Reflectance Spectrum of Methylene Blue on

Pigment A.

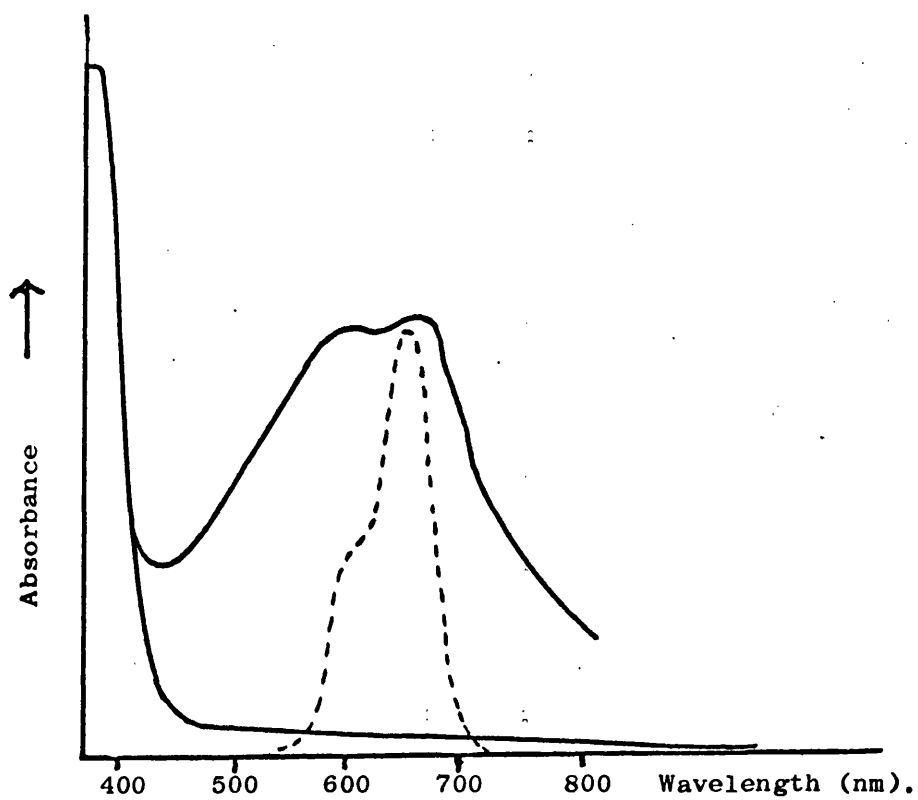
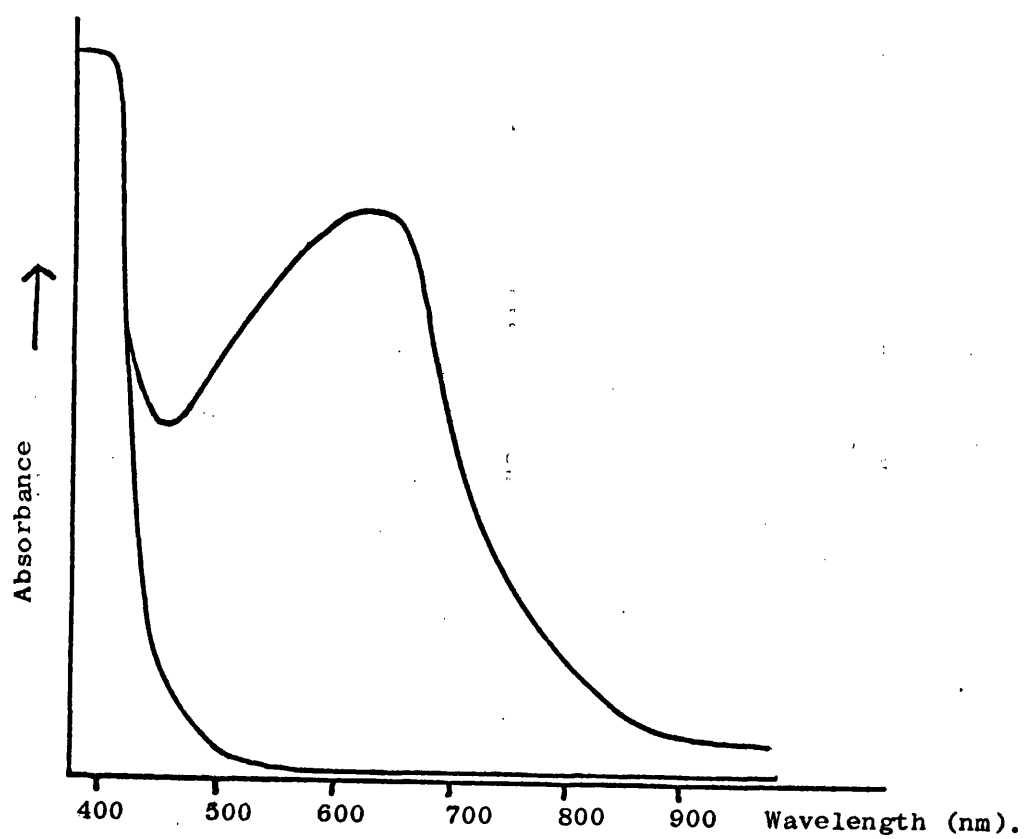


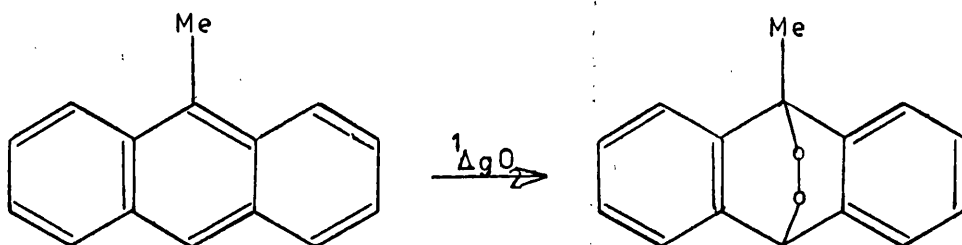
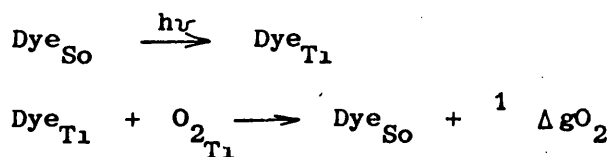
Fig. 39b. Ultra-Violet Reflectance Spectrum of Methylene Blue on Zinc

Oxide.



4.3 Sensitized Photo-oxidation of 9-methylanthracene by Methylene Blue on Titanium Dioxide.

9-Methylanthracene undergoes photo-oxidation sensitized by dyes in solution in the presence of oxygen¹²¹. This occurs via the sensitized formation of singlet oxygen.



The sensitizing ability of methylene blue on pigment A was followed by the photo-oxidation of 9-methylanthracene

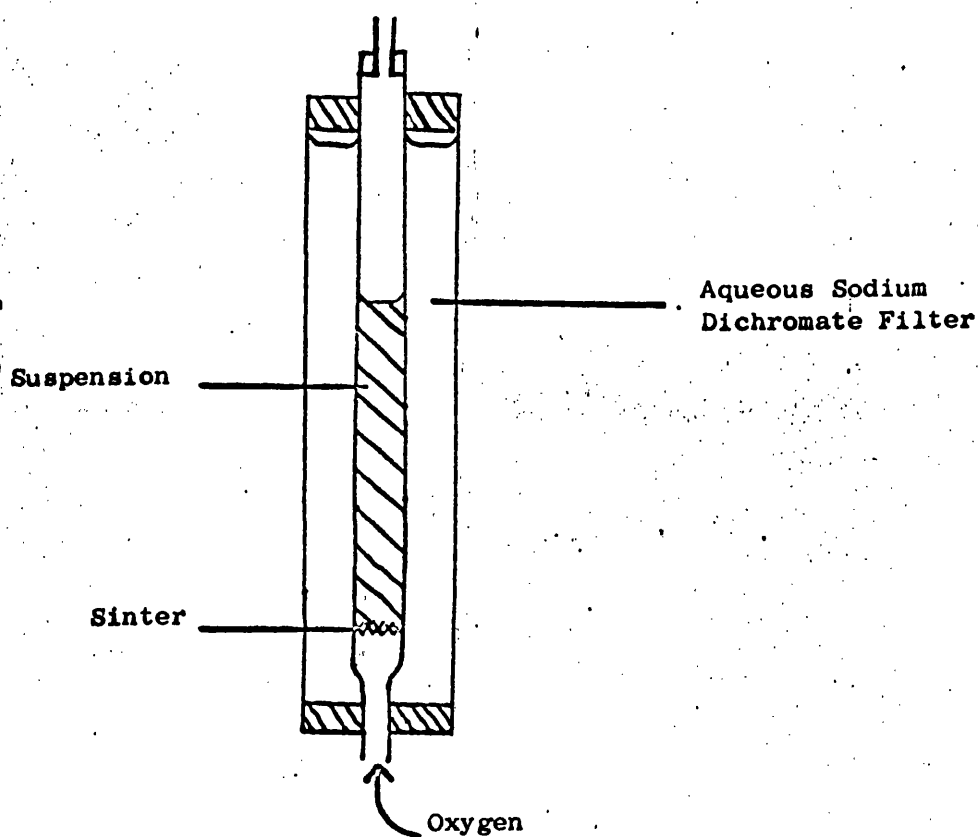
4.3(a) Experimental.

A suspension of pigment A containing 1% w/w methylene blue was prepared in 20ml of a 1.75×10^{-4} M solution of 9-methylanthracene in sodium dried benzene by use of a Dawe Instruments ultra sonic probe for a period of five minutes. Methylene blue is insoluble in dry benzene.

The suspension was placed in the apparatus in fig. 40. The sodium dichromate solution filters out ultra-violet light which would cause photo-dimerization of 9-methylanthracene. Oxygen flows through the suspension from the bottom of the apparatus which aids the maintenance of a stable suspension. The suspension was irradiated by a bank

of daylight tubes surrounding the apparatus. Changes in the concentration of 9-methylanthracene were followed by ultra-violet absorption spectroscopy; small samples of suspension being taken, the pigment centrifuged down and the optical density of the solution being measured at 370nm.

Fig. 40.



4.3(b) Results.

The optical density of the 9-methylanthracene solution was found to decrease when irradiated in the presence of methylene blue containing pigment suspension. The decrease in optical density of 9-methylanthracene with irradiation time for 20mls of suspension containing 0.01g, 0.02g, and 0.04g of 1% w/w methylene blue on pigment

A are plotted in fig. 41. The slope of the lines are for 0.01g, 6.0×10^{-9} moles/s, for 0.02g 5.9×10^{-9} moles/s, and for 0.04g, 6.0×10^{-9} moles/s.

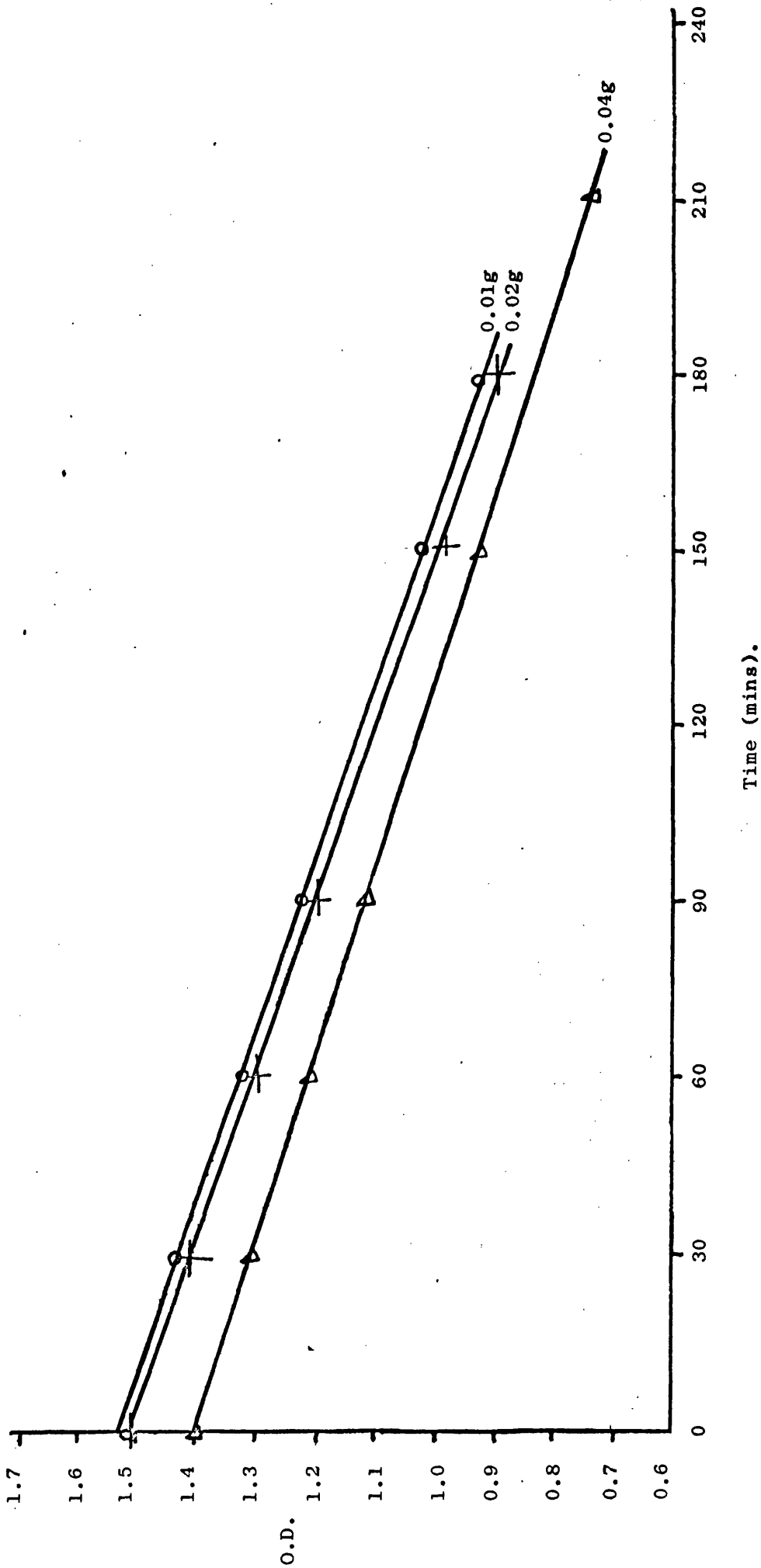
4.4 Discussion.

The parts of the fluorescence spectra where the fluorescence intensity goes off scale is due to reflected light. This occurs when the excitation wavelength and the detection monochromator setting are of comparable wavelength and the photomultiplier tube receives light reflected from the titanium dioxide. This problem occurs with both measurement of fluorescence and excitation spectra. To partly overcome this problem of separating reflected light from the emission, increasingly shorter wavelengths of excitation light can be used so that the observation of reflected light is complete before the wavelengths at which fluorescence occurs are reached. Likewise for recording excitation spectra the longest wavelength part of the fluorescence spectrum is used so that the effective excitation wavelengths have been passed before reflection occurs.

Attempts at recording the excitation spectra of the pigments alone were unsuccessful, with only reflected light being observed.

The difference in the wavelength of the higher energy fluorescence band for anatase and rutile pigments, 406nm and 420nm, may be due to the difference in their absorption spectra. If fluorescence occurs at wavelengths within the pigment absorption band then this light would be reabsorbed by the pigment and therefore not observed. Rutile pigments absorb to slightly longer wavelengths than anatase and the effect of this on the shorter wavelength fluorescence band would be to distort the band

Fig. 41. Photo-Oxidation of 9-methylanthracene.



so that it was centred at a longer wavelength. The fluorescence occurs with excitation wavelengths of band gap energy and therefore seems to be concerned with band gap transitions.

Only three of the four fluorescence peaks of anthracene appear; the one of shortest wavelength (378nm in ethanol solution) is absorbed by the pigment. The second peak, 400nm in ethanol¹²² has undergone a shift to 423nm. The most interesting feature concerns the excitation spectra of anthracene fluorescence. In ethanolic solution the excitation spectrum maximum is at 368nm but on the pigments this has been shifted to 418nm and 408nm on pigments A and I respectively, i.e. away from the absorption wavelengths of the pigments. When excitation wavelengths of band gap energy are used the anthracene fluorescence is of low intensity which suggests the possibility of energy transfer from the excited anthracene molecule to the pigment. For molecules whose excitation wavelengths lie outside the titanium dioxide absorption band, excitation with band gap light produces only the titanium dioxide fluorescence spectrum. Fluorescence quenching for λ excitation = 365nm has been reported for dyes on zinc oxide¹¹⁹.

Perylene in ethanol solution fluoresces at 450nm_(max), 475nm, 505nm and a small band at 555nm. The increase in the fluorescence at 555nm when on titanium dioxide may be due to the dimer fluorescence¹²³. The excitation spectrum maximum at 475nm may also be due to excitation of the dimer.

Methylene blue is known to form dimers and trimers in concentrated aqueous solutions. The monomer has λ max = 665nm and a slight shoulder at 615nm; the dimer has λ max = 605nm and the trimer has λ max = 575nm¹²⁴. In methanol solution λ max = 655nm for the monomer with a shoulder at

605nm. The general broadness of the reflectance spectrum of methylene blue on titanium dioxide and the shifting of λ_{\max} to 600nm may be attributed to dimers and trimers on the pigment surface.

Energy transfer from triplet methylene blue on titanium dioxide to oxygen still occurs and methylene blue on titanium dioxide could be used as a convenient sensitizer since it allows methylene blue to be used in solvents in which it is insoluble and separation of products from methylene blue only requires filtration.

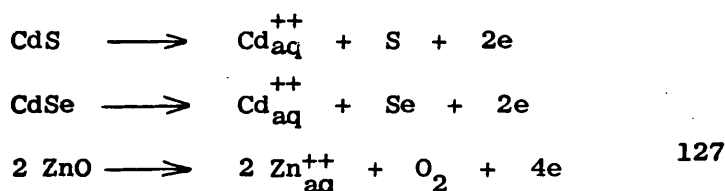
CHAPTER 5

PHOTO-ELECTRIC PROPERTIES OF TITANIUM DIOXIDE

CELL SYSTEMS.

5.1 Introduction.

Photovoltaic effects have been known to occur in binary compounds for many years since Becquerel discovered the photovoltaic properties of silver chloride.¹²⁵ Williams¹²⁶ made a survey of binary semiconductors showing photovoltaic effects by irradiating single crystals in contact with an electrolyte using a saturated calomel reference electrode and measuring the voltage change, and the direction of the change brought about by light. He divided the semiconductors into two main types; those in which the photovoltaic effects bring about a chemical reaction of the electrode material itself which would eventually lead to the destruction of the electrode, and those which are inert. For example the reactions found to occur at irradiated cadmium sulphide, cadmium selenide, and zinc oxide electrodes have been shown to be



The inert electrodes such as gallium arsenide participate in an exchange of electrons with an oxidation-reduction couple in solution. Titanium dioxide electrodes are not decomposed by light and so belong to the second type of electrodes. Williams found that n type semiconductors gave negative photovoltaic effects, i.e. upon irradiation the potential change is such that the semiconductor electrode becomes negative with respect to the reference electrode; for example this occurred with ZnS, CdS, CdSe, and ZnO. Conversely p type semiconductors such as CuI, Cu₂O and AgBr showed positive photovoltaic effects.

Attention has only recently been turned to titanium dioxide photo-electric effects for a number of applications. These involve its potential use in cell systems for the conversion of solar energy,¹²⁸⁻⁹ its application in photographic processes,¹³⁰⁻¹³² and the development of rectifying behaviour.¹³³⁻¹³⁵ Studies of the photo-electric properties of titanium dioxide can be broadly divided into two kinds, those involving its photo-electric properties when in contact with electrolytes (usually aqueous), and those studies of photoconductivity, and contact potentials where the oxide is either in contact with gases or is in vacuum.

Fujishima¹²⁸⁻⁹ observed oxygen evolution upon irradiation of a reduced titanium dioxide single crystal electrode in an aqueous cell system at the titanium dioxide electrode, and hydrogen evolution at the platinum black counter electrode. This system was used for an electro-chemical determination of the photo-reduction of methylene blue on titanium dioxide.¹³⁶ An open circuit potential of one volt was obtained for a system comprised of a reduced titanium dioxide layer on titanium, formed by oxidation of titanium, and a 5N potassium hydroxide electrolyte.¹³⁷ A cell system using a reduced titanium dioxide crystal with an alkaline electrolyte at the titanium dioxide electrode and acidic electrolyte at the platinum counter electrode was reported to give an enhanced emf.

Memming¹³² recently reported an investigation of the photocatalytic deposition of palladium on titanium dioxide layers. These layers were formed on titanium or stannic oxide substrates by spraying a titanium acetylacetonate solution onto the hot substrate. This system in an aqueous electrolyte also gave oxygen evolution from the titanium dioxide electrode upon irradiation.

These single crystals and reduced layers of titanium dioxide designed to give maximum photo-effects can show little resemblance to pigmentary titanium dioxide where the emphasis has been to produce samples with minimal photocatalytic properties.

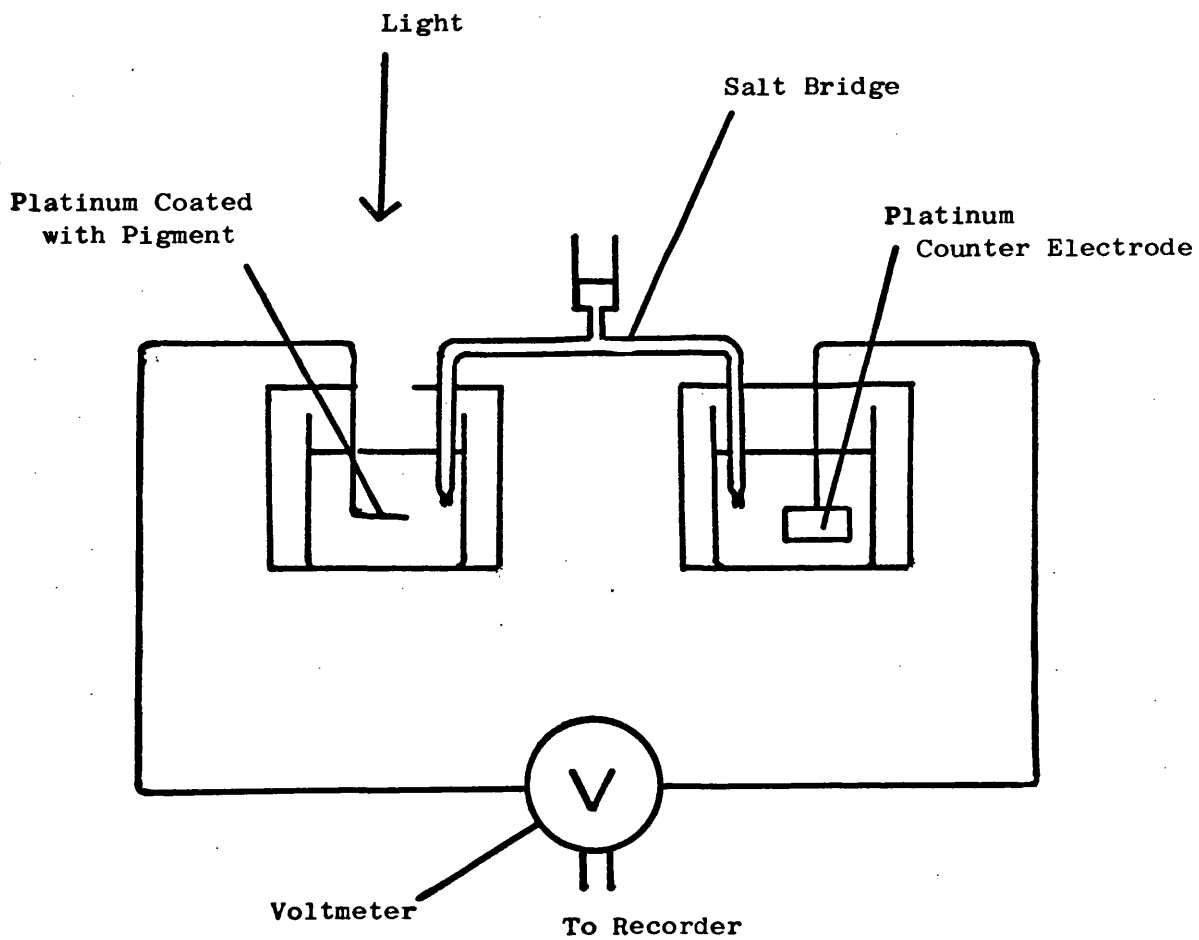
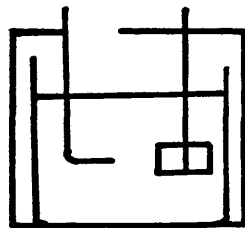
Studies of the photo-electric properties of single crystals of titanium dioxide in contact with gases have revealed that the photo-desorption of oxygen is involved in the photoconductivity of titanium dioxide and adsorption of oxygen involved in the decay of the photo-effect after illumination has ceased.¹³⁸

Contact potential measurements were made of titanium dioxide in a binder relative to a platinum reference electrode in vacuum and in air, the photo responses being related to adsorption-desorption phenomena.¹³¹ A related work on titanium dioxide single crystals and powder layers concluded that the photo-currents in powder layers were determined by surface adsorption while for single crystals this was only partially true, the slow decay times of photocurrents for single crystals being due to slow trap emptying.¹³⁰

5.2 Photo-Voltage Measurements.

5.2(a) Experimental.

For photo-voltage determinations of pigments the apparatus in Fig. 42 was used. Two types of cell systems were used, which were, (1) a double cell system where the platinum counter electrode and electrode containing titanium dioxide were in separate compartments connected by a glass tube salt bridge of 0.1M aqueous potassium chloride solution. A syringe was used as a reservoir for the bridge. In this system additions of material to the 0.1M KCl electrolyte could be made

Fig. 42. Apparatus for Photo-Voltage Measurement.Single Cell

separately to each half cell. (2) A cell system, which avoids the disadvantages of using a salt bridge. The double cells were constructed from cut down 100 ml beakers enclosed in plastic holders. The single cell was made from a cut down 150 ml beaker enclosed in a similar plastic holder.

Electrolytes were prepared with deionized water, the pH of the unbuffered electrolyte being adjusted to pH7 by small additions of potassium hydroxide solution and hydrochloric acid, experiments were performed at room temperature.

The potential difference between the two electrodes was measured on a Phillips High Impedance DC Microvoltmeter and for the scale used the voltmeter had an impedance of $10^8 \Omega$. The chart recorder output from the voltmeter was used to obtain a plot of potential difference versus time. Three light sources were used; firstly a 500 watt and a 200 watt high pressure mercury lamp with the light beam being focussed vertically onto the titanium dioxide electrode were used, quartz lenses being used for the 500 watt lamp system and pyrex lenses for the 200 watt lamp system together with a filter transmitting light of wavelength 300nm - 400nm. A 2Kw xenon lamp was used with the light beam being focussed by pyrex lenses through the side of the cell compartment on to the titanium dioxide electrode. For this system an aqueous saturated copper sulphate solution in a 1500 ml pyrex beaker circulated through copper tubing cooled in ice was placed in the light beam as a heat filter. A glass filter transmitting only the wavelengths 300 nm to 400 nm was also placed in the light pathway.

The potential generated across a 100Ω resistor by a selenium photo-cell was taken as a measure of the light intensity. The selenium

photocell was positioned in the vertical light beam of the 500 watt lamp and the light intensity adjusted by a Variac controlling the lamp prior to measurements. For the system using a 200 watt lamp the selenium cell was positioned to receive scattered light from the optical system for light intensity measurements. For the xenon lamp system the selenium cell was positioned in the light beam for intensity measurements prior to photo-effect measurements.

The electrodes were made of 15mm x 30mm platinum mesh, the counter and test electrodes being identical. The method of preparation of an electrode using titanium dioxide poses some problems. The method used by Gerisher¹³⁹ of zinc oxide suspensions in contact with an inert electrode can be seen to have several disadvantages; these include, (a) obtaining a sufficient light intensity at the electrode since the pigment particles not in contact with the inert electrode would absorb radiation while not contributing to a photo-effect, hence the inert electrode would have to be placed near to the electrolyte surface. (b) Ensuring that no light reaches the counter electrode in a single cell system which would create an opposing photo-effect. (c) The maintenance of stable suspensions of titanium dioxide in water over extended periods would cause major difficulties.

The method of electrode preparation chosen was to deposit a layer of pigment particles onto the platinum support. The physical stability of such a coating might be expected to be small but coatings prepared were found to have adequate stability. A simple technique of "painting" an aqueous slurry of pigment onto the platinum with a small brush and drying the coating with a hot air blower was first used and this was developed into two standard procedures for electrode preparation.

Method 1.

0.2 g of pigment was dispersed in 5ml of deionized water using an ultra-sonic bath. The platinum electrode was immediately dipped into the suspension, removed and the coating dried with a hot air blower.

Method 2.

2 g of pigment were dispersed in 25 ml deionized water by use of a Dawe Instruments Ultra-Sonic Probe for one minute at power setting 5. This dispersion was then used for electrode preparation as in Method 1.

After experimentation the electrodes were cleaned by removing the pigment coating by using the ultra-sonic probe in water. The electrodes were then dried and placed in molten potassium bisulphate for several minutes. The bisulphate was removed from the platinum in boiling hydrochloric acid and the platinum washed in deionized water.

5.2(b) Results.

Upon connecting a titanium dioxide coated electrode into the cell system the dark potential of this electrode with reference to the platinum can be measured. It was noted for the pigments that the dark potentials were negative when measured soon after immersion of the TiO_2/Pt electrode in the electrolyte. The dark potentials drift quite rapidly at first towards positive potentials and then more slowly taking approximately two hours to give a good straight base line for the dark potential. The dark potential generally equilibrated at small positive values, the actual values of the dark potentials being non-reproducible.

Irradiation of the TiO_2/Pt electrode was found to cause the potential of the TiO_2/Pt electrode to move towards negative potentials with respect to the platinum counter electrode. A typical response

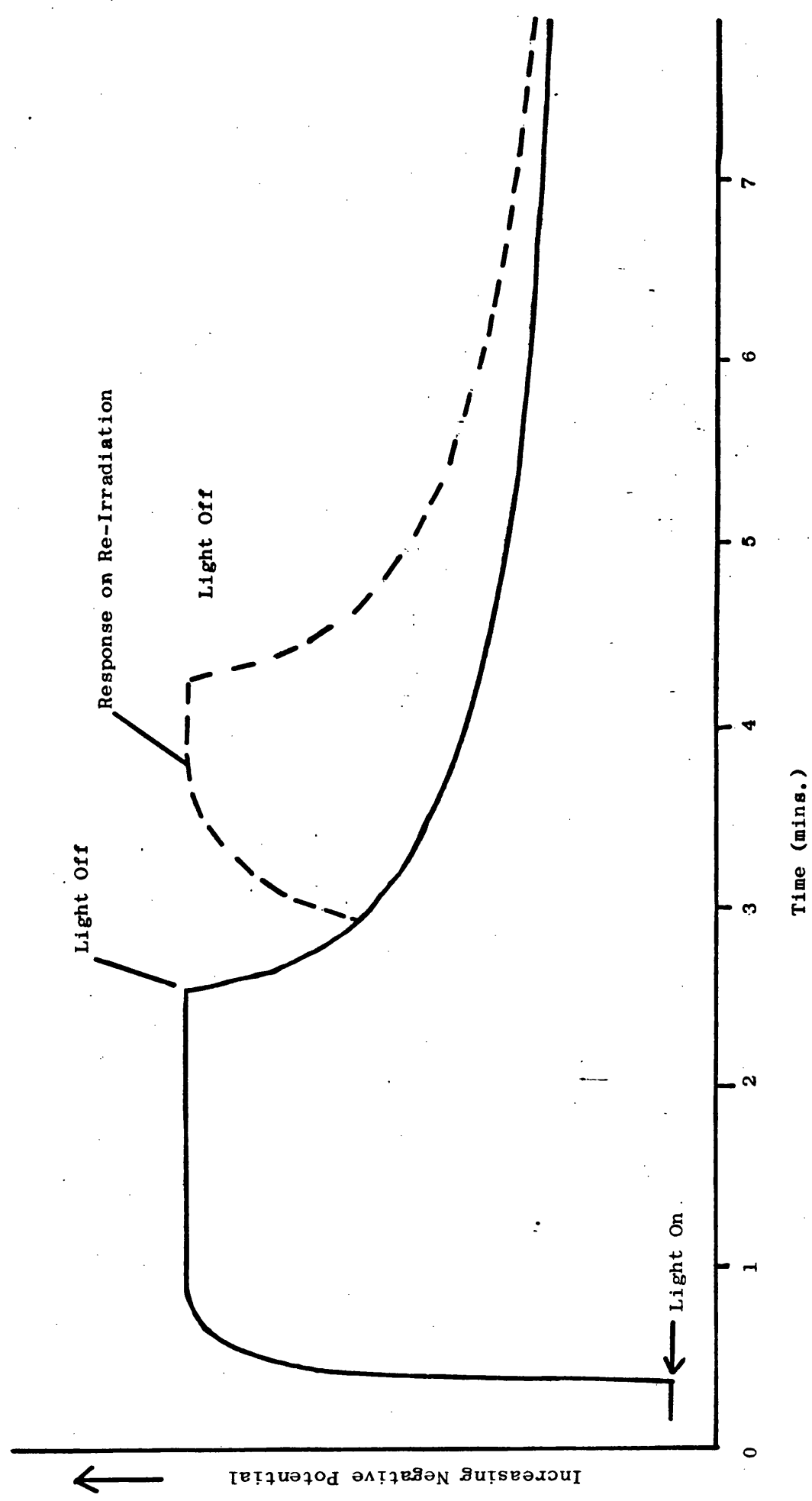
is illustrated in Fig. 43. The voltage changes rapidly at first and then rounds off to give a level potential. The photo-voltage is the difference between the dark potential and the level potential reached upon irradiation. On switching the light source off the potential decays back towards the dark potential value, sharply at first, then at a decreasing rate; the potential taking as much as thirty minutes to fall back to the dark potential. If the light beam is interrupted for a few seconds the potential falls back towards the dark potential but returns to the same potential achieved before when the electrode is re-irradiated (Fig. 43 dashed line).

The photo-voltages were found to increase with the time that the TiO_2/Pt electrode has been immersed in the electrolyte. For example the photo-voltage of an electrode coated with pigment E was determined to be only 5 mv 20 minutes after immersion (measured against a drifting dark potential base line), 20 mv two hours after immersion, and 53 mv after being immersed overnight. After immersion overnight the maximum photo-voltage was reached, immersion for longer periods did not lead to an increase in the photo-voltage. When the TiO_2/Pt electrode was not connected into the cell system but left immersed in electrolyte overnight the maximum photo-voltage was observed upon connecting it into the cell, the dark potential usually being small and positive.

Effect of Oxygen.

The effect on the photo-voltage of saturation of the electrolytes with oxygen was investigated by bubbling oxygen and oxygen free nitrogen into the cell compartments of the double cell system for periods of twenty minutes. Thus both cells were saturated with nitrogen, nitrogen saturation at the pigment A/Pt electrode, oxygen saturation at the

Fig. 43. Typical Photo-Voltage Response of Titanium Dioxide.



platinum counter electrode, oxygen saturation at both electrodes, oxygen saturation at the pigment A/Pt electrode and nitrogen at the platinum counter electrode. Bubbling gases through the electrolytes disturbs the dark potentials and therefore before each photo-voltage measurement the flow of gas through the electrolyte was stopped but the gases were blown on top of the electrolytes in each compartment. The dark potential was allowed to steady out to a straight base line after each gas treatment before the electrode was irradiated. Within experimental error the photo-voltages were found to be the same for whatever combination of gases that were used. The dark potentials to which the system equilibrated after each gas treatment were -

Pigment A/Pt	Pt	Dark Potential (mv)
N ₂	N ₂	+100
N ₂	O ₂	- 57
O ₂	O ₂	+ 46
O ₂	N ₂	+180

The values of the dark potentials were non reproducible, but the order of dark potentials were the same.

Variation of Photo-Voltage with Light Intensity.

The light intensity reaching the titanium dioxide electrode was varied by placing neutral density filters in the light beam. The photo-voltage variation was measured for each relative light intensity available starting with the lowest intensity since the level potential value is reached more quickly when exposing the titanium dioxide

electrode to increasing light intensity than when reducing the light intensity and allowing the photo-voltage to decay downwards to another level value. The light intensity variation of photo-voltage was measured for several pigments, the maximum light intensity not being the same as that used in a later comparative study of photo-voltages.

The increase in photo-voltage is seen to level off towards a maximum value (Fig. 44a). A graph of photo-voltage versus log (Light Intensity) gives a good straight line plot as shown in (Fig. 44b).

Determination of the Photo-Voltages of Pigments.

The photo-voltages of the pigment samples were determined after the pigment/Pt electrode had been immersed in electrolyte in the cell system overnight. A second determination of the photo-voltage was performed on an electrode which had been stored in electrolyte overnight and then quickly placed in the cell system. The results are illustrated in bar diagrams. The first set of results, Fig. 45a, were determined using the double cell system irradiated with the 500 watt mercury lamp. The titanium dioxide electrodes were prepared by method 1. Gases were not bubbled through the electrolytes which were unbuffered at pH 7.

The second set of results, Fig. 45b, were determined using a single cell system, illuminated by the 200 watt mercury lamp, the electrolyte being unbuffered pH 7.

The third set of results, Fig. 45c, refer to photo-voltage measurements of pigments immersed overnight in a pH 7 buffered 0.1 M KCl electrolyte (B.D.H. mixed phosphate buffer) using a single cell illuminated by the 200 watt mercury lamp. The equilibrium dark potentials for the electrodes are recorded in Tables 5, 6, and 7.

Fig. 44a. Variation of Photo-Voltage with Light Intensity.

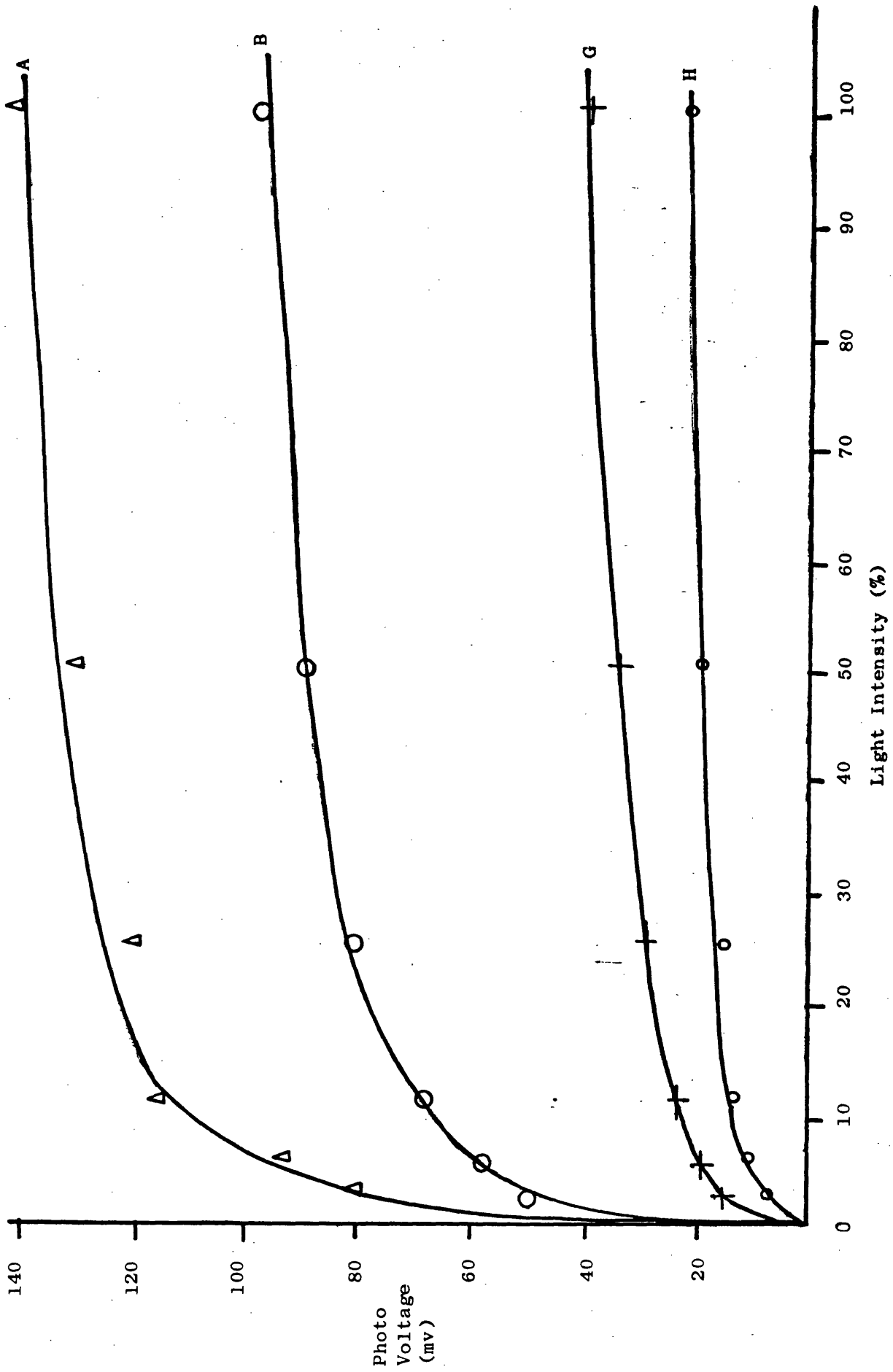


Fig. 44b. Variation of Photo-Voltage with Log (Light Intensity).

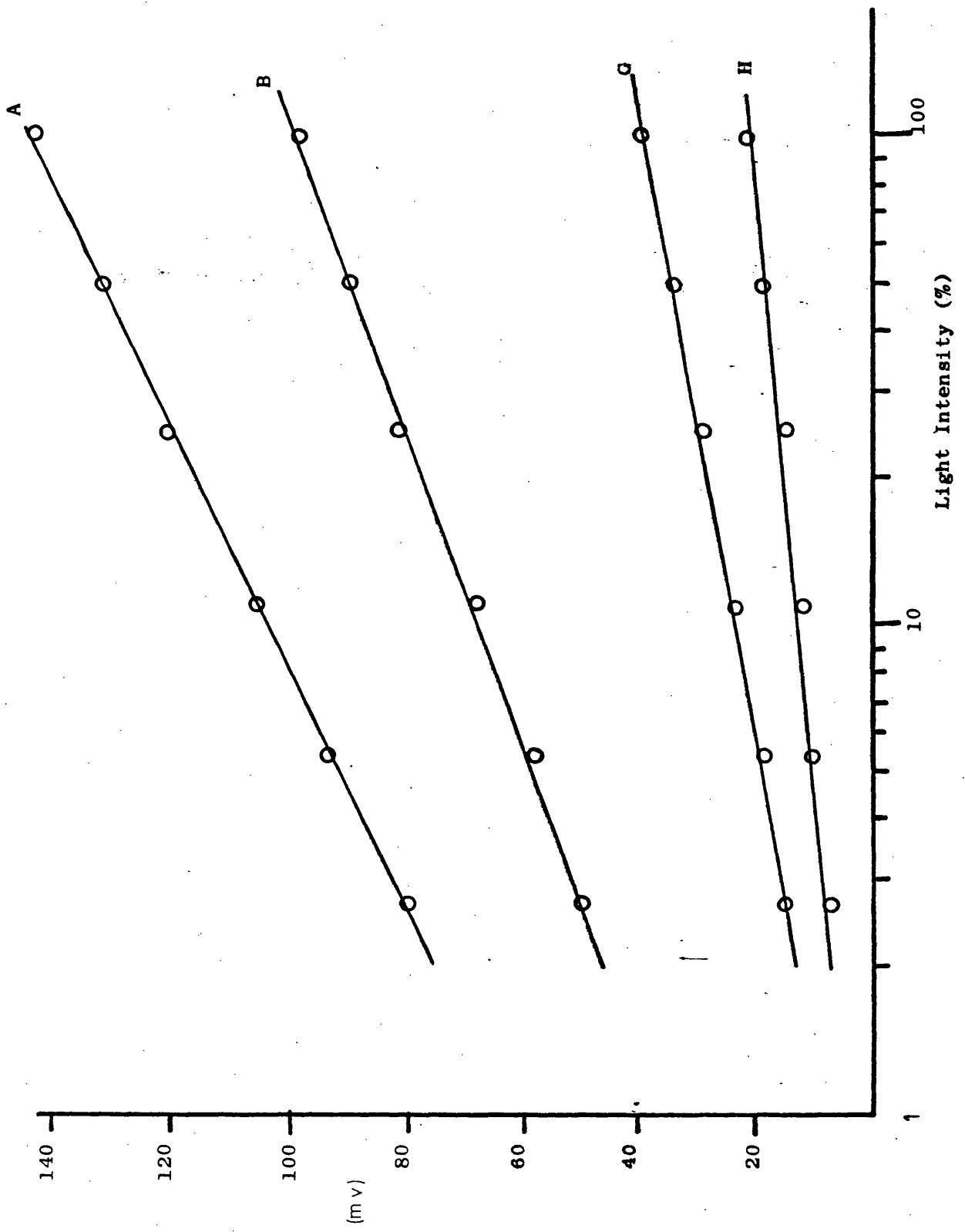


Fig. 45a,b,c. Photo-Voltage Measurements.

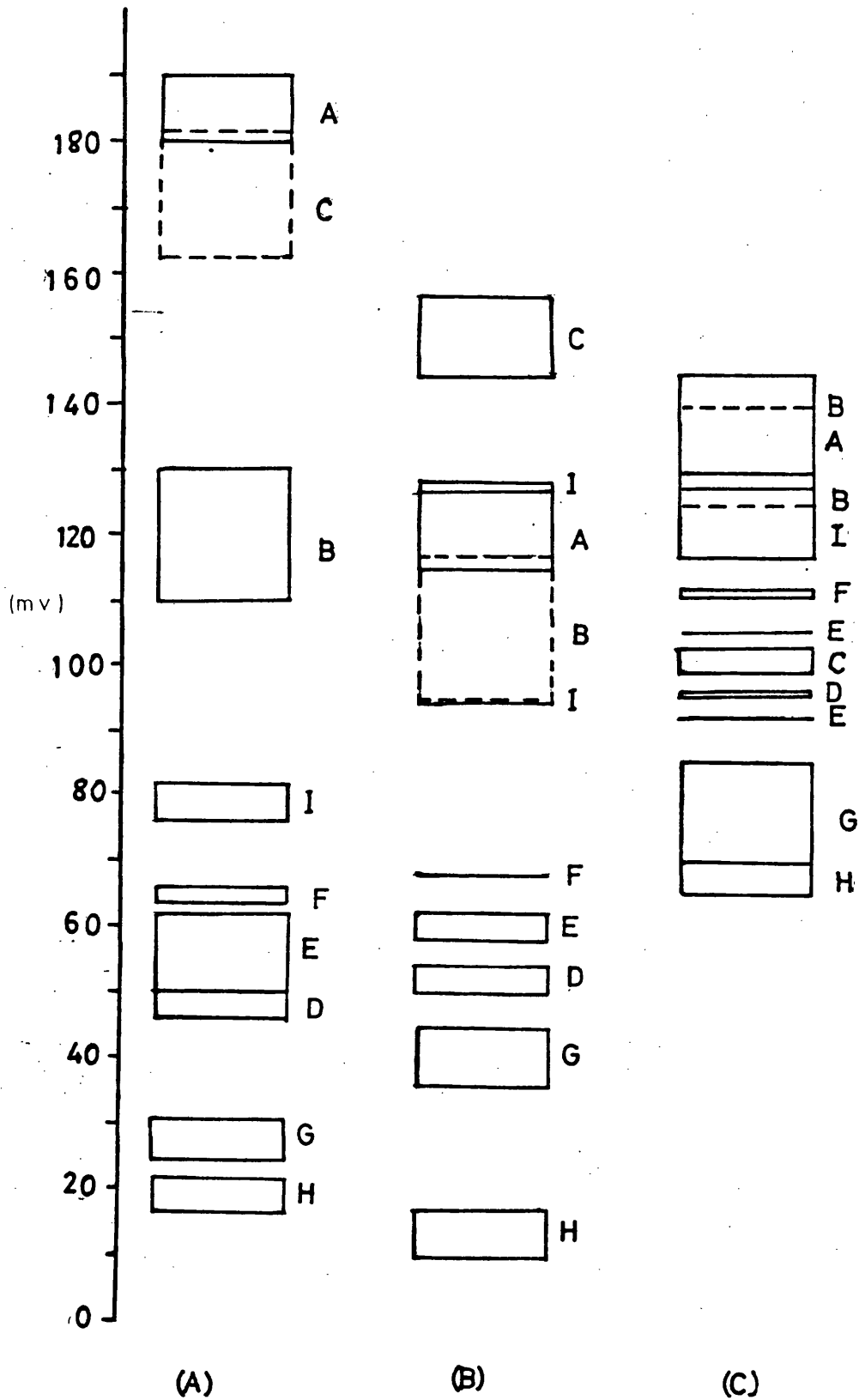


TABLE 5 Photo-Voltage and Dark Potentials (First Set).

Pigment	Dark Potential (mv)	Photo-Voltage (mv)
A	- 36	190
A	+ 19	180
B	+ 99	130
B	+ 78	110
C	+ 85	162
C	+ 20	181
D	+ 30	50
D	+ 50	46
E	+ 125	50
E	+ 5	62
F	+ 45	66
F	+ 19	63
G	+ 35	31
G	+ 35	25
H	- 27	17
H	+ 3	23
I	+ 81	82
I	+ 66	76

TABLE 6 Photo-Voltages and Dark Potentials (Second Set).

Pigment	Dark Potential (mv)	Photo-Voltage (mv)	Weight of Pigment (mg.)
A	+ 16	127	14
A	+ 18	115	9
B	+ 135	95	15
B	+ 35	117	11
C	+ 35	145	18
C	+ 10	157	14
D	+ 46	54	14
D	+ 45	50	12
E	+ 40	62	21
E	+ 40	58	15
F	+ 25	68	11
F	- 55	68	10
G	+ 98	36	16
G	+ 78	45	11
H	+ 115	17	16
H	+ 80	10	11
I	+ 170	95	4
I	+ 109	128	10

TABLE 7 Photo-Voltages and Dark Potentials (Third Set).

Pigment	Dark Potential (mv)	Photo-Voltage (mv)	Weight of Pigment (mg)
A	+ 30	145	10
A	+ 10	130	15
B	+ 25	140	17
B	+ 25	125	13.5
C	+ 70	100	11
C	+ 40	103	19
C	+ 8	136	7
C	+ 30	111	9
D	+ 25	95	11
D	+ 18	96	12
E	+ 20	105	11
E	+ 20	92	18
F	+ 20	112	9
F	0	113	9
G	+ 2	86	11
G	+ 20	85	15
H	+ 25	70	9
H	+ 12	65	16
I	+ 8	128	31
I	+ 8	117	21

Measurements of the weight of pigment on the platinum support for the second and third sets of results are given. These were measured by drying the electrodes after experimentation using a hot air blower, weighing the electrode, and weighing the platinum support after it had been cleaned.

Photo-Voltage Decay Kinetics.

If a = level photo-voltage (in mv)

and x = decrease of photo-voltage (mv) time, t , after the irradiation has ceased, then for second order kinetics,

$$\frac{dx}{dt} = k(a - x)^2$$

$$\int \frac{dx}{(a - x)^2} = \int k dt$$

$$\frac{x}{a(a - x)} = kt$$

$$\frac{1}{(a - x)} - \frac{1}{a} = kt$$

$$\frac{1}{(a - x)} = kt + \frac{1}{a}$$

Thus a plot of $\frac{1}{(a-x)}$ versus t would give straight line plots if second order decay kinetics are obeyed, having slope = k and intercept = $\frac{1}{a}$. Figs. 46a and b show second order plots for the photo-voltage decay of the pigments. Values of k appear in Table 8.

Figs. 46a and b show a plot of photo-voltage ($a - x$) versus the

Fig. 46(a). Second Order Plot for Photo-Voltage Decay.

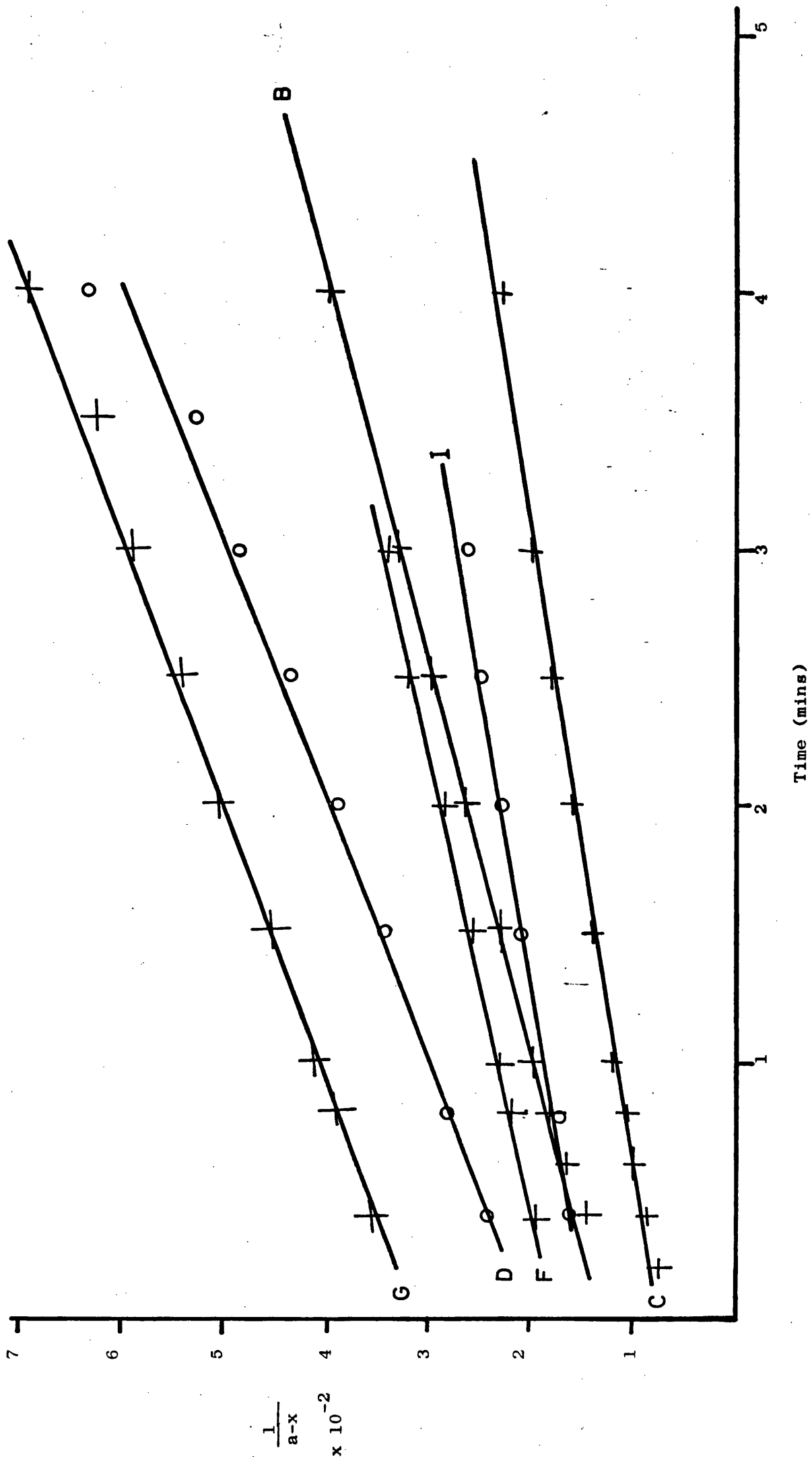
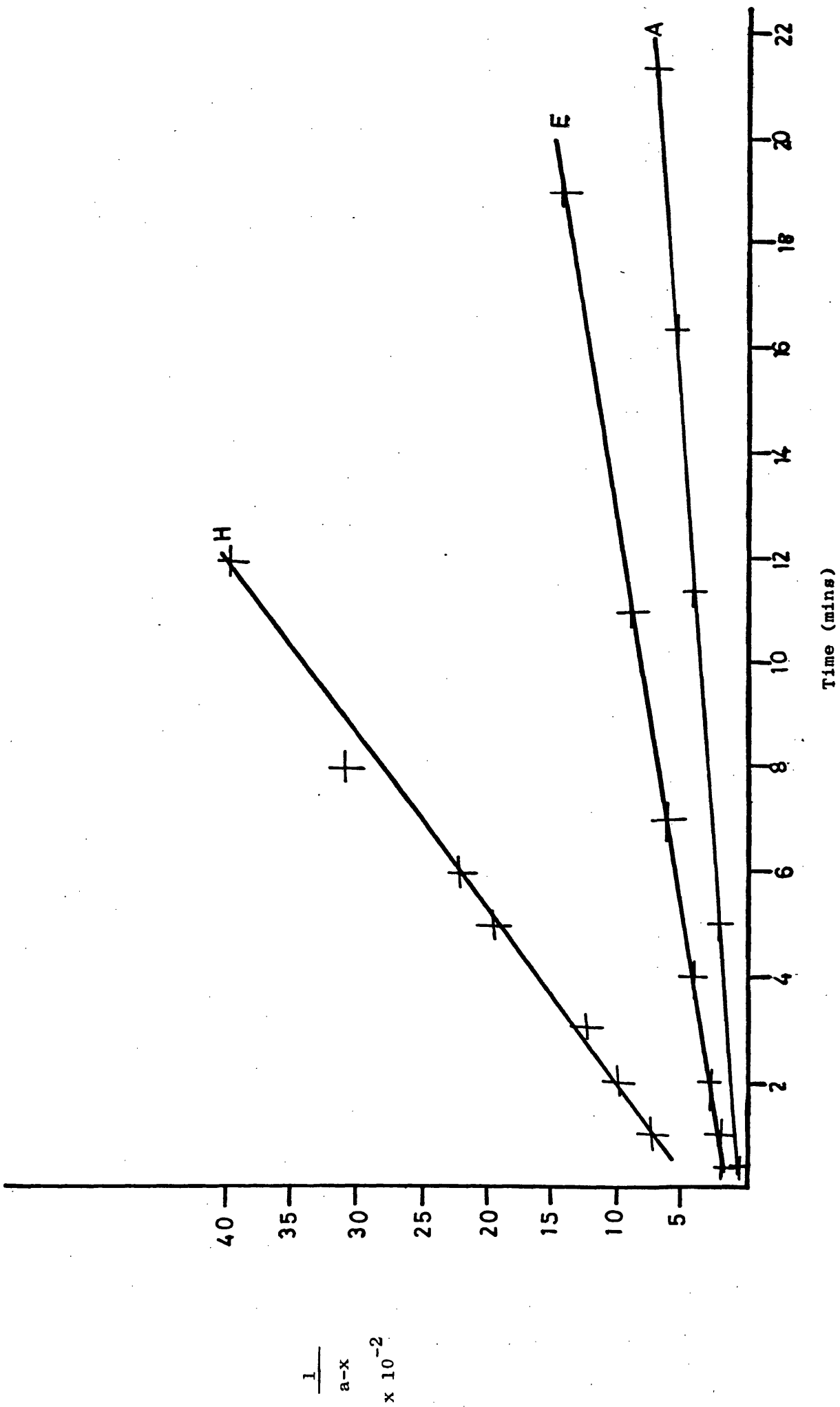


Fig. 46(b). Second Order Plot for Photo-Voltage Decay.



logarithm of the time after irradiation of the electrode has ceased.

TABLE 8

<u>Pigment</u>	<u>$k v^{-1} s^{-1}$</u>
A	5.14×10^{-2}
B	1.18×10^{-1}
C	7.5×10^{-2}
D	1.56×10^{-1}
E	1.1×10^{-1}
F	1.01×10^{-1}
G	1.62×10^{-1}
H	5.0×10^{-1}
I	7.8×10^{-2}

5.2(c) Discussion.

Electrical potential differences appear at the interface between two electrically conducting phases in contact, an example being the electrode potential of a metal in an electrolytic solution. When a semiconductor is in contact with an electrolyte an electrical double layer consisting of excess ions on the surface and an outer layer of oppositely charged ions is formed; these comprise the Helmholtz layer and its structure is not unlike that of a capacitor.

The charged layer on the surface creates an equal and opposite space charge layer in the semiconductor. If the net excess charge on the surface of the semiconductor is negative the electron energy levels of the valence band and conduction band in the space charge layer will be raised, and conversely the energy level for holes will be lowered.¹⁴⁰

Fig. 47(a). Decay of Photo-Voltage versus Log (time).

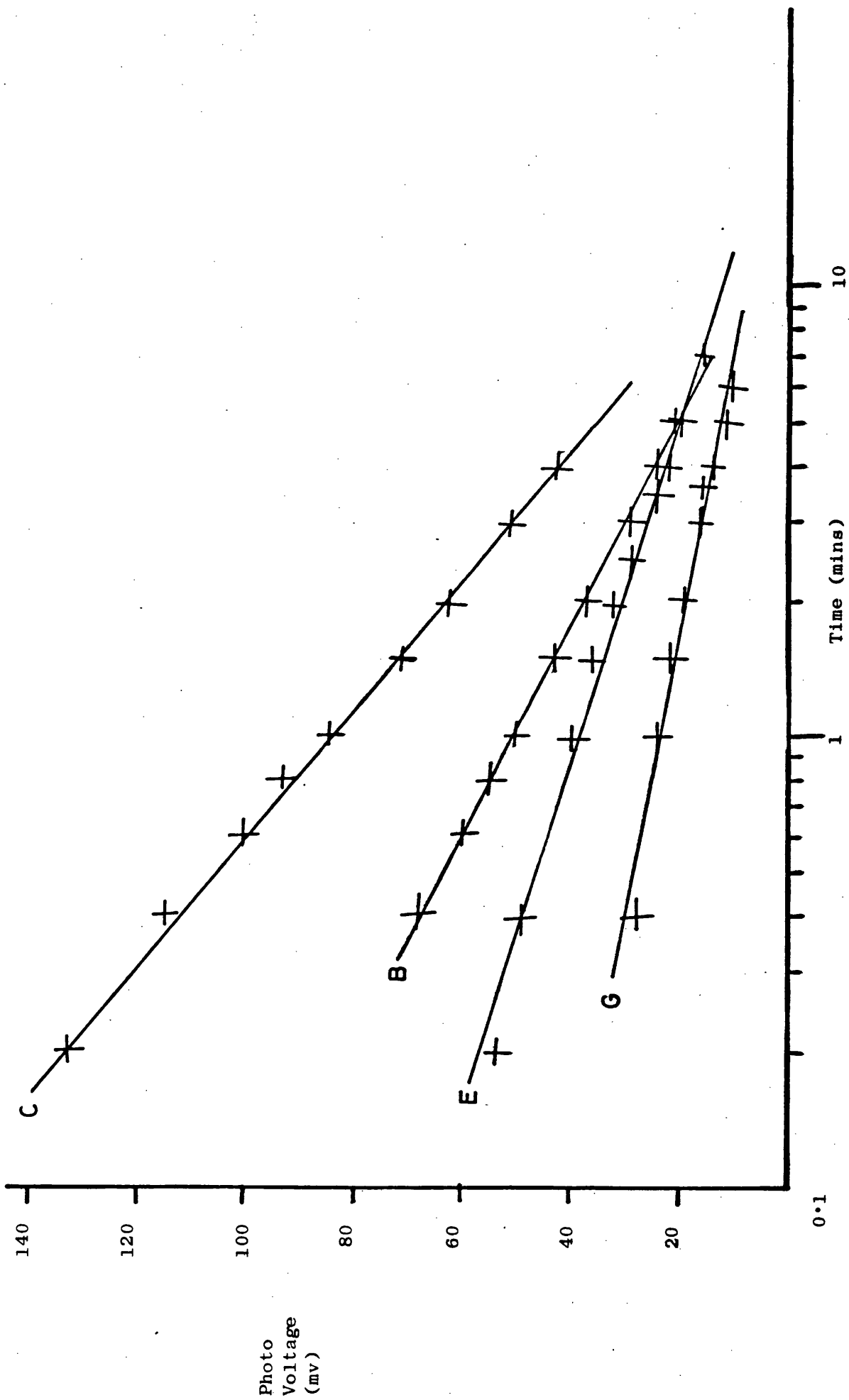
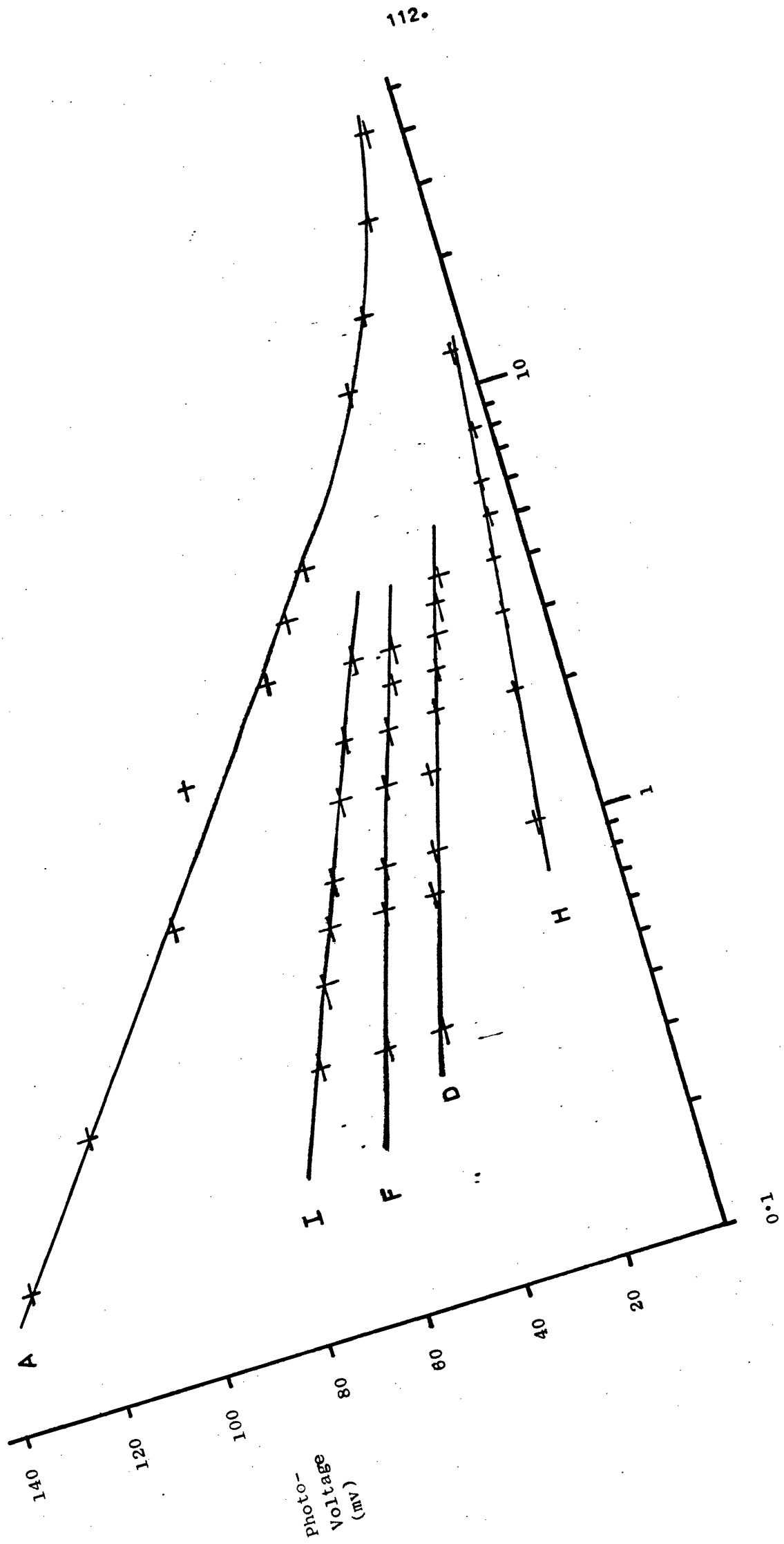


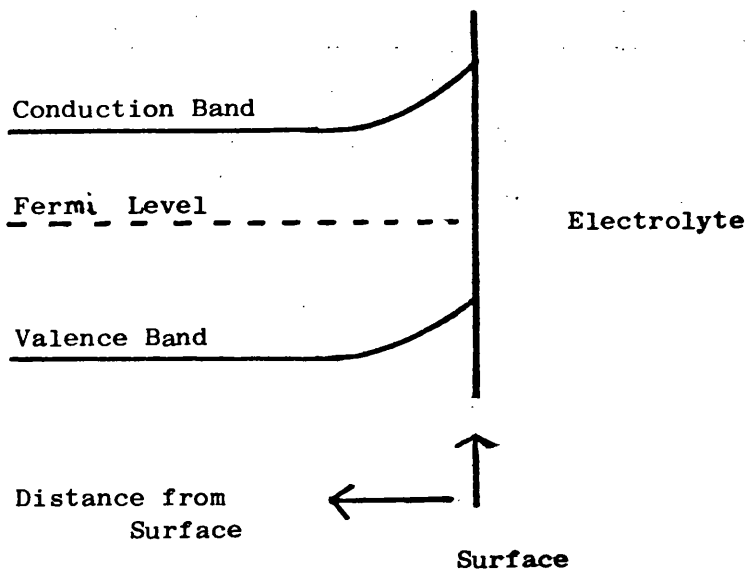
Fig. 47(b). Decay of Photo-Voltage versus Log (time).



The interior of the semiconductor will be relatively positively charged with respect to the surface. For n type titanium dioxide this situation will result in the formation of a spacecharge layer which is a depletion layer, i.e. this region will be devoid of electrons and holes.

Fig. 48 shows the band structure for titanium dioxide in contact with electrolyte with upward band bending at the surface.

Fig. 48



Upon exposure of titanium dioxide to light of band gap energy electron-hole pairs are created in the surface region since light absorption occurs within this region. Electrons are attracted towards the positive interior, i.e. they can flow down the conduction band energy level away from the surface. Holes in the valence band are attracted towards the negatively charged surface; the accumulation of holes at the surface and the movement of electrons towards the interior will reduce the band bending at the surface. It is this reduction in the band bending under the action of light which gives the observed photo-voltage.

Immersion of the pigment/Pt electrode in the electrolyte at first gives negative dark potentials indicating that the movement of

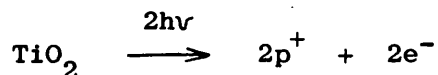
electrons in the dark would be from the pigment to solution. This process seems to reach equilibrium slowly. The transfer of electrons from titanium dioxide to solution in the dark would gradually make the titanium dioxide electrode the positive terminal of the cell. The phenomena of the photo-voltage increasing with time of immersion of the pigment in the electrolyte can be explained by the slow build up of the space charge and Helmholtz layers. If we view the photo-voltage as the change in band bending upon irradiation, then the increase of photo-voltage with time indicates that the upward band bending is increasing with time, this being caused by the pigment and electrolyte slowly coming to equilibrium.

This effect of increasing photo-activity of titanium dioxide pigments with immersion time in liquids has been noted for the photo-catalytic oxidation of isopropanol by pigments.¹⁴¹

The variation of photo-voltage with the logarithm of the light intensity is predicted from theory for n type semiconductors.¹²⁷ The logarithmic response means that the photo-voltages tend towards limiting values with increasing light intensity (Fig. 44a), this would correspond to a change in the band bending under illumination to the flat band condition where the valence and conduction band levels are flat up to the surface.

The direction of the photo-voltage, (titanium dioxide electrode moving towards negative potentials), indicates that the reaction giving rise to the photo-voltage is a transfer of electrons from the electrolyte to the titanium dioxide. Electrons promoted to the conduction band travel the external circuit, arrive at the platinum counter electrode and react with a solution species. In the photo-voltage experiment virtually no current is allowed to flow and therefore no reaction will occur.

The reaction of a water molecule with a photo-hole at the titanium dioxide surface was proposed as a reaction mechanism¹²⁹



At the titanium dioxide

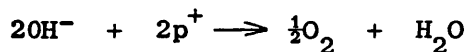


and at the platinum counter electrode



this results in oxygen evolution at the titanium dioxide electrode and hydrogen evolution at the counter electrode.

Perhaps a better formulation of the reaction is the reaction of hydroxide ions with photo-holes.¹⁴² At titanium dioxide

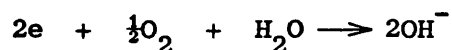


at counter electrode



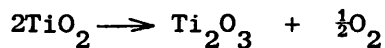
The reaction at titanium dioxide above is the trapping of a hole by a surface OH^- ion forming an OH^\cdot radical which is desorbed, and a solution OH^- ion being adsorbed in its place.

Oxygen absorption at the platinum counter electrode was observed by Keeney¹³⁷ instead of hydrogen evolution, however the electrolyte used was 5N KOH. The cathodic reaction proposed was

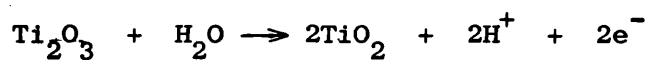


An alternative but equivalent reaction scheme for oxygen evolution

at the titanium dioxide electrode would be oxygen photo-desorption³²



followed by reformation to fully oxidized titanium dioxide by reaction with water.



For all reaction schemes H^+ is formed in solution at titanium dioxide and OH^- at the platinum counter electrode, which indicates that the reaction will be dependent upon the pH of the solution.

Upon irradiation of titanium dioxide the level photo-voltage condition is reached when the rate of promotion of electrons to the conduction band equals the rate at which electrons and holes recombine. Since there is essentially no current flow for the photo-voltage measurement the photo-voltage decay will be by electron-hole recombination in the semiconductor. This can be seen to be a slow process from the decay curves. Memming¹³² has recently noted a long decay time for the photo-voltage of a titanium dioxide film and this can be ascribed to the existence of electron traps which are able to trap out electrons and slow the recombination of holes and electrons.

The recombination would be expected to be a second order process due to it depending upon the concentration of holes and electrons. The photo-voltage decay closely follows second order kinetics (Figs. 46). The plots deviate from straight lines at large t values but this may be due to increasing errors in $\frac{1}{(a-x)}$ since as x increases $(a-x)$ becomes increasingly small and subject to larger errors.

The linear dependence of the photo-voltage ($a - x$) with the logarithm of time indicates a Elovich type decay law found for the photo-voltage decay of titanium dioxide in a binder by Vohl,¹³¹ and also found for the photo-oxidation of ethylene and propylene on titanium dioxide.¹⁴³ The law is indicative of chemisorption phenomena where the chemisorption rate decreases exponentially with the amount adsorbed.

The rate law is of the type

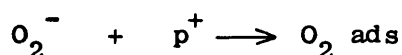
$$\Delta N = \lambda \ln (t/t_0 + 1)$$

where ΔN = increase in concentration of chemisorbed species,

t = time, t_0 and λ are constants.

If adsorbed oxygen molecules act as recombination centres for photo-holes and electrons then the photo-voltage decay rate would depend upon the rate of chemisorption of oxygen. Oxygen being photodesorbed during the irradiation.

Recombination



The photo-voltages of the pigments cover a wide range of values, from around 20 mv to about 200 mv. The photo-voltage determinations are found to spread slightly, this is probably due to non-reproducibility of the electrode preparation as indicated by the measurements of the weight of pigment on the platinum support.

For the first and second set of results the order of the pigments having increasing photo-voltages is essentially the same. The pigments giving the most reproducible photo-voltages are those that disperse

easily and form uniform coatings on the platinum support. Pigments such as C tend to flocculate quickly after ultra-sonic treatment making electrode preparation more difficult.

The order of the pigments as determined by photo-voltage measurement, excluding pigment I is that of the durability of the pigments as established by weathering tests. Thus the uncoated rutile pigments A, B, and C are less durable pigments whereas the coated pigments E, D, G, and H show much smaller photo-voltages and are known to be more durable in paint media. The photo-voltage measurements are able to distinguish between the most durable pigment H and the slightly less durable pigments G, D, and E.

Pigment I (untreated anatase) is the least durable of the pigments but this is not reflected in its photo-voltage. This may be due to it having a different absorption spectrum from rutile pigments, which causes it to absorb less ultra-violet light and therefore it does not protect binders as effectively as rutile pigments. Also the possibility exists that anatase engages in a photo-catalytic mechanism which is not indicated in photo-voltage measurements.

For the third set of results performed in phosphate buffer the range of photo-voltages has been compressed, although the pigment order remains essentially the same. The photo-voltages of coated pigments have been increased dramatically. This is most likely due to the interaction of the pigment surface with the mixed KHPO_4 , Na_2HPO_4 phosphate buffer which increases the band bending and hence increases the measured photo-voltage.

The photo-voltages of the pigments are related to the durability of the pigments, probably by the different extent of the band bending

for each pigment. A larger band bending would lead to more efficient separation of holes and electrons giving a larger photo-catalytic activity and fewer electrons and holes recombining with no net reaction. The role of surface coating can be seen as a method of decreasing the upward band bending at the surface and hence increasing pigment durability.

The determination of photo-voltages provides a quick test method for the estimation of the durability of a pigment avoiding the delay resulting from natural weathering or accelerated weathering tests. Rapid test methods for durability have been developed in the past, relying mainly on chemical reactions. These have included the reduction of pigments by ultra-violet light in the presence of mandelic acid,⁹⁶ photo-bleaching of adsorbed dyes,¹⁴⁴ reaction of silver compounds on titanium dioxide,¹⁴⁵⁻⁶ as well as measuring the drying time of dryerless lacquers pigmented with titanium dioxide.¹⁴⁷

5.3 Photo-Current Measurement.

5.3(a) Experimental.

The apparatus shown in Fig. 49 was used for the measurement of photo-currents. It consists of a single cell with a platinum counter electrode and a pigment/Pt electrode prepared by method 2 and stored in electrolyte overnight. The electrolytes used were pH7 unbuffered 0.1M aqueous potassium chloride and aqueous 0.1M potassium chloride containing phosphate pH7 buffer.

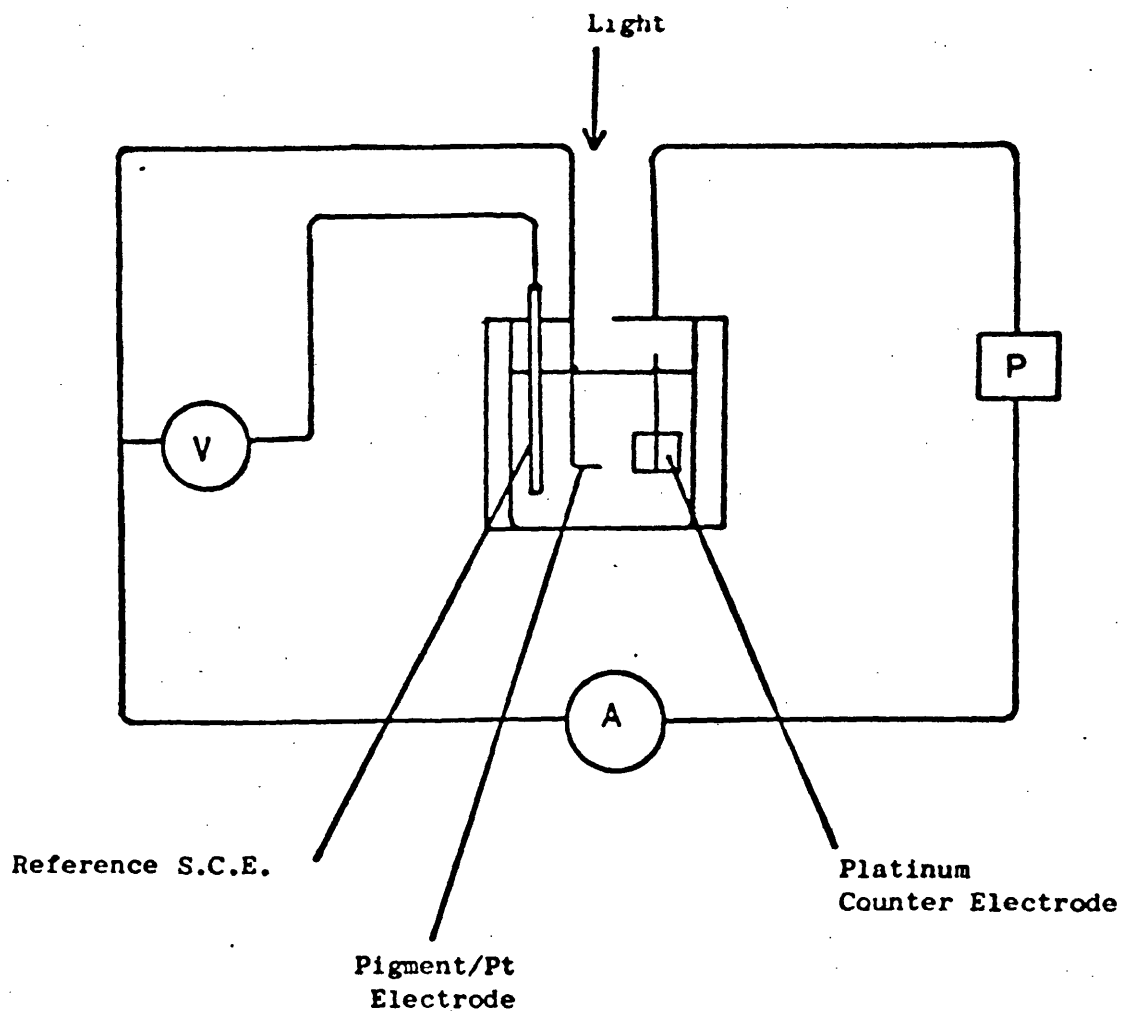
The circuit is basically that used by Gerisher.¹⁴⁸ A Heath polarography module EAU 19/2 containing inbuilt potentiostat (P), ammeter (A) and voltmeter (V) was used for current measurement. The

recorder output for current of the polarography module was used to follow changes of current with time.

Current measurement is made at constant potential; the potentiostat provides current to the platinum counter electrode so that the potential between the pigment/Pt electrode and the saturated calomel reference electrode remains constant, this being measured by the voltmeter. The polarography module has facilities for the measurement of the potential between the pigment/Pt electrode and the reference electrode by an external voltmeter. A Phillips DC Micro-voltmeter was used for this purpose, providing more accurate potential measurements. The saturated calomel electrode in the cell was of the "dip in" type used with glass electrodes.

Current can be measured from a maximum of 10^{-3} amps to about 10^{-7} amps; below this the signal to noise ratio becomes unacceptable. The 200 Watt mercury lamp was used as the main light source, filtered to transmit light of wavelength 300-400 nm only. Light intensity was measured by a selenium photo-cell.

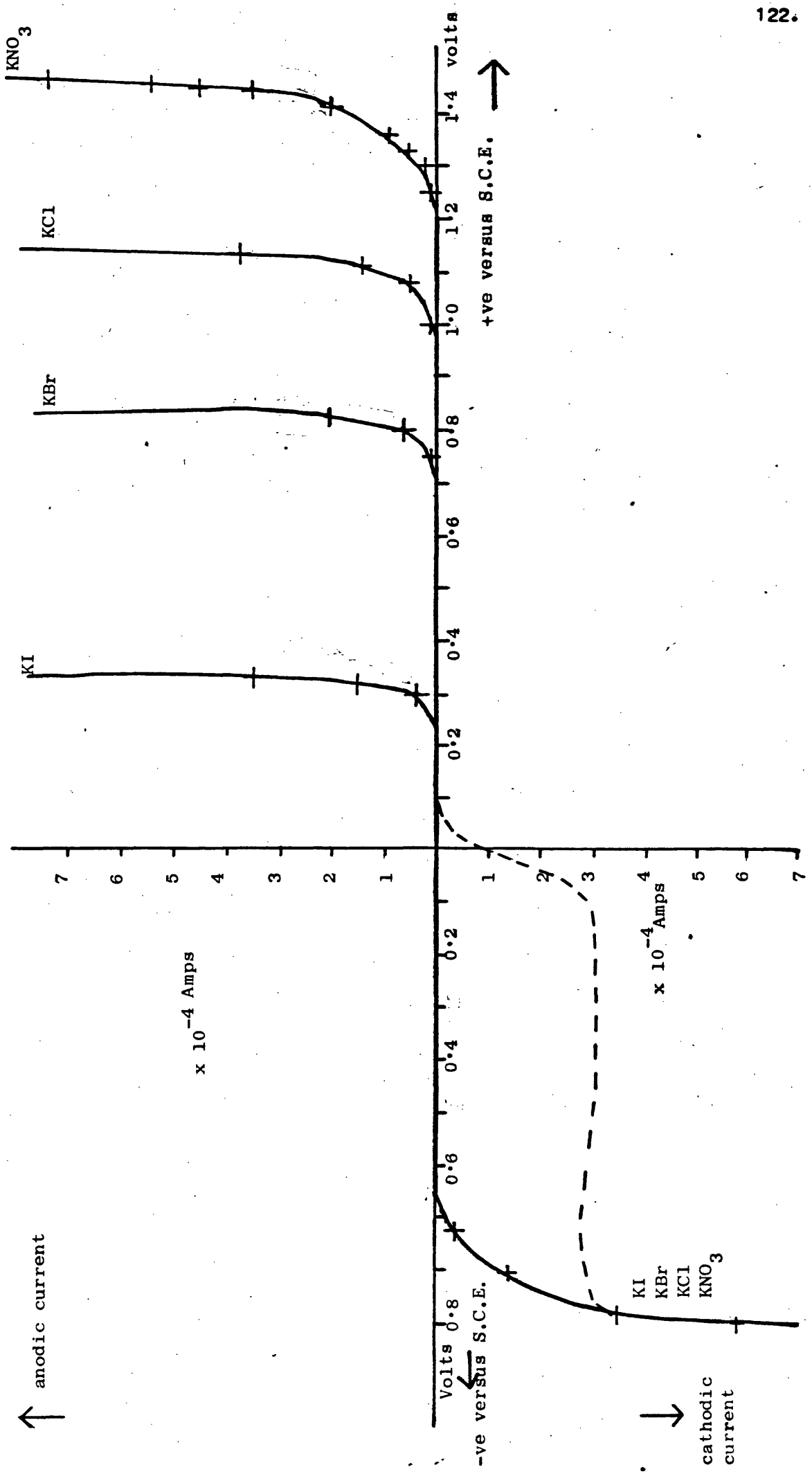
Fig. 49.



5.3(b) Results.

The variation of the dark current with applied potential was determined for a number of electrolytes de-oxygenated by bubbling nitrogen through for twenty minutes. The presence of pigment on the electrode makes no difference to the dark current, the same curves being observed using electrodes of clean platinum (Fig. 50). If oxygen is not removed from the electrolyte a non-reproducible dark current appears at cathodic potentials (dashed line Fig. 50).

Fig. 50. Dark Current-Voltage Curves.



Anodic current infers a flow of electrons from the pigment/Pt electrode to the platinum counter electrode. Cathodic current infers a flow of electrons from the platinum counter electrode to the pigment/Pt electrode. Anodic biasing is the application of positive potentials to the pigment/Pt electrode and cathodic biasing is the application of negative potentials to the pigment/Pt electrode relative to the reference electrode.

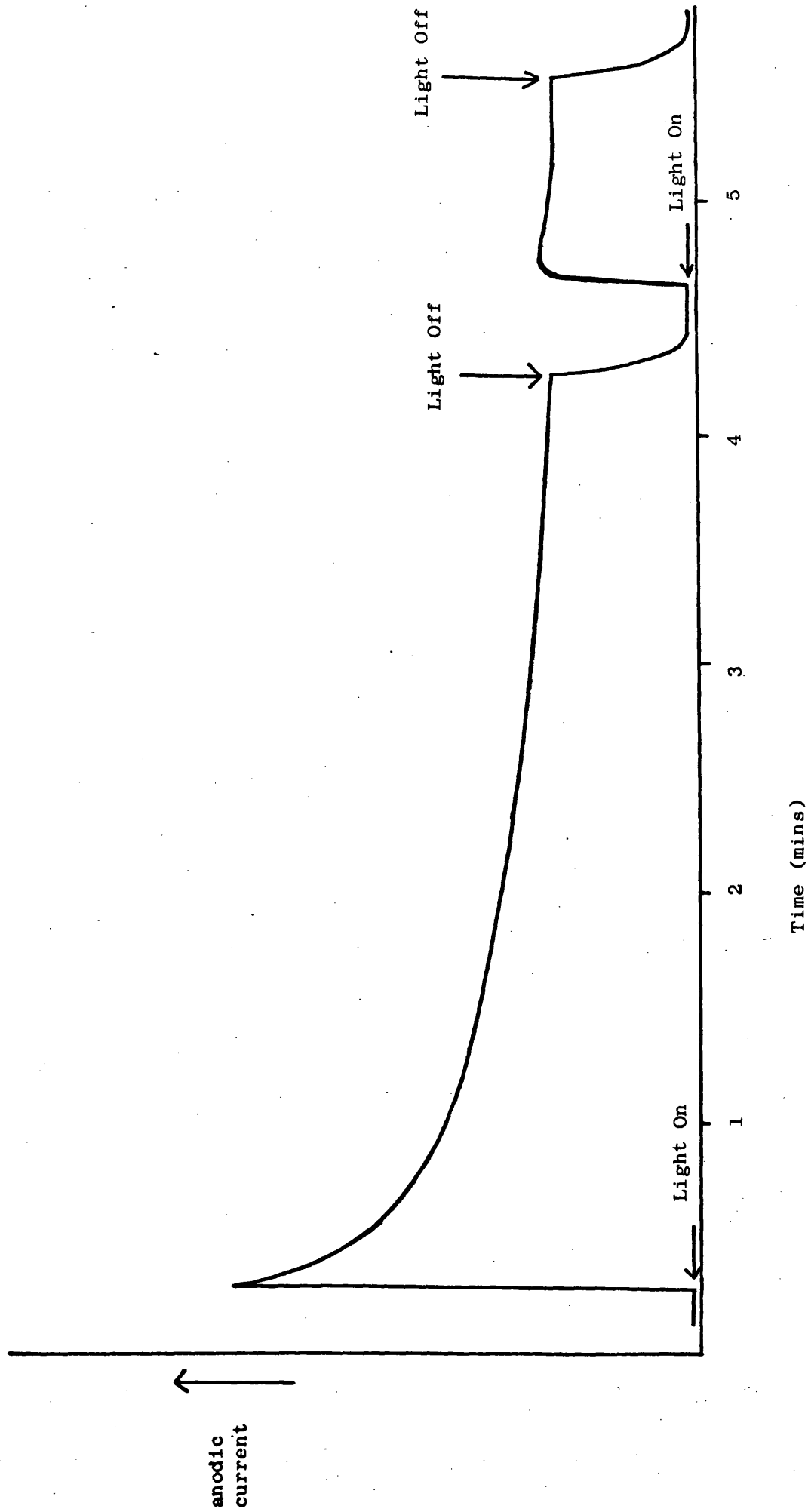
Photo-Current Response.

Irradiation of the pigment/Pt electrode under anodic biasing was found to give anodic photo-currents. The photo-current is the increase in current observed upon irradiation of the pigment. A typical photo-current response is shown in Fig. 51. The photo-current quickly reaches a peak value and then decays to a level photo-current. Switching off the light returns the current to the small dark current value almost immediately. Re-irradiation of the pigment a few seconds after the first irradiation results in the photo-current increasing to a level photo-current or only a small peak in the photo-current being observed. If the pigment/Pt electrode is left in darkness for a short period (approximately five minutes) after irradiation, the "peak" photo-current returns upon re-irradiation of the pigment.

The peak photo-current is observed for all pigments at 0.5v anodic biasing, and has been observed for pigments A and F at 1.0v anodic biasing in pH7 electrolyte. A steady increase to a level photo-current is observed for pigments A and F in 0.1M HCl KCl electrolyte and for pigments E and H in pH7 electrolyte.

During irradiation of the pigment no gas evolution was observed at either electrode. Removal of oxygen from the electrolyte by bubbling nitrogen through for twenty minutes did not result in any

Fig. 51. Typical Photo-Current-Current Response.



change in the photo-current nor did saturating the electrolyte with oxygen change the photo-current.

Determination of Photo-Currents of Pigments.

The level photo-currents of pigments were determined at 0.5v anodic biasing. The same electrodes that were used for the second and third sets of photo-voltage measurements were used for the photo-current determination. The results are shown in bar diagrams in Fig. 52. The first set of values were determined in unbuffered pH7 electrolyte and the second set of values were determined in pH7 phosphate buffered 0.1M KCl electrolyte.

Variation of Photo-Current with Applied Biasing.

The variation of level photo-current with anodic biasing of pigment A was determined using an unbuffered pH7 potassium nitrate electrolyte. The biasing was varied from +1.2v to +0.1v with measurement of the level photo-current after the dark current had been allowed to settle. Large dark currents were observed at high anodic biasing which prevented the use of biasing above +1.2v due to the difficulty of measuring a small photo-current against a large dark current. Fig. 53 shows a plot of photo-current versus anodic biasing.

Using the xenon lamp which provides a more intense light source, a small cathodic photo-current was observed when a pigment A electrode in 0.1M KCl unbuffered pH7 electrolyte at 0.5v cathodic bias was irradiated. When operating at cathodic bias oxygen has to be removed from the electrolyte so that dark currents are small enough to enable a small photo-current to be measured. A peak response was noted for the cathodic photo-current, decaying to a small level

Fig. 52. Level Photo-Current Measurements.

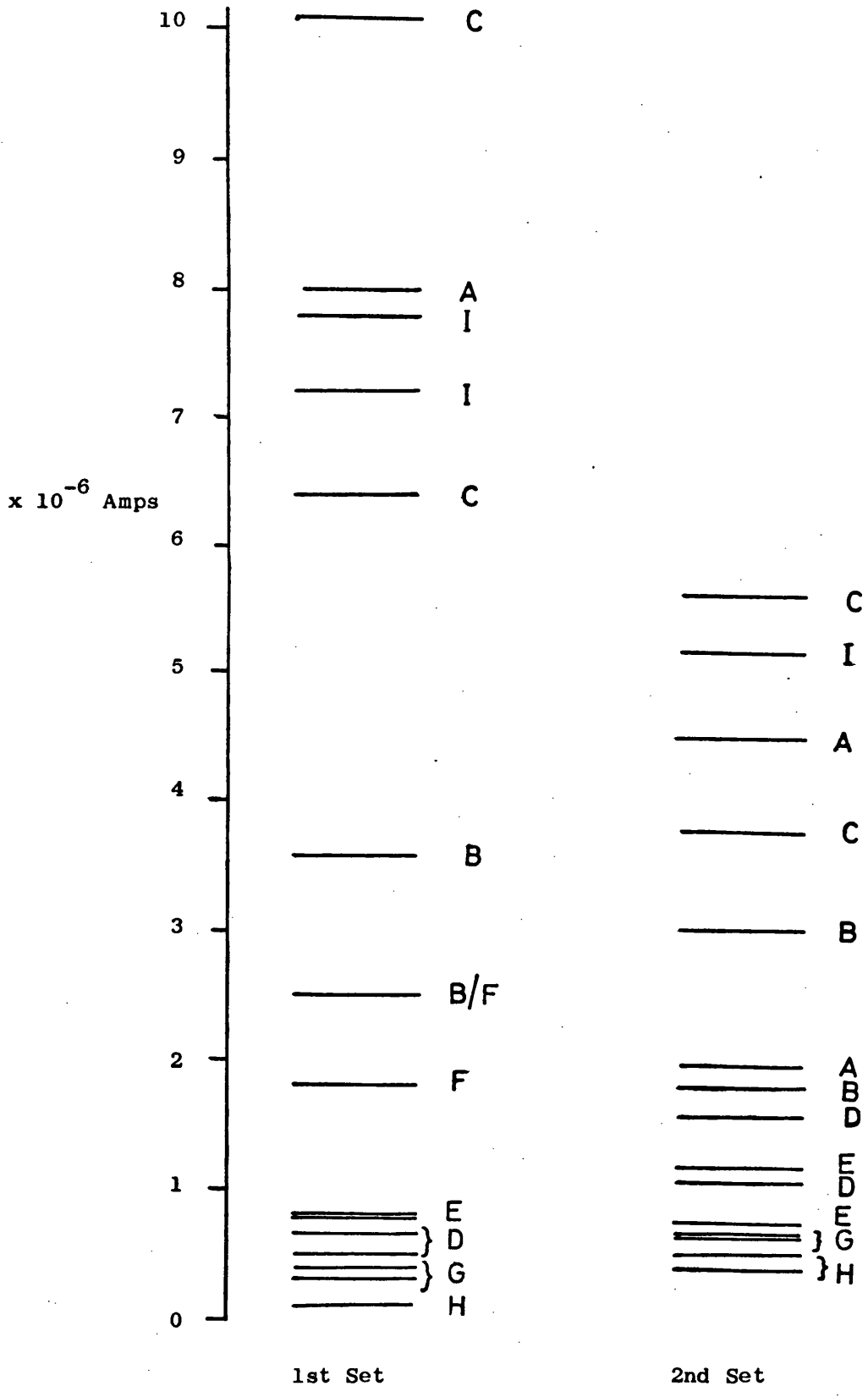


Fig. 53. Variation of Level Photo-Current with Potential Biasing.

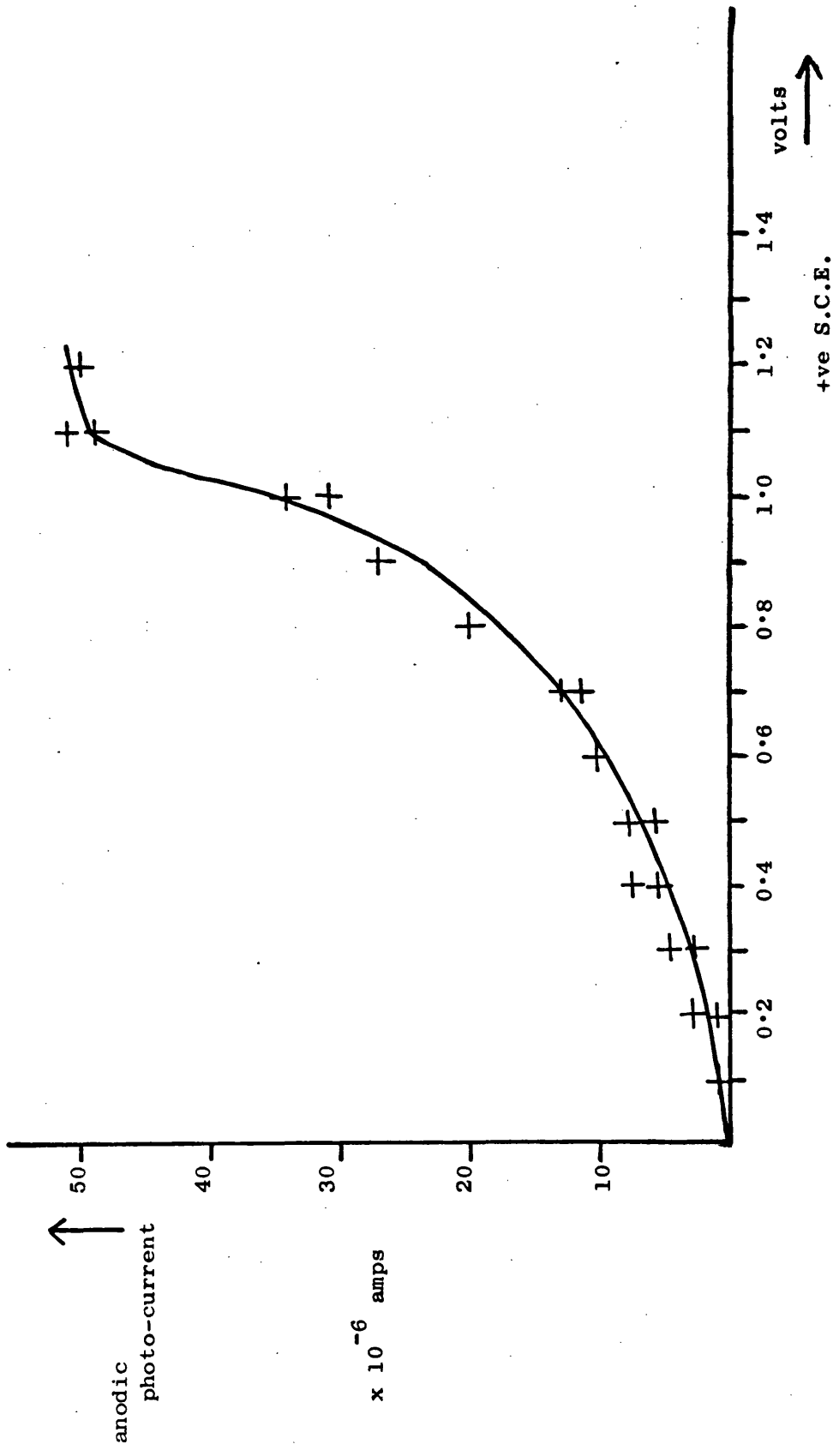


photo-current of approximately 1×10^{-6} amps. The photo-currents observed for pigment A are variable, but under 1.0v anodic bias the level photo-current can be of the order of 80 to 100×10^{-6} amps and approximately 30×10^{-6} amps at 0.5v anodic bias using the xenon lamp light source, so that the observed cathodic photo-current is relatively very small.

5.3(c) Discussion.

Anodic biasing favours the flow of electrons from the pigment/Pt electrode to the platinum counter electrode. This occurs since the anodic reaction, electron injection into titanium dioxide would become more favourable as the pigment/Pt is made more positive. Conversely cathodic biasing of the pigment/Pt electrode disfavors the anodic reaction and favours a cathodic reaction, i.e. electron flow from the platinum counter electron to the pigment/Pt electrode.

The two situations can be viewed in terms of changes of the band bending in titanium dioxide. Under anodic biasing the upward band bending is increased, resulting in more efficient separation of photo-holes and electrons and an increased anodic reaction. Cathodic biasing decreases the upward band bending, thus reducing the energy barrier for electron flow to the titanium dioxide surface.

The biasing that can be applied is limited by the dark current-voltage for the various electrolytes. Systems using single crystal electrodes do not suffer from this problem since dark currents do not occur at high anodic biasing,^{129,133} but a cathodic dark current occurs at cathodic bias due to electrolysis of water. The anodic dark currents of the pigment/Pt-platinum system corresponds to the oxidation of I^- , Br^- and Cl^- for KI, KBr, and KCl electrolytes, e.g. $2I^- \rightarrow I_2 + 2e$.

The anodic dark current for KNO_3 electrolyte and the cathodic dark current for all the electrolytes corresponds to electrolysis of water. The variation of anodic photo-current differs from that reported for a single crystal¹²⁹ which reaches a saturation photo-current at lower potential biasing.

The level photo-currents obtained for pigments are of the order of a factor of 10^3 times smaller than that obtained for reduced single crystal.¹²⁹ A calculation from the photo-current flowing indicates that the extent of reaction occurring is very small and that gas evolution would be undetectable. Reduction treatment of single crystals gives them a much lower resistance whereas the resistance of pigments is high. The main cell resistance would be due to the pigment resistance and the platinum pigment interface resistance. If the pigment particles which are irradiated are not in direct contact with the platinum support then electrons will have to be transferred from one particle to another overcoming the space charge barrier at the particle surfaces and this will add to the resistance of the pigment layer.

Single crystals used in electrochemical studies only have a small surface area of the order of a few square centimetres and current densities can therefore be calculated. For a layer of pigment on platinum although the weight of pigment can be measured the surface area of the pigment exposed to light is not known.

The reactions proposed for the photo-cell have been discussed in section 5.2(c). The anodic photo-current corresponds to reaction of holes at the surface of titanium dioxide resulting in oxygen evolution. The small cathodic photo-current observed for pigments under cathodic bias could be considered the reverse of the anodic reaction, i.e. hydrogen evolution at titanium dioxide¹³² by reaction of photo-electrons

at the surface with hydrogen ions.

Memming¹³² also observed peak photo-currents for layers of titanium dioxide on stannic oxide which were attributed to the existence of traps in the space charge layer or at the titanium dioxide surface. The peak photo-current would correspond to emptying of the electron traps. When the traps are empty the photo-current observed is due to reaction of photo-holes at the pigment surface. This provides an explanation for the photo-current having little or no peak effect upon immediate re-irradiation since the electron traps have been emptied by the previous irradiation. The traps are refilled during a dark period and the peak effect is observed when irradiation occurs after a period. The electron traps could be considered to be the same as those which cause the slow decay of the photo-voltages.

The rapid fall of the photo-current when the light is switched off would be expected because holes and electrons can be rapidly effectively recombined by the cell reaction since the electrodes are at virtual short circuit so that the remaining electrons in the conduction band can flow to the counter electrode and the remaining holes in the valence band are destroyed by electron injection.

The absence of an effect of oxygen on the photo-currents may again reflect the incomplete removal of oxygen by nitrogen bubbling considering the small photo-currents involved. If the cathodic process at the platinum counter electrode is hydrogen evolution then the oxygen concentration would have no effect on this reaction. It is likely that adsorbed oxygen on the pigment surface would swamp any effect of oxygen in solution.

The level photo-current results for the pigments vary much more than the corresponding photo-voltage measurements, although they

roughly follow the same order, i.e. pigments A, B, C and I giving the largest photo-currents while pigments E, D, and G give small photo-currents and pigment H gives a very small photo-current. Phosphate buffer increases the photo-currents for coated pigments (Fig. 52) paralleling the trend found for the photo-voltage measurements. The variation in the level photo-current measurements suggests that the photo-currents may be more susceptible to variation in the electrodes due to preparation.

5.4 Photo-Current Sensitization.

5.4(a) Experimental.

The effect of alcohols upon the photo-current was investigated by measuring the level photo-currents obtained after successive additions of alcohols to a cell system containing 100 mls of 0.1M KCl pH7 unbuffered electrolyte. After each alcohol addition the system was left in darkness for thirty minutes before photo-current measurement. The 200 watt mercury lamp was used as light source for the majority of experiments. Titanium dioxide electrodes were stored in electrolyte as before.

5.4(b) Results.

Methanol, ethanol, isopropanol, benzyl alcohol, and pentaerythritol were found to increase the level photo-current when added to the electrolyte. The sensitization was followed with increasing concentration for isopropanol for a number of pigments at 1.0v anodic biasing; a maximum photo-current being reached, (Fig. 54). The photo-current sensitization for pigment A at 1.0v anodic bias by methanol is shown in Fig. 55 and by pentaerythritol at 0.5v anodic bias

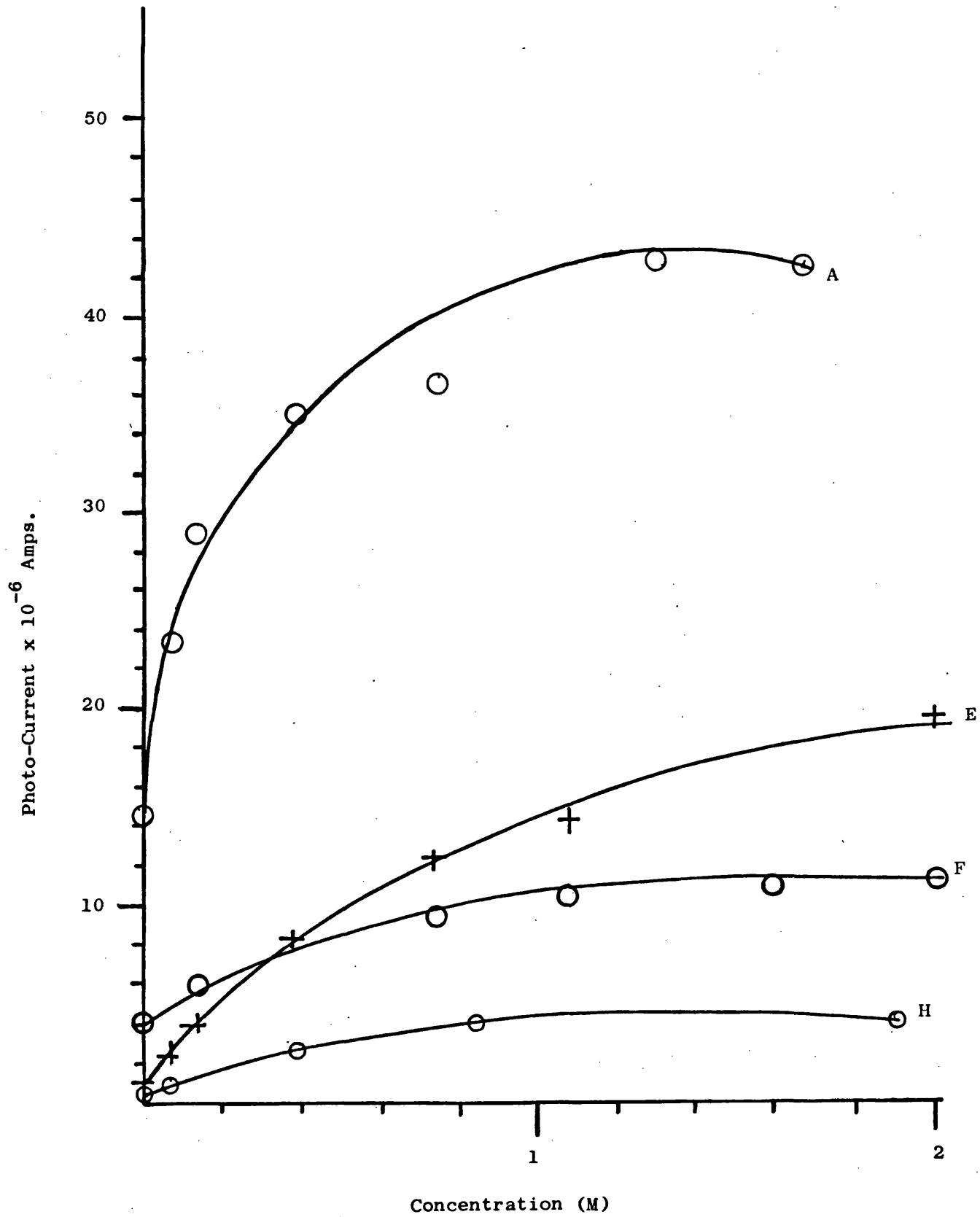
Fig. 54. Photo-Current Sensitization by Isopropanol.

Fig. 55. Photo-Current Sensitization of Pigment A by Methanol.

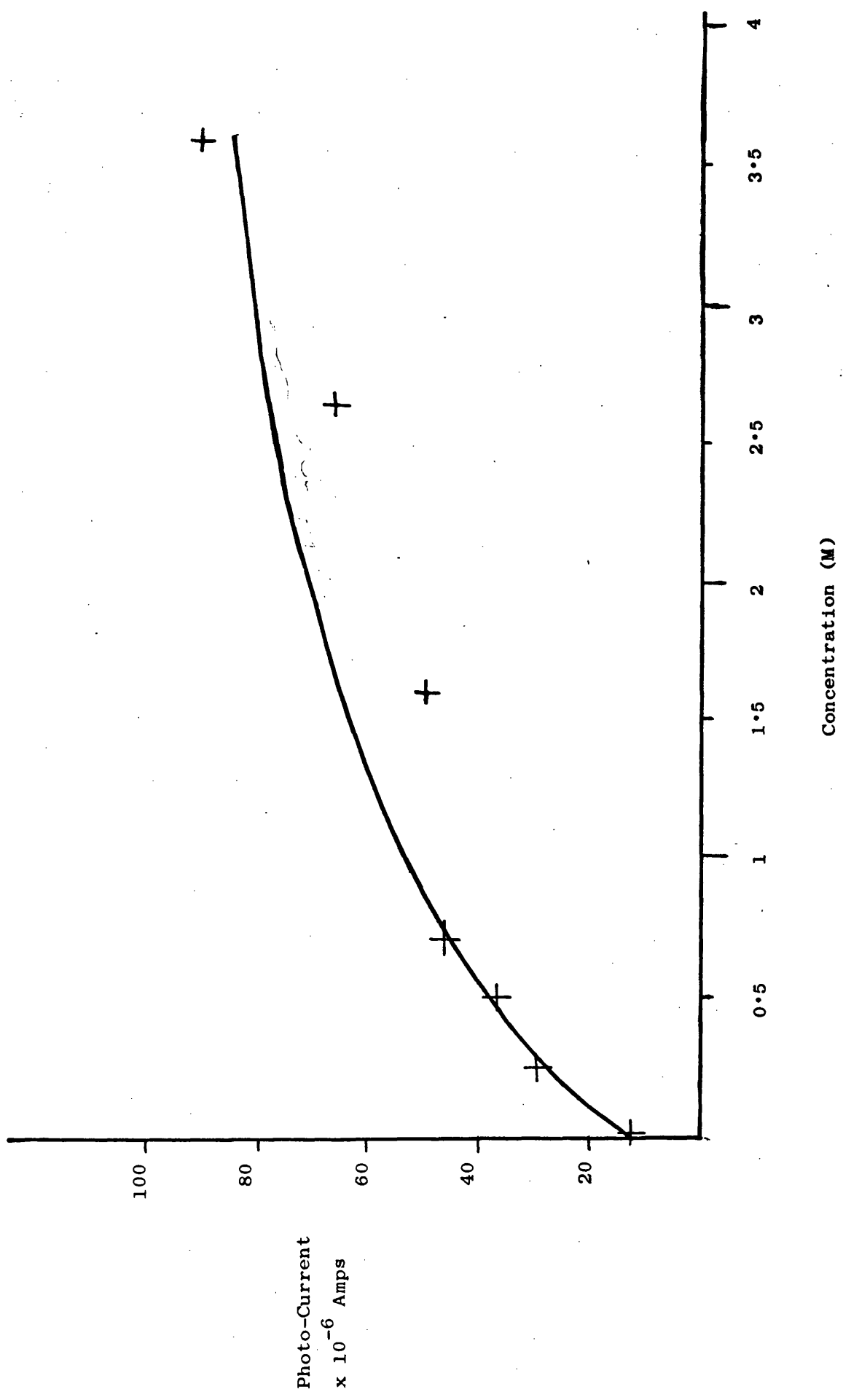
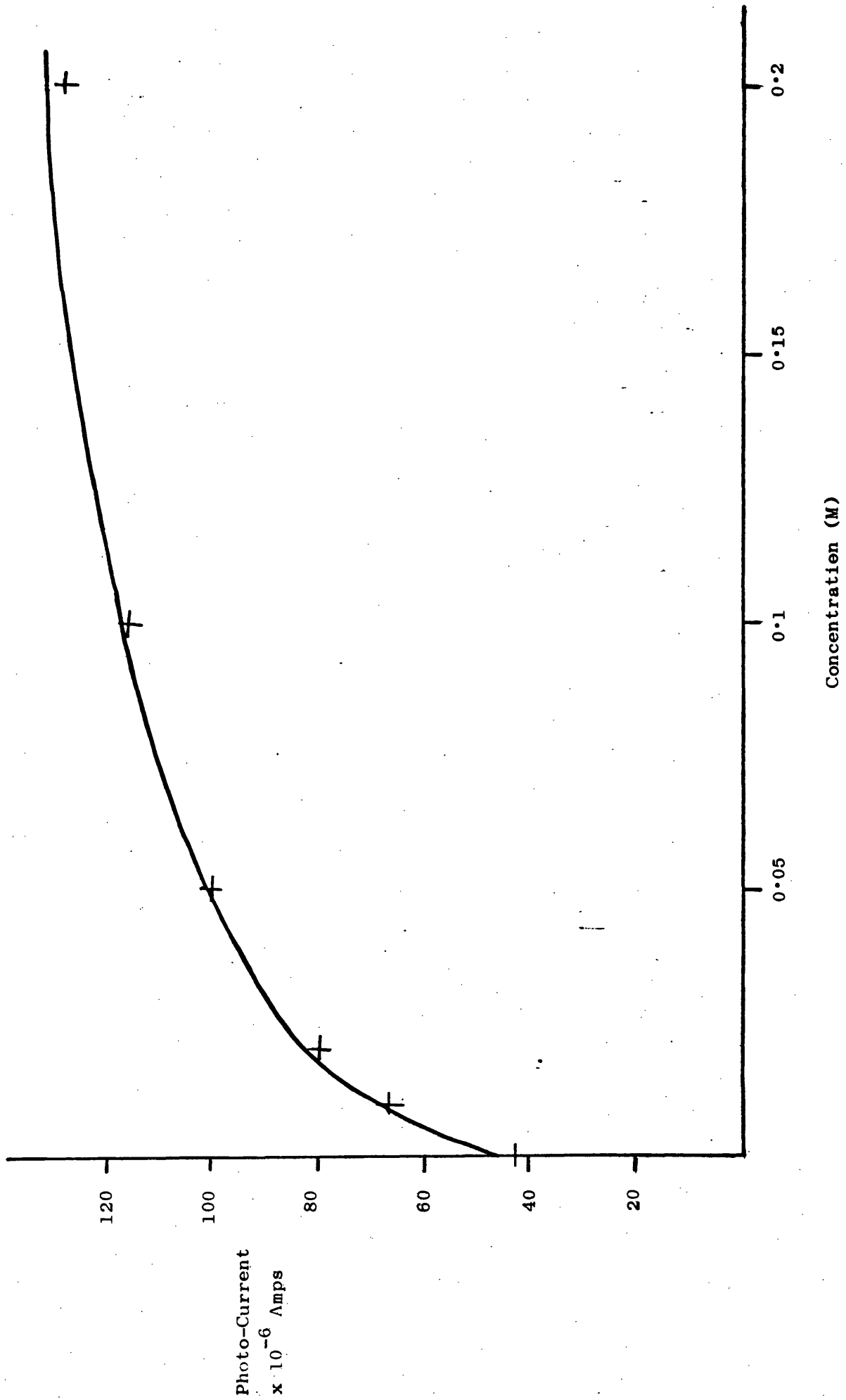


Fig. 56. Photo-Current Sensitization of Pigment A by Penta-Erythritol.



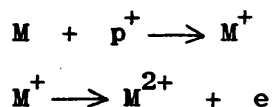
in Fig. 56. Pentaerythritol was only soluble in the electrolyte to less than 0.4 Molar, and the photo-current obtained in the saturated solution was $162\mu\text{A}$. Pentaerythritol sensitization was performed using the xenon lamp as the light source.

The small cathodic photo-current observed at 0.5v cathodic bias was reversed to a level anodic photo-current by addition of methanol, although the transient photo-effect is initially in the cathodic direction.

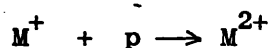
The dark current was noted to increase slightly upon addition of alcohols to the electrolyte, but this was only due to slight changes in the current-voltage characteristics of the cell due to the presence of the two platinum electrodes.

5.4(c) Discussion.

Morrison¹⁴⁹⁻⁵⁰ has noted sensitization of the photo-current obtained from zinc oxide by the addition of multivalent reducing agents to the electrolyte. This he termed "current doubling" since the photo-current became nearly double. This phenomenon was attributed to the reaction of the reducing agents with photo-holes.



Here the product M^+ injects an electron into the semiconductor conduction band instead of reacting with another hole.

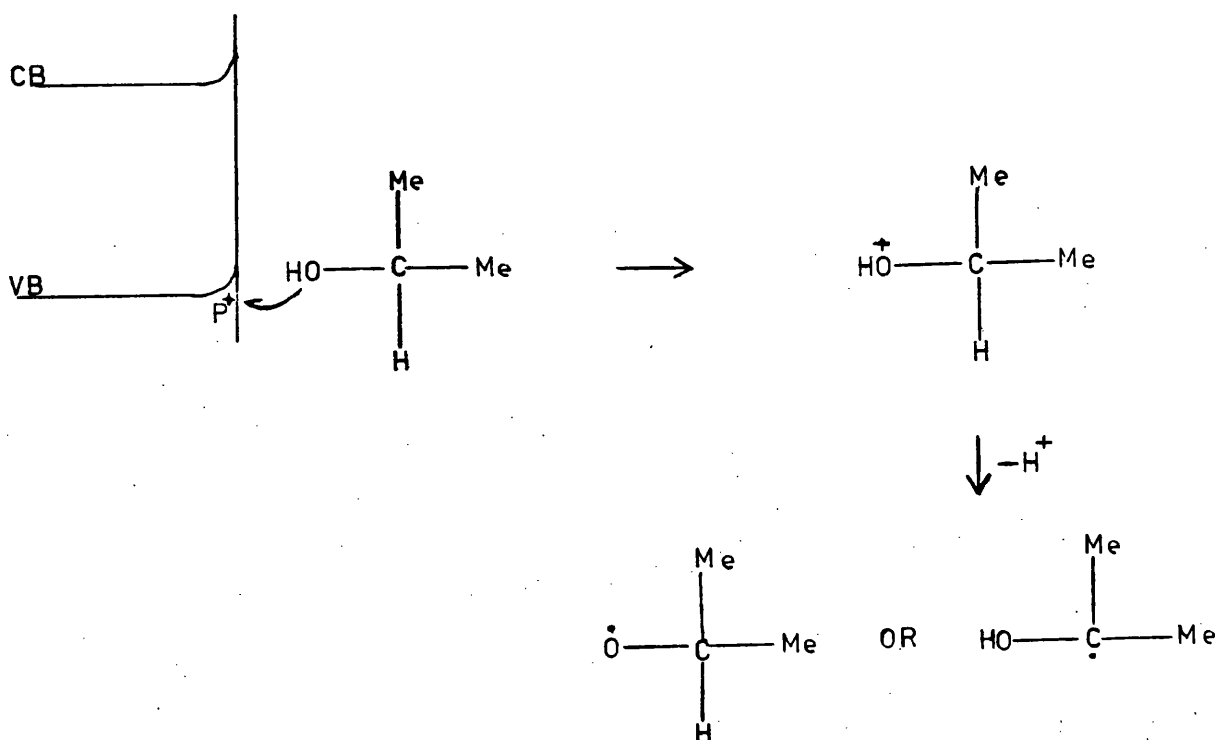


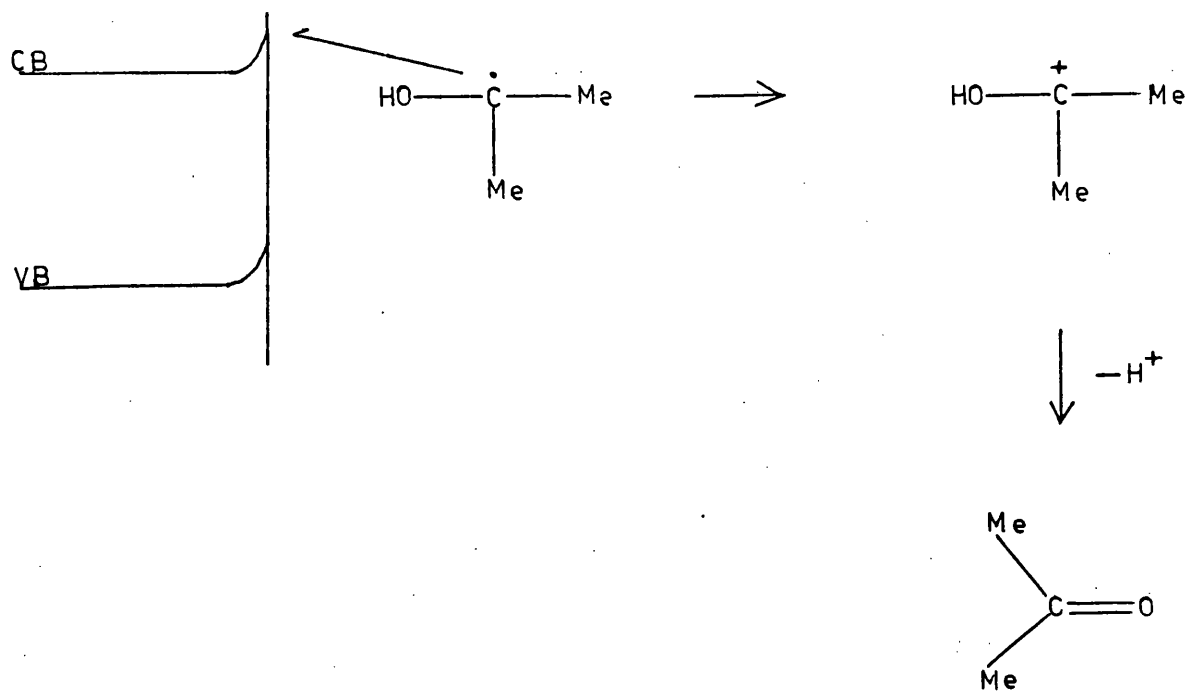
The light intensity controls creation of photo-holes and the

photo-current is dependent upon the hole concentration. The reaction of M^+ with another hole would not lead to any photo-current sensitization. If M^+ injects an electron into the conduction band this will increase the photo-current because the reaction of one hole has led to the injection of two electrons into the semiconductor. If every hole reacted with M and every M^+ molecule injected an electron into the conduction band the photo-current would exactly double. Photo-current increase of a single crystal of titanium dioxide by methanol has been noted.¹³⁶

The photo-current increases observed for pigmentary titanium dioxide reach a constant value at sufficiently high alcohol concentration as would be expected if the alcohol competes with water or surface hydroxide ions for photo-holes. However, the photo-currents are more than doubled for which the above scheme alone would not account.

The reaction of isopropanol as a two equivalent reducing agent would be





If alcohol molecules were capable of reacting with photo-holes that were of insufficient energy to react with water molecules or surface hydroxide ions, and which would therefore recombine without reaction then photo-currents could be expected to more than double.

Increased pigment-electrolyte "contact" by alcohol addition may also contribute to photo-current increase. The band bending appears not to be affected by isopropanol addition as the photo-voltage does not change.

The reaction of alcohols at illuminated pigment electrodes is closely related to the photo-reduction of pigments with alcohols. Electron injection occurs resulting in reduction since there is no circuit or counter electrode for the electron flow.

The sensitization of anodic photo-current at cathodic bias is an indication of the competition between cathodic and anodic processes. Both reactions are occurring but the overall direction of the current depends upon which reaction is occurring to the greatest extent. Alcohol addition sensitizes the anodic reaction but not the cathodic reaction resulting in a level anodic photo-current at cathodic bias. The transient response attributed to electron traps near or at the surface would not be affected by the current sensitization.

5.5 Spectral Distribution and Light Intensity Variation of Photo-Current.

5.5(a) Experimental.

The photo-current of a pigment A electrode (immersed in electrolyte overnight) was measured at 1.0v anodic bias using the 200 watt mercury lamp and varying the light intensity with neutral density filters. The electrode was irradiated with full light intensity until a level photo-current was obtained, the light intensity then being reduced and the lower photo-currents measured. The light intensity variation of pigment F at 0.5v anodic bias was determined in the same way.

For the determination of the spectral distribution of pigment A the xenon lamp was used as the light source, giving a more even light output, and a Bausch and Lomb monochromator was used to control the light

wavelength. Because the light intensity is much reduced by the monochromator, methanol was added to the cell electrolyte to increase the photo-current to make measurements more accurate. The electrode was at 1.0v anodic bias. A Cambridge Instruments zinc black thermopile was used for measurement of the light output.

5.5(b) Results.

The variation of level photo-current for pigments A and F with light intensity is shown in Fig. 57 and a plot of photo-current versus the square root of light intensity is shown in Fig. 58.

For spectral distribution determination the light intensity variation of a pigment A electrode was determined three times, and the results graphed as photo-current versus $\sqrt{\text{light intensity}}$ (Fig. 59). The uncorrected wavelength response of the photo-current was determined by recording the level photo-current at 10 nm intervals.

The relative light intensity variation of the xenon lamp measured by the thermopile is shown in Fig. 60. The light intensities were calculated by correcting the thermopile readings for wavelength since a thermopile measures light energy and not intensity. The spectral distribution of the photo-current was corrected for light intensity using the xenon lamp light intensity graph and the graph of photo-current versus light intensity. Fig. 61 shows the corrected photo-current spectral distribution.

5.5(c) Discussion.

The saturation photo-current for titanium dioxide is reported to be linear with light intensity.^{128,132} The response observed for pigments even at 1.0v anodic bias is a distinct curve and the plots of photo-current versus square-root light intensity give approximate

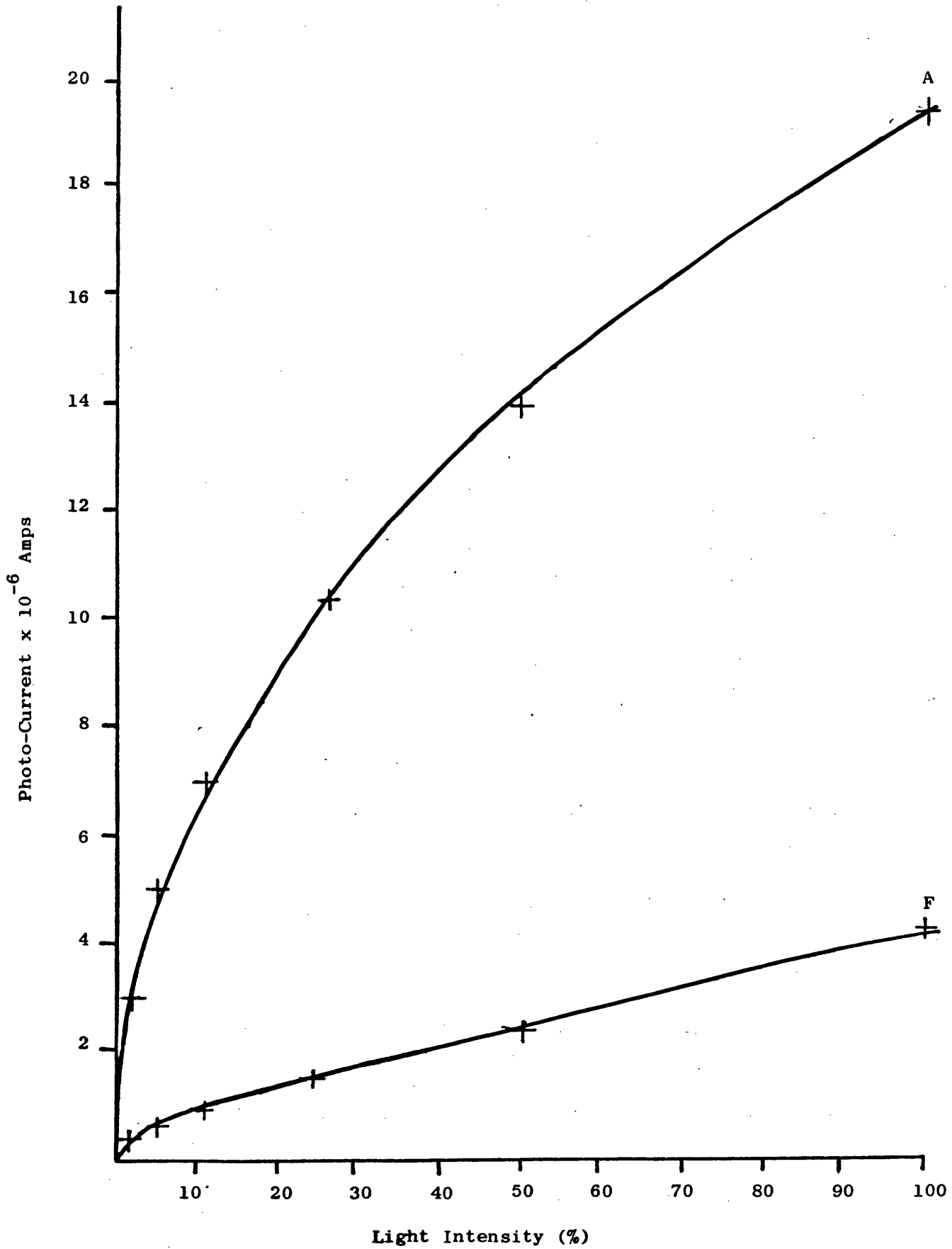
Fig. 57. Variation of Photo-Current with Light Intensity.

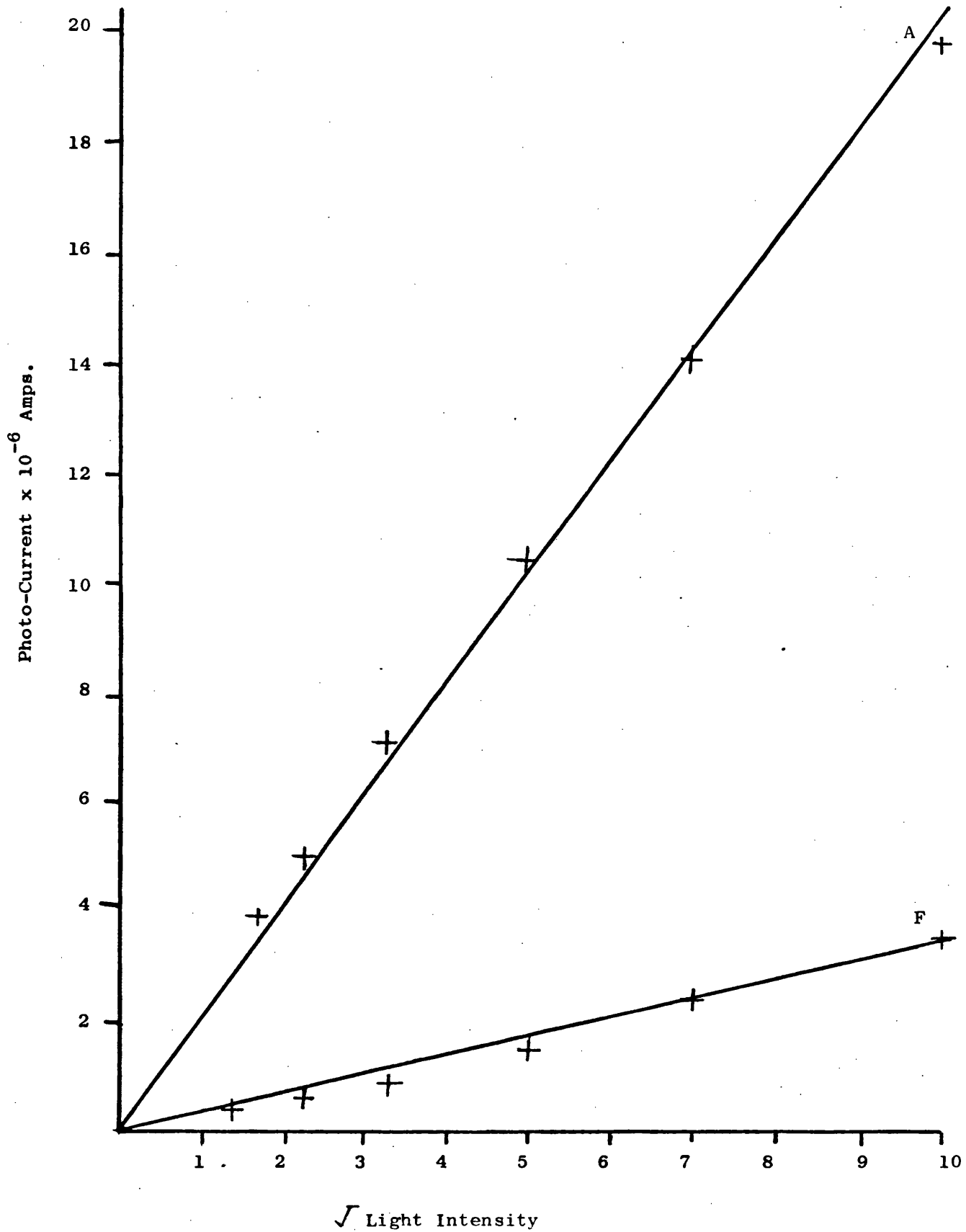
Fig. 58. Photo-Current Versus Square Root Light Intensity.

Fig. 59. Variation of Photo-Current with $\sqrt{\text{Light Intensity}}$ at 395 nm for Pigment A.

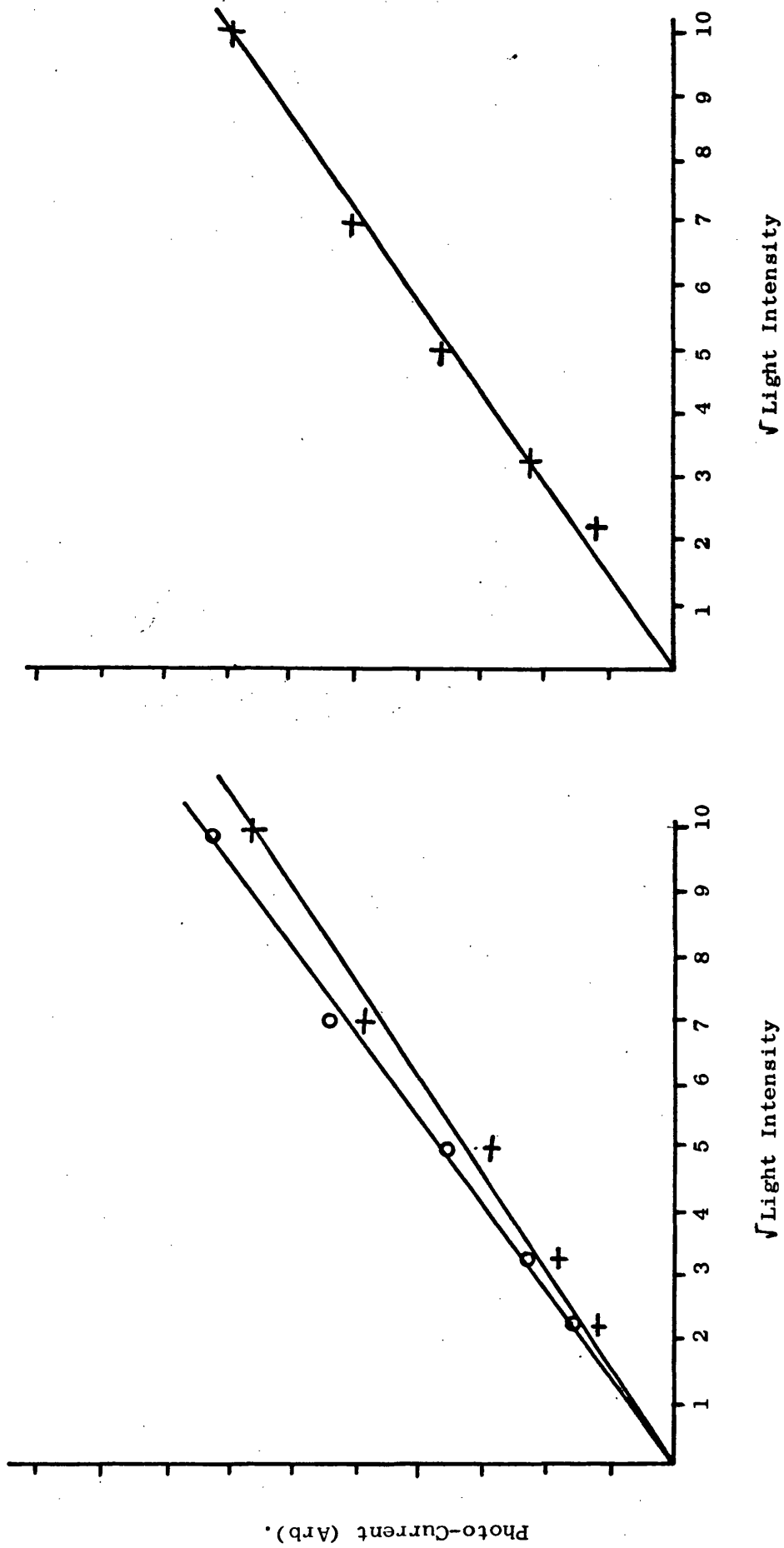


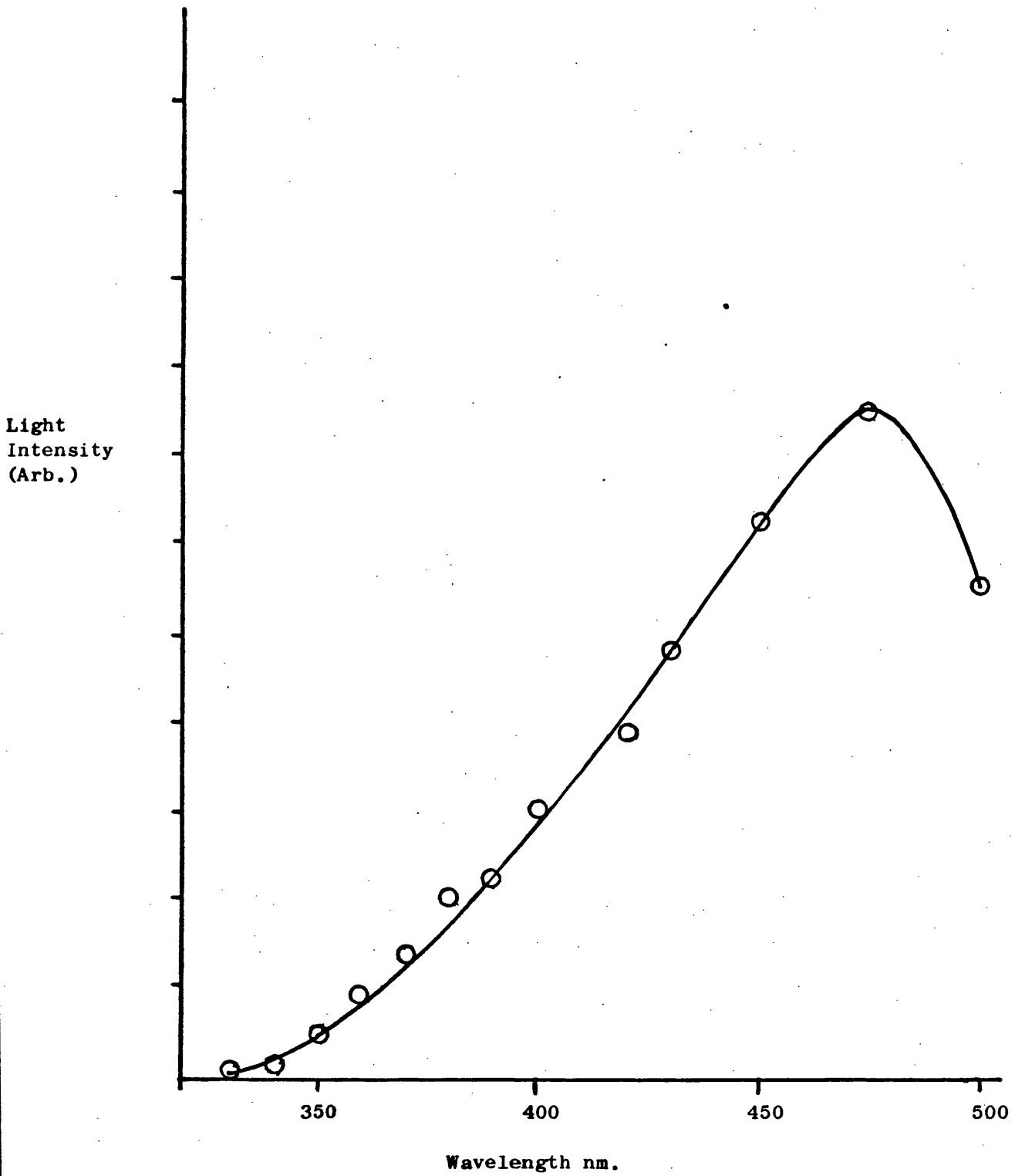
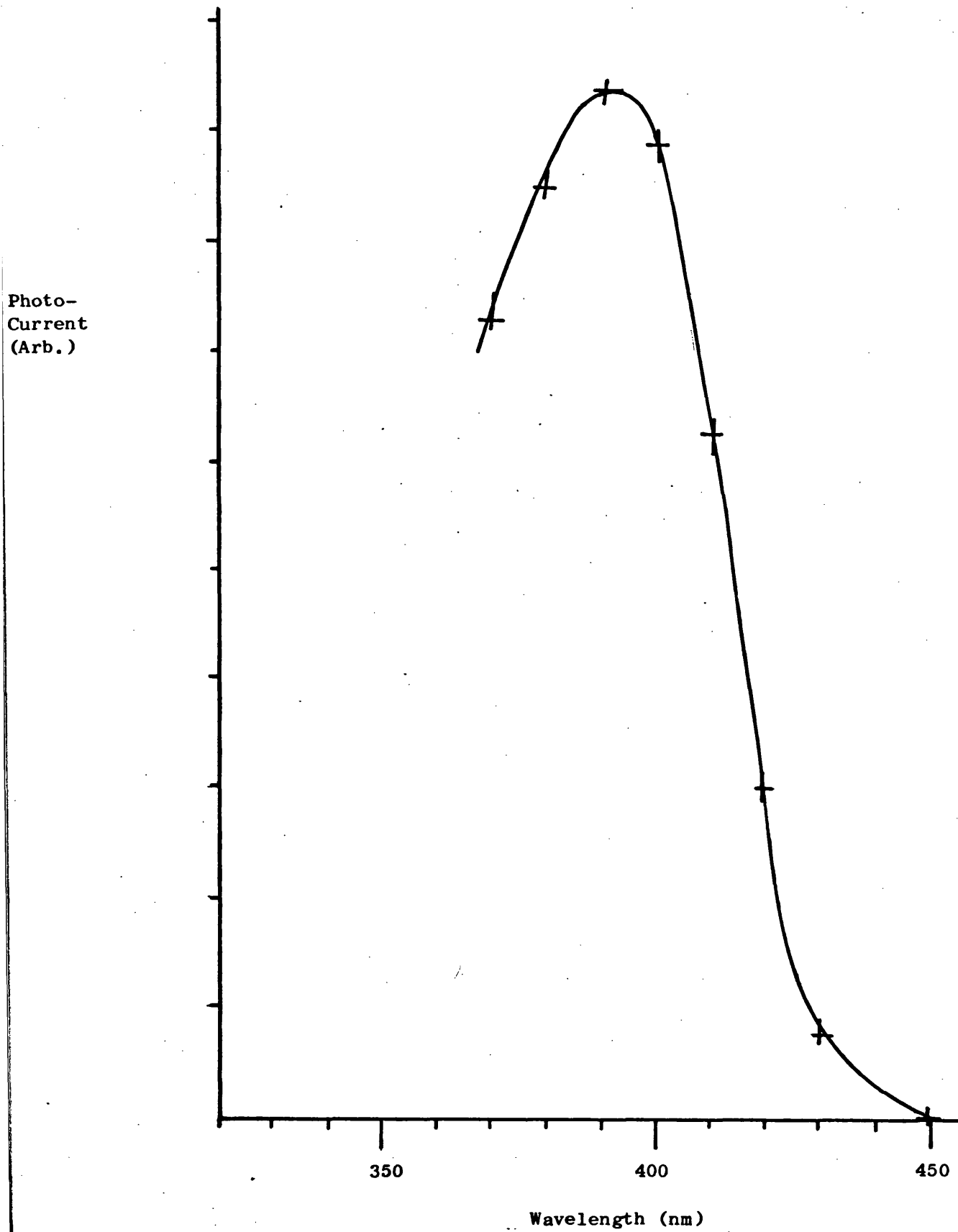
Fig. 60. Xenon Lamp Light Intensity Variation with Wavelength.

Fig. 61. Photo-Current Spectral Distribution.

straight lines. The non linear dependence of photo-current may well be due to the electrode being under insufficient anodic bias to give saturation photo-currents. Biassing greater than 1.0v is not possible due to the increasing dark current. Saturation photo-currents are reached when further increases in biassing do not increase the photo-current which indicates that the biassing applied is sufficient to separate practically all photo-holes and electrons. The number of electron-hole pairs produced would be dependent upon the number of quanta of light absorbed.

Memming¹³² found that the λ maximum for the photo-current spectral distribution of a titanium dioxide layer on stannic oxide and titanium moved to longer wavelengths for layers of increasing thickness. The maximum photo-current for pigment A occurred for a light wavelength of about 390 nm which corresponds to light of band gap energy. This longer wavelength for λ maximum is probably an indication of the thickness of the pigment layer on the platinum support.

5.6 Temperature Dependence of the Photo-Electric Effects of Titanium Dioxide.

5.6(a) Experimental.

The temperature of unbuffered 0.1M KCl electrolyte of a cell system containing a pigment A electrode was increased by use of a contact thermometer and heater immersed in the electrolyte. The cell system was encased in an expanded polystyrene jacket and sealed as far as possible to prevent heat losses and evaporation of the electrolyte. The xenon lamp was used as light source for the temperature dependence study.

The photo-voltage was measured at thirty minute intervals while increasing the temperature in 10°C steps during the dark period.

Separate pigment A electrodes were used for the photo-current measurements at 1.0v anodic bias; the temperature being increased in the same manner as for the photo-voltage measurements and thirty minute dark periods being observed before each photo-current measurement. The calomel reference electrode potential is known to change very slightly with temperature,¹⁵¹ therefore comparison measurements were made using the platinum electrode as both the reference and counter electrodes.

5.6(b) Results.

The photo-voltage variation with temperature for pigment A is shown in Fig. 62. The results of three experiments on pigment A electrodes are presented. The light intensity was not the same for each experiment. The electrodes had been immersed in electrolyte at room temperature prior to the experiments for (1) 7 days, (2) 2 days, (3) 3 days. The photo-voltages were found to increase slightly at first and then to decrease sharply with increasing temperature.

The results of several determinations of the photo-current variation with temperature of pigment A are shown in Fig. 63. Fig. 63a, b, c, and d were determined using a saturated calomel reference electrode and Fig. 63e was determined using the platinum counter electrode as the reference electrode. The level photo-current was found to increase fairly linearly with temperature resulting in an approximate doubling of the level photo-current as the temperature is increased from 20°C to 80°C. The peak photo-currents remain fairly constant up to 40°C - 50°C and then increase sharply with increasing temperature. The temperature variations are quite qualitatively reproducible. The photo-currents obtained after allowing the electrodes to cool to 20°C overnight were found to be larger than the photo-currents obtained at

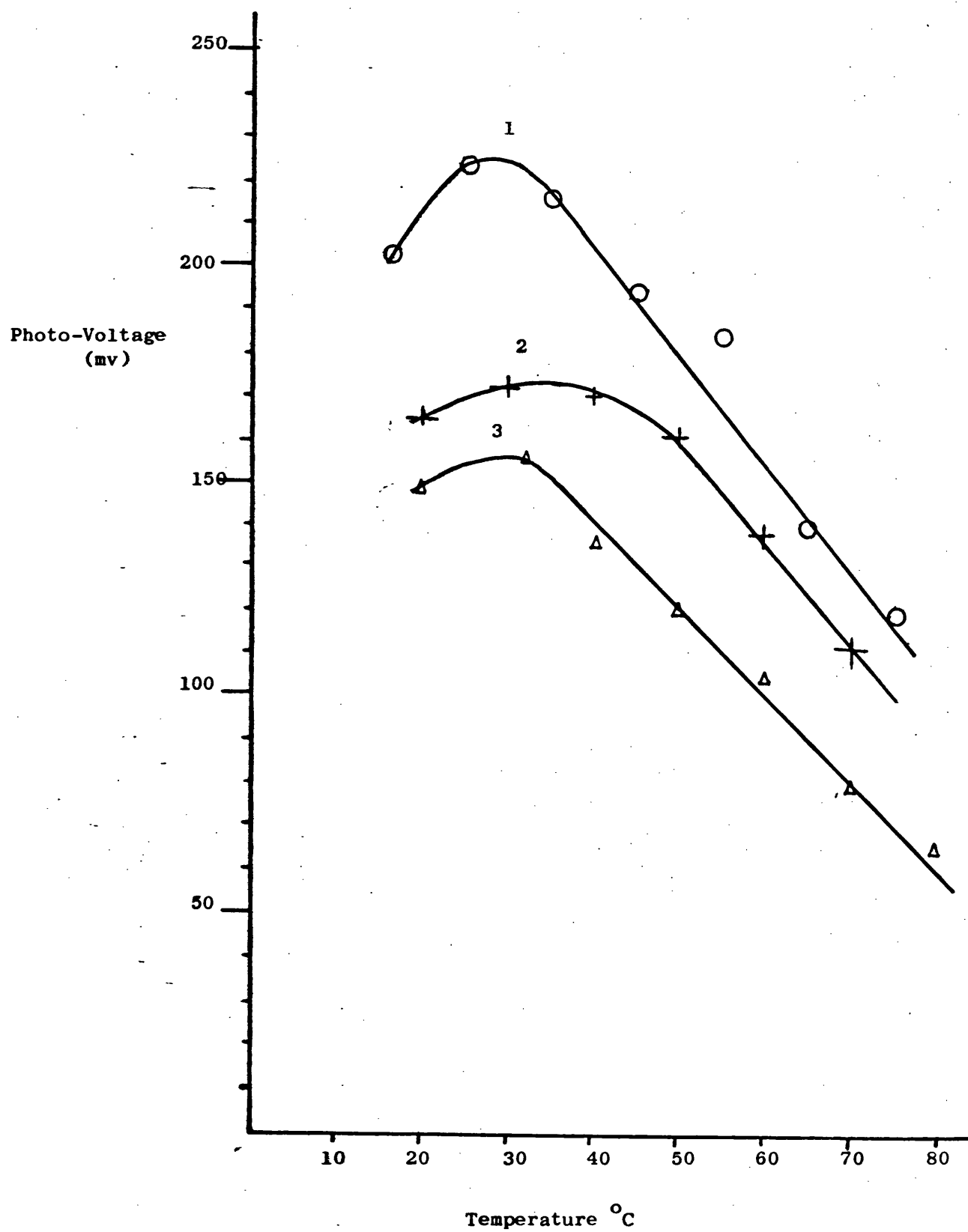
Fig. 62. Temperature Dependence of Photo-Voltage.

Fig. 63a. Temperature Dependence of Photo-Current.

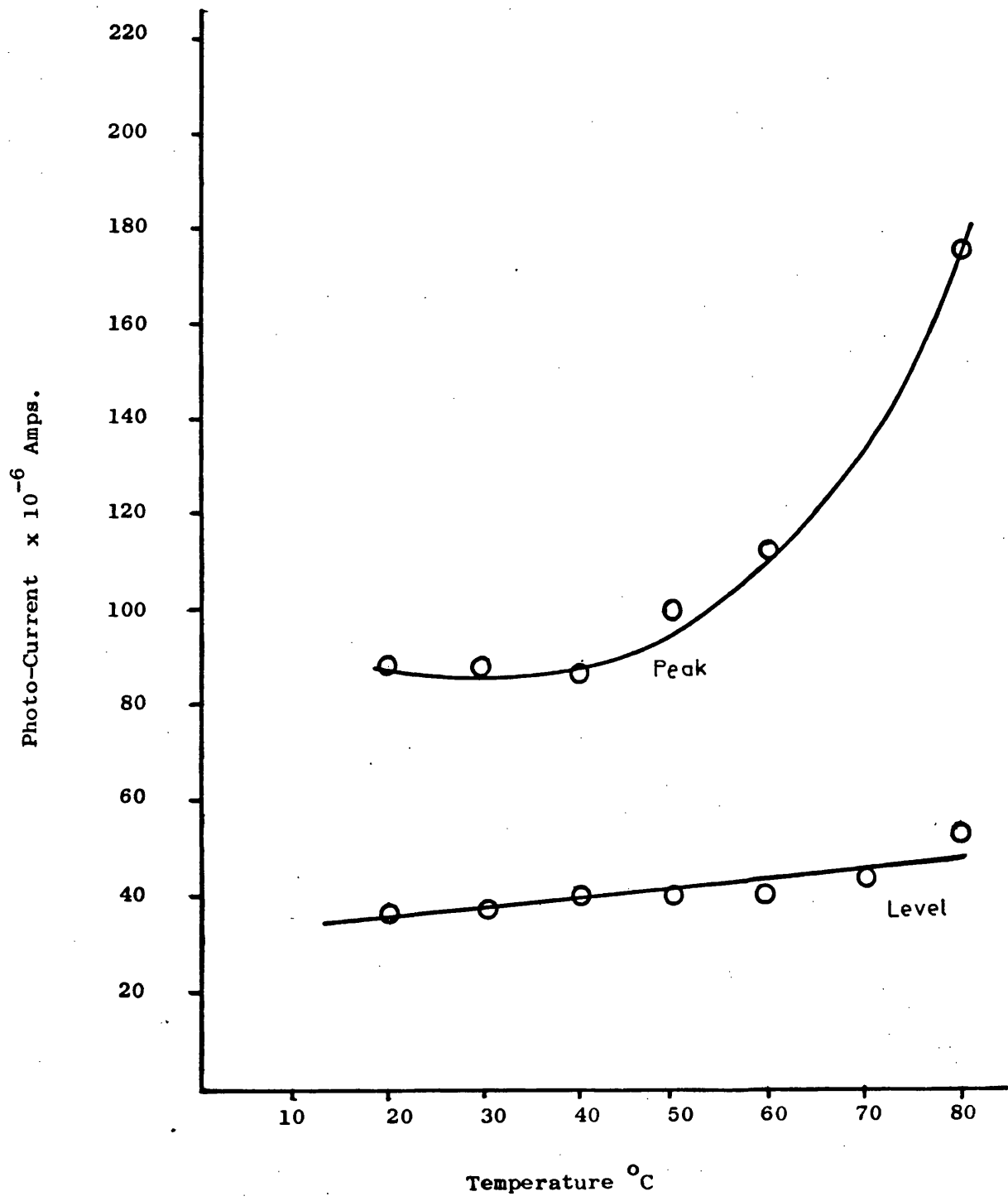
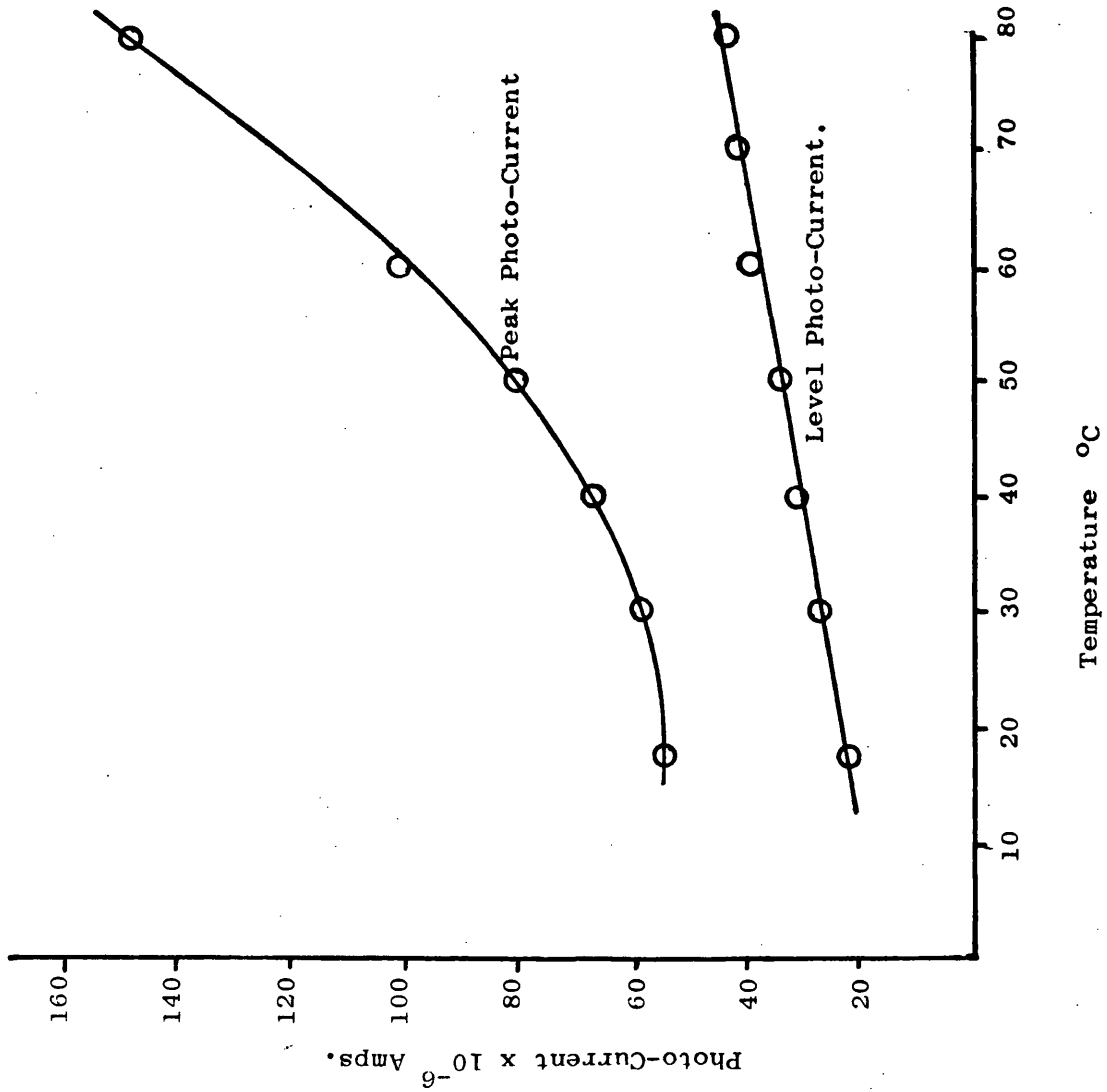


Fig. 63 (b and c) Temperature Dependence of Photo-Current.

(b)



(c)

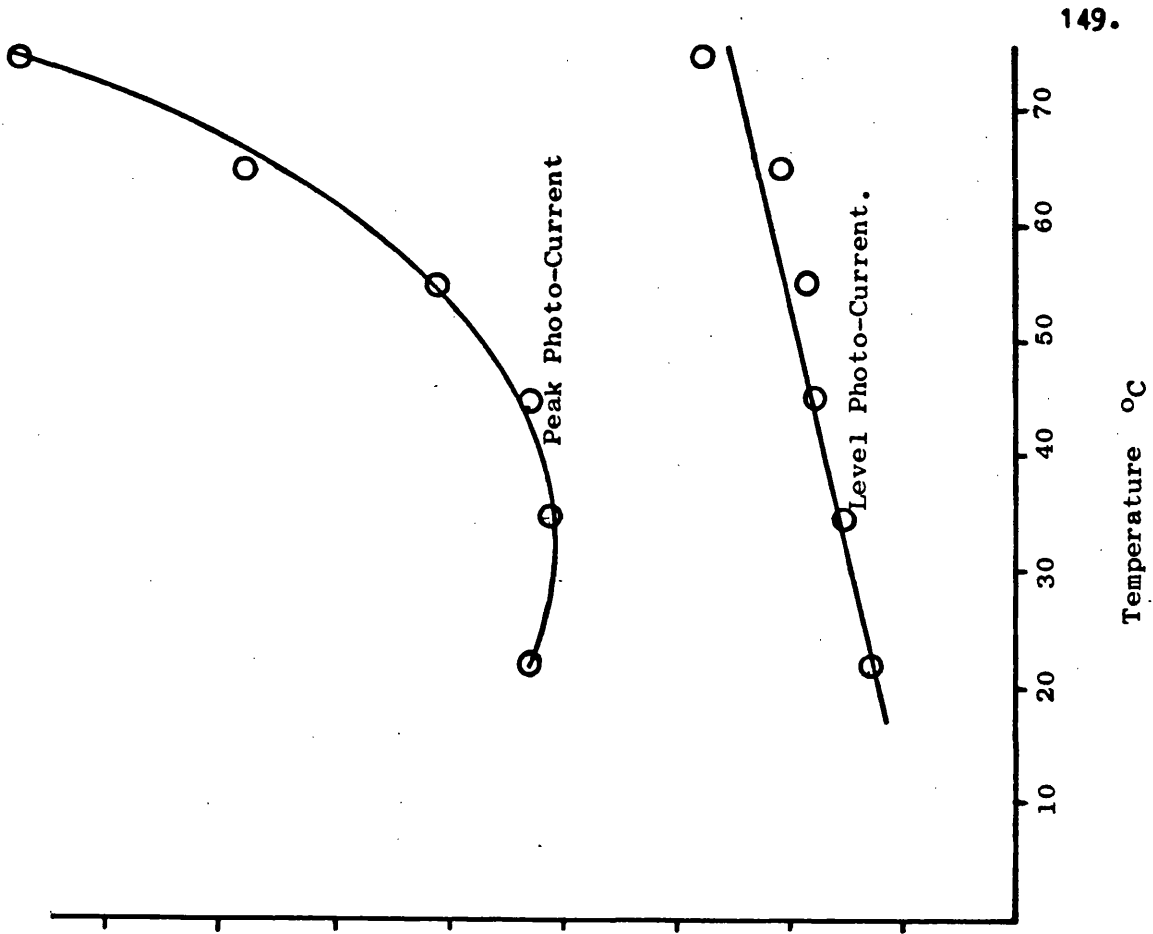
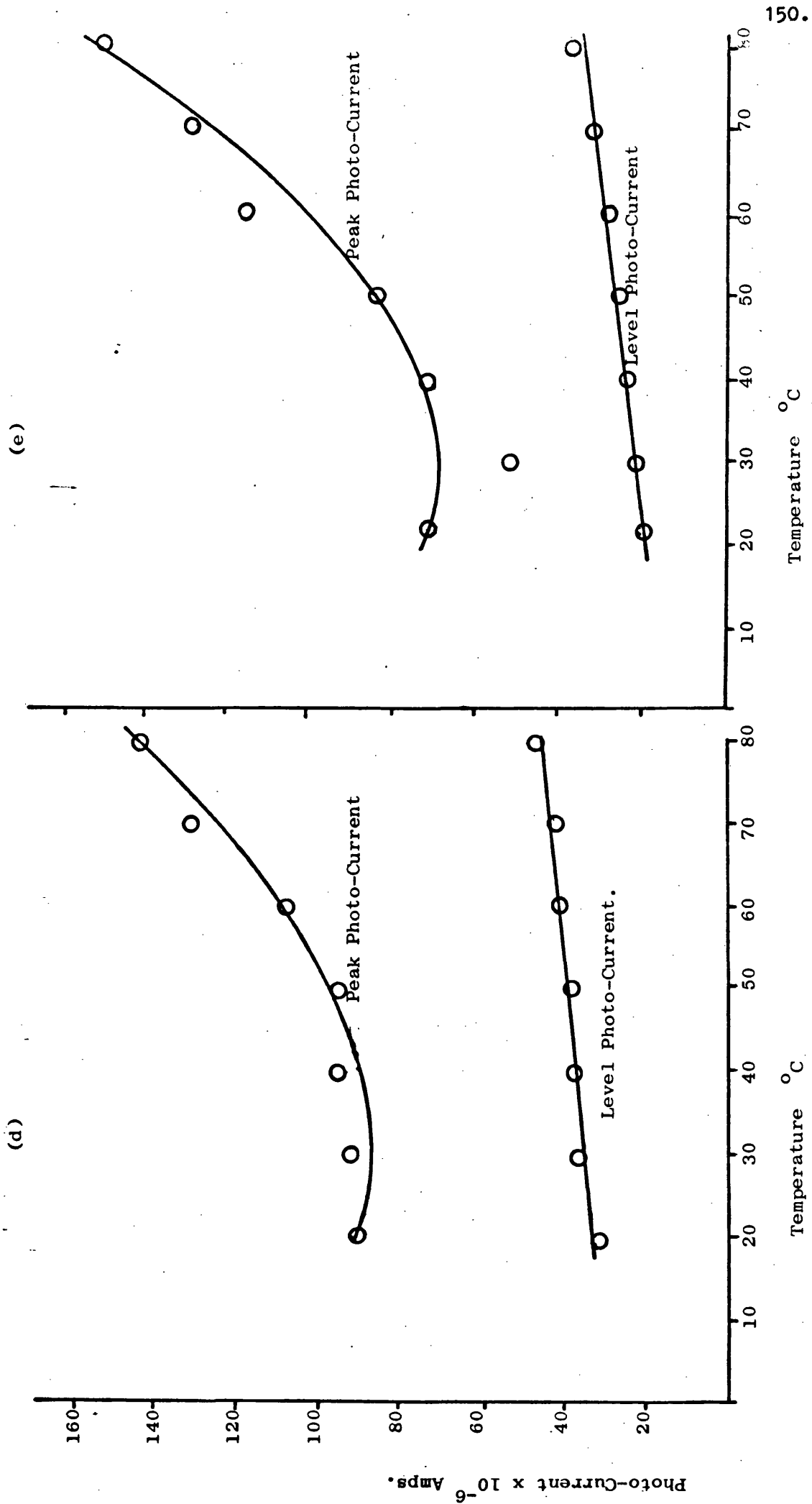


Fig. 63 (d and e). Temperature Dependence of Photo-Current.



20°C before the electrolytes were heated but less than the photo-currents obtained at 80°C.

5.6(c) Discussion.

The decrease of the photo-voltage with temperature indicates a reduction of the band bending. This may be due to increased mobility of holes and electrons within the pigment.

The photo-voltage decreases with temperature but the photo-currents increase with temperature. This is not a contradiction since the measurements are made under different conditions. For the photo-current the potential, and therefore the band bending is maintained at constant potential relative to the reference electrode. For the photo-voltage measurement the potential of the pigment electrode is allowed to change but there is no current flow.

The level photo-current undergoes a relatively small increase over a 60°C temperature range. This is probably due to the level photo-current being representative of a catalytic process. The current increase may originate in the increase in the rate of adsorption-desorption of hydroxide ions and hydroxyl radicals from the pigment surface, increasing the efficiency of the reaction of photo-holes. Likewise the faster diffusion of photo-holes to the surface due to higher temperatures would lead to photo-current increases.

The peak photo-current, which was attributed to charge displacement by removal of electrons from traps near or at the titanium dioxide surface, increases rapidly for temperatures above 50°C. This may be qualitatively attributed to the lower probability of electrons being retrapped in the interior of the pigment and to the increased electron mobility which would result in the observation of increased current flow

The heat treatment appears to result in a permanent increase in photo-current when the photo-current is remeasured at 20°C. An increase in the "wetting" of the pigment surface by immersion in hot electrolyte would be expected to lead to larger photo-currents.

5.7 Effect of Anions on the Photo-Electric Effects of Titanium Dioxide.

5.7(a) Experimental.

Preliminary investigations of the effects of iodide and bromide ions upon the photo-electric effects were performed with pigment A electrodes stored in 0.1M KI or 0.1M KBr pH7 unbuffered electrolytes overnight and the photo-currents were measured in the respective electrolytes using the 200 watt mercury lamp as light source. The potential biasing had to be within the limits for the electrolyte set by the dark current-voltage curves (Fig. 50).

The determination of the variation of photo-electric properties with concentration was performed by making small additions of potassium iodide or bromide solutions to a single cell system containing a pigment A electrode and 100 ml of 0.1M KCl pH unbuffered electrolyte. The xenon lamp was used as the light source. The photo-voltage and photo-current measurements (on separate electrodes) were made after a thirty minute dark period after the halide ion concentration had been adjusted.

5.7(b) Results.

The preliminary investigations resulted in the observation of a small positive photo-voltage (of 16 mv), for pigment A in potassium iodide electrolyte, i.e. the dark potential of the titanium dioxide electrode moved towards positive potentials upon irradiation. The photo-voltage for pigment A in potassium bromide electrolyte was smaller

than that obtained in potassium chloride electrolyte being only 50 mv but in the normal negative direction.

At 0.1v anodic bias pigment A in potassium iodide electrolyte gave a small cathodic photo-current of approximately $3\mu\text{A}$ and at 0.1v cathodic bias a cathodic photo-current of $6.4\mu\text{A}$ was observed. Pigment A in potassium bromide electrolyte at 0.5v anodic biasing gave only a small anodic photo-current of $3\mu\text{A}$.

A double cell system, with the salt bridge and cell compartments containing 0.1M KCl pH7 unbuffered electrolyte was used to investigate the reaction of iodide ions in the cell system. For this system a photo-voltage of 191 mv (-ve) was obtained for a pigment A electrode when the iodide concentration was zero. Upon making the pigment electrode compartment 10^{-3}M in KI a photo-voltage of 161 mv (+ve) was observed. When the experiment was repeated with another pigment A electrode the photo-voltage when the iodide concentration was zero was 214 mv (-ve). After making the counter electrode compartment 10^{-3}M in KI the photo-voltage was 184 mv (-ve).

The effect upon the photo-voltage of pigment A of progressive increases in iodide concentration in the electrolyte is shown in Fig. 64 as a plot of photo-voltage versus $\log(\text{concentration } \text{I}^-)$. The experiment was performed twice with different pigment A electrodes and qualitative agreement was achieved. Iodide ion concentrations had significant effects upon the shapes of the photo-voltage response curves. The photo-voltage curves are illustrated in the series of diagrams of Fig. 65. An iodide ion concentration is reached where the photo-voltage decay is initially towards more negative potentials and then decays slowly towards positive potentials. At higher concentrations the initial direction of the photo-voltage is in a positive direction but reverts to

Fig. 64. Variation of Photo-Voltage with Potassium Iodide Concentration.

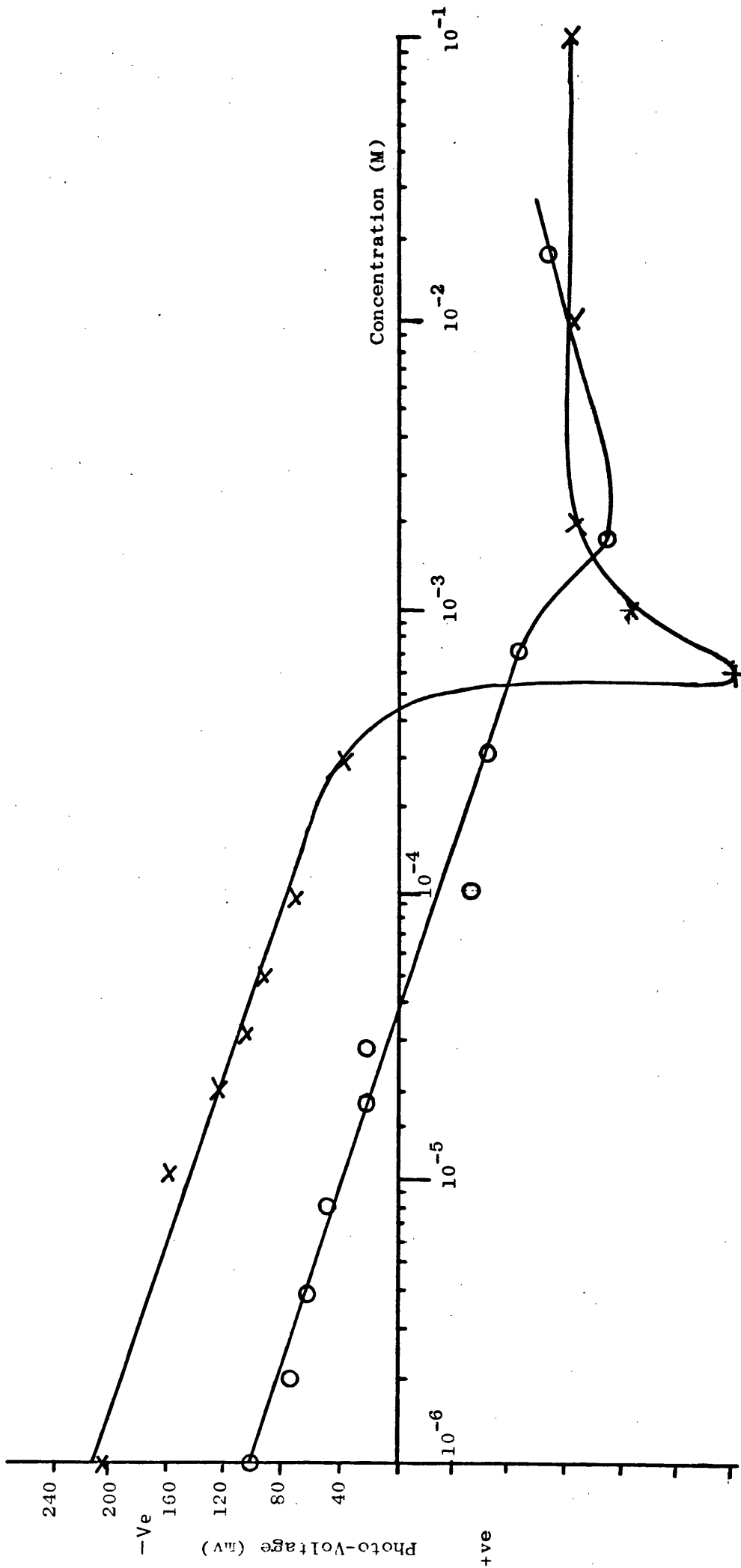
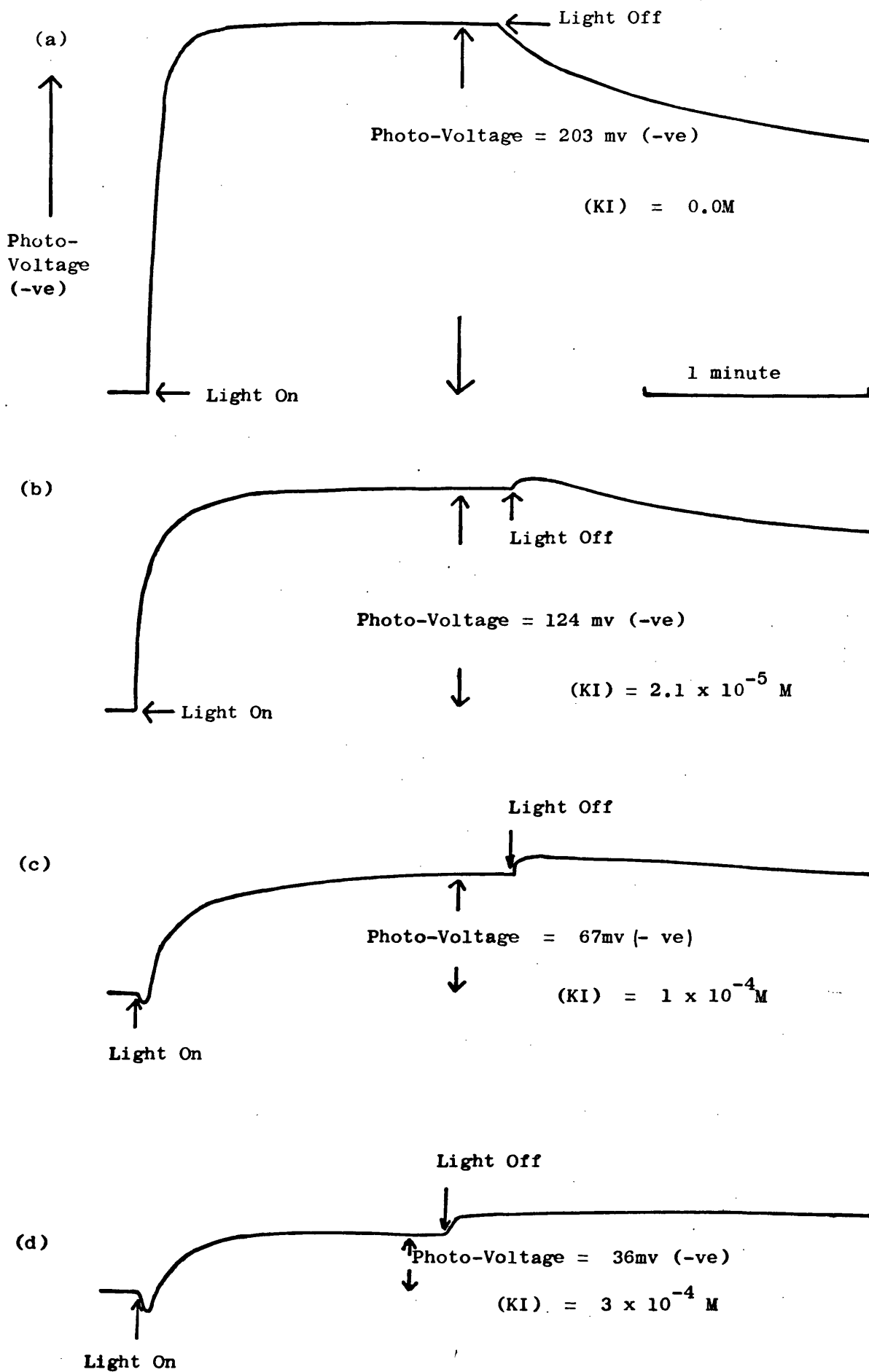
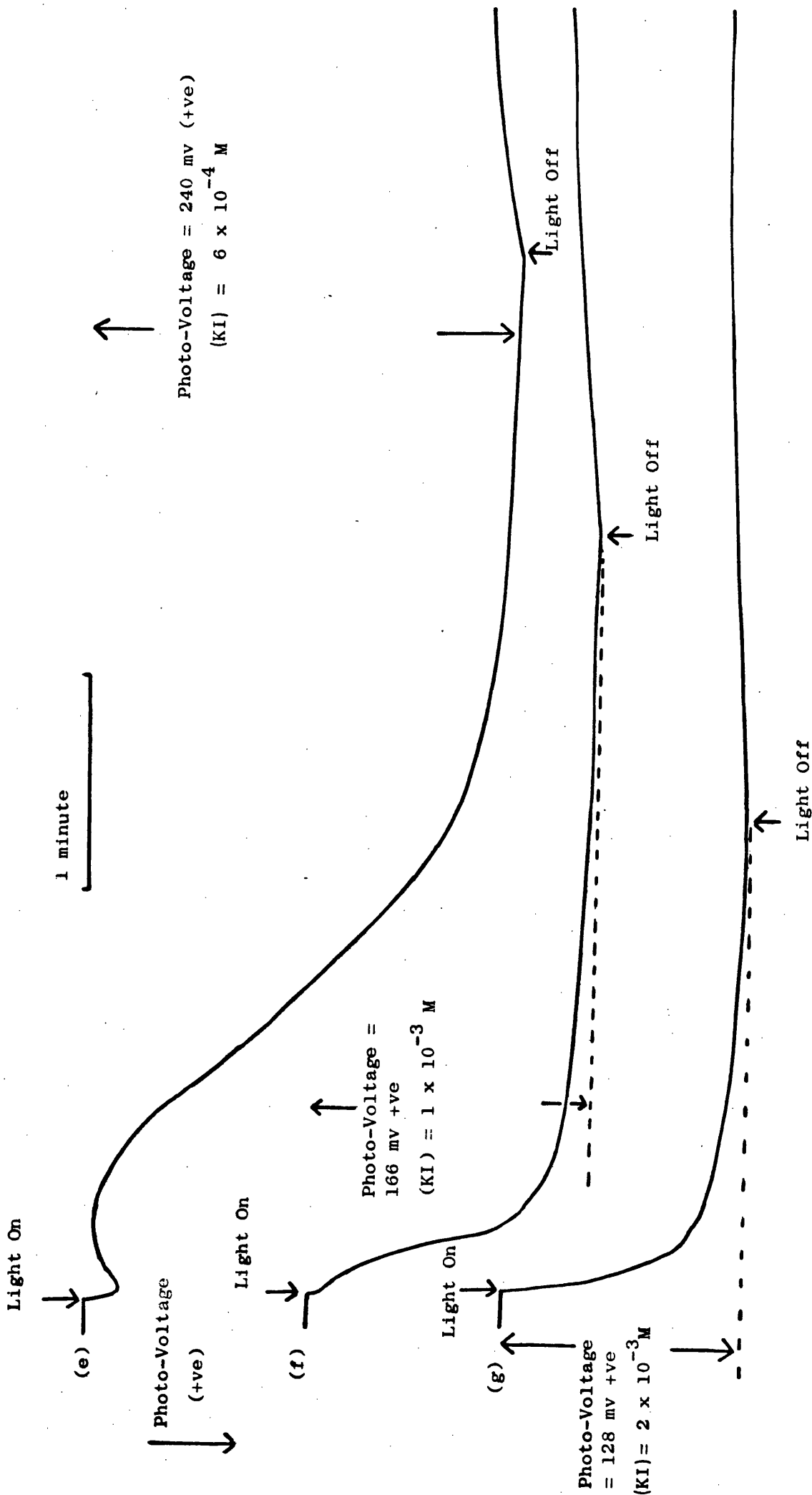


Fig. 65. Variation of Photo-Voltage with Potassium Iodide Concentration.



the normal negative direction. The photo-voltages eventually become positive.

The level anodic photo-currents of a pigment A electrode at 0.5v anodic biasing were found to decrease with increasing KI or KBr concentration as shown in Fig. 66. The dark current at 0.5v anodic biasing was not too large to prevent photo-current measurement since the concentration of potassium iodide used was low.

The effect upon the cathodic photo-current of pigment A at 0.5v cathodic bias was investigated. Oxygen was removed from the electrolyte by nitrogen bubbling. A small level cathodic photo-current of $1.5\mu\text{A}$ was increased to $6\mu\text{A}$ when the concentration of I^- was 10^{-4}M but increasing the concentration further did not increase the cathodic photo-current.

The effect of potassium iodide on the photo-current of an unbiased system was studied. This was effected by using the platinum counter electrode as both counter and reference electrodes and by setting the biasing to zero, so that the potentiostat ensured that there was no potential difference between the pigment A/Pt electrode and the platinum electrode.

The small anodic photo-current which was observed decreased upon addition of potassium iodide to the electrolyte as shown in Fig. 67 and eventually gave a small cathodic photo-current. Additional transient effects were noted for the photo-current response as the iodide concentration was increased. These are illustrated in Fig. 68.

5.7(c) Discussion.

Iodide and bromide ions were reported to undergo oxidation in competition with oxygen evolution at irradiated single crystal titanium dioxide electrodes.¹²⁸⁻⁹ This mode of reaction for iodide ions was also noted at illuminated cadmium sulphide electrodes.¹⁵² For an irradiated

Fig. 66. Variation of Photo-Current with KI and KBr Concentration.

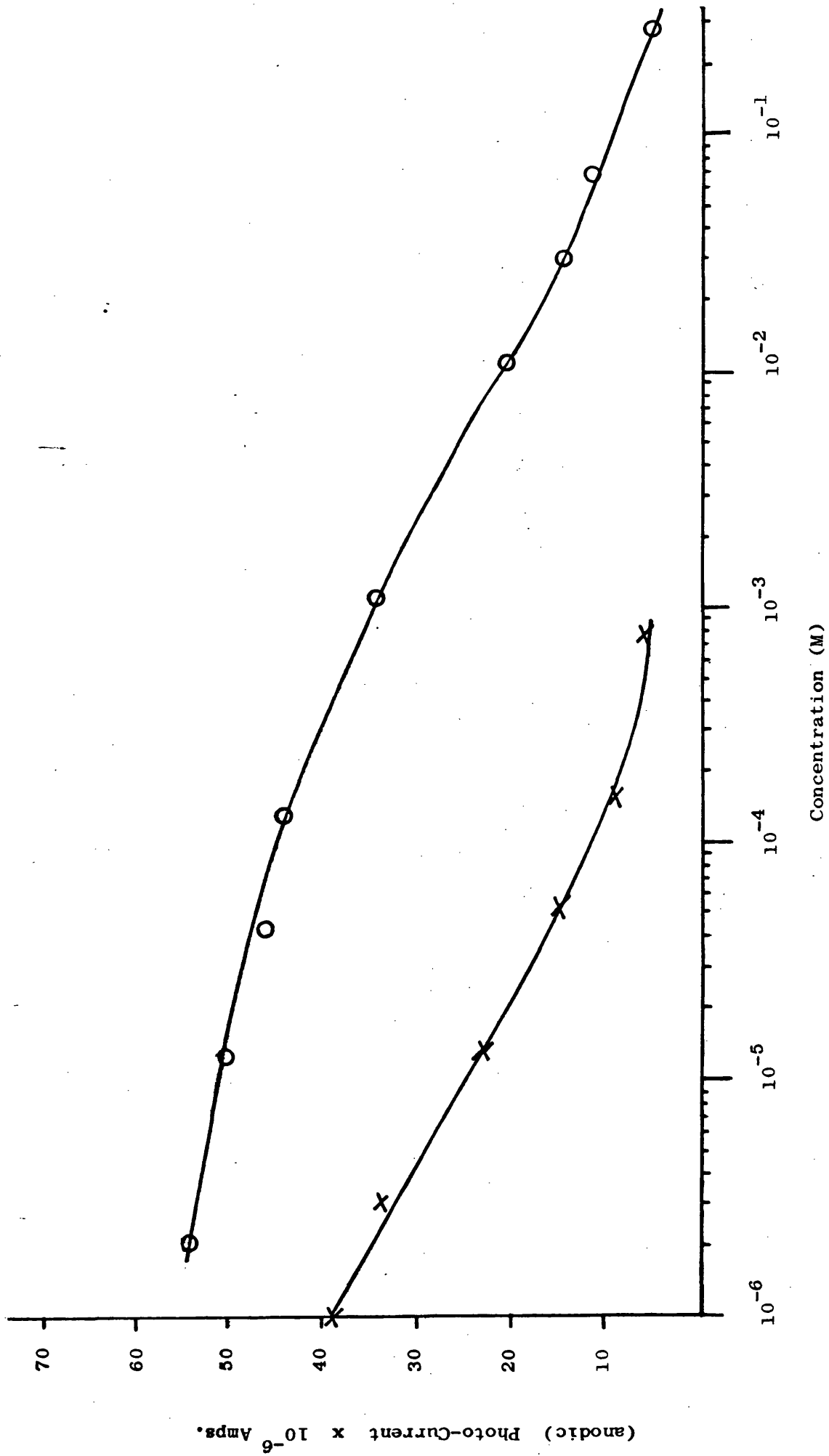


Fig. 67. Variation of Photo-Current (Under Zero Biasing) with KI Concentration.

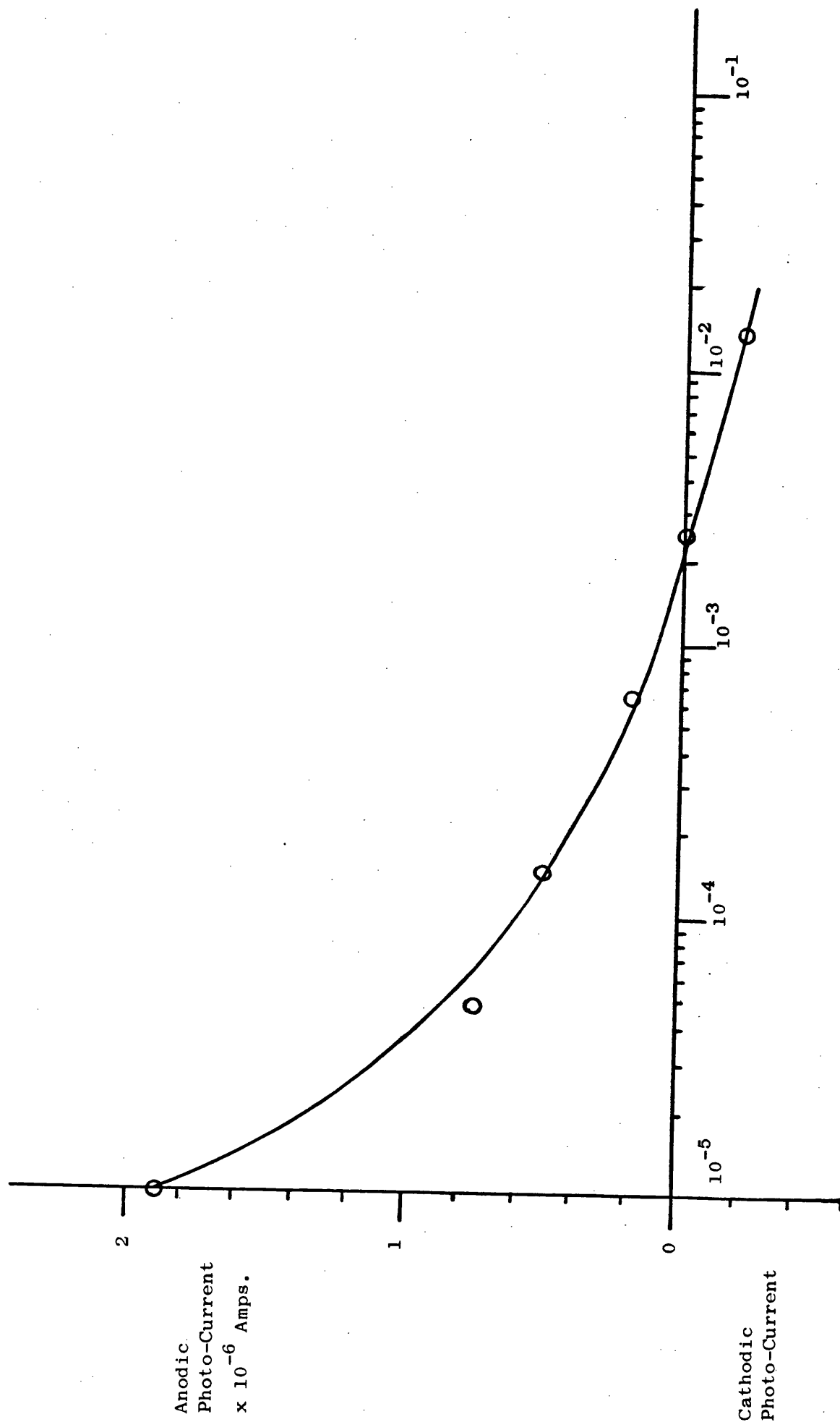
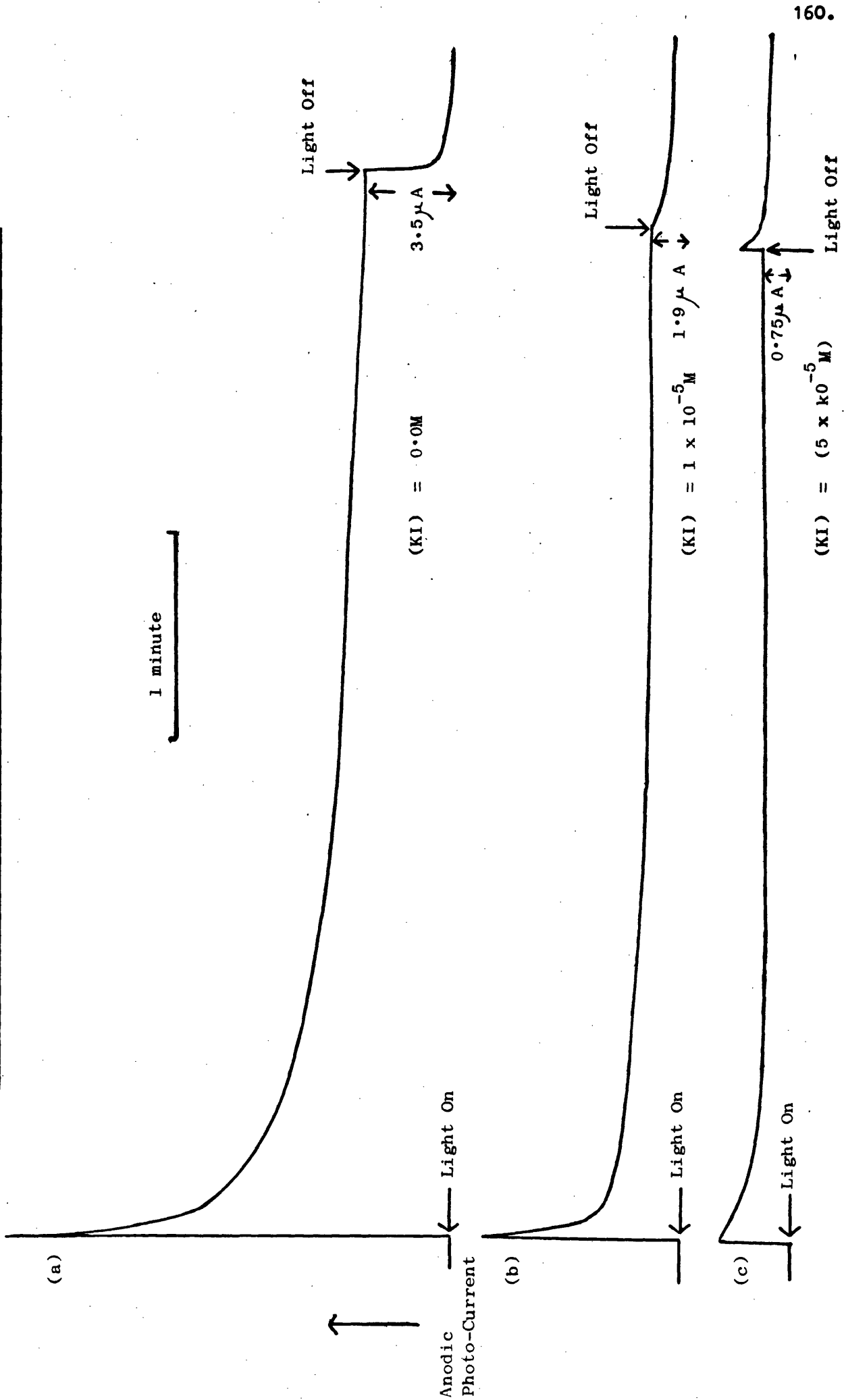
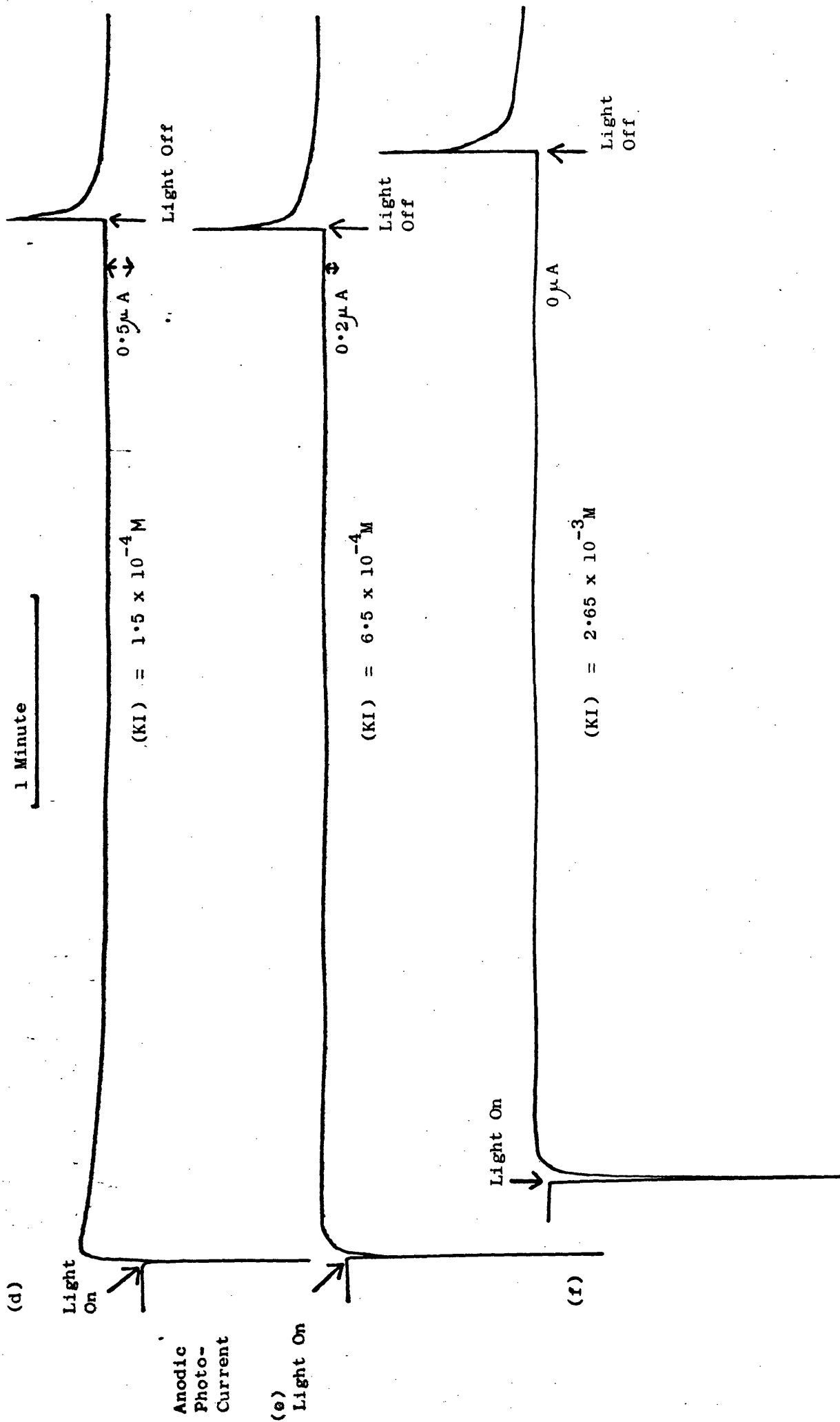
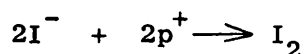


Fig. 68. Variation of Photo-Current at Zero Biasing with Potassium Iodide Concentration.





zinc oxide electrode the oxidation of I^- and Br^- occurs in preference to dissolution of zinc oxide.¹⁵² The oxidation would be due to the reaction of iodide ions with photo-holes.



This would lead to an anodic photo-current and for halide ions reacting in this way their addition to an electrolyte would not lead to any change in the anodic photo-current.

The oxidation of iodide ions at irradiated cadmium selenide electrodes was detected by the decrease in the current doubling effect by Vanden Berghe.¹⁵³ Thus when I^- was added to a cadmium selenide cell system sensitized with a current doubling agent the photo-current was found to decrease due to the competition for photo-holes between the current doubling agent and iodide ions. Reaction of iodide ions with a photo-hole would result in the injection of only one electron in the cadmium selenide electrode whereas reaction of the current multiplying agent with a photo-hole would lead to the injection of two electrons. Bromide ion was shown by this method not to undergo oxidation at irradiated cadmium selenide.

From the experiments with the double cell system it is clear that the reaction of I^- only occurs at irradiated titanium dioxide and that I^- concentrations at the counter electrode have no effect. The slight decrease of the photo-voltage when potassium iodide was added to the counter electrode compartment is most likely due to the diffusion of a small amount of potassium iodide to the pigment compartment via the salt bridge. Even very concentrated aqueous potassium iodide solutions have no absorption in the region 300nm - 400nm and a control experiment

of the irradiation of a clean platinum electrode in potassium iodide electrolyte gave no photo-effects. The effects observed for iodide and bromide ions on the irradiated pigment electrode do not indicate a simple oxidation of the halide ions as noted for titanium dioxide single crystals.¹²⁸⁻⁹

The decrease of the photo-voltage for pigment A is linear with the logarithm of iodide concentration for low concentrations.(Fig. 64.)

This suggests that the behaviour may be described by the Nernst Equation

$$E = E_0 - \frac{RT}{zF} \log_e [A_I^-]$$

where E and E₀ are dependent upon light intensity. z is the number of electrons involved in the reaction. If z = 1, $2.303 \frac{RT}{F}$, the slope of the graph of E against $\log_{10}(I^-)$ has a value of -0.059v. The values of the slopes of the lines in Fig. 64 are 0.072v and 0.068v giving fairly good agreement with theory. The deviation from straight lines at higher iodide concentrations may be attributed to iodide concentrations becoming unrepresentative of the activity of the iodide ions.

The observation of positive photo-voltages implies that there has been a reversal of the surface band bending, i.e. the energy levels are now bending downwards as they approach the surface and irradiation of the pigment produces electron-hole pairs which are separated by the potential field, electrons moving towards the surface and holes towards the interior. This would reduce the downward band bending and lead to the observation of positive photo-voltages. The change in the direction of band bending would appear to be brought about by the effect of I⁻ ions upon the double layer.

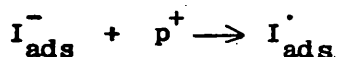
The transient effects noted in the photo-voltage response

immediately suggests that we are observing the competition between two effects operating in opposing direction being affected by I^- concentrations. In Fig. 65(b) the decay of the photo-voltage is initially towards more negative potentials and very slow decay rates occur. This effect seems to be due to the opposing photo-voltaic effects having different decay rates. Likewise in Fig. 65(c) upon irradiation the initial small positive photo-voltage could be due to the opposing photo-voltages having different charging rates. The resulting level photo-voltages in each case would be equal to (+ ve photo-voltage - -ve photo-voltage).

The anodic photo-current under anodic biasing is decreased by iodide and bromide ion concentrations; bromide ions being less effective in their behaviour than iodide ions. The photo-current does not become cathodic due to the anodic biasing maintaining upward band bending.

Photo-current measurement at zero biasing relative to platinum is directly comparable to photo-voltage measurement. The photo-currents measured in this way are very small even with the high light intensity of the xenon lamp. The photo-current behaviour mirrors remarkably the effects seen for the photo-voltages. Slower decay rates are observed for the photo-current curves and transient increases in the anodic current upon switching the light off are noted (Fig. 68c). At higher iodide ion concentrations the peak photo-currents occur in the cathodic direction and the level photo-current eventually becomes cathodic.

Iodide and bromide ions may be acting as electron-hole recombination centres for the irradiated pigment



Although if this was the only action of iodide ions the result would be a continual decrease of the anodic photo-current towards zero.

Photo-produced e.s.r. signals from zinc oxide in aqueous suspensions attributed to conduction band electrons have been shown to be quenched by iodide ions¹⁵⁴ which may imply its action as a recombination centre.

The effect of halide ions upon the photo-electric properties of the pigment/Pt electrode suggests the use of cell systems for the rapid investigation of additives for pigment preparation which may improve durability.

5.8 Effect of Amines on Pigment Photo-Currents.

5.8(a) Experimental.

Preliminary experiments have been performed on the effect of amine addition to cell systems.

Aqueous amines were added to the 100 ml of 0.1M KCl pH7 unbuffered electrolyte of a single cell system containing a pigment A electrode; the xenon lamp being used as the light source. When required after each addition of amine the pH was returned to pH7 by small additions of hydrochloric acid. The cell system was allowed to stand in darkness for thirty minutes after each amine addition before photo-current measurement. The anodic biasing applied was limited to 0.5v due to the dark current-voltage curves of the amines.

5.8(b) Results.

The level anodic photo-current of Pigment A at 0.5v anodic biasing decreased with additions of triethanolamine when the pH was not corrected to pH7 due to the electrolyte becoming alkaline (Fig. 69). Upon adjusting the pH to neutral a large increase in the level photo-

Fig. 69. Variation of Photo-Current with Triethanolamine (pH uncorrected).

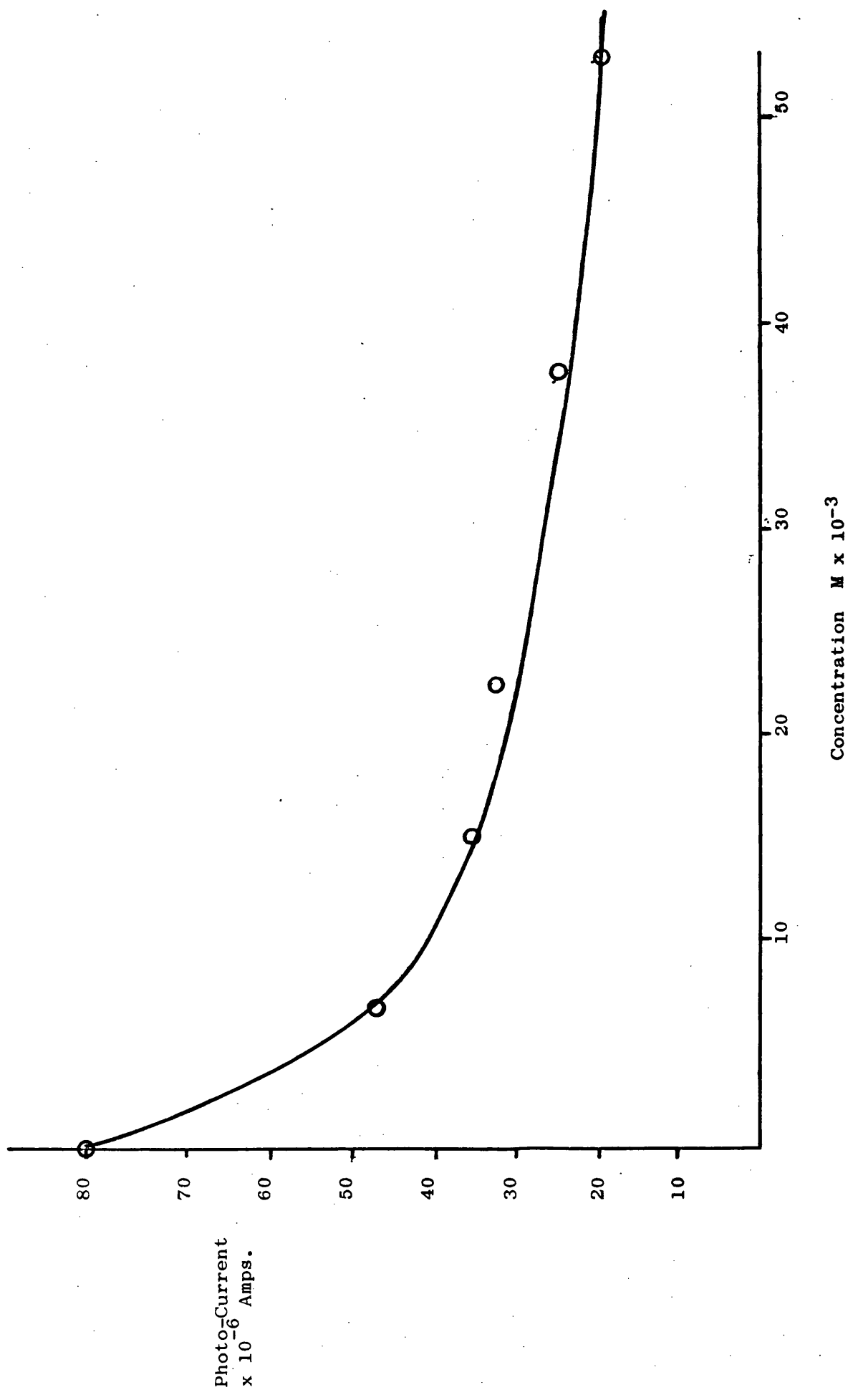
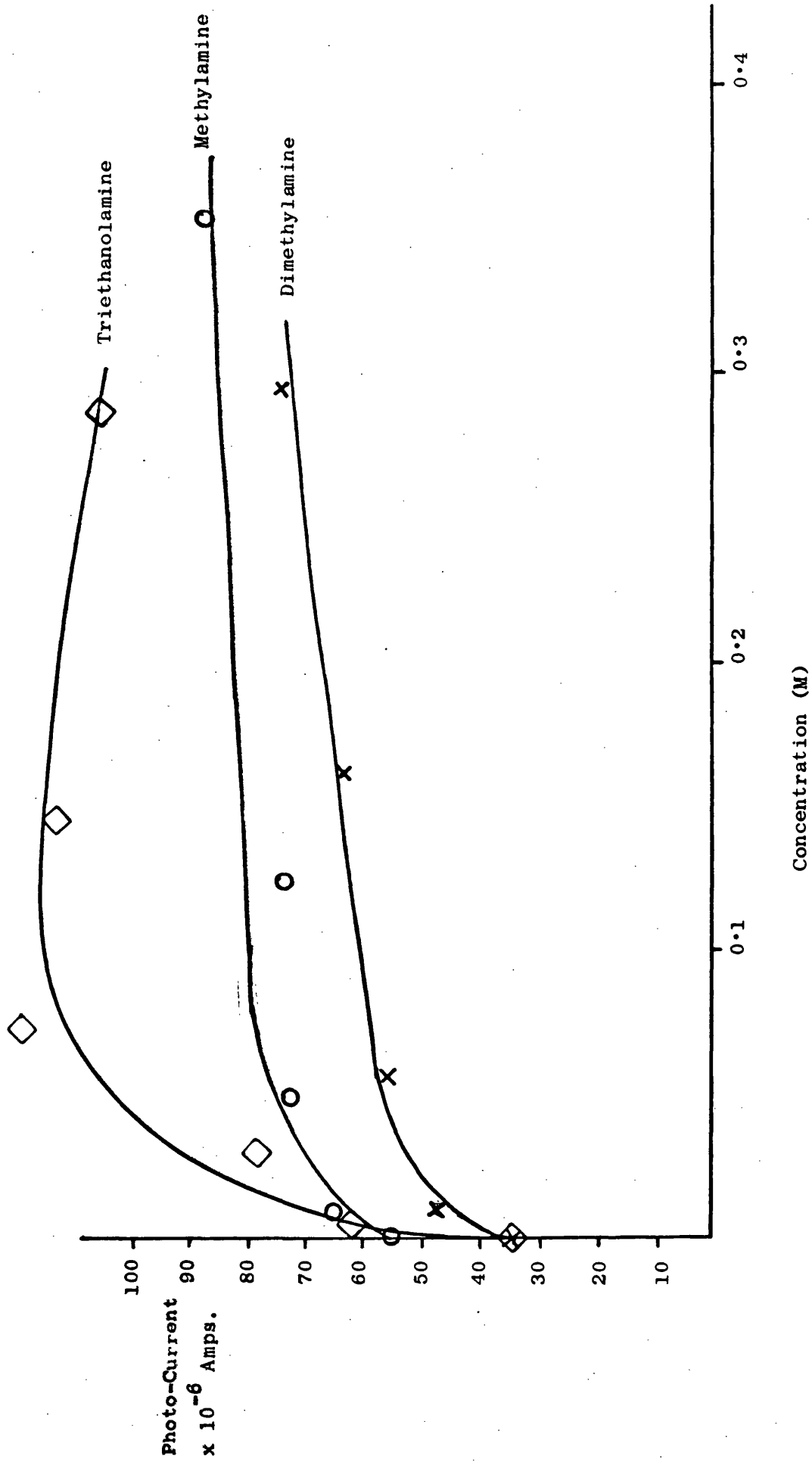
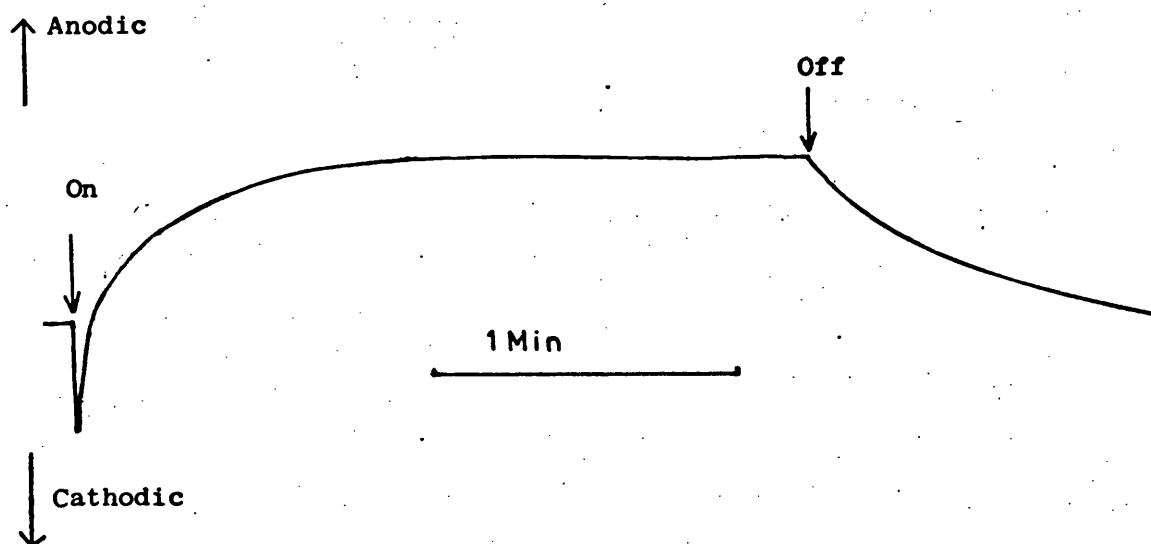


Fig. 70. Variation of Photo-Current with Amine Concentration (pH corrected).

-current was observed. Fig. 70. With readjustment to pH7 addition of methylamine and dimethylamine causes increases in the level anodic photo-current (Fig. 70).

For the cell system at 0.5v cathodic bias addition of triethanolamine to the electrolyte (after oxygen removal by nitrogen bubbling) without any pH adjustment led to the following photo-current response having a level photo-current of about $10\mu\text{A}$.

Fig. 71.



If the electrolyte is saturated with oxygen a level anodic direction photo-current of $200-250\mu\text{A}$ is observed at 0.5v cathodic bias against a large dark current due to the oxygen concentration in the electrolyte. At 0.5v anodic bias the photo-current was only $50\mu\text{A}$. The same effects of increase of photo-current with oxygen concentration are observed for methylamine and dimethylamine at cathodic bias.

When after triethanolamine addition the pH is adjusted to neutral a small level anodic direction photo-current of $20\mu\text{A}$ was observed which increased to $90\mu\text{A}$ when the electrolyte was saturated with oxygen.

If potassium hydroxide is added to the electrolyte instead of amines a similar photo-current response to Fig. 71 is observed but this is not increased by saturation of the electrolyte with oxygen.

Experiments were also performed at 0.5v cathodic bias using the double cell system. Triethanolamine was added to both cell compartments without pH adjustment. The electrolyte in the pigment compartment was saturated with oxygen and the counter electrode electrolyte was saturated with nitrogen. Under these conditions a level anodic direction photo-current of approximately $250\mu\text{A}$ was observed. When the pigment compartment electrolyte was saturated with nitrogen and the counter electrode electrolyte saturated with oxygen a level anodic direction photo-current of only $15\mu\text{A}$ was observed. With the normal concentration of dissolved air in the electrolyte the photo-current was $46\mu\text{A}$ in the anodic direction.

Addition of methanol to the electrolyte of a single cell system at 0.5v cathodic bias changed the small level photo-current to level anodic photo-current, but the initial peak photo-current was still in a cathodic direction. Saturation of the electrolyte with oxygen did not increase the photo-current.

5.8(c) Discussion.

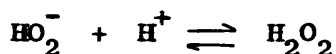
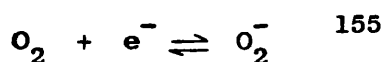
An increase of the anodic photo-current at cathodic bias is a consequence of the change from neutral to alkaline pH. Under anodic biasing this pH change leads to a decrease in the anodic photo-current. The anodic photo-current is also reduced in acidic electrolyte.

From the double cell experiment it appears that a reaction involving triethanolamine, methylamine, or dimethylamine, oxygen and

irradiated titanium dioxide is occurring at cathodic potentials. The anodic photo-current increase appears to be favoured in alkaline electrolytes which may be due to the amines being present in the free form instead of as the hydrochloride. The amines do not absorb light between the wavelengths 300nm to 400nm.

A reaction between amines and oxygen photo-catalysed by titanium dioxide might lead to a lowering of the oxygen concentration in the immediate vicinity of the pigment electrode which would reduce the cathodic dark current. This effect would not be observed at anodic biasing because the presence of oxygen in the electrolyte does not cause dark currents at anodic biasing.

The cathodic dark current due to oxygen in the electrolyte would be caused by oxygen reduction at the Pigment/Pt electrode.



The anodic photo-current at anodic biasing is sensitized by triethanolamine (at constant pH) and this most likely occurs by the same mechanism as for methanol and ethanol, i.e. by electron injection into the conduction band from the intermediate formed by the reaction of triethanolamine with a photo-hole. Methylamine and dimethylamine also appear to increase the anodic photo-current but to a much lower

extent. The presence of methanol and oxygen does not lead to large anodic photo-currents under cathodic bias which indicates that it is the nitrogen function of the triethanolamine molecule which is responsible for the effect noted with oxygen.

5.9 Chalking Mechanisms.

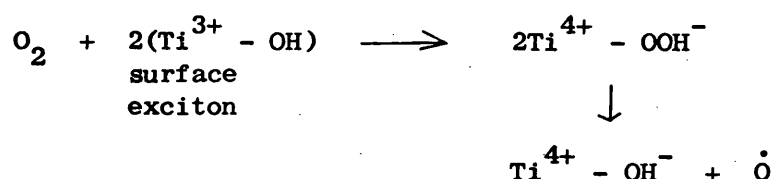
It has long been established that for chalking of a paint film to occur water and oxygen as well as ultra-violet light must be present.^{96,97} Jacobsen⁹⁶ quantified the earlier work of Renz⁹⁵ into a pigment testing method and inferred the atomic oxygen as the cause of chalking arising from photolysis of titanium dioxide.



Titanium dioxide would be re-oxidized in the presence of oxygen.

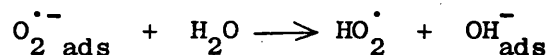
Clark¹⁵⁶ extended the idea of atomic oxygen as the reactive species, but being produced from adsorbed molecular oxygen and not from lattice ions. The beneficial action of Zn^{2+} ions and surface treatments on durability was explained by their ability to trap atomic oxygen.

Hughes³ also suggested that irradiation of titanium dioxide would lead to atomic oxygen.

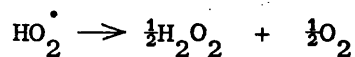


These mechanisms do not account for the involvement of water in the photo-catalytic process.

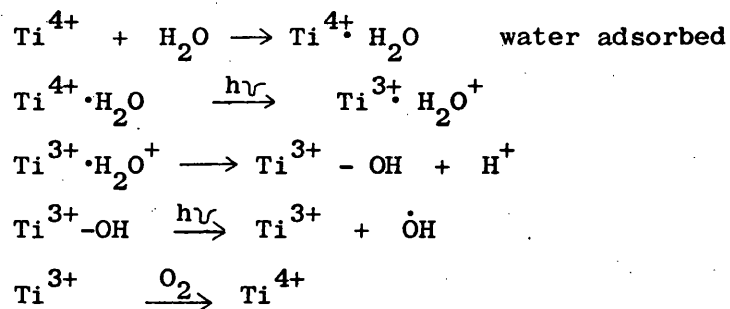
Photo-produced superoxide anions on titanium dioxide¹⁰²⁻³ may reaction with water to produce hydroperoxyl radicals.



This would lead to hydrogen peroxide production



The hydroxyl radical was first implicated as the reactive species by its detection over irradiated TiO_2 /aqueous dye systems by the hydroxylation of benzene to phenol.¹⁵⁷ Volz¹⁵⁸ recently reported the direct observation of hydroxyl radicals in irradiated aqueous pigment suspensions by e.s.r. He proposed the following mechanism for their formation



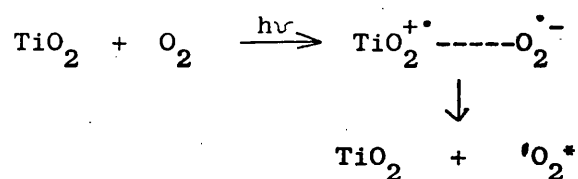
The last reaction should lead to $\text{O}_2^{\cdot-}$ formation and its associated reactions. Volz confirmed the ability of water to permeate a paint film and measured a passage of 1 ml of water per hour over a square metre of film with a partial pressure head of 18 torr. This passage was a factor of 10^3 times greater than the passage of oxygen through the film.

The above reaction scheme may be considered analogous to electron injection from water molecules proposed for the titanium dioxide cell reaction. Further evidence is provided by oxygen photo-adsorption being enhanced by the presence of water.¹¹⁰ Stone¹¹⁰ proposed that the action of water is to provide a source of surface OH^- ions which can trap photo-holes, producing hydroxyl radicals, and allowing the photo-electron to react with oxygen to form adsorbed O_2^- ions. In the cell system the photo-electron is able to react at the counter electrode and would not need to react with adsorbed molecules.

Irradiation of zinc oxide aqueous suspensions has long been known to produce measurable quantities of hydrogen peroxide.¹⁵⁹ It has been reported that irradiation of aqueous titanium dioxide does not produce hydrogen peroxide,¹⁶⁰⁻¹⁶¹ but hydrogen peroxide was detected in the presence of reducing agents such as benzene. The formation of hydrogen peroxide in irradiated aqueous titanium dioxide systems has been recently reported along with evidence for the formation of singlet oxygen.¹⁶²

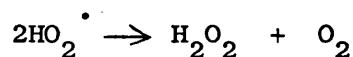
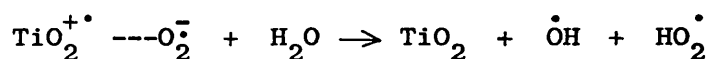
The production of singlet oxygen was detected in irradiated methanolic suspension of titanium dioxide containing furan by the formation of the singlet oxygen product 2-methoxy-5-oxo-2,5-dihydrofuran. Irradiation times of 4 - 5 days were necessary. Irradiations of aqueous suspension of titanium dioxide for the same time were reported as producing small quantities of hydrogen peroxide.

The mechanism of singlet oxygen formation proposed involved an electronic energy transfer from the pigment to oxygen via a titanium dioxide-oxygen complex



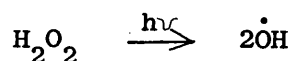
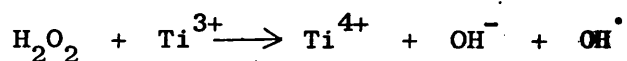
This is equivalent to oxygen acting as a recombination centre for photo-holes and electrons resulting in the formation of singlet oxygen by the transfer of energy of recombination to the oxygen molecule.

The proposed mechanism of formation of hydrogen peroxide was via the reaction of the titanium dioxide-oxygen complex with water leading to hydroperoxy radicals which form hydrogen peroxide



This provides an alternative mechanism for hydroxyl radical formation.

A steady state concentration of hydrogen peroxide is reached due to its decomposition over irradiated titanium dioxide by the mechanism¹⁶²



If singlet oxygen formation was occurring in the titanium dioxide cell system the reaction would not be detected by a photo-current since it is equivalent to a quenching reaction.

REFERENCES

1. R.J.H. Clark, The Chemistry of Titanium and Vanadium, Elsevier Publishing Company, 1968.
2. P. Nylén and E. Sunderland, Modern Surface Coating, Interscience Publishers, 1965.
3. W. Hughes, 8th Fatipec Congress, 1970, 67.
4. J. Dunderdale, W.E. Crake, and J.H. Collings, 12th Fatipec Congress, 1974, 69.
5. H.B. Weiser, W.O. Milligan, and E.L. Cook, J. Phys. Chem., 1941, 45, 1227.
6. D.J.C. Yates, J. Phys. Chem., 1961, 65, 747.
7. M. Primet, P. Pichat, and M.V. Mathieu, J. Phys. Chem., 1971, 75, 1216.
8. K.E. Lewis and G.D. Parfitt, Trans. Faraday Soc., 1966, 62, 204.
9. P. Jackson and G.D. Parfitt, Trans. Faraday Soc., 1971, 67, 2469.
10. P. Jones and J.A. Hockey, J.C.S. Faraday I, 1972, 68, 907.
11. H. Knozinger, Z. phys. Chem. (Frankfurt), 1970, 69, 108.
12. P. Jackson and G.D. Parfitt, J.C.S. Faraday I, 1972, 68, 896.
13. P. Jones and J.A. Hockey, Trans. Faraday Soc., 1971, 67, 2679.
14. M. Primet, P. Pichat, and M.V. Mathieu, Compt. Rend. Ser. B., 1968, 267, 799.
15. H.P. Boehm, Adv. Catal., 1966, 16, 249.
16. H.P. Boehm and M. Herrman, Z. anorg. allg. Chem., 1967, 352, 156.
17. H.P. Boehm and M. Herrman, Z. anorg. allg. Chem., 1969, 368, 73.
18. H.P. Boehm, Angew. Chem. Internat. Edn., 1966, 5, 533.
19. H.P. Boehm, Disc. Faraday Soc., 1971, 52, 264.

20. G.D. Parfitt, J. Ramsbotham, and C.H. Rochester, Trans. Faraday Soc., 1971, 67, 1500.
21. G.D. Parfitt, J. Ramsbotham, and C.H. Rochester, Trans. Faraday Soc., 1971, 67, 841.
22. G.D. Parfitt, J. Ramsbotham, and C.H. Rochester, Trans. Faraday Soc., 1971, 67, 3100.
23. I.T. Smith, Nature, 1964, 201, 67.
24. M. Primet, P. Pichat, and M.V. Mathieu, J. Phys. Chem., 1971, 75, 1221.
25. T. Morimoto, M. Nagao, and T. Omori, Bull. Chem. Soc. Japan, 1969, 42, 943.
26. R. Fell, Laporte Industries Limited, Organics and Pigments Division, Private Communication.
27. R.T. Kyi, Phy. Rev., 1962, 128, 151.
28. A.V. Kiselev and A.V. Urarov, Surface Sci., 1967, 6, 399.
29. B.A. Goodman and J.B. Raynor, Adv. Inorg. Chem. Radiochem., 1970, 13, 135.
30. D.L. Carter and A. Okaya, Phy. Rev., 1960, 118, 1485.
31. E. Yamaka and R.G. Barnes, Phy. Rev., 1962, 125, 1568.
32. W.A. Weyl and T. Forland, Ind. Eng. Chem., 1950, 42, 257.
33. H.J. Gerritsen and E.S. Sabisky, Phy. Rev., 1963, 132, 1507.
34. H.J. Gerritsen, S.E. Harrison, H.R. Lewis, and J.P. Wittke, Phy. Rev. Lett., 1959, 2, 153.
35. T. Takamura and J. Kashiwakura, Bull. Chem. Soc. Japan, 1963, 36, 1538.
36. B.D. Flockhart, C. Naccache, J.A.N. Scott, and R.C. Pink, Chem. Comm., 1965, 238.

37. B.D. Flockhart, I.R. Leith, and R.C. Pink, Chem. Comm., 1966, 885.
38. V.V. Subba Rao, R.D. Iyengar, and A.C. Zettlemyer, J. Catalysis, 1968, 12, 278.
39. C. Naccache, Y. Kodratoff, R.C. Pink, and B. Imelik, J. Chim. Phys., 1966, 63, 341.
40. B.D. Flockhart, I.R. Leith, and R.C. Pink, Trans. Faraday Soc., 1969, 65, 542.
41. B.D. Flockhart, I.R. Leith, and R.C. Pink, Trans. Faraday Soc., 1970, 66, 469.
42. B.D. Flockhart, I.R. Leith, and R.C. Pink, J. Catalysis, 1967, 9, 45.
43. M. Eigen and P. Matthies, Chem. Ber., 1961, 94, 3309.
44. D.M. Brouwer, Chem. Ind., 1961, 177.
45. J.K. Fogo, J. Phys. Chem., 1961, 65, 1919.
46. W.K. Hall, J. Catalysis, 1962, 1, 53.
47. D.M. Brouwer, J. Catalysis, 1962, 1, 372.
48. J.J. Rooney and R.C. Pink, Trans. Faraday Soc., 1962, 58, 1632.
49. A. Terenin, V. Barachevsky, E. Kotov, and V. Kolmogorov, Spectrochim. Acta, 1963, 19, 1797.
50. B.D. Flockhart, J.A.N. Scott, and R.C. Pink, Trans. Faraday Soc., 1966, 62, 730.
51. J.A.N. Scott, B.D. Flockhart, and R.C. Pink, Proc. Chem. Soc., 1964, 139.
52. Y. Kodratoff, C. Naccache, and B. Imelik, J. Chim. Phys., 1968, 65, 562.
53. Y.D. Pimenov, V.E. Kholmogorov, and A.N. Terenin, Doklady Akad. Nauk S.S.S.R., 1965, 163, 935.

54. Y.A. Zarif'yants, S.N. Karyagin, V.F. Kiselev, S.V. Khrusteleva, and G.D. Chukin, Doklady Akad. Nauk. S.S.S.R., 1972, 202, 109.
55. A.I. Mashchenko, G.B. Pariishii, and V.B. Kazanskii, Kinetika i Kataliz, 1967, 8, 704.
56. J. Cunningham and A.L. Penny, J. Phys. Chem., 1974, 78, 870.
57. M. Che, C. Naccache, and B. Imelik, J. Catalysis, 1972, 24, 328.
58. M. Che, C. Naccache, B. Imelik, and M. Prettre, Compt. Rend. Ser. C., 1967, 264, 1901.
59. H. Hosaka, T. Fujiwara, and K. Meguro, Bull. Chem. Soc. Japan, 1971, 44, 2616.
60. H. Hosaka, N. Kawashima, and K. Meguro, Bull. Chem. Soc. Japan, 1972, 45, 3371.
61. H. Hosaka and K. Meguro, Colloid. and Polymer Sci., 1974, 252, 322.
62. H. Ueda, Bull. Chem. Soc. Japan, 1970, 43, 319.
63. Y.D. Pimenov and V.E. Kholmogorov, Ser. Fiz. i Khim., 1966, 2, 21.
See Chem. Abs., 65. 11554a.
64. M. Che, C. Naccache, and B. Imelik, J. Chim. Phys., 1968, 65, 1301.
65. P.B. Asycough, Electron Spin Resonance in Chemistry, p. 156,
Methuen and Co. Ltd., 1967.
66. L.R. Melby, R.J. Harder, W.R. Hertler, W. Mahler, R.E. Benson, and W.E. Mochel, J. Amer. Chem. Soc., 1962, 84, 3374.
67. G. Briegleb, Angew. Chem. Internat. Edn., 1964, 3, 617.
68. A. Fulton, Aust. J. Chem., 1968, 21, 2847.
69. M.E. Peover, Trans. Faraday Soc., 1962, 58, 1656.
70. M.E. Peover, Trans. Faraday Soc., 1962, 58, 2370.
- 71a. W.D. Phillips and J.C. Rowell, J. Chem. Phys., 1960, 33, 626.
- 71b. L.A. Blymenfel'd and B.I. Sukhorukov, Doklady Akad. Nauk. S.S.S.R., 1964, 157, 1199.

72. D.C. Reitz, F. Dravnieks and J.E. Wertz, J. Chem. Phys., 1960, 33, 1880.
73. B. Venkatarman, B.G. Segal, and G.K. Fraenkel, J. Chem. Phys., 1959, 30, 1006.
74. I. Bergman, Trans. Faraday Soc., 1954, 50, 829.
75. E.S. Pysh, and N.C. Yang, J. Amer. Chem. Soc., 1963, 85, 2124.
76. A.J. Bard, K.S.V. Santhanam, J.T. Maloy, J. Phelps, and L.O. Wheeler, Disc. Faraday Soc., 1968, 45, 167.
77. H. Baba, I. Omura, and K. Higasi, Bull. Chem. Soc. Japan, 1956, 29, 521.
78. S.S. Lord and L.B. Rogers, Anal. Chem., 1954, 26, 284.
79. M. Kinoshita, Bull. Chem. Soc. Japan, 1962, 35, 1609.
80. L.F. Fieser, J. Amer. Chem. Soc., 1930, 52, 5204.
81. T.I. Gornyxh and A.G. Pozdeeva, Zhur. Priklad. Khim., 1954, 27, 118. See Chem. Abs., 48.5676a.
82. E.T. Seo, R.F. Nelson, J.M. Fritsch, L.S. Marcoux, D.W. Leedy, and R.N. Adams, J. Amer. Chem. Soc., 1966, 88, 3498.
83. F. Becker, Chem. Ber., 1963, 86, 1150. See Chem. Abs., 48.2450i.
84. P. Bischof, J.A. Hashmall, E. Heilbronner, and V. Hornung, Tetrahedron Letters, 1969, 4025.
85. P.B. Ayscough, Electron Spin Resonance in Chemistry, p.442. Methuen, 1967.
86. U. Eisner and R.P. Linstead, J. Chem. Soc., 1955, 3749, and D. Walker and J.D. Hiebert, Chem. Rev., 1967, 67, 153.
87. Y. Iida, Bull. Chem. Soc. Japan, 1971, 44, 1777.
88. C.S. Johnson and H.S. Gutowsky, J. Chem. Phys., 1963, 39, 58.

89. R.M. Elofson and R.L. Edsberg, Can. J. Chem., 1957, 35, 646.
90. R.F. Homer and T.E. Tomlinson, J. Chem. Soc., 1960, 2498.
91. W.R. Boon, Chem. Ind., 1965, 782.
92. R.F. Homer and T.E. Tomlinson, Nature, 1959, 184, 2012.
93. R.D. Iyengar and M. Codell, Advan. Colloid Interface Sci., 1972, 3, 365.
94. P. Meriaudeau, M. Che, P.C. Gravelle, and S.J. Teichner, Bull. Soc. Chim. France, 1971, 13.
95. C. Renz, Helv. Chim. Acta., 1921, 4, 961.
96. A.E. Jacobsen, Ind. Eng. Chem., 1949, 41, 523.
97. J. Petit and R. Poisson, Compt. Rend., 1955, 240, 312.
98. Y.I. Abramov, Lak. Mat., 1973, 1, 10.
99. P.F. Cornaz, J.H.C. Van Hooff, F.J. Pluijm, and G.C.A. Schuit, Disc. Faraday Soc., 1966, 41, 290.
100. C. Naccache, P. Meriaudeau, and M. Che, Trans. Faraday Soc., 1971, 67, 506.
101. A.I. Maschenko, V.B. Kazanskii, G.B. Pariiskii, and V.M. Sharapov, Kinetika i Kataliz, 1967, 8, 853.
102. P.C. Gravelle, F. Juillet, P. Meriaudeau, and S.J. Teichner, Disc. Faraday Soc., 1971, 52, 140.
103. M. Formenti, F. Juillet, P. Meriaudeau, and S.J. Teichner, Bull. Soc. chim. France, 1972, 69.
104. V.B. Kazanskii, V.V. Nikishina, and B.N. Shelimov, Doklady Akad. Nauk, 1969, 188, 112.
105. M. Che and C. Naccache, Chem. Phys. Letters, 1971, 8, 45.
106. R.D. Iyengar and R. Kellerman, J. Colloid Interface Sci., 1971, 35, 424.

107. R.D. Iyengar and R. Kellerman, Z. phys. Chem. (Frankfurt), 1969, 64, 345.
108. R.D. Iyengar, M. Codell, J.S. Karra, and J. Turkevich, J. Amer. Chem. Soc., 1966, 88, 5055.
109. C. Hauser and P. Cornaz, Chem. Phys. Letters, 1970, 5, 226.
110. R.I. Bickeley, G. Munuera, and F.S. Stone, J. Catalysis, 1973, 31, 398.
111. R.D. Iyengar, M. Codell, J. Karra, and J. Turkevich, Disc. Faraday Soc., 1966, 41, 325.
112. R.R. Addiss, A.K. Ghosh, and F.G. Wakim, Applied Physics Letters, 1968, 12, 397.
113. R.B. Lauers and A.K. Ghosh, Applied Physics Letters, 1970, 16, 341.
114. S.K. Deb, Solid State Communications, 1972, 11, 713.
115. F.A. Kröger and H.J. Vink, J. Chem. Phys., 1954, 22, 250.
116. G. Oster and M. Yamamoto, J. Applied Physics, 1966, 37, 823.
117. I.A. Akimov, Zhur. Nauch. i Priklad. Fot. i Kinematog., 1959, 4, 64. See Chem. Abs., 53.15761g.
118. M. Popovici, A.D. Petrescu, A. Redes, I. Atanasie, E. Armasar, and E. Popovici, Rev. Fiz. Chim. Ser. A., 1970, 7, 31. See Chem. Abs., 72. 123003X.
119. E. Lendvay, J. Phy. Chem., 1965, 69, 738.
120. D. Oelkrug, M. Radjaipour, and H. Erbse, Z. Phy. Chem. (Frankfurt), 1974, 88, 23.
121. K. Gollnick, Advances in Photochemistry, 1968, 6, 1.
122. J.G. Calverts and J.N. Pitts, Photochemistry, Wiley, 1966.
123. J.B. Birks and L.G. Christophoron, Proceedings Royal Society London (A), 1964, 277, 571.
124. E. Braswell, J. Phy. Chem., 1968, 72, 2477.
125. Becequerel, Compt. Rend., 1839, 9, 561.

126. R. Williams, J. Chem. Phys., 1960, 32, 1505.
127. H. Gerisher, J. Electrochem. Soc., 1966, 113, 1174.
128. A. Fujishima and K. Honda, Bull. Soc. Chem. Japan, 1971, 44, 1148.
129. A. Fujishima and K. Honda, Nature, 1972, 238, 37.
130. R.R. Addiss and F.G. Wakim, Photo. Sci. Eng., 1969, 13, 111.
131. P. Vohl, Photo. Sci. Eng., 1969, 13, 120.
132. F. Möllers, H.J. Tolle, R. Memming, J. Electrochem. Soc., 1974, 121, 1160.
133. P.J. Boddy, J. Electrochem. Soc., 1968, 115, 199.
134. K. Hirata, H. Yoneyama, and H. Tamura, Electrochim. Acta., 1972, 17, 793.
135. K. Hirata, H. Yoneyama, and H. Tamura, Electrochim. Acta, 1972, 17, 805.
136. H. Yoneyama, Y. Toyoguchi, and H. Tamura, J. Phy. Chem., 1972, 76, 3460.
137. J. Keeney, D.H. Weinstein, and G.M. Haas, Nature, 1975, 253, 719.
138. R. Keezer, J. Applied Physics, 1964, 35, 1866.
139. H. Gerisher and K. Cammann, Berichte der Bunsengesellschaft, 1972, 76, 385.
140. The Surface Chemistry of Metals and Semiconductors, H.C. Gatos, Wiley, 1959.
141. R. Marwick, Laporte Industries, Organics and Pigments Division, Private Communication.
142. A. Fujishima, K. Kohayakawa, and K. Honda, Bull. Chem. Soc. Japan, 1975, 48, 1041.
143. I.S. McLintock and M. Ritchie, Trans. Faraday Soc., 1965, 61, 1007.
144. C.F. Goodeve, Trans. Faraday Soc., 1937, 33, 340.

145. W. Sbrolli and E. Bertotti, Ann. Chim. Rome, 1959, 49, 1143.
See. Chem. Abs., 54.6268c.
146. A. Goetz and E.C.Y. Inn, Rev. Mod. Physics, 1948, 20, 131.
147. S. Keifer, Defazet-Dtsch. fa-ben.Z. 1974, 28, 364. CA.82.100131
148. H. Gerischer and H. Tributsky, Berichte der Bunsen-Gesellschaft, 1968, 72, 437.
149. S.R. Morrison and T. Freund, J. Chem. Phys., 1967, 47, 1543.
150. S.R. Morrison and T. Freund, Electrochim. Acta., 1968, 13, 1343.
151. A. Findlay, Practical Physical Chemistry, Longmans, Green, 1945.
152. A. Fujishima, E. Sugiyama, and K. Honda, Bull. Chem. Soc. Japan, 1971, 44, 304.
153. R.A.L. Vanden Berghe, W.P. Gomes, and F. Cardon, Z. phy. Chem. (Frankfurt), 1974, 92, 91.
154. J. Cunningham and S. Corkery, J. Phy. Chem., 1975, 79, 933.
155. J. Koryta, J. Dvorak, and V. Bohackova, Electrochemistry, Methuen, 1970.
156. A.G. Vondjidis and W.C. Clark, Nature, 1963, 198, 279.
157. G.A. Korsunovskii, Doklady Akad. Nauk S.S.S.R., 1957, 113, 853.
158. H.G. Volz, X Fatipec Cong. 1970, 107.
159. G.A. Korsunovskii and Yu. S. Lebedev, Russian J. Phy. Chem., 1961, 35, 528.
160. G.A. Korsunovskii, Russian J. Phy. Chem., 1960, 34, 241.
161. M.C. Markham and K.J. Laidler, J. Phy. Chem., 1953, 57, 363.
162. S.P. Pappas and R.M. Fischer, Pigment and Resin Tech., 1975, 3.